

***A Hydrogeochemical Evaluation of Groundwater in Fractured  
Rock Aquifers using Trace Elements and Stable Isotopes at  
Loxton in the Central Karoo.***

***By***

***L.H. Marais***

Thesis submitted in partial fulfillment  
of the requirements for the degree



***MAGISTER SCIENTIAE***

In the Faculty of Science,  
Department of Geology,  
University of Stellenbosch.

***Studyleader: Dr. G.J. Greeff***

***March 2001***

## **Declaration**

I, the undersigned, hereby declare that: A Hydrogeochemical Evaluation of Fractured Rock Aquifers by using Trace Elements and Stable Isotopes in Loxton, Central Karoo, to be my own work and that all the sources I have quoted, have been indicated and acknowledged by means of complete references.

## **Ethical consideration**

The results of this study would be made available to the Loxton municipality and farmers of the region. The author hopes that this study would form the basis of a continues study to optimise the development and management of groundwater resources in the Karoo.

Leánder Hugo Marais  
March 2001

## Abstract

This study was conducted to assess groundwater characteristics of geologically different fracture rock aquifers, at different depths, by means of chemical, isotope and  $^{14}\text{C}$ -dating results and to test for a "deeper seated aquifer", with different characteristics.

Jurassic dolerite dykes and sills, Cretaceous kimberlite fissures and pipes, as well as EW trending sinusoidal megafolds, comprise the structural domains of the study area. Fluvial sandstone and mudstone of the Beaufort Group are the dominant lithology of the study area.

The main water type found in the area is a water type not dominated by any anions or cations in particular. The second is a water type in which  $\text{Na-SO}_4$  is dominant, followed by a  $\text{Na-HCO}_3$  dominated water and to a lesser extend a  $\text{Ca-SO}_4$  type water.

The main cause of groundwater salinity is the infiltration of evaporated water to the subsurface, suggested by the isotopic enrichment of  $\delta^{18}\text{O}$  and  $\delta^2\text{H}$ , indicating very slow recharge from ponded water during excessive rainfall events.

There is a fair difference in isotopic values between surface measurements and measurements taken at depth, enforcing the possibility of a "second deeper seated aquifer". The water with the lower  $^{18}\text{O}$  values, for samples at depth suggest that this water has a source further inland, from rainfall on the range to the NE, the Hex River Mountain or Pramberge, which has greatly depleted  $^{18}\text{O}$  values relative to SMOW.

Most of the groundwater samples taken at depth indicated a  $^{14}\text{C}$ -dating of century age ( $\pm 200$  years), although in an evolutionary sequence the water is not such an old (evolved) water type, lending support to the theory about the migration of deeper seated water and thus a "second deeper seated aquifer system".

The chemical character of the groundwater is predominantly controlled by the infiltration of evaporated surface and subsurface water, the topographical nature of the catchments, geological influences (i.e. the process of dissolution, precipitation and ion exchange) and the influence of man.

Variability in water quality is caused by differences in rainfall, recharge, evaporation, topography, soil type and thickness, vegetation cover and antropogenic activities. Micro-scale differences

occur due to the nature of groundwater flow in Karoo rocks, namely the resulting variations within matrix and fracture components of the groundwater flux. The residence times are often different for these two main components and give rise to the differences in mineralization and solute proportion in passing groundwater.

This project should be seen as a basis of continuing study to provide the concrete answers needed to manage groundwater projects in the fractured rock aquifers of the Karoo.

Enslin (1950) expresses the classical hydrological conceptualisation of Karoo dolerite dykes - ***“the effect of induration and crushing of the sedimentary rock is that the permeability has been increased and the contact zone has been changed into an aquifer lying between the solid dyke and the saturated, low permeability country rock”.***

## Samevatting

Hierdie studie was onderneem met die doel om grondwater eienskappe te ondersoek in geologies verskillende gekraakte / genate aquifere en by verskillende dieptes met die hulp van chemiese, isotopiese en  $^{14}\text{C}$ -datering resultate, om sodoende te toets vir 'n "tweede dieper liggende aquifeer", met verskillende eienskappe.

Doleriet gange en plate (Jura), kimberliet gange en pype (Kryt), sowel as OW lopende sinusvormige mega-verskuiwings en monoklienes van die Kaapse Plooi Gordel, vorm die strukturele omgewings in die studie gebied. Die dominante litologie in die studie gebied is fluviaal gedeponeerde sandsteen en moddersteen van die Beaufort Groep.

Die opvallendste water-tipe wat in die studie gebied waargeneem word is 'n grondwater wat geen dominante katione of anione toon nie, tweedens is daar 'n  $\text{Na-SO}_4$  tipe grondwater wat gevolg word deur 'n  $\text{Na-HCO}_3$  tipe water en daarna 'n  $\text{Ca-SO}_4$  grondwater tipe.

Die hoof oorsaak van saliniteit in the grondwater is die infiltrering van verdamppte water na die grondwater-tafel, deur die verryking in  $\delta^{18}\text{O}$  en  $\delta^2\text{H}$ , wat stadige infiltrasie van water na hewige reënval episodes voorstel.

Die verskil van isotoop waardes by vlak en dieper watervlakke, steun die moontlikheid van die aanwesigheid van 'n "tweede dieper liggende aquifeer". Water met die lae  $^{18}\text{O}$ -waardes (met diepte) dui op 'n opvangsgebied meer na die noordoostelike binneland, soos byvoorbeeld die Hex Rivier Berge en die Pramberge.

Meeste van die grondwater monsters wat geneem is by 'n redelike diepte toon 'n  $^{14}\text{C}$ -datering waarde van ongeveer 200 jaar, alhoewel die water uit 'n evolutionere oogpunt nie so oud is nie en sodoende ondersteuning bied aan die teorie van die beweging van dieper liggende water en die bestaan van 'n "tweede dieper liggende aquifeer".

Die chemiese karakter van grondwater word hoofsaaklik beheer deur die infiltrering van verdamppte oppervlak water na die grondwater-tafel, die topografiese geaardheid van die opvangsgebied, geologiese invloede (soos die prosesse van presipitering, oplossing en ion uitruiling), sowel as die invloed van die mens.

Wisselvalligheid in die kwaliteit van grondwater word veroorsaak deur verskille in reënval, infiltrasie, evaporasie, topografie, grond tipe en diepte, plantegroei en die aktiwiteite van die mens. Verskille op mikro-vlak word veroorsaak deur die aard van die grondwater vloei deur die Karoo gesteentes, volgens die verskil in hidroliese geleiding tussen vloei in die matriks en vloei in die krake / nate. Daar is ook 'n verskil in die tydsbestek wat grondwater in die twee hoofstrukturele komponente deurbring en so die verskil in mineralisasie en saliniteit in die dinamiese grondwater veroorsaak.

Die projek moet gesien word as die basis vir voortdurende studie om konkrete antwoorde te verseker vir die gebruik in grondwater bestuur projekte van die gekraakte / genate rots aquifere in die Karoo.

Enslin (1950) konseptualiseer Karoo doleriet gange as volg: **“die effek van indringing en verbrokkeling van sedimentêre gesteentes is dat die deurlaatbaarheid verhoog word en dat die kontak sone verander is na 'n aquifeer wat lê tussen die soliede gang en die versadigde, lae deurlaatbare wand-gesteentes”.**

## Acknowledgements

The Water Research Commission of South Africa funded this project and also made it possible for the researcher to study for the year 2000, by means of a bursary.

I thank Dr. G.J. Greeff (Geology Department, University of Stellenbosch) for his input, guidance and constructive comments during this project.

I am indebted to Dr. Luc Chevallier from the Council of Geoscience for the information provided on the geology and relevant topics regarding the study area, as well as for his informative discussions, in the initial stages of the project. The Council is acknowledged for providing the caravan during the field work stage of this project.

Thanks to Shafick Adams (University of the Western Cape) for his thesis which provided strong guidance to the drafting of this project, as well as some useful software and to Mr. R. Titus for the use of a "bakkie" during my first visit to Loxton.

To Dr. Harris (Stable Isotope Laboratory, University of Cape Town), Prof. Verhagen (Shönland Center, University of the Witwatersrand) and INFRUITECH (Reggie Olivier) for producing good quality analysis.

To God, my family and friends, who supported me and made me feel like everything is possible: "Thank you".

## Abbreviations

AEC	-	Atomic Energy Corporation
b.g.l.	-	below ground level
b.g.w.l.	-	below groundwater level
CSIR	-	Council for Scientific and Industrial Research
DWA&F	-	Department of Water Affairs and Forestry
Fig.	-	Figure
GMWL	-	Global Meteoric Water Line
m.a.m.s.l.	-	meters above mean sea level
pers. comm.	-	personal communication
SMOW	-	Standard mean ocean water
WRC	-	Water Research Commission

Name	Abbreviation	Unit
Correlation coefficient	r	
Deuterium	$^2\text{H}$ or D	per mil
Electrical conductivity	EC	mS/m
Meters	m	m
Milligrams per liter	mg/l	mg/l
Oxygen-18	$^{18}\text{O}$	per mil
Partial pressure of <i>carbon dioxide</i>	$p\text{CO}_2$	atm
Parts per million	ppm	ppm
Redox potential	Eh	mV
Saturation index	SI	
Total dissolved solids	TDS	ppm or mg/l
Tritium units	T.U.	T.U.

## Table of Contents

### Chapter 1

#### General Introduction

<b>1.1. Introduction</b> .....	<b>1</b>
<b>1.2. Research objectives</b> .....	<b>1</b>
<b>1.3. Research requirements</b> .....	<b>2</b>
<b>1.4. Organisation of the study</b> .....	<b>3</b>

### Chapter 2

#### Theoretical considerations

<b>2.1. Introduction</b> .....	<b>4</b>
<b>2.2. Previous work</b> .....	<b>4</b>
<b>2.3. Literature review</b> .....	<b>5</b>
2.3.1. Fractured rock aquifers .....	5
2.3.2. Intergranular semi- to unconsolidated aquifers .....	7
2.3.3. Recharge .....	8
2.3.4. Natural hydrochemistry .....	9
2.3.4.1. Weathering and Dissolution .....	10
2.3.4.2. Cation Exchange .....	12
2.3.4.3. Precipitation and Saturation states .....	13
2.3.4.4. Elemental Sources .....	14
2.3.4.5. Salinization of Groundwater .....	19
2.3.4.6. Hydrochemical Evolution .....	19
2.3.5. Environmental isotope hydrology .....	22
2.3.5.1. Radioactivity .....	24
2.3.5.2. Fractionation .....	25

2.3.6. Radioactive isotopes .....	25
2.3.6.1. Tritium ( <sup>3</sup> H) .....	25
2.3.6.2. Radiocarbon ( <sup>14</sup> C) .....	26
2.3.7. Stable isotopes .....	30
2.3.7.1. Oxygen-18 & Deuterium .....	31
2.3.7.2. Carbon-13 .....	32
2.3.7.3. Nitrogen-15 .....	33
2.3.7.4. Dissolved gasses .....	34
2.3.8. Groundwater pollution .....	36
2.3.9. Statistics in hydrogeochemistry .....	36

## Chapter 3

### Study area

<b>3.1. Introduction .....</b>	<b>38</b>
<b>3.2. Location and extent of the area .....</b>	<b>38</b>
<b>3.3. Climate .....</b>	<b>38</b>
<b>3.4. Vegetation .....</b>	<b>41</b>
<b>3.5. Drainage .....</b>	<b>41</b>
<b>3.6. Geology .....</b>	<b>42</b>
3.6.1. Introduction .....	42
3.6.2. Lithology and Mineralogy .....	44
3.6.3. Structure .....	47
A) Site 1 : Loxton Allotment .....	54
B) Site 2 : De Wilg .....	54
C) Site 3 : Midland .....	55
D) Site 4 : Nuweland .....	55
E) Site 5 : Taaibosch .....	55
F) Site 6 : Môreson .....	57

3.6.3.1. Sill and ring complexes .....	58
3.6.3.2. Fracturing associated with Sill and Ring-Structures .....	61
3.6.3.3. Breccia plugs and Volcanic Vents .....	65
3.6.3.4. Kimberlite and associated Alkaline Intrusive Complexes ...	67
3.6.3.5. Regional lineaments .....	74
3.6.3.6. Folding .....	77
3.6.3.7. Vertical faulting and master jointing .....	78
3.6.3.8. Bedding-Plane Fracturing .....	82
<b>3.7. Geohydrology .....</b>	<b>83</b>
3.7.1. Beaufort Group .....	83
3.7.2. Karoo Dolerites .....	84
3.7.3. Distance from Dyke Contact .....	90
3.7.4. Width of Dyke .....	91
3.7.5. Dip of Dyke .....	91
3.7.6. En-échelon Dyke Segmentation .....	92
3.7.7. Transgressive Fracturing .....	92
3.7.8. Jointing Parallel to the Dyke Contact .....	92
3.7.9. Effect of Dyke Attitude and Drainage .....	93
3.7.10. Dyke / Sill Intersections .....	94
<b>3.8. Seismicity, Neotectonics and Unloading .....</b>	<b>95</b>
<b>3.9. Geomorphology, Fluvial terraces and Pedocrete .....</b>	<b>96</b>
3.9.1. Geomorphology .....	96
3.9.2. Fluvial terraces .....	97
3.9.3. Pedocrete .....	101
<b>3.10. Diagenesis, Paleo-fluid movement &amp; Thermo-metamorphism ...</b>	<b>103</b>

## Chapter 4

### Methodology and Conceptual Models

<b>4.1. Introduction</b>	<b>105</b>
<b>4.2. Methodology</b>	<b>105</b>
4.2.1. Sample localities	105
4.2.2. Sampling methods	105
4.2.3. Laboratory analysis	106
<b>4.3. Conceptual models</b>	<b>107</b>
4.3.1. Model I - Geology	109
4.3.1.1. Influence of the lithology on the groundwater chemistry	109
4.3.2. Model II - Recharge	111
4.3.3. Model III - Topography	113
<b>4.4. Groundwater Flow Models</b>	<b>115</b>
<b>4.5. Groundwater Flow Modeling</b>	<b>118</b>
<b>4.6. Groundwater Management Principles</b>	<b>120</b>

## Chapter 5

### Hydrogeochemistry

<b>5.1. Introduction</b>	<b>123</b>
<b>5.2. Precipitation Chemistry</b>	<b>123</b>
<b>5.3. Surface Water Chemistry</b>	<b>123</b>
<b>5.4. Groundwater Chemistry</b>	<b>124</b>
5.4.1. Statistical Analysis	124
5.4.1.1. Introduction	124
5.4.1.2. Descriptive Statistics	125
5.4.1.3. Correlation Matrices	127
5.4.1.4. Factor Analysis	129

5.4.2.	Groundwater Types of the Study area	132
5.4.2.1.	Introduction	132
5.4.2.2.	Groundwater Types	132
5.4.2.3.	Description of the Chemical Constituents	135
5.4.2.4.	Groundwater Evolution	147
<b>5.5.</b>	<b>Factors Affecting Groundwater Chemistry</b>	<b>148</b>
5.5.1.	Influence of Topography on the Groundwater Chemistry	148
5.5.2.	Influence of Evapotranspiration on the Groundwater Chemistry	150
5.5.3.	Influence of Geology on the Groundwater Chemistry	154
5.5.3.1.	Introduction	154
5.5.3.1.1)	Site 1 : Loxton Allotment	155
5.5.3.1.2)	Site 2 : De Wilg	156
5.5.3.1.3)	Site 3 : Midland	157
5.5.3.1.4)	Site 4 : Nuweland	158
5.5.3.1.5)	Site 5 : Taaibosch	159
5.5.3.1.6)	Site 6 : Môreson	160
5.5.3.2.	Physical Weathering	161
5.5.3.3.	Weathering of Dolerite	161
5.5.3.4.	Weathering of Sedimentary Rock	162
5.5.3.5.	Role of Carbon Dioxide	162
5.5.3.6.	Mineralogy	163
5.5.3.7.	Dissolution	165
5.5.3.8.	Precipitation and Saturation States	166
5.5.3.9.	Cation Exchange	170
5.5.3.10.	Isotopes	172
5.5.3.11.	Redox Controlled Reactions	173
5.5.4.	Influence of Human Activity on Groundwater Chemistry	174
5.5.5.	Spatial Distribution of Major Constituents	175
5.5.5.1.	Summary of the Chemical Parameters	177
5.5.5.2.	Major Cations	179
5.5.5.3.	Major Anions	184

5.5.5.4. Silica .....	189
5.5.6. Variability of the major constituents .....	190
5.5.7. Groundwater quality with respect to drinking water guidelines .....	190

## **Chapter 6**

### **Conclusions and Recommendations**

<b>6.1. Introduction .....</b>	<b>192</b>
<b>6.2. Groundwater chemistry and variations .....</b>	<b>193</b>
<b>6.3. Groundwater characteristics .....</b>	<b>194</b>
<b>6.4. Groundwater model .....</b>	<b>198</b>
<b>6.5. Hydrogeochemical conditions of groundwater .....</b>	<b>200</b>
<b>6.6. Recommendations .....</b>	<b>202</b>

<b>References .....</b>	<b>204</b>
-------------------------	------------

<b>Appendices .....</b>	<b>222</b>
-------------------------	------------

**Appendix A : Data tables**

**Appendix B : Chemical analyses**

**Appendix C : Geological information**

**Appendix D : LOG - activities**

## List of Figures

<b>Figure 2.3.2.</b>	Geohydrological section across the Caroluspoot alluvial-bedrock aquifer	8
<b>Figure 3.2.</b>	Loxton locality map	40
<b>Figure 3.6.1.</b>	North-south cross-section of the Main Karoo Basin	43
<b>Figure 3.6.2.A.</b>	Distribution of lithological units in the Main Karoo Basin	46
<b>Figure 3.6.2.B.</b>	Generalised stratigraphy of the Karoo Supergroup	47
<b>Figure 3.6.3.A.</b>	Mega lineaments extracted from LINCOMP	50
<b>Figure 3.6.3.B.</b>	Lineament structural domains	51
<b>Figure 3.6.3.C.</b>	Lineament map of Loxton	52
<b>Figure 3.6.3.D.</b>	Exploration drilling sites at Loxton	53
<b>Figure 3.6.3.E.</b>	Vertical dislocation of the De Wilg Shear dyke	56
<b>Figure 3.6.3.1.</b>	Major dolerite Ring Complex System	59
<b>Figure 3.6.3.2.A.</b>	Fractures associated with sill and ring complexes	62
<b>Figure 3.6.3.2.B.</b>	Mechanisms of emplacement of dolerite sill / ring systems	64
<b>Figure 3.6.3.4.</b>	Geohydrology of the Jagersfontein Kimberlite Diatreme	73
<b>Figure 3.6.3.5.</b>	Pre-Karoo structures	76
<b>Figure 3.7.2.A.</b>	En-échelon dolerite dyke, Thermal joints, Tectonic reactivation	86
<b>Figure 3.7.2.B.</b>	Structural domains and emplacement of dolerite dykes	89
<b>Figure 3.9.1.A.</b>	The African and Post-African surface	98
<b>Figure 3.9.1.B.</b>	The drainage system near Victoria West	99
<b>Figure 4.3.A.</b>	Typical conceptual model for Karoo aquifers	108
<b>Figure 4.3.B.</b>	Vertical fracture indicating perpendicular flow	109
<b>Figure 4.3.2.</b>	D vs. $^{18}\text{O}$ diagram	112
<b>Figure 4.4.A.</b>	Idealised flow lines for a confined aquifer	116
<b>Figure 4.4.B.</b>	Idealised flow lines for a isotropic, unconfined, phreatic aquifer	117
<b>Figure 5.4.2.2.A.</b>	Histogram of the main water types in the area	132
<b>Figure 5.4.2.2.B.</b>	Piper diagram of all groundwater at Loxton	134

<b>Figure 5.4.2.2.C.</b>	Expanded Durov diagram of all the groundwater at Loxton	134
<b>Figure 5.4.2.3.A.</b>	Electrical conductivity map of the area	136
<b>Figure 5.4.2.3.B.</b>	Sodium (ppm) map of the area	137
<b>Figure 5.4.2.3.C.</b>	Calcium (ppm) map of the area	138
<b>Figure 5.4.2.3.D.</b>	Sulphate (ppm) map of the area	139
<b>Figure 5.4.2.3.E.</b>	Chloride (ppm) map of the area	140
<b>Figure 5.4.2.3.F.</b>	Potassium (ppm) map of the area	141
<b>Figure 5.4.2.3.G.</b>	Nitrate (ppm) map of the area	142
<b>Figure 5.4.2.3.H.</b>	Bicarbonate (ppm) map of the area	143
<b>Figure 5.4.2.3.I.</b>	Strontium (ppm) map of the area	144
<b>Figure 5.4.2.3.J.</b>	Fluoride (ppm) map of the area	145
<b>Figure 5.4.2.3.K.</b>	Topographical map for the study area	146
<b>Figure 5.5.1.</b>	Relationship between Cl & TDS & topography	149
<b>Figure 5.5.2.A.</b>	Deuterium vs. oxygen-18 for all samples at Loxton	151
<b>Figure 5.5.2.B.</b>	Chloride vs. oxygen-18	152
<b>Figure 5.5.2.C.</b>	Altitude vs. oxygen-18	153
<b>Figure A-</b>	Site 1. Loxton Allotment	155
<b>Figure B-</b>	Site 2. De Wilg	156
<b>Figure C-</b>	Site 3. Midland	157
<b>Figure D-</b>	Site 4. Nuweland	158
<b>Figure E-</b>	Site 5. Taaibosch	159
<b>Figure F-</b>	Site 6. Môreson	160
<b>Figure 5.5.3.8.A.</b>	Activity-activity diagram for calcite saturation	167
<b>Figure 5.5.3.8.B.</b>	Activity-activity diagram for gypsum saturation	168
<b>Figure 5.5.3.8.C.</b>	Activity-activity diagram for strontianite saturation	168
<b>Figure 5.5.3.8.D.</b>	Activity-activity diagram for barite saturation	169
<b>Figure 5.5.3.8.E.</b>	Activity-activity diagram for fluorite saturation	169
<b>Figure 5.5.3.10.</b>	Carbon-14 vs. Tritium plot for Loxton groundwater	173

<b>Figure 5.5.5.2.A.</b> Calcium concentration (geometric mean)	179
<b>Figure 5.5.5.2.B.</b> Magnesium concentration over elementary lithological units	181
<b>Figure 5.5.5.2.C.</b> Sodium concentration	182
<b>Figure 5.5.5.2.D.</b> Na:Cl ratio in the Karoo Basin	183
<b>Figure 5.5.5.3.A.</b> Chlorite concentration (geometric mean)	186
<b>Figure 5.5.5.3.B.</b> Sulphate concentration	187
<b>Figure 5.5.5.3.C.</b> Nitrate (as N) concentration	188
<b>Figure 5.5.5.3.D.</b> Fluoride concentration	189

## List of tables

<b>Table 4.2.2.1.</b>	Physical and chemical determinants	106
<b>Table 4.3.1.1.</b>	Average element composition (ppm) of the major rock types	110
<b>Table 5.4.1.2.</b>	Univariate statistical overview of the data set	126
<b>Table 5.4.1.3.</b>	Pearson's correlation matrix for the Loxton data	128
<b>Table 5.4.1.4.</b>	Factor analyses of Loxton data with Varimax rotation	131
<b>Table 5.4.2.4.A.</b>	Assumed hydrochemical facies and regimes of the groundwater	147
<b>Table 5.4.2.4.B.</b>	Hydrochemical facies and regimes of groundwater according to TDS	147
<b>Table 5.5.1.</b>	Average groundwater chemistry for various topographical settings	149
<b>Table 5.5.3.6.</b>	Mineralogy of the major rock types in Loxton	165
<b>Table 5.5.3.8.</b>	Mineral solubility product	167

## List of plates

<b>Plate 3.6.3.4.</b>	Kimberlite fissure and pipe at Nuweland (Loxton)	70
<b>Plate 3.6.3.7.</b>	Prominent master joints	81

## CHAPTER 1

### General Introduction

#### **1.1. Introduction**

Groundwater has always been an important natural resource in the Karoo region. Variability in the groundwater quality and quantity puts extra strain on the domestic and agricultural needs of this region.

The variability in groundwater quality is the result of various surface and subsurface processes and activities. The importance of understanding geohydrological and groundwater characteristics of the region, that influence the chemical composition of groundwater, can be used to describe the interaction of groundwater with its environment.

Delineating areas with distinctive groundwater chemistry, by identifying the main factors and processes that determine groundwater chemistry variations in space (horizontally as well as vertically) and time (most probable movement and recharge histories) is possible.

This research project is aimed at assessing groundwater characteristics of the geologically different fractured rock aquifers, at different depths, found in the Loxton area. The main factors (hydrogeochemical) and processes (exchange reactions, etc.) that determine groundwater chemistry variations (quality) in space and time are to be identified by means of chemical, isotope and  $^{14}\text{C}$ -dating results, in order to test for a possible "second deeper seated aquifer system", with different characteristics.

#### **1.2. Research objectives**

This Water Research Commission funded project entitled: ***Hydrogeochemical Evaluation of Groundwater in Fractured Rock Aquifers, using Trace Elements and Stable Isotopes at LOXTON, Central Karoo*** attempts to:

1. Delineate areas with distinctive groundwater chemistry and the variations in space and time.
2. Assess groundwater characteristics of the aquifers found in the study area and correlation / comparison of the results (chemical, isotope and  $^{14}\text{C}$ ) obtained with the physical environment, mainly in the determination of the chemical composition of groundwater (quality).
3. Derive a model of the groundwater bodies in the study area.
4. Identify the hydrogeochemical conditions and exchange reactions with different bedrock zones that influence the chemical composition of the groundwater.

### **1.3. Research requirements**

The research requirements identified, to achieve the project objectives were:

- Purchase of a pump, suitable for the extraction of groundwater over a period of time, to allow for the establishment of equilibrium conditions in the water chemistry from a specific depth, in a number of boreholes (39) drilled in the Karoo, by the Department of Water Affairs (DWA&F) at Loxton.
- Fitting of a hydraulic packer to the stem of the pump, to enable sampling of groundwater at selected depths, within the boreholes, to make comparative analyses of the chemical composition, trace element and stable isotope content of these samples.
- Assembly and testing of the solar powered water pump and the function of the hydraulic packer fittings and the flow-through-cell sampling device.
- Transport of the sampling pump to the research area for the drawing of groundwater samples from different parts of the boreholes for chemical, isotope and  $^{14}\text{C}$ -dating analyses, by INFRUITEC, UCT and Shönland Center (UWits) respectively.

- Extraction of groundwater samples from discrete zones in a large number of boreholes from the six sites, drilled by DWA&F in the area around Loxton. Selection of boreholes (twelve  $^{14}\text{C}$ -samples from the six sites at vertically different geological formations) expected to provide the most information regarding chemical and isotope analyses of groundwater at different depths, using the solar powered packer pump. This would provide information to evaluate fractured rock aquifers in the Loxton area and to test for a “second deeper seated aquifer system”, with different characteristics.
- Analysis and evaluation of the major anions and cations, trace elements, the environmentally stable isotopes (D and  $^{18}\text{O}$ ) and  $^{14}\text{C}$ -dating analysis of groundwater samples from the fractured rock aquifers, for a quality assessment. The sampling of groundwater for trace elements (acidified with  $\text{HNO}_3$ ) and macro element (unacidified), as well as for D and  $^{18}\text{O}$  isotopes (unacidified) at different depths. Samples will also be taken at twelve selected boreholes for  $^{14}\text{C}$  determination.
- Assessment and evaluation of data from groundwater samples by means of graphic and other programs, in order to derive a model of the groundwater bodies in the area.

#### **1.4. Organisation of the study**

1. Theoretical considerations – *Chapter 2.*
2. Description of study area – *Chapter 3.*
3. Hydrogeochemistry – *Chapter 4.*
4. Methodology and Conceptual model – *Chapter 5.*
5. Conclusions and Recommendations – *Chapter 6.*

## CHAPTER 2

### Theoretical Considerations

#### 2.1. Introduction

The literature study, comprising of both local and international literature, contributed to the compilation of a conceptual model for the study area, outlined in Chapter 4. Relevant literature (areas experiencing similar conditions i.e. arid to semi-arid climate and similar geological conditions) is also incorporated as an aid to interpretation.

#### 2.2. Previous Work

A report on the chemistry of Beaufort-West groundwater was supplied by the Geological Survey, dating October 1976. This report deals with chemical variations of borehole water with depth and a discussion of available analyses from groundwater of boreholes and wind-pumps, around Beaufort-West.

This project was run in conjunction with another Water Research Commission Project (K5/653): The regional characterisation and mapping of Karoo fractured aquifer systems - An integrated approach using a geographical information system and digital image processing. A total of thirty-nine boreholes were drilled in the area of Loxton, into different geological structures and pumptests were performed.

A brief survey using a variety of isotopic and other environmental tracers of ground water at Beaufort West was conducted by the CSIR (*Vogel et al., 1980(b)*) as an adjunct to major development of groundwater resources in the area. The town itself is situated on a fairly featureless plain. The area is underlain by a variable sequence of Beaufort Group siltstone, mudstone and intercalated sandstone.

Radiocarbon and tritium values plot along the general trend expected from the exponential model, indicating that the more mobile groundwater in the area is effectively phreatic. Boreholes at higher elevation all show high  $^{14}\text{C}$  and  $^3\text{H}$  values, indicating rapid groundwater fluxing. Much slower moving (older) groundwater and higher mineralization was found in the plain, more rapid turnover and fresher water (local recharge) was found at various locations.

Recently, a groundwater study involving some isotopic measurements (SRK, 1997) was conducted in the same general area of Beaufort West. Most  $\delta^2\text{H}$  and  $\delta^{18}\text{O}$  values lie on the GMWL and cover a much wider range than those observed by Vogel et al. (1980(b)). The tritium and radiocarbon values show active recharge. Very little correlation was seen between groundwater mineralization and radioactive and stable isotope content.

## **2.3. Literature Review**

### **2.3.1. Fractured rock aquifers**

A statistical study has shown that 90% of aquifers in South Africa are fractured aquifers (Kirchner and Van Tonder, 1995). It is also well known that the quality of groundwater varies considerably over short distances in many of South Africa's fractured aquifers (Parsons and Tredoux, 1993).

The term fracture was defined (Kirchner and Van Tonder, 1995) as cracks, fissures, joints and faults, which are caused mainly by:

1. Tectonic movement, secondary stresses, release of crustal pressure, shrinkage, weathering, chemical action and thermal action.
2. Petrological factors like the composition of minerals, internal pressure and grain size.

A fractured rock mass can be considered a multi-porous medium, consisting of two main components, namely matrix rock blocks and fractures. Fractures are conductive conduits for flow, whilst the matrix blocks may be permeable or impermeable and most of the storage is contained within the permeable matrices (Kirchner and Van Tonder, 1995). Density of fractures may be a factor in storing significant amounts of water, which depends on the lithology and structural components of the geological setting. Thinner sedimentary rock units can be more susceptible to fracturing, than thicker sedimentary rock units (Domenico and Schwartz, 1990). Sandstone fractures in response to stresses, while mudstone behaves in a more ductile fashion, due to the clay content (Hughes and Sami, 1991). Fractures may close at depth, in response to the weight of the overburden and fracture dewatering. Wright stated in 1994, that openings typically develop in the upper part of the earth's crust, but are generally restricted to the upper 100 m.

Theoretically, lineament studies should be most applicable in hard rock terrains, where the primary permeability is negligible and where groundwater occurs mainly in zones of fracture-induced secondary permeability. It is expected therefore that boreholes located on or at the intersection of such zones, should have relatively higher yields than those away from these features (*Woodford et al., in press*).

The hydrogeological significance of a particular lineament will depend on the degree of deformation and stress in the host rock. Under normal deformation conditions in the upper crust, rocks fracture in a brittle manner by a pure shear mechanism, during which failure occurs along one or two sets of conjugate shears, which are essentially compressional features. Tension joints may form as an early response to stress, but do not normally continue to propagate, once shearing commences (*Woodford et al., in press*).

Structures may undergo reactivation during later stress deformation so that their geometry may not always provide information relating to the current stress environment. Abundant steep joints and surface-parallel sheeting are often of recent origin and indicate that the near surface-zone, 50-100m below ground level, is under decompression and tension caused by erosional unloading and / or tectonic uplift. Under these conditions many pre-existing fractures regardless of their origin, could be under tension and open to movement of groundwater.

Karoo aquifers are associated with dolerite intrusions. Experience has proven that high yielding boreholes can be sited on these structures, due to the fracturing caused in the adjacent country rock, with intrusion (*Enslin, 1950*). Joints are common along these intrusive contacts, which are particularly valuable on the up-slope side of the hydraulic gradient in Karoo sediment (*Robins, 1980*). The Karoo sediments have a poor primary permeability, but intrusive contacts form high permeability conduits, capable of drawing water from a wide area of sediments, supporting yields of up to 6 l/s, found by Robins in Swaziland in 1980. Fracturing and other deformational features such as fold axes and faults can be associated with increased yields. Weaver et al. (1993) found, in the Strydenberg region, that not all dolerite contacts yield water.

Most of the groundwater in the Karoo Basin is abstracted from shallow fractured-rock aquifers via shallow (< 60m deep) boreholes. These boreholes are normally open holes that are only equipped with a short length of solid steel casing, which extends from the surface to the base of the unconsolidated overburden. This simple borehole construction often results in borehole collapse and loss of pump equipment, especially in high-yielding holes, where blocks of highly fractured rock are dislodged from the wall of the borehole (*Woodford et al., in press*).

### 2.3.2. Intergranular semi- to unconsolidated aquifers

Composite alluvial / jointed-bedrock aquifers are an important exploitable groundwater resource in the central and western Karoo Basin, although not extensive in area. They form shallow aquifers that do not require drilling deeper than 30m. Production boreholes in these aquifers are designed to ensure that the formation remains stable and that abstraction takes place at a maximum efficiency without influx of fine aquifer material into the hole. Production boreholes in highly weathered / decomposed hardrock, especially coarse-grained dolerite bodies, and the so-called “calcrete” aquifers often require a similar design (*Woodford et al., in press*).

Productive alluvial-bedrock aquifers, such as the Caroluspoort aquifer near De Aar (**Figure 2.3.2**), exhibit the following characteristics (*Woodford et al., in press*):

- The thickness of the alluvium varies between 8 and 30m, with 10 to 15m being more common.
- The upper section of the alluvium is commonly fine grained (silts and clays) and acts as a confined or leaky semi-confined layer.
- The basal section is generally coarse grained, consisting mainly of fine-grained sand to coarse gravel. This zone is typically 1 to 5m thick and is the most transmissive portion of the aquifer.
- The bedrock is weathered and / or jointed and also acts as a conductive layer, to a lesser extent. The depth and degree of weathering of the rock decreases from eastern to the western Karoo, i.e. at Calvinia in the western Karoo this zone is approximately a metre in thickness, while in Graaff-Reinet it varies between 2-5m.
- The waterlevel is normally very shallow (i.e. less than 5m below ground level).
- The groundwater quality is typically more saline than that of the adjoining fractured-rock aquifers.

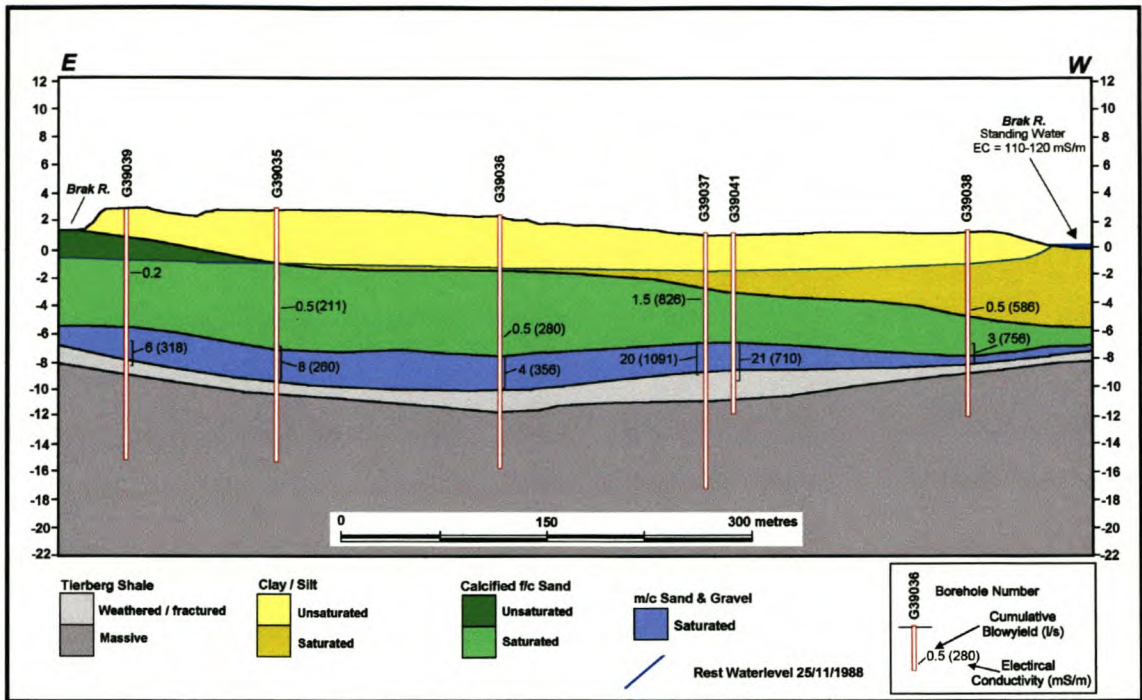


**Figure 2.3.2: Geohydrological Section across the Caroluspoort alluvial-bedrock aquifer, De Aar (Woodford et al., in press).**

### 2.3.3. Recharge

Groundwater quality or salinity depends on the amount of rainfall and infiltration that contributes to recharge. Areas receiving less than 2250 mm / annum, tend to exhibit the poorest water quality, thus the higher the rainfall the better the groundwater quality, but superimposed on this are local specific factors, influencing the groundwater quality (AEC, 1990). Water in the Karoo Supergroup is generally of poor quality, as stated by De Beer and Blume (1985).

Water bearing formations in South-Africa are recharged by rainfall infiltration, amounting to 3% of the mean annual rainfall in the west (250 mm average annual rainfall), to 23% in the east (1200 mm average annual rainfall) (Simonis and Kok, 1989). Secondary Karoo aquifers have limited storage ( $S = 0.004$ ) and recharge rates of 2-5% of the annual precipitation (Bredenkamp et al., 1995; Van Tonder and Kirchner, 1990). The amount of recharge is dependant on the differential head and hydraulic properties of the aquifer. Natural recharge sources include the following (US Dept. of the Interior, 1981):

1. Deep percolation of precipitation, as a major source of groundwater recharge.
2. Seepage from surface water bodies. In arid regions where the entire flow of a stream may be lost to aquifer recharge, seepage may be of major significance.
3. Recharge from a nearby, hydraulically connected aquifer, by means of underflow.

The amount of recharge is influenced by vegetative cover, topography, the type and nature of soils and the intensity and frequency of precipitation (*US Dept. of the Interior, 1981*). Groundwater levels tend to rise after rainy periods with heavy storms, due to the joints penetrated by the boreholes being in hydraulic continuity with the joints that are open to recharge (*Robins, 1980*). In Karoo aquifers the favored recharge mechanism is flow along preferred pathways (*Van Tonder and Kirchner, 1990*). Groundwater moves from areas of higher potential energy levels to areas with lower potential energy in general, which is essentially the result of elevation and pressure (*Davis and De Wiest, 1966*). Generally shallow water levels occur in areas of outcrop and recharge, while deep water levels coincide with basement depressions, having thickened beds and lack of recharge (*Levin, 1981*).

Recharge in Karoo aquifers is highly variable due to varying thickness of the soil overburden, rock outcrops, collection of surface water in depressions and surface runoff. In addition spatial and temporal variations of rainfall are normally high. The most reliable methods of estimating recharge are therefore based on groundwater-balance methods and / or mass-balance methods (i.e. chloride method).

#### 2.3.4. Natural Hydrochemistry

The chemical composition of groundwater, unaffected by human activities is determined by a series of complex physical, chemical and biological processes occurring as precipitated water moves through the saturated - and unsaturated zone of soil, as stated by Katz and Choquette (1991). The hydrochemistry of groundwater reflects the source of water, lithology of the aquifer and local chemical conditions, such as, temperature, pressure and redox potential (*Henderson, 1986*). Groundwater hydrochemistry is useful for determining groundwater potability (*Ophori and Toth, 1988*). The environment of groundwater occurrence, the geological, biospherical and human influence are reflected in the chemical constituents of groundwater (*Malomo et al., 1990*).

An intimate knowledge of the chemical evolution of the water in an aquifer is required, according to Tredoux and Kirchner (1981), in order to classify the water sources and to identify the groundwater mixture.

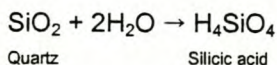
The inorganic constituents contained naturally in water are the major cations, calcium, magnesium, sodium and potassium, while the major anions are, chloride, sulphate, carbonate and bicarbonate. Silica can also be a non-ionic, but major constituent. Minor constituents may be present, such as, iron, manganese, fluoride, nitrate, strontium and boron (*Fetter, 1988*).

#### 2.3.4.1. Weathering and Dissolution

Weathering of rock is both a chemical and mechanical process (*Henderson, 1986*). Weathering entails the interaction of an aqueous solution with rock material, to produce a solution of different composition from the reactant one. A residue of insoluble solids of the initial rock and other solids that form secondary mineral phases, is the result (*Henderson, 1986*). Water incorporates major and trace elements on encountering soil and rock, decomposing and dissolving rock materials. This is mostly due to the reaction of the H<sup>+</sup>-ion with carbonate and alumino-silicate minerals, to liberate cations and silica into solution and leave clay minerals behind (*Rose et al., 1979*). Incoming acidity can thus be neutralised by chemical weathering. Two types of reactions are generally exhibited by weathering of minerals (*Henderson, 1986*):

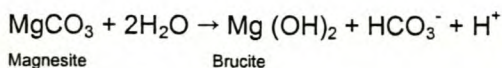
1. Congruently, whereby all minerals dissolve completely.

*Example:*



2. Incongruently, whereby some minerals dissolve and others recombine, to form a new solid phase.

*Example:*



The pH of water is largely controlled by the amount of carbonates, bicarbonates and dissolved carbon dioxide (CO<sub>2</sub>) in the water (*El Ghandour et al., 1985*). It is also governed by the type of contamination bases, degree of ionisation, extent of hydrolysis and buffering action. Katz and Choquette (1991) stated, that strong acids from precipitation, together with carbonic acid from biological processes in the soil, attack minerals and release dissolved components to the water if it is a strong acid, the accompanying anions (SO<sub>4</sub><sup>2-</sup>, NO<sub>3</sub><sup>-</sup> or Cl<sup>-</sup>), will balance the base cations released. If carbonic acid is the principal weathering agent, the bicarbonate anion will balance the cations released (*Katz and Choquette, 1991*).

Carbonate ions are mainly derived from calcium carbonate rocks, which generally have a low solubility, but in the presence of dissolved CO<sub>2</sub>, become highly soluble, forming bicarbonate (*El Ghandour et al., 1985*), thus the content of bicarbonate in solution is dependant on the amount of CO<sub>2</sub> in the water. Carbon dioxide is present in soil gas and will react with infiltrating water in the unsaturated zone, due to methanogenesis and other bacterially mediated processes in groundwater (*Katz and Choquette, 1991*). An initial source of CO<sub>2</sub> is rain, which leads to the dissolution of CaCO<sub>3</sub> to its equivalent calcium and bicarbonate ions, additional CO<sub>2</sub> is released by the biological activity in the soil and chemical processes, increasing the bicarbonate contamination of groundwater (*El Ghandour et al., 1985*).

Chemical characteristics of groundwater differ with depth. The different groundwater compositions are produced by factors such as the effect of temperature and pressure on the mineral solubilities, ion complexing and aging of deep groundwater (*Freeze and Cherry, 1979*).

Katz and Choquette (1991) stated that, groundwater chemistry is dominated by faster reacting minerals [muscovite, andesine (feldspar), calcite and chlorite], while the influence of slow reacting minerals, such as quartz, is negligible. Carbon dioxide charged water reacts with feldspars and forms water with predominantly dissolved sodium, calcium or potassium bicarbonate, depending on the type of feldspars (*Mazor et al., 1980*). Paleozoic and Mesozoic sedimentary rocks contribute major ions such as carbonates, chlorides, calcium, magnesium and sulphates, to the water in the area (*DWA&F, 1993*).

The effect of variable cooling of dykes following intrusion is apparent in the way in which dykes weather in the Western Karoo, namely (*Woodford et al., in press*):

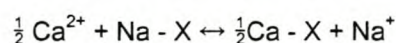
1. Thick dykes (>8m) generally exhibit a prominent chill-margin containing a fine grained, porphyritic, melanocratic dolerite that weathers to produce well-rounded, small, white-speckled boulders (i.e. spheroidal weathering). This zone is normally only 0.5 to 1.5m wide and exhibits well-developed thermal-shrinkage joints. The central portions of such dykes consist of medium- to coarse-grained, mesocratic and occasionally leucocratic dolerite that decomposes to a uniform "gravelly" material, which exhibits an exfoliation type of pattern. Sporadic fractures or meta-sedimentary veins are encountered in this zone, often not extending into the country rock. Magnetic traverses across these features normally produce two distinctive peaks.
2. Thin dykes (<3m) commonly consist of fine-grained, porphyritic, melanocratic dolerite (*Vandoolaeghe, 1979*). These tend to be more resistant to weathering than the thicker dykes and in outcrop exhibit a uniform pattern of shrinkage-joints. The dyke weathers to produce small rounded, white-speckled boulders set in a finer angular groundmass.

#### 2.3.4.2. Cation Exchange

The property of exchanging cations within a structure and with cations in the surrounding water, is exhibited by numerous minerals (*Talma, 1981*). Ionic exchange is dependant on the charge, ionic radius and valency of the participating ions (*Cogho et al., 1992*). Further ionic exchange occurs later in the sedimentary cycle, where the clay minerals adjust geochemically to the depositional environment, by exchanging some of the "detrital" elements with those present in the surrounding aqueous environment (*Zawada et al., 1988*). The most common exchange combination is the replacement of Na in a Cl dominated water, by an equivalent amount of Ca, derived from the aquifer rock, exemplified by Appelo and Postma, (1994):



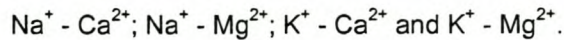
The process of reverse ion exchange or refreshing (*Appelo and Postma, 1994*), may be represented by:



where:

X = soil exchangers

Refreshing occurs when Na replaces Ca in solution, by the action of reverse cation exchange. The most important cation exchange reactions in groundwater systems are between the following divalent and monovalent cations (*Freeze and Cherry, 1979*):



Ion replacement follows the following sequence:



and it becomes increasingly more difficult to remove the ions from a clay mineral, as the affinity for adsorption is greater (*Cogho et al., 1992*).

#### 2.3.4.3. Precipitation and Saturation states

Minerals precipitate due to the dissolution of other minerals, because of weathering and the subsequent exchange between cations. Once the equilibrium-state of mineral phases has been surpassed, precipitation of the minerals can commence. Precipitation (i.e. rain and snow) and groundwater, as the two end-members of a sequence, can be compared by using mass-balance calculations, to evaluate the relative importance of weathering (mineral dissolution) and precipitation reactions in controlling the chemical composition of groundwater (*Katz and Choquette, 1991*).

The saturation indices (SI) are indicative of the saturation-state of a specific water, with respect to specific mineral phases. Saturation indices were calculated with the NETPATH computer program, through a WATEQF subroutine as by *Plummer et al., 1992*.

The SI is expressed as (*Appelo and Postma, 1994*):

$$\text{Degree of saturation} = \log \text{IAP} / \text{KT}$$

where:

IAP = Ion activity product  
 KT = Solubility product

if:

SI = -0.1 to 0.1 (Saturated)  
 SI = -1.0 to -0.1 (Unsaturated)  
 SI = 0.1 to 1.0 (Oversaturated)

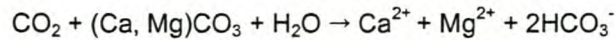
Equilibrium states are not common in groundwater (i.e. SI = 0) and the saturation states of the groundwater merely indicate the direction in which a process may proceed, if at all (*Appelo and Postma, 1994*). Minerals (if present) will precipitate out of solution in case of oversaturation, and dissolution of minerals will occur if the solution is undersaturated. The uncertainty in the pH measurement in this study, is the reason for not taking SI = 0 as equilibrium. An error of  $\pm 0.05$  pH units leads to an uncertainty of  $\pm 0.05$  units in SI of minerals and of uncertainties in  $\text{Ca}^+$ ,  $\text{Mg}^{2+}$  and  $\text{HCO}_3^-$  analysis. The total uncertainties are in the order of  $\pm 0.1$  units of SI (*Langmuir, 1971*).

#### 2.3.4.4. Elemental Sources

The processes mentioned above may be the reason for the origin of various dissolved constituents in water (or the lack thereof) (*Adams, 1998*).

**Carbonate and bicarbonate ions** in groundwater are mostly derived from  $\text{CO}_2$  in the atmosphere,  $\text{CO}_2$  in soil and in the solution of carbonate rock (*Davis and De Wiest, 1966*). Atmospheric  $\text{CO}_2$  content (0.03 %), is increased up to a hundred-fold in the soil, due to root respiration and the decay of organic matter.

CO<sub>2</sub> in a water solution, dissolves carbonate minerals by this reaction (*Talma, 1981*):



The weathering of silica rock is another reaction forming bicarbonate in groundwater, as well as the oxidation of sedimentary organic material (*Talma, 1981*). Sodium bicarbonate and carbonate are highly soluble and remain in the water, while calcium bicarbonate is removed by ion exchange and replaced by sodium. Sodium bicarbonate water is suggested to be formed in this way (*Mazor et al., 1980*).

If CaCO<sub>3</sub> is precipitating, it would deplete both the Ca<sup>2+</sup> and HCO<sub>3</sub><sup>-</sup> content, thereby reducing the pH (*Adams, 1998*).

Most of the **calcium** in subsurface water, which is in contact with sedimentary rocks of marine origin, is derived from calcite, aragonite, dolomite, anhydrite, fluorite and gypsum (*Davis and De Wiest, 1966; Hem, 1989*). Weathering also releases calcium from minerals such as apatite, wollastonite, fluorite and various members of the feldspar, amphibolite and pyroxene groups in igneous and metamorphic rocks (*Davis and De Wiest, 1966*). Calcium carbonates are easily soluble in water provided there is an abundant supply of H<sup>+</sup> (*Davis and De Wiest, 1966*). The dissociation of carbonic acid is one of the most important sources of hydrogen ions (*Davis and De Wiest, 1966*).

**Magnesium** is most commonly found in the hydrosphere in the dolomite of sedimentary rocks, olivine, biotite, hornblende, magnesite and augite in igneous rocks and serpentine, talc, diopside and tremolite in metamorphic rocks (*Davis and De Wiest, 1966*). Some magnesium is also contained in calcite. Abundant magnesium and calcium can be yielded from a limestone solution (*Davis and De Wiest, 1966*). A major source of magnesium in water is the pyroxene and olivine reactions with CO<sub>2</sub>-containing water (*Mazor et al., 1980*).

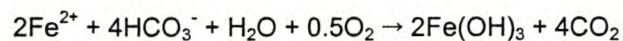
**Sodium** is released in natural water primarily from the soluble products that form during the weathering of plagioclase feldspars (*Davis and De Wiest, 1966*). Sodium concentrations range from 0.2 ppm in rain and snow to over 100 000 ppm in brines in contact with salt beds (*Davis and De Wiest, 1966*). A halite solution is important, in areas of evaporite deposits. Large quantities of exchangeable sodium may be released by clay minerals in certain conditions. Measurable amounts of sodium are contained in all natural water, where less important sodium sources are

the minerals nepheline, sodalite, stilbite, natrolite, jadeite, arfvedsonite, glaucophane and aegerite (Davis and De Wiest, 1966). These minerals are abundant in some igneous and metamorphic rocks, but are quantitatively of minor importance in comparison with the feldspars (Davis and De Wiest, 1966). A sodium residual is left behind from irrigation runoff, which is much higher in concentration than the original irrigation water (Hem, 1989).

**Potassium** sources are the weathering products of orthoclase, microcline, biotite, leucite and nepheline, in igneous and metamorphic rocks (Davis and De Wiest, 1966).

**Iron** is released naturally in the aquatic environment, by the weathering and leaching of sulphide ores (Pyrite, FeS<sub>2</sub>) in igneous, sedimentary and metamorphic rocks. Iron is only released under reducing conditions (DWA&F, 1993). Hem (1989) stated that the most common iron specie found in groundwater is ferrous iron (Fe<sup>2+</sup>). Important minerals and mineral groups that may contain large amounts of iron are pyroxene, amphiboles, magnetite, pyrite, biotite, olivine and garnets (DWA&F, 1993; Hem, 1989). Weathering of these minerals releases iron, which is usually converted to the relatively stable ferric iron oxide (Davis and De Wiest, 1966).

When ferrous iron containing groundwater is exposed to the atmosphere, this reaction occur (Davis and De Wiest, 1966):



The removal of OH<sup>-</sup> ions in this reaction tends to lower the pH, but the ferric hydroxide solubility is so low in normal pH, that the iron will be precipitated (Davis and De Wiest, 1966).

**Sulphates** are mostly derived from the oxidation of marcasite and pyrite in sedimentary rocks, in particular organic shales. Sulphate-reducing bacteria in subsurface water obtain energy from oxidation of organic compounds, deriving oxygen from the sulphate ions (Davis and De Wiest, 1966). Hydrogen sulphide gas is a by-product in the reduction of sulphate ions. Iron sulphide may precipitate if iron is present in the water, under moderately reducing conditions, removing iron as well as sulphide from the water. Most of the hydrogen may escape directly to the atmosphere if soil bacteria facilitate the sulphate reduction (Adams, 1998).

Sulphate ion (SO<sub>4</sub><sup>2-</sup>) is not generally adsorbed or precipitated, once it has entered into the natural water. As sulphate is not governed by the same control-mechanisms as the other elements, it behaves quite independently (Woodford et al., in press).

**Fluoride** concentrations in surface and groundwater are high in the Karoo, posing domestic water use problems (DWA&F, 1993). It is thought that fluoride is the main ion responsible for the solubilising of beryllium, scandium, niobium, tantalum and tin in natural water (DWA&F, 1993). The natural fluoride concentration appears to be limited by the solubility of fluorite ( $\text{CaF}_2$ ), which is about 9 ppm F in natural water (Davis and De Wiest, 1966).

Elevated fluoride concentrations in groundwater are often reported by geohydrologists working at various localities in the Karoo Basin. Three possible sources of fluoride in Karoo aquifers are (Woodford *et al.*, *in press*):

1. Leaching and concentration of fluorine from rocks and soils during weathering and alteration processes.
2. Dissolution of secondary hydrothermal–pneumatolytic fluoride-rich minerals.
3. Circulation and regional-flow of a deeper-seated (thermal) groundwater.

Fluorine is the most abundant halogen in sedimentary rocks and has to be considered as a major source of fluoride in groundwater. This does not however account for the marked fluoride variability on a local scale in “shallow” aquifers (upper 150m below ground level), where the host-rocks are similar. This suggests that fluoride concentrations are not only controlled by the near-surface lithology (Woodford *et al.*, *in press*).

During recent drilling in the Loxton area, where elevated fluoride values are known to occur, typical hydrothermal F-bearing fracture mineralization was commonly encountered in the form of apophyllite in association with calcite (Woodford and Chevallier, 1998). Fluorine-bearing hydrothermal-pneumatolytic mineralization was commonly reported in breccia plugs in the Western Karoo (Woodford and Chevallier, *in press*) which are known for their anomalously high fluoride-bearing groundwater. Drill cores from the Calvinia breccia plugs showed fracture mineralization of quartz, calcite, fluorite, apophyllite, tourmaline, gypsum, chlorite, siderite, baryte, pyrite, pyrrhotite, chalcopyrite, galena, marcasite, bornite and covellite (Hallbauer *et al.*, 1995). Groundwater samples from these breccia plugs showed fluoride concentrations of up to 12 mg/l. It is postulated that fluorine-bearing minerals were precipitated in certain fracture systems in the Karoo Basin by hydrothermal-pneumatolytic fluids during and after the emplacement of the dolerite and kimberlite intrusives (Woodford *et al.*, *in press*).

The southern Karoo was demonstrated to contain deep-seated groundwater by two SOEKOR boreholes that struck thermal-artesian water. The water was highly saline and considered to be partly connate and of marine origin – having entered the rocks during an extensive marine transgression during early Dwyka times (Upper Carboniferous) (*Kent et al., 1965*).

Studies by Kent (1972) revealed that warmer, and thus deeper circulating groundwater contains more fluoride (up to 5 mg/l) than nearby “cold-water” springs and shallow aquifers (0.2 mg/l). Many thermal springs which rise along dolerite dykes and faults in the Beaufort and Ecca Group contain more than 1.5 mg/l of fluoride.

Investigation of the flooding of the Orange-Fish River tunnel near Venterstad indicated that thermal springs are located along the presumed extension of the fissure present at this site, including the well-known Badsfontein spring (*Woodford et al., in press*).

This evidence points to a relationship between age, origin, temperature and fluoride content of groundwater in certain areas of the Karoo Basin. It therefore seems likely that deep-seated thermal water may rapidly transport fluoride upwards from greater depths as a constituent of connate or paleo-meteoric water and / or dissolve fluorine-bearing minerals along its flow-path to the surface along discrete fracture zones due to an increase in solubility with temperature. This water will normally be mixed in the near-surface with the recent, shallow, meteoric water of local recharge (*Woodford et al., in press*).

A definite relationship exists between the **total dissolved solids** of water and the surface slope. The idea is that the steeper the slope, the higher the groundwater velocity, implying that such water is meteoric, with a low TDS (total dissolved solids) content (*Woodford et al., in press*).

The assumption made that the TDS is a function of the flow rate, implying that the flow rate is a measure of groundwater age, has never been proven. However TDS in groundwater is controlled by the chemical composition of the host rock, as well as by the age of the water, making these two parameters essential in hydrogeochemical data interpretation. The total dissolved solids concentration depends to a greater degree on the chemistry of the host rock, than on the flow rate of the underground water (*Woodford et al., in press*).

Calcrete may be responsible for high TDS values in this system of fresh and brackish water. A dolerite barrier may indicate more stagnant and mature water and may explain the higher TDS. TDS is not a function of borehole depth (*Woodford et al., in press*).

**Hardness**,  $\text{HCO}_3^-$  and pH are very closely associated, as they make up part of the carbonic system. It also appears as if  $\text{Na}^+$ ,  $\text{Cl}^-$ ,  $\text{Mg}^{2+}$  and TDS are associated, although to a lesser degree (Woodford *et al.*, *in press*).

**Uranium** concentrations remain constant with depth, but decrease laterally from a possible mineralized area (Woodford *et al.*, *in press*).

#### 2.3.4.5. Salinization of Groundwater

Groundwater recharge can contribute to the salinity of the water. Salinity may be derived from incompletely leached evaporite horizons in closed surface basins, such as pans and salt loads build up in the unsaturated zone during periods of low rainfall (Verhagen, 1985). As evaporation exceeds precipitation throughout the year, leaching is limited and soluble salts tend to accumulate near the surface (Sami, 1992).

Percolation and runoff periodically flush these salts into streams and the groundwater after heavy rain events. Sodium chloride (NaCl) is dissolved mainly from the Ecca shales (Mazor *et al.*, 1980). The two factors of importance in arid and semi-arid regions are precipitation of minerals and evapotranspiration of water (Adams, 1998).

Dissolved solids may concentrate to a significant degree by means of water evaporation and transpiration from plants (Rose *et al.*, 1979). In dry climates the salt content tend to be higher of sodium chloride (NaCl) and sodium sulphate ( $\text{Na}_2\text{SO}_4$ ) (Rethati, 1983). The water quality problems of arid regions are therefore quite significant, as the slow circulation of groundwater catalyses mineralization. Evaporation of groundwater from discharge areas results in salt deposition, contributing to high salinities in the soil and shallow groundwater (Fetter, 1988).

#### 2.3.4.6. Hydrochemical Evolution

The chemical composition of water in an aquifer can be influenced by the length of the groundwater flow paths and residence times (Katz and Choquette, 1991). The chemical quality of water in the recharge zone is the primary function in the progressive mineralization, along a valley-wide flow path (Kauffman, 1977).

Contributing factors in progressive mineralization along a flow path is the type, distribution and adsorptive capacity of the geological matrix, the porosity and permeability of rocks and sediments

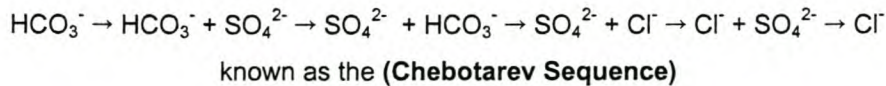
and the course followed by water (*Kauffman, 1977*). Freeze and Cherry (1979) postulated that, the order in which groundwater encounters strata of different mineralogical compositions can exert an important control on the water chemistry. It was also stated that as groundwater flows through strata of different mineralogical composition, it undergoes adjustments caused by imposition of new mineralogically controlled thermodynamic constraints. Water may attain local equilibrium in some strata, with respect to some mineral phases, but the continuous flow of the water causes disequilibrium, as the water moves into strata comprising of different minerals (*Freeze and Cherry, 1979*).

Many groundwaters in stratified sedimentary sequences feature  $\text{Na}^+$  and  $\text{HCO}_3^-$  as dominant ions (*Freeze and Cherry, 1979*). Significant changes in groundwater chemistry occur across the boundary between confined and unconfined regions of sandstone aquifers, indicated by the results of a field sampling program in Dodge and Fond du Lac counties, Wisconsin (USA). An increase in sulphate, chloride, sodium and potassium concentrations and a less pronounced increase in radium activity, is also included (*Weaver and Bahr, 1991*). The influence of the geology in the determination of water chemistry can be indicated by hydrological contour maps, where the contours cut across geological boundaries.

The contrast in chemical quality of water in the common groups of sedimentary rocks (i.e. sandstone, shale and carbonates), are usually quite definably marked. Shale contains higher amounts of iron and fluoride, with a low pH between 5.5 and 7.0 (*Davis and De Wiest, 1966*). Abundant minerals such as illite and quartz in shale, are relatively unreactive in the weathering environment and therefore contribute little to runoff chemistry. Water that drains shales sometimes contains chloride and sodium which are thought to have originated from seawater trapped in the shale during the time of deposition, but the form of ion storage is not known (*Drever, 1988*). Shale drained water is therefore highly variable in composition.

Sulphate and chloride are the major anions and the water exhibits a lower silica to total cation ratio, than water draining igneous rocks. Limestone will have greater amounts of calcium and magnesium, a lower silica ( $\text{SiO}_2$ ) content and pH values above 7.0 (*Drever, 1988*). As limestone weathers more rapidly than igneous rocks, the water draining the limestone will also be more concentrated in dissolved ions (*Drever, 1988*). The water quality of sandstone-drained water is more variable, as it depends on the adjacent rock types, the mineral composition of the sand and aquifer depth (*Davis and De Wiest, 1966*). Water with a very high salinity can form due to evaporite dissolution. Sulphate and / or chloride are the principle anions, with sodium and calcium being the principle cations, depending on the nature of the evaporite (*Drever, 1988*).

A series of regional sequential changes can occur in dominant ions along flow lines (*Freeze and Cherry, 1979*) as:



In large sedimentary basins the Chebotarev sequence can be correlated with depth, described in terms of three main zones (*Freeze and Cherry, 1979*):

1. Upper zone of mainly  $\text{HCO}_3^-$ -water, low in TDS.
2. Intermediate zone of higher TDS and  $\text{SO}_4^{2-}$  as the major anion.
3. A lower zone with high TDS and a high concentration of  $\text{Cl}^-$ .

Groundwater should evolve naturally from a bicarbonate facies in recharge areas, to a sulphate or chloride dominant facies in the discharge area (*Ophori and Toth, 1988*). As water moves toward the discharge area, the increase rate of  $\text{CO}_3^{2-} + \text{HCO}_3^-$  decreases in favor of  $\text{SO}_4^{2-}$ , which is acquired readily from bedrock strata (*Ophori and Toth, 1988*).

The chloride content of water normally increases gradually in relation with the residence time in the natural groundwater environment. Chloride is an excellent tracer and reference ion (*Tredoux and Kirchner, 1981*). Evapotranspiration is the primary cause of the increase in chloride concentration of groundwater in unconfined aquifers, due to the dissolution of sodium chloride. The chloride increase is dependant on the availability of chloride in the host rock and the groundwater circulation rate; permeability changes of the host rock will affect the flow rate and therefore the chloride concentration in the groundwater (*Adams, 1998*).

The lowest sodium percentage of groundwater is generally near the recharge area of the Auob Sandstone aquifer in Namibia (*Tredoux and Kirchner, 1981*). The sodium concentration increase accompanies the decrease in dissolved magnesium, calcium and potassium concentration, the latter being adsorbed on the interbedded and confining shales, in exchange for the desorbed sodium ions (*Tredoux and Kirchner, 1981*). The equilibrium of the calcium-magnesium-carbonic acid-calcite system is disturbed by the decrease of calcium and magnesium concentration in solution, resulting in the dissolution of additional calcite (*Tredoux and Kirchner, 1981*). The calcium ions are also exchanged for sodium in solution, with the overall effect of these reactions being an increase in sodium, alkalinity and pH, with a concurrent decrease of calcium and magnesium (*Tredoux and Kirchner, 1981*). This is also true for the study at Loxton.

Three distinct groundwater types, based on chemical and isotope data, were found by *Talma (1981)* in sandstone, siltstone and shales, intruded by dolerite dykes and covered by colluvium, in the Beaufort Group near Venterstad:

- I. Recent (<20 years) Ca, Mg, HCO<sub>3</sub>-water;
- II. Very pure (Old) Na HCO<sub>3</sub>-water and;
- III. Old NaCl-water, with little Ca<sup>2+</sup> and HCO<sub>3</sub><sup>-</sup>.

The main reason for two boreholes close together (between 1m - 10m) having a dissimilar hydrogeochemistry, is the fact that they may tap different aquifers (*Woodford et al., in press*).

A study of trace element content appears to be the most meaningful in the determination of groundwater homogeneity. A slight chemical variation with depth is probably related to change in the rock-type and hydrodynamical pattern of water flow. However vertical stratification plays an insignificant role and is overridden by lateral chemical changes as a function of distance away from a mineralized zone. Groundwater velocity, which affects the mineralization, is dependant on rock-permeability, pressure, density, geological structures and the water supply in the catchment area (*Woodford et al., in press*).

### 2.3.5. Environmental isotope hydrology

The most important recharge mechanism to groundwater is by diffuse infiltration of rainwater through the vadose sone (unsaturated sone). Piston-like or plug intergranular-flow of moisture is usually assumed, modified by various processes of dispersion. To study this flow requires ideally a thick (tens of meters) and reasonably uniform sand / soil cover, from which samples can be taken at various depths. The column of moisture at any one moment contains components of various rainfall events with variable isotopic characteristics (oxygen-18 and deuterium) over a period of time, which may be employed to assess the transport of water towards the water table. Evaporative moisture losses from just below the ground surface may be reflected in the enrichment of the stable isotopes near the top of the profile (*Woodford et al., in press*).

The depth of penetration of the thermonuclear bomb peak of tritium gives a measure of the amount of water retained in the zone since the mid-sixties. Another approach is comparing the total amount of tritium in the profile containing the peak with the total amount of tritium in the rainfall over the same period. Although in principle much simpler than the tritium method, the

chloride method suffers from the difficulty of estimating adequately the input concentration (Beekman *et al.*, 1996), a factor much better known and widely monitored for tritium.

Although tritium concentrations in present-day rainfall have returned to near-natural values and the bomb tritium peak has been flushed out of all but very thick (tens of metres) vadose zones, bomb tritium can still be identified in certain instances. Thus Beekman *et al.* (1996) concluded from a recent study of Kalahari sand profiles that by-pass flow through root-holes, and animal and insect burrows, probably constitutes the bulk of the downward transport of moisture, rather than intergranular flow. As soils are generally poorly developed in the Karoo, it is therefore clear that the use of isotopic tracers in vadose zone investigations holds out little potential in assessing recharge in this environment (Woodford *et al.*, *in press*).

Environmental isotopes have found a firm place amongst the large variety of techniques with which ground water can be studied and resources can be assessed (e.g. IAEA (1983), Fontes (1980), Mazor (1991), Verhagen *et al.* (1991)). Initially confined largely to academic studies, isotope techniques are now firmly established as practical, even indispensable, tools in ground water investigations.

Environmental isotope tracers constantly "label" groundwater, principally during recharge from the surface. At any one time, a groundwater body reflects its isotopic history, or the cumulative input of the isotopic tracers. The basic approach in their application is that of the "isotope snapshot", i.e. the analysis of isotope, chemical and other environmental tracers of groundwater samples from a particular area reflecting the origins and mobility of the different groundwater occurrences. These need to be interpreted in terms of other meaningful information, using various concepts and models (Woodford *et al.*, *in press*).

Isotope techniques can be employed at various phases of a groundwater investigation. If little else is known on the local geohydrology, the isotope results are efficient in suggesting a conceptual model. In cases where an *a priori* conceptual model exists, isotope data can set boundary conditions to these concepts. When the isotope data has been interpreted quantitatively in terms of known aquifer parameters, it can be used to calibrate, or at least set limits to conclusions from, numerical groundwater management models (Woodford *et al.*, *in press*).

The radioactive isotope  $^3\text{H}$  and the non-radioactive or stable isotopes  $^{18}\text{O}$  and  $^2\text{H}$  label the water molecule itself. The radioactive isotope  $^{14}\text{C}$  and stable isotope  $^{13}\text{C}$  label the total dissolved inorganic carbon (TDIC). Other isotopes label other dissolved compounds such as the stable species  $^{15}\text{N}$  in dissolved nitrate (Woodford *et al.*, *in press*).

### 2.3.5.1. Radioactivity

Radioactivity is the process through which unstable atoms (nuclides) spontaneously emit one or more particles or quanta to reach stability. This process is random, with the emission rate being proportional to the number of radioactive atoms (*Woodford et al., in press*):

$$dN/dt = -\lambda N$$

where

$N$  = the number of radioactive atoms,

$t$  = the time, and

$\lambda$  = the decay constant or probability.

Integrated over a time period  $t$ , this equation becomes:

$$N = N_0 e^{-\lambda t}$$

where

$N_0$  = the number of radioactive atoms at time  $t = 0$

when

$N/N_0 = 1/2$ , the time elapsed is called the half-life  $t_{1/2}$

The half life and decay constant are related by:

$$t_{1/2} = 0.693 / \lambda \quad \text{equ. A}$$

Equation A governs the concept of radioactive dating. When the initial and final concentration of radioactive atoms is known, the time  $t$  since the initial condition can be determined. Groundwater cannot strictly be "dated", as a fluid undergoes processes such as mixing, hydrodynamic dispersion and diffusion (*Woodford et al., in press*).

### 2.3.5.2. Fractionation

Molecules of a compound have different masses as do the isotopes of the elements making up molecules, which differ in mass. These mass differences influence factors such as vapour pressure, diffusivity etc. During phase processes, such as evaporation, condensation and exchange reactions the abundance of the isotopes of individual elements change, or undergo fractionation. Such processes are usually operative at the interface of different phases or compounds containing the same elements, such as vapour in contact with a liquid, a liquid in contact with a solid etc. These changes in abundance can be traced through natural and other systems (*Woodford et al., in press*).

The unit fractionation factor ( $\alpha$ ) is defined as:

$$\alpha = R_A/R_B$$

where  $R_A$  and  $R_B$  are the ratios of the abundance of the rare (heavier) isotope to the more abundant (light) isotope in phases A and B respectively, and  $\alpha$  is temperature dependent.

As isotopic abundances and changes in these abundances are generally small, it is customary to express these changes as fractional differences in  $\delta$  per mille with respect to the value of a reference standard

$$\delta = [(R_S/R_R) - 1] \times 1000 (\text{‰}) \quad \text{equ. B}$$

where the measured ratios for the heavy to the light isotope are  $R_S$  for the sample and  $R_R$  for the reference standard, respectively.

### 2.3.6. Radioactive isotopes

#### 2.3.6.1. Tritium ( $^3\text{H}$ )

This hydrogen isotope is formed in the upper atmosphere through cosmic ray reactions. Oxidised to  $^3_1\text{H}^1\text{HO}$  it reaches the surface of the earth as part of rainwater, in which it is essentially a

conservative tracer. The isotopic ratio  $^3\text{H} / ^1\text{H}$  established by this natural source in continental environments is approximately  $5 \times 10^{-18}$ , or 5 TU (tritium units). The half-life of tritium is 12.43 years. When rainwater is isolated from the atmospheric source, i.e. during groundwater recharge, no new tritium is added and the tritium concentration will decrease with this characteristic half-life (*Woodford et al., in press*).

The useful range of measurement of environmental tritium in geohydrological applications spans four to five half-lives. It is therefore measurable only in and acting as an indicator of recently recharged ground water. From the mid 1950's the atmospheric input increased due to nuclear weapons fallout. Since the middle sixties, rainwater tritium levels have declined from the "bomb peak" to reach about pre-bomb levels in non-industrialised areas at present (*Woodford et al., in press*).

Tritium levels in ground water with a mean residence time (MRT) in excess of about 200 years, lie at or below the limit of detectability (routinely  $0.2 \pm 0.2$  TU). At present, a TU value of greater than 1 unequivocally indicates that groundwater body received significant recharge during the thermonuclear era (the past 45 years) (*Woodford et al., in press*).

#### **Sampling:**

A 1-litre sample of water is required for determination of low-level tritium. The sample bottle is rinsed with the sample-water, completely filled and tightly stoppered. The water should not be treated in any way before sampling. Samples can be taken by field technical personnel, under guidance from the participating laboratory (*Woodford et al., in press*).

#### 2.3.6.2. Radiocarbon ( $^{14}\text{C}$ )

Formed in the upper atmosphere by processes similar to tritium, radiocarbon is oxidized to  $^{14}\text{CO}_2$  and becomes part of atmospheric carbon dioxide, in which the natural isotopic ratio  $^{14}\text{C} / ^{12}\text{C} \sim 10^{-12}$ , is called 100 pMC (100 per cent modern carbon). The  $^{14}\text{C}$  half-life is 5730 years. As with tritium, thermonuclear tests increased the atmospheric level of radiocarbon to peak in the early 1960's. Plants assimilate atmospheric carbon dioxide through photosynthesis. Humus and roots liberate  $\text{CO}_2$  labeled with environmental  $^{14}\text{C}$ , which dissolves in infiltrating groundwater, rendering the water chemically aggressive, which leads to the various species of  $^{14}\text{C}$ -labeled total dissolved inorganic carbon (TDIC) (*Woodford et al., in press*).

Thus, radiocarbon:

- (a) Becomes a time dependent radioactive tracer of ground water, and
- (b) Allows for the estimation of ground water residence times.

In contrast to tritium, radiocarbon is not strictly a conservative tracer of water, as numerous chemical processes can alter the  $^{14}\text{C} / ^{12}\text{C}$  ratio. Attempts have been made by several authors (*Verhagen et al 1991*) to develop correction models, based on hydrochemistry and  $\delta^{13}\text{C}$  values. These models all assume that the hydrochemical processes occur principally during the initial development phases of, and therefore affect the initial isotopic ratio established in the TDIC of ground water (e.g. during recharge). Once the hydrochemistry has been stabilised, the  $^{14}\text{C} / ^{12}\text{C}$  ratio is taken to effectively alter only through radioactive decay. Vogel (1970) suggested a rule-of-thumb initial (recharge) value of about 85% of atmospheric  $\text{CO}_2$  for many aquifers. In principle however, this initial value may be as low as 50% in carbonate aquifers, approaching 100% in purely crystalline terrain and has to be assessed for each individual terrain. Subsequent water / rock interactions in the saturated zone of established aquifers are usually regarded as negligible.

In spite of its potentially complex hydrochemistry, radiocarbon is the principal radioactive environmental tracer of deeper-seated groundwater, its useful range of measurement in geohydrological applications spanning five to six half-lives (*Woodford et al., in press*).

During the early sixties, atmospheric  $^{14}\text{C}$  concentrations rose due to thermonuclear fallout, and have since declined. In qualitative terms therefore, ground water radiocarbon values of > 100 pMC can be interpreted as falling in the thermonuclear era, i.e. substantially recharged over the past four and a half decades. Within this time-span, interpretations can be further constrained by tritium data (*Woodford et al., in press*).

### **Sampling:**

About 1-2 g of carbon is needed for measurement. The most common field procedure is to collect and treat about 50 litres of water, at a TDIC of 200 mg/l, in a suitable closed container. The water is rendered alkaline and the carbonate precipitated by e.g. barium or strontium chloride. The supernatant is decanted and the precipitate transferred to a sample bottle for transport to the laboratory. These procedures can be performed by technical field personnel under guidance from the collaborating laboratory (*Woodford et al., in press*).

The plastic bag method for collecting and preconcentrating carbonate from groundwater for radiocarbon analysis, was used during the field investigation at Loxton: (*Chemicals and method provided by Schönland Research Centre, University of the Witwatersrand, Johannesburg*)

- 1) The object is to obtain enough carbon (minimum 2g) for a radiocarbon measurement. This is ensured by precipitating the  $\text{HCO}_3 / \text{CO}_3$  at 200mg/l, from 100 liters of water. Roughly adjusting the amount of water according to the total alkalinity.
- 2) The "bag" method of carbonate precipitation is most efficient when employed close to the sample point, where the bag can be filled with a hose leading from the pump, source or syphon from a sediment settling tank.
- 3) Select a reasonably smooth area, preferably with a slight slope, which will allow up to 150 liters of water to drain away. Spread out the bag having ensured that there are no large thorns, sharp stones or other object likely to puncture the bag.
- 4) Cut off one corner of the bag and prop up the opening by 10-15cm with a small heap of sand or rock.
- 5) Empty a 100g sachet of  $\text{BaCl}_2$  powder into a bucket, pour in a few liters of the sample water and stir until dissolved. (One sachet is enough for some 100 liters of water at a total alkalinity of 300mg/l.).

**Please note:**

$\text{BaCl}_2$  is non-corrosive but poisonous. Avoid inhaling fine dust or ingesting. ( $\text{SrCl}_2$  is mainly used).

- 6) Insert hose-pipe carrying the sample water into the bag opening. When the bag is about halfway full of water, insert a funnel next to the hose-pipe.
- 7) Whilst water flows into bag, pour into funnel:
  - I) A dash of phenolphthalein solution (Shake bottle first).
  - II) 300ml Specially cleaned NaOH solution (Caustic). Do not disturb the precipitate at the bottom of the NaOH bottles. Pour clear liquid gently and ensure that precipitate remains in bottle, by not emptying the bottle entirely.
  - III) All the  $\text{BaCl}_2$  solution.
- 8) The water will turn pink on the addition of the NaOH and a cloud of precipitate will form when  $\text{BaCl}_2$  solution is added. These should mix by the swirl of the inflowing water. If needed, the bag may be gently prodded to effect further mixing. If the pink colour disappears, add more NaOH solution.
- 9) When full (thickness ~ 10cm) the bag will contain some 150 liters of water. Preferably do not fill to much less than ~ 100 liters. Remove hose and funnel, coax out excessive air and close the opening by tying with string.

- 10) Leave bag undisturbed until all precipitate has collected on the bottom surface and the liquid is clear. This may take an hour or two. In cases where logistics demand, this period can be shortened somewhat, but the bag should not normally be removed until the bottom is at least visible and water slightly turbid.
- 11) Drain the bag by slashing the sides with a pen / knife. Ensure that one corner of the bag remains undamaged for the final collection of the precipitate. Label this corner boldly with a marking pen. The speed of draining should be such that as little as possible of the precipitate is swept out of the bag. On uneven terrain, various slashes may be needed to drain the bag in a controlled fashion.
- 12) When 3-5 liters of fluid are left, or when significant amount of precipitate begins to emerge, raise the bag smoothly with an undamaged corner downwards and drain the contents into this corner, forming a cone.
- 13) Place a large funnel into the mouth of a 5 litre container (one litre glass-bottle in this study). Lower the tip of the filled cone of the bag into the funnel and puncture the tip. Collect the remaining content of the bag. If the volume of fluid appears too great, wait a few minutes to allow the precipitate to settle in the cone. This will allow minimal loss, should the bottle overflow.
- 14) Stopper bottle tightly. After a day or so, the precipitate will have settled considerably. Most of the clear supernatant can be poured off and saved. The precipitate can now be gently shaken and transferred into a smaller container, and topped up with the supernatant.
- 15) Expose the alkaline fluid as briefly as possible to air, to limit CO<sub>2</sub> absorption.
- 16) Incinerate bag or retain for re-cycling.
- 17) Collect a one litre sample of water from the same source for other isotope measurements.

***Radiocarbon and tritium can be employed as:***

- (a) Long-lived and short-lived radioactive tracers, respectively, of the infiltrating rainwater. In this way, their isotopic ratio is employed as a qualitative or semi-quantitative indicator of actively “turned-over” or dynamic groundwater. As such, they can be used to delineate recharge areas and in tracking hydrochemical processes. The isotopic ratio of radiocarbon defines the concentration in the TDIC. When the ratio is multiplied by the TDIC concentration (usually closely approximated by the alkalinity), a factor is obtained which is proportional to the radiocarbon concentration in the water. It then becomes a tracer akin to tritium (*Verhagen et al. 1996*).
- (b) Suitable models to interpret groundwater residence times, which can give information on groundwater dynamics and estimates of recharge rates (*Woodford et al., in press*).

### 2.3.7. Stable Isotopes (Oxygen-18 and Deuterium)

Several factors may influence the difference in isotopic composition of groundwater. The factors controlling isotopic variation in precipitation are (Mook, 1994):

- 1) Temperature
- 2) Latitude
- 3) Altitude
- 4) Seasonality

Processes responsible for changes in the oxygen-18 ( $^{18}\text{O}$ ) and deuterium ( $^2\text{H}$ ) concentrations, relative to the global meteoric water line (GMWL), are indicated on a plot of  $^2\text{H}$  vs.  $^{18}\text{O}$ , (**Figure 4.3.2 p. 112**).

The effect of processes such as evaporation before infiltration,  $\text{CO}_2$ -exchange, condensation, hydration of silicates,  $\text{H}_2\text{S}$ -exchange and exchanges between the rock minerals and water can be identified, using these stable isotopes (Domenico and Schwartz, 1990).

The GMWL is determined from (Craig, 1961):

$$\delta\text{D} = 8(\delta^{18}\text{O}) + 10$$

where:

$8$  = a general constant

$10$  = the intercept, called the deuterium (d)-excess

The  $\delta$  notation is expressed as parts per thousand ( $\lambda$ ) or permil (Weaver *et al.*, 1996).

$$\delta = [\text{R}_x - \text{R}_s] / \text{R}_s \times 1000$$

where:

$\text{R}_x$  = the isotopic ratio of the sample

$\text{R}_s$  = the isotopic ratio of the standard - VSMOW (Vienna Standard Mean Ocean Water)

The RMWL (regional meteoric water line) was determined by (Dr. C. Harris, UCT, pers. comm., 2000):

$$\delta D = 6.15(\delta^{18}O) + 10.87$$

### 2.3.7.1. Oxygen-18 and Deuterium

Oxygen-18 ( $^{18}O$ ) and deuterium ( $^2H$ ) are present in water in isotopic abundance (or ratios, R) of about  $^{18}O / ^{16}O = 0.20\%$  and  $^2H / ^1H = 0.015\%$ . In various combinations, these isotopes make up water molecules, principally of masses 18, 19 and 20. In phase processes such as evaporation and condensation, the different vapor pressures of these molecules produce isotope fractionation, the heavier isotopes tending to concentrate in the denser phase. These small changes can be expressed as a fractional deviation  $\delta$  from a standard called SMOW (standard mean ocean water) (Woodford *et al.*, *in press*).

Values of  $\delta$  can be diagnostic of water from different origins. Water vapor rising from the ocean is depleted in the heavy isotopes. Vapor masses moving inland are subject to equilibrium (or Rayleigh) isotopic exchange processes, the depletion of the heavy isotopes continuing on the vapor trajectories inland due to rainout. Consequently, the stable isotopic content of meteoric water lies on a regression line (Woodford *et al.*, *in press*):

$$\delta^2H = s \delta^{18}O + d \quad \text{equ. C}$$

where

s = the slope, and

d = the intercept d on the  $\delta^2H$  axis (deuterium excess).

The line with s = 8 and d = +10 is called the global meteoric water line (GMWL). The position of any pair of  $\delta^2H$  and  $\delta^{18}O$  values on this line for rainwater worldwide will depend on local climatological conditions (temperature, latitude, altitude, rainfall effects).

Surface water bodies, such as dams, lakes and pans will develop an enrichment in their heavy isotope content when undergoing significant kinetic (non-equilibrium) evaporation. Light isotopes are preferentially transferred to the vapor phase. The surficial layer of the water body is thus enriched in the heavy isotopes and is then readily mixed into the bulk of the water body through convective processes (Woodford *et al.*, *in press*).

This evolutionary enrichment produces  $\delta^2\text{H}$  and  $\delta^{18}\text{O}$  values which lie to the right of the meteoric water line, and plot on an evaporation line of lesser slope (s of usually 4 - 5) and lower d than the GMWL. Groundwater derived through infiltration from such water bodies will carry this distinctive evaporative isotopic signal (*Woodford et al., in press*).

Evapotranspiration losses from soil and groundwater system generally occur under isotopic equilibrium, i.e. without fractionation. In semi-arid environments such as the Karoo, isotopic values of groundwater derived directly from rain will therefore lie on or close to, the GMWL. They will tend however to be displaced to  $\delta$ -values more negative (or "lighter") than the weighted mean in rain, due to the process of rainfall selectivity (*Vogel and van Urk 1975; Verhagen, 1984*). Major rainfall events, which produce isotopically lighter precipitation, with more negative  $\delta$ -values, may contribute proportionately more to recharge. Different processes of rainfall recharge (viz. diffuse, channeled, bank infiltration) can be distinguished by different stable isotope ranges on the GMWL (*Woodford et al., in press*).

#### **Sampling:**

A 20ml sample suffices for the measurement both of  $\delta^2\text{H}$  and  $\delta^{18}\text{O}$ . The bottle should be rinsed with the untreated sample water, completely filled and securely stoppered, preventing any leaks. Sampling can be performed by technical field personnel, under guidance from the collaborating laboratory (*Woodford et al., in press*).

#### 2.3.7.2. Carbon-13

The isotopic abundance  $^{13}\text{C} / ^{12}\text{C}$  of atmospheric carbon dioxide, is about  $\delta^{13}\text{C} = -7\text{‰}$  with respect to a marine limestone isotopic standard PDB (PeeDee belemnite). During photosynthesis, this abundance is modified through biological isotope fractionation, which establishes organic values of about  $\delta^{13}\text{C} = -25\text{‰}$  in C3 plants (e.g. trees) and  $-12\text{‰}$  in C4 plants (e.g. grasses). The soil  $\text{CO}_2$  produced by such plants will have similar isotopic ratios. These ratios can be modified through isotopic exchange and dilution processes, such as the dissolution of soil or rock carbonate of differing carbon isotopic abundance, resulting in isotopic ratios in the different TDIC species in groundwater, governed by appropriate fractionation factors (*Woodford et al., in press*).

The  $\delta^{13}\text{C}$  is therefore diagnostic of some of the chemical processes which groundwater has undergone, and can provide information of the provenance of the TDIC, and thus of the water itself. It is also useful in assessing the  $^{14}\text{C} / ^{12}\text{C}$  ratio, as this is also modified by such processes, and forms the basis of  $^{14}\text{C}$  correction models (*Woodford et al., in press*).

**Sampling:**

For hydrological purposes,  $\delta^{13}\text{C}$  usually is measured on the same precipitate sample taken for radiocarbon, and requires no separate sampling (*Woodford et al., in press*).

### 2.3.7.3. Nitrogen-15

The study of nitrogen isotopes provides a method of monitoring the migration of nitrogenous compounds in groundwater. As nitrogen compounds are altered chemically within a system, the stable isotopes  $^{14}\text{N}$  and  $^{15}\text{N}$  may undergo isotopic fractionation. If such fractionation is unique, then nitrogen isotopes can be used to determine major sources of nitrate (*Woodford et al., in press*).

The isotope ratio  $^{15}\text{N} / ^{14}\text{N}$  in the atmosphere is 0.3663 %. Small deviations from this value as standard are given as  $\delta^{15}\text{N}$  ‰.  $\delta^{15}\text{N}$  values in terrestrial nitrogen compounds generally fall in the range -15‰ to +20‰ (*Hübner 1986*).

As with the isotopes of hydrogen and oxygen, fractionation occurs through either equilibrium (reversible) or kinetic (unidirectional) reactions. The equilibrium processes occur mainly in the atmosphere. More important in the hydrosphere are kinetic reactions, facilitated by bacteria, producing dissolved nitrate with depleted values of  $\delta^{15}\text{N}$ . Nitrogen isotope variations in groundwater therefore allow at best semi-quantitative interpretation (*Heaton 1986*).

A considerable range of values of  $\delta^{15}\text{N}$  in nitrate, derived from different sources is covered by each of the main source categories, which sometimes overlap. For most practical purposes the only source which can potentially be clearly distinguished in groundwater nitrate is animal and human waste. Extreme positive values of  $\delta^{15}\text{N}$  can be found accompanying high nitrate and coliform bacteria. Heaton (1986) was able to show a marked positive correlation between bacterial content and  $\delta^{15}\text{N}$  in four boreholes near Pretoria.

Very positive values of  $\delta^{15}\text{N}$  in groundwater nitrate may also result from denitrification through anaerobic bacterial reactions, which proceed under anoxic conditions in the aquifer. One is reasonably assured that the original (recharge)  $\delta^{15}\text{N}$  values are being conserved only if oxic conditions can be shown to prevail throughout the system being studied (*Woodford et al., in press*).

As yet, no applications of nitrogen isotopes in the main Karoo Basin have been reported. However, the usefulness of this method is likely to increase. No nitrogen isotope study has been conducted in the study at Loxton.

**Sampling:**

A sample of about 1 litre of water is required, depending on  $\text{NO}_3$  concentration. The water should be filtered and  $\text{HgCl}_2$  added in order to arrest any biological activity in the sample. These procedures can be performed by technical field personnel, under guidance from the collaborating laboratory (*Woodford et al., in press*).

#### 2.3.7.4. Dissolved gases

Gases dissolved in rainwater during the process of infiltration can be used as tracers of groundwater and reflect conditions at the time of infiltration (*Vogel et al. 1980 (a),(b); Mazor and Verhagen, 1983*). The concentration of gases in water is dependent on their atmospheric gas partial pressure and solubility, which is temperature dependent, at equilibration before the water is removed from effective atmospheric contact. If there is reasonable assurance that the water has been held under closed-system conditions, the relative concentrations of gases such as  $\text{N}_2$  and the noble gases He, Ne, Ar, Kr, Xe give information about the conditions at infiltration, such as temperature (*Woodford et al., in press*).

**Radon-222:** is a daughter product in the radioactive decay chain of uranium. It is short lived ( $t_{1/2} = 3.82$  days) and emits high-energy  $\alpha$  rays. It therefore has a high specific activity. Being a noble gas, it is very mobile and can easily diffuse from the aquifer rock, which contains the parent uranium, into the groundwater (*Andrews, 1972*). Aquifer porosity is a critical parameter in this diffusive process and faults and fractures conduct radon rapidly.

$^{222}\text{Rn}$  in groundwater therefore reflects aquifer conditions and can be a sensitive indicator of deep-seated highly conductive zones (*Woodford et al., in press*).

Of particular interest are **chlorofluorocarbons** (CFC's): these gases have been released into the atmosphere since the 1950's, their concentrations steadily increasing, with new compounds being added over the past few decades. When carefully sampled and measured, the concentrations of the different CFC's give a measure of the time since infiltration of groundwater (*Busenberg and Plummer, 1992*). The water can therefore be "dated" in principle over a span of some 4 decades, a very useful range covered also by thermonuclear tritium. The latter exhibits a peak in its input concentration, rendering its interpretation terms of short residence times ambiguous. Measurements of radiocarbon values can assist in removing this ambiguity. A similar function may be fulfilled by CFC's in that the concentrations in the atmosphere have been steadily rising, or leveling off.

As the source of the dissolved CFC's is the atmosphere itself, extreme care has to be exercised in obtaining samples. Contact with the atmosphere has to be rigorously avoided, requiring elaborate equipment to obtain sealed samples. Rigorous conditions also have to apply to extracting water from a borehole, avoiding any atmospheric contact. Several parallel samples have to be collected and the lowest of the results usually taken as the most reliable. Busenberg and Plummer (1992) recommend simultaneous tritium measurements in order to assess the degree of atmospheric contamination.

**Sampling:**

Special procedures are required in sampling for CFC's where extreme care has to be taken in avoiding atmospheric contact, both in extracting water from the borehole and in producing the sealed samples. These field operations require special equipment and are usually performed by the personnel of the collaborating laboratory (*Woodford et al., in press*).

Isotopes can provide information on groundwater origin, recharge and mobility in the Karoo Basin. However, the full potential of such environmental tracer techniques may be achieved only when they can be integrated into well-conducted geohydrological investigations or groundwater development programs (*Woodford et al., in press*).

Extensive isotope hydrology studies have been conducted over the past 15 years in the Karoo aquifers of the Kalahari Basin. Three of these were conducted by the Schönland Research Centre (then the NPRU). The first addressed the influence of ephemeral surface drainage on regional groundwater systems. The second was a detailed evaluation of a groundwater flow regime at the hand of integrated isotope and other data. The third was concerned with the determination of recharge by isotopes and by independent means in a project specifically designed as a model for fractured Karoo aquifers in South Africa (*Woodford et al., in press*).

The Karoo Basin is characterised by fractured rock aquifers that are bisected by numerous dolerite intrusions. These conditions produce a complex hydrogeological system, which complicates the study and development of groundwater. Universal models of groundwater flow hardly apply to these conditions, and the geohydrologist needs additional tools with which to understand the movement and chemical evolution of groundwater. Environmental isotope techniques and their use in Karoo aquifers is intended to draw attention to this powerful and efficient tool to be used by geohydrologists. One of the most important of these is hydrochemistry, and programs such as FLOWPATH, with which evolutionary trends in the data may be followed. As mentioned above, the potential of environmental isotopes has not properly been exploited in the main Karoo Basin, and their use in groundwater investigations is encouraged (*Woodford et al., in press*).

### 2.3.8. Groundwater Pollution

The sources of groundwater pollution include animal waste, human waste, irrigation and the results of agricultural tillage. Nitrate, phosphorous, potassium and sulphates are the main nutrients manifesting pollution (*Schot and Van der Wal, 1992; Tredoux, 1993*). Potassium and sulphate ions are obtained from the geological environment (*Hem, 1989*). South African geology is not contributing significantly to the nitrate loading of subsurface water (*Tredoux, 1993*). The sporadic occurrence of water containing high nitrate values, are usually the result of point-source pollution (*Heaton, 1984*).

Nitrates and bacterial-activity, are the main pollutants from animal and human waste. Pathogens are rare or absent, due to the fact that water is naturally filtered (*Helweg, 1978*). A common source of nitrates in agricultural areas, is the mineralization of natural soil's organic nitrogen and leaching thereof, when a virgin field is turned to tillage. Contaminants mainly affect the shallow groundwater sources (*Lynch et al., 1994*).

### 2.3.9. Statistics in Hydrogeochemistry

Readily available computer supported statistical packages are STATISTICA, STATSOFT and various geohydrological programs (WISH), that can perform statistical analyses on large data sets in a very short time.

Correlating multi-element hydrogeochemical data is simplified by producing a matrix which contains the correlations among all possible pairs of the elements being considered (*Levinson, 1980*). Two variables in a specific data set are correlated if a simple bivariate scatter plot of the data indicate a linear trend (*Swan and Sandilands, 1995*). Dissimilar physico-chemical environments cause marked differences in correlation. Symmetrical correlation matrices contain the correlation coefficients for all the pairs of selected elements. The correlation coefficients are a measure of the degree of linear correlation (*Swan and Sandilands, 1995*), being the ratio between the covariance and the square root of the product of the variance (*Johnston, 1989*).

A useful tool in aid of the interpretation of geohydrochemical data is factor analysis (*Schot and Van der Waal, 1992; Usunoff and Guzman-Guzman, 1989*). Factor analysis essentially aims to find groups of variables with shared common variances (*Johnston, 1989*). Classical graphical approaches are not as advantageous as that of factor analysis. It can be used for interpreting neutral chemical species and non-chemical data (e.g. temperature, pH, Eh and pCO<sub>2</sub>) as well as variations in ions in small concentrations (e.g. trace elements), which are not masked by chemically similar ions in greater concentration (e.g. Cl) in the data sets (*Usunoff and Guzman-Guzman, 1989*). Each factor is assigned a numerical value ranging from +1,00 to -1,00. These loadings are a measure of the extent to which each factor is associated with a particular value. If two loadings of the same factor have the same sign (either positive-positive or negative-negative) then they are positively correlated, but negatively correlated if they have opposite signs.

R- and Q-mode analysis are applied in factor analysis. The similarities between variables are described by R-Mode analysis, while the Q-mode describes the correlation between sampling sites (*Hitchon et al., 1971; Reeder et al., 1972*). Data are usually rotated (varimax rotation) to reduce the factor loading to a simple structure by placing the highest possible loadings on the fewest number of variables, while preserving the independence of each factor and reducing the complexity further by allowing the factors to become slightly correlated (*Levinson, 1980*). These new combinations are then examined for significance in terms of process, type of samples, geological and geochemical information (*Rose et al., 1979*).

## CHAPTER 3

### Study Area

#### 3.1. Introduction

Vertical, local and regional chemical variations in groundwater are dependant upon the physical character of the environment and on linear structures (dykes, faults, master joints, fissures etc.) which constitutes aquifers in the study area. Groundwater analysis may provide a method whereby such aquifer systems may be more meaningfully classified in terms of groundwater occurrence and quality.

#### 3.2. Location and extent of the study area

The study area is located between 22°00' & 22°45' E longitude and 31°15' & 31°45' S latitude, in the Permo-Triassic Karoo Basin (**Figure 3.2**). The Main Karoo Basin covers an area of approximately 630 000km<sup>2</sup>. Surface altitude ranges between 800m to 3650m above mean sea level ( $\pm$  1500m above mean sea level in the study area) and decreases from east to west.

The main structural domains of the study area are the Jurassic dolerite dykes and sills, the Cretaceous kimberlite fissures and pipes, as well as E-W trending sinusoidal megafolds and shears. Fluvial sandstone and mudstone of the Beaufort Group are the dominant geological components in the lithology of the area.

#### 3.3. Climate

Karoo climate is determined by the degree of latitude, distance from the sea and the topography, as well as elevation of the area. A subtropical high-pressure belt with a characteristic dry upper air layer influences the climate. The major part of the Karoo Basin receives summer rain from October to March, with the exception of the southwestern parts and southeastern coastal zone, receiving both summer and winter rains (*Venter et al., 1986*).

Rainfall in the winter is minimised due to intensified high-pressure systems, causing inversion layers and preventing maritime air from reaching the interior. Summer months are frequented with sporadic thunderstorms, caused by moisture-laden air which flows in from the Indian Ocean and penetrates the interior. The mean annual precipitation decreases from east to west, with the central regions receiving less than 200mm per annum. The eastern escarpment receives the highest rainfall of up to 2000mm per annum. Reliability of rainfall also decreases from south to north. River flow is at a maximum in the east, the area of maximum rainfall.

Evaporation is highest during the hot summer months, with the evapotranspiration increasing from east to west (*Simonis and Kok, 1989*) and from south to north (*Venter et al., 1986*). These factors determine the amount of rainfall that is available to recharge the groundwater sources in the area, which in turn determines the quality of the water (*AEC, 1990*). Poor water quality is related to areas experiencing very low rainfall, as areas with high rainfall generally have good water quality. In the Karoo seasonal temperature fluctuations are large, with a 25°C difference between day and night temperatures.

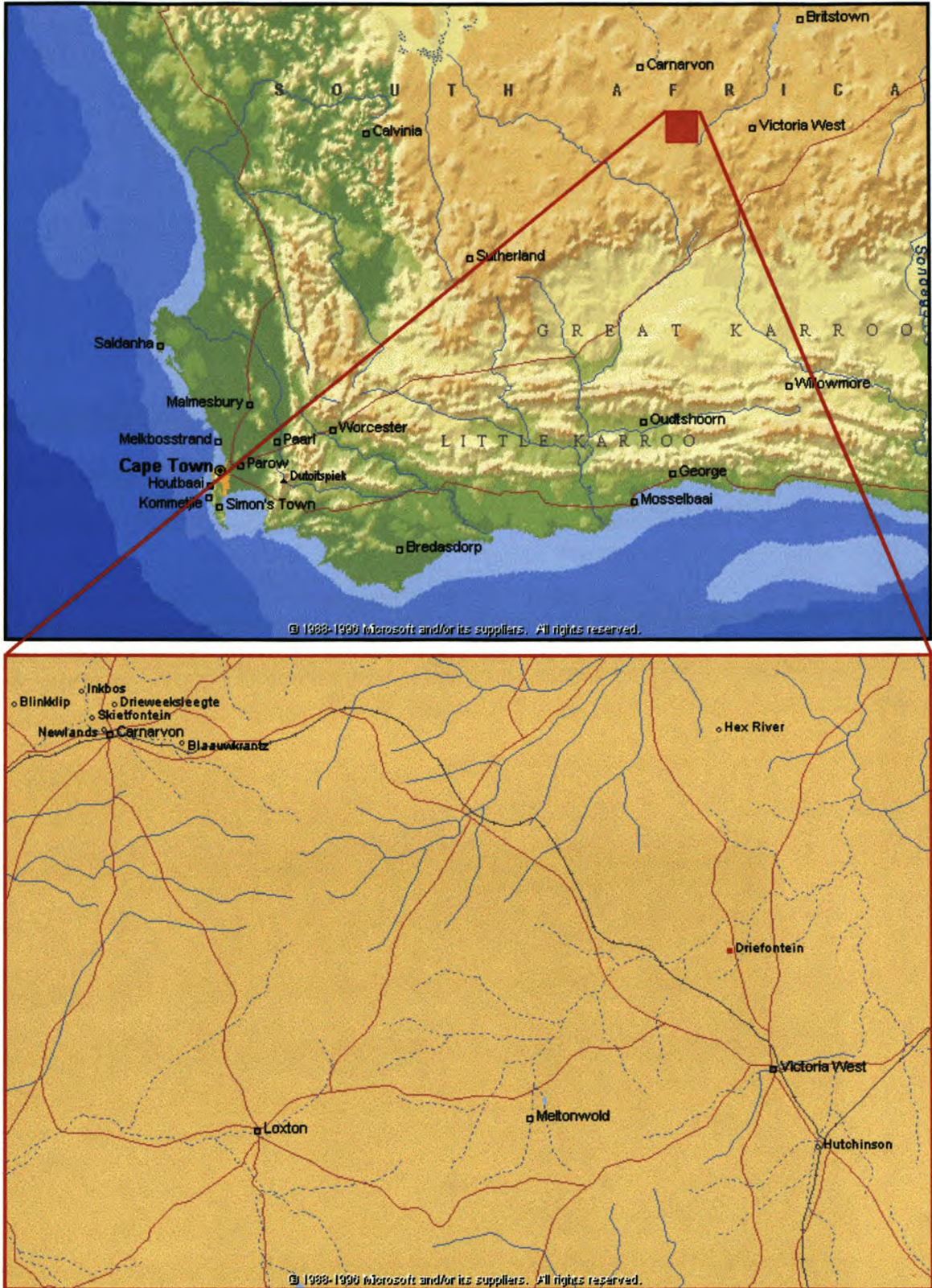


**Figure 3.2. Loxton locality map.**

### **3.4. Vegetation**

The study area is dominated by Karoo and Karrooid plants, with stunted shrubs and thornveld. Vegetation near water sources is larger and greener than that found in dry areas as can be seen in the relationship between vegetation and fracture zones (linear growth pattern of vegetation on dolerite or other intrusions and along joints of water bearing bedrock). Dominating plant life in the area is represented by: rosemary, perdebos, bitterbos, harpuisbos, plakkies and renosterbos.

Vegetation is influenced by environmental factors such as water (rain, runoff and soil moisture) and evaporation in arid areas such as the Karoo. Significant fluctuation in Karoo vegetation is due to short term shifts in seasonal rainfall and the grazing factor (*Roux, 1981*). Removal of the thin topsoil layer by nature or man could be detrimental to the growth and re-establishment of vegetation (*Roux and Opperman, 1986*).

The topsoil cover is generally shallow, increasing in thickness along rivers, valleys and flatter plains. The amount of soil cover determines the amount of CO<sub>2</sub> available in the unsaturated and saturated zones, which relates to the amount of mineral weathering in these zones (*Adams, 1998*).

### **3.5. Drainage**

The major drainage features of the Karoo include the Orange River with its perennial tributaries, as well as the Vaal and Caledon Rivers, all flowing from east to west.

A number of non-perennial rivers that only flow during peak rainfall periods in the study area, are responsible for most of the groundwater recharge. Damming of the non-perennial rivers for irrigation and stock watering provides a recharge source for groundwater, but the high evapotranspiration rate means that most of the water is lost to the atmosphere (*Adams, 1998*).

Runoff depends on the annual precipitation frequency, topography, soil nature and the geology of the area. The amount of rain retained over a year is a function of the precipitation frequency, gradient of the catchment area, nature and density of vegetation (as vegetation controls interception and retardation of runoff). Runoff is the product of precipitation after interception, surface retention and initial infiltration. Human induced pathways such as roads and a high relief lead to a high runoff (*Adams, 1998*).

## 3.6. Geology

### 3.6.1. Introduction

The Karoo Basin developed as an east-trending linear foreland basin (related to the Cape Fold Belt tectonics) in southwestern Gondwana due to combined sagging of the crust, compression and uplift. Glacigenic sedimentation (Dwyka Group) predominated.

The **first folding phase** at 278 Ma corresponds to the last glacial cycle in the Dwyka Group (Visser, 1997).

The **second tectonic event** at 258 Ma affected the basin significantly, as the southern and western branches of the Cape Fold Belt were probably lifted above sea level. Deep-water fans are replaced by fluvially dominated sandy deltas of the upper Ecca and lower Beaufort.

The **third tectonic phase** at 247 Ma resulted in a pulse of coarse-grained, braided sands of the Katberg Formation (upper Beaufort).

The **fourth tectonic paroxysm** at 230 Ma corresponds to further narrowing of the basin with deposition of fluvial sands (Molteno Formation) from alluvial fans emanating from the Cape Fold Belt, southeast of the basin.

The history of the Main Karoo Basin was controlled by four major geodynamic events (Woodford *et al.*, *in press*):

1. The uplift of the Cape Fold Belt and the deposition of the Karoo sediments,
2. The break-up of Gondwanaland with the extrusion of the Karoo basalts and intrusion of dolerites,
3. Localised mantle up-welling and the intrusion of kimberlites, and
4. Cessation of regional tectonism, uplifting, modern geomorphology and deposition of recent sediments.

This classic foreland basin was filled with a thick sedimentary succession in a linear trough along the landward side of the rising Cape Fold Belt, to the north of which it thins and wedges out over

the adjacent craton (**Figure 3.6.1**). Fluid migration and progressive diagenesis accompanied the development of the basin and the rising of the belt (*Duane and Brown, 1992*).

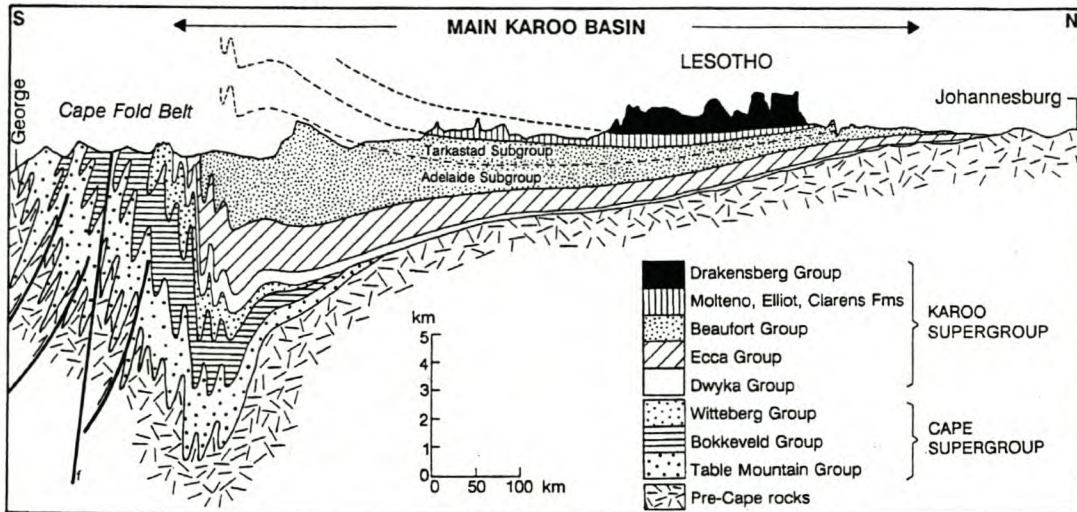


**Figure 3.6.1. North-South cross-section of the Main Karoo Basin.**

Basin fill of the Main Karoo Basin took place from the late Carboniferous (280 Ma) to early Jurassic (100 Ma) (*Visser et al., 1980*). The Karoo Supergroup lies unconformably on the Cape Supergroup, which in turn lies unconformably on the Precambrian floor of Malmesbury beds and younger Cape granite intrusives (*De Wet, 1975*).

The study area is comprised of the Abrahamskraal Formation (2500m thick), overlain by the Teekloof Formation (1000m thick), both part of the late Permian Adelaide Subgroup of the Beaufort Group. The sandstone comprising the Teekloof Formation (400m thick) overlies the Abrahamskraal Formation which predominates in the south of the study area (*Johnson et al., 1997*).

The Abrahamskraal Formation consists of fine to medium grained sandstone, interlayered with grey to green mudstone. The mudstone to sandstone ratio is 4:1. The Adelaide Subgroup in the study area consists of alternating bluish-grey, greenish-grey or greyish-red mudstone and grey, very fine to medium-grained, lithofeldspathic sandstone (*Woodford et al., in press*).

The sandstone and mudrock units normally form fining-upward cycles. These cycles rest on erosion-surfaces overlain in many cases by a thin intra-formational mud-pellet conglomerate. The cycles vary from a few metres to a few tens of metres in thickness and were probably formed by the lateral migration of meandering rivers. Sandstone units with an average thickness of 6m to

60m maximum are observed, with calcareous concretions in some sandstone layers of 20cm to 100cm in diameter. Palaeocurrent data indicate that the bulk of the sediment was derived from a source area situated to the south and southeast of the basin, with subordinate influx from the southwest, west-northwest and northeast (*Woodford et al., in press*).

The strata in the study area are approximately horizontal in orientation, with a maximum regional dip of 4° southwards (*Woodford et al., in press*).

### 3.6.2. Lithology and Mineralogy

Karoo basalt extruded onto the surface of the Karoo sediments during a period of extensive magmatic activity in the Jurassic (180 Ma: *Duncan et al., 1997*) and was accompanied by one of the early-stages of the Gondwanaland break-up phases (*Hunter and Reid, 1987, White, 1997*). Flood basalts originate from large mantle plumes (convection-cells) that result in the upwelling of abnormally hot material at the base of the lithosphere. A mantle plume situated on the East coast of Southern Africa is proposed by Storey and Kyle (1997). This magmatic activity generated an extremely large volume of hypabyssal dolerite intrusives (dykes and sills), now outcropping over an area covering almost two-thirds of South Africa. The tremendous heat flow generated by the intrusives was responsible for the widespread hydrothermal metamorphism of the sediments (*White, 1997; Rowsell and De Swart, 1976*).

Kimberlite and associated alkaline-rich igneous rocks (i.e. carbonatite, olivine melilitite) of the Main Karoo Basin were intruded during the Cretaceous period between 130 Ma to 70 Ma (*Allsop et al., 1986; Duncan et al. 1978; Smith et al., 1985; Smith et al., 1994*). Some radiometric dating also gives ages between 140 and 190 Ma (*Davis, et al., 1966, Nixon et al. 1983, Smith et al. 1994*), indicating that some of the kimberlite may have been intruded directly after the Karoo dolerite. Kimberlites have their source in the mantle (>200 km) and therefore differ totally in origin and composition from dolerites and basalts. Kimberlite fissures (or dykes) and pipes occur in clusters and their activity did not produce large volumes of magmatic material or any noticeable regional geomorphological features. Furthermore, they did not result in any significant regional or even local contact metamorphism due to a lack of high and sustained heat flow during intrusion (*Woodford et al., in press*).

Major uplift during the Miocene and Plio-Pleistocene resulted in the formation of the circum-country Great Escarpment, the development of the present course of the Orange River and the completion of the African weathering surface (*Du Toit, 1954; Partridge and Maud, 1987*).

Whether or not the South African continent is presently undergoing a renewal of tectonic activity is still a matter of controversy. For some authors neotectonics and seismicity in South Africa are indicative of a renewed era of tectonic activity (*Patridge, in press; Hartnady, 1990, 1998*). For others the African Plate has been at rest with respect to the mantle for the past 40-30 Ma (*Burke, 1996*). The present day seismic activity over Southern Africa indicates a number of distinctive seismo-tectonic provinces that could be linked to the development of a new structural and plate tectonic framework (*Woodford et al., in press*).

The lithostratigraphic units of the Karoo Supergroup outcrop concentrically around the Main Karoo Basin (**Figure 3.6.2.A**). More detailed sections portraying the entire stratigraphic succession in different parts of the basin are contained in **Figure 3.6.2.B**. Lateral facies changes, particularly in the lower half of the succession, have given rise to intertonguing of formations in various parts of the basin. No major regional unconformities are known to exist within the basin, with the possible exception of one at the base of the Molteno Formation. The description which follows is a summary from Johnson et al. (1997). Other recent reviews of the Main Karoo Basin are those by Cole (1992), Tankard et al. (1982), Smith (1990), Smith et al. (1993) and Veevers et al. (1994).



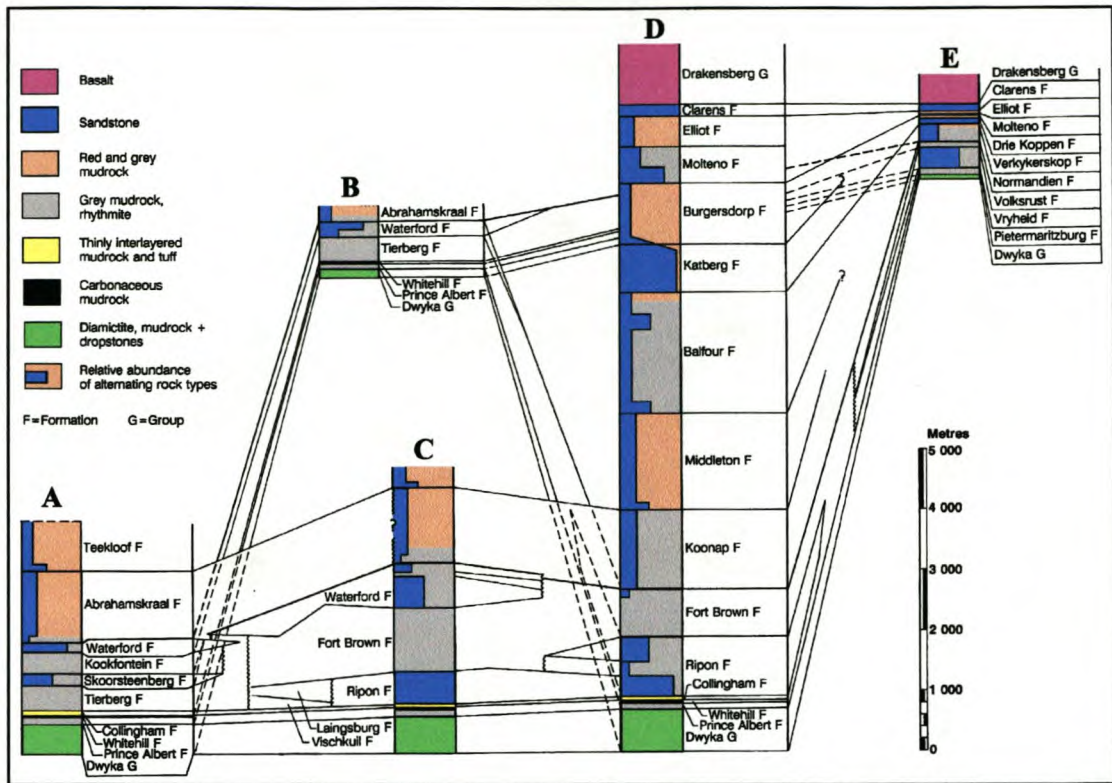


**Figure 3.6.2.B: Generalised stratigraphy and lithology of the Karoo Supergroup of the Main Karoo Basin. (Johnson et al., 1997).**

### 3.6.3. Structure

An exhaustive structural interpretation was carried out in the Western Karoo on the Victoria West and Beaufort West 1:250 000 sheets as part of a Water Research Commission project (Woodford and Chevallier, 1998). The first phase of the research involved:

1. Assessment of the different techniques of lineament mapping,
2. Structural analysis of the lineaments and determination of the stress field history, and
3. Spatial analysis of the lineament dataset.

The second phase of the research program was to assess the relationship between the structural information and the occurrence of groundwater. The third phase of the project, given this relationship, was to compile a groundwater productivity (yield) map of the study area using the structural information to extrapolate between borehole information, using a GIS. Exploration

drilling was conducted in Loxton area to scientifically assess the structural evaluation of the lineaments in terms of groundwater occurrence (*Woodford et al., in press*).

Three different tectonic styles and patterns of lineaments characterise the study area, namely: dolerite dykes, kimberlites fissures and master-joints (the project excluded the folding to the south of latitude 30°S, as well as the dolerite sills). Many examples of tectonic reactivation were observed in the field (*Woodford et al., in press*).

The network of dolerite dykes in the area shows two distinct tectonic patterns:

- A right-lateral E-W shear-dislocation zone, and
- A series of NNW intrusions.

The master-joints form two regional systems, trending NNW and NNE. The emplacement of the kimberlite dykes was controlled by the dolerite or master-joint tectonic trends. The NNW fractures appear to be the most prominent structural feature in the study area and they exhibit many signs of tectonic reactivation, as well as neotectonic movements (*Woodford et al., in press*).

A NW horizontal crustal compressional system has prevailed since the break-up of Gondwanaland and this accounts for the E-W shear zone and the reactivation of NNW trending structures. The modern regional tectonic stress field seems to be characterised by a WNW compressional system (*Woodford et al., in press*).

A near-surface stress system also plays a dominant role in the reactivation of fractures. Near-surface stresses are created by uplift and thermal cooling as a result of erosional unloading. Analysis of the surface stresses in the study area shows that a general NE tensional stress should be expected (*Woodford et al., in press*).

Following the structural and stress analysis of lineaments in the study area, it is estimated that the N 90° and 150° trending structures are the most likely to have been reactivated and opened during recent times. High density fracturing seems to be related to structural “knots”, i.e. where two or more major lineaments intersect one another. Analysis indicates a strong overprint of the EW shear pattern and the NNW fracture trends (*Woodford et al., in press*).

The mega-lineaments define a number of corridors of preferential, extensive and dense fracturing. The fractures can be of different origin or age (**Figure 3.6.3.A**). The lineaments are

generally expressed as non-linear features, which may be curved, jagged, undulating, broken or offset and / or anastomosed (*Woodford et al., in press*).

A number of distinct structural domains (**Figure 3.6.3.B**) were defined (*Woodford et al., in press*):

- Three E-W trending (Northern, Central and Southern) domains: the *Central Domain* (Loxton, Victoria West and Richmond) represents a zone of major E-W shearing. Its boundaries correspond to an envelope that contains most of the prominent R- (riedel) and P-type shear fractures, which form a series of “bulges” and “necks”. It also includes the mega-lineaments. The central domain is characterised by the greatest concentration of rough lineaments. The northern and southern E-W domains have less pronounced structural features.
- Six NNW trending domains correspond to major NNW corridors of fracturing and are delimited by mega-lineaments.
- Four kimberlite domains correspond to the four clusters (areas of kimberlite pipe occurrence), as indicated on Figure 3.6.3.B.

The width of many dykes were measured in the field. No significant relationship could, however, be found between dyke width and length, probably because the long lineaments are often segmented or offset (*Woodford et al., in press*).

Six sites were selected for exploration drilling by the Department of Water Affairs and Forestry at Loxton (**Figure 3.6.3.C**). Different structural parameters were used to select each site: type of fracture, major lineaments, orientation, stress-field, reactivation, structural domain and roughness, as well as density of fracturing. Detailed site plans of the six sites at Loxton are available in **Figure 3.6.3.D** (*Woodford et al., in press*).

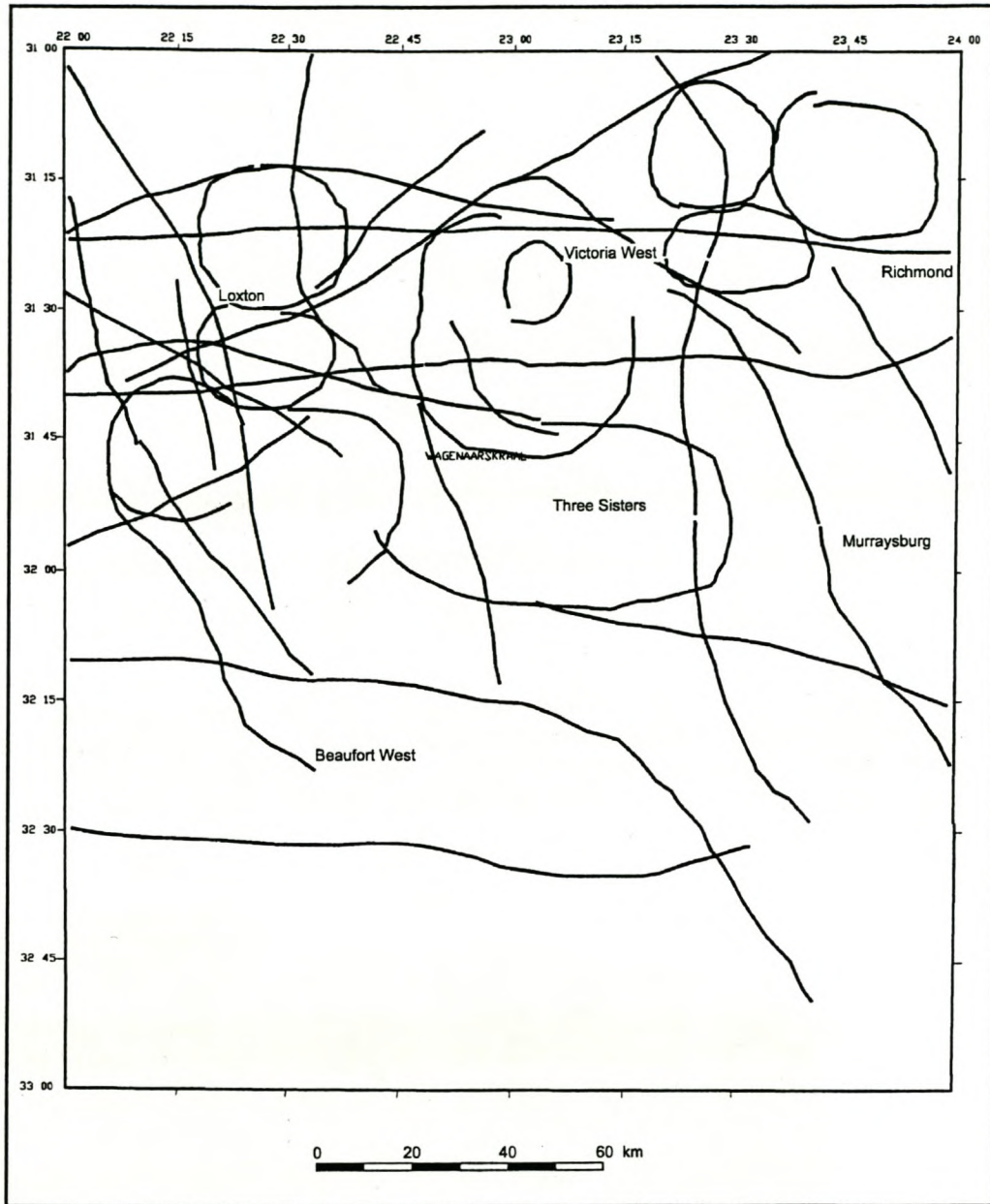


**Figure 3.6.3.A. Mega-Lineaments extracted from LINCOMP (Woodford et al., in press).**

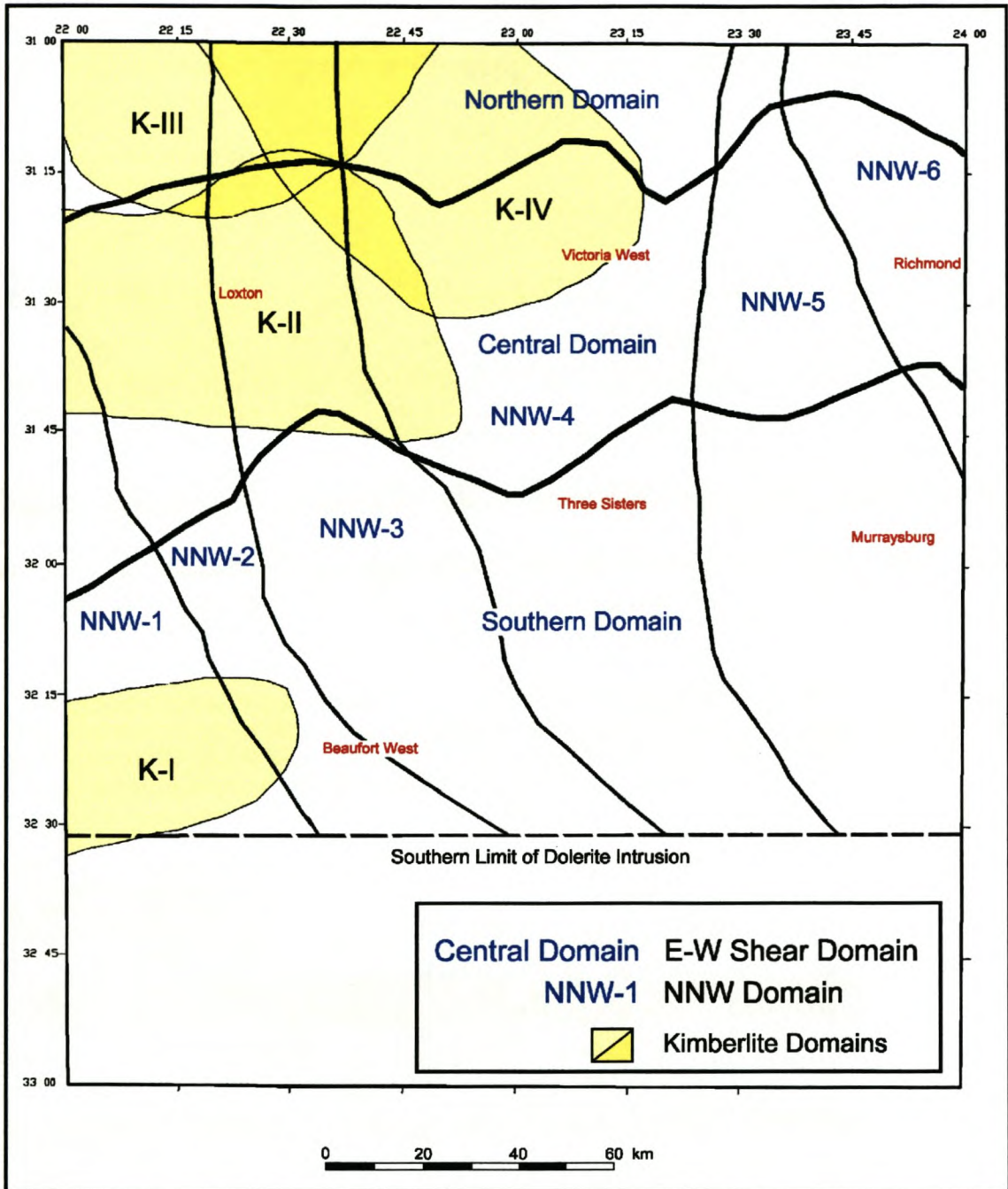


**Figure 3.6.3.B.** Lineament structural domains (Woodford et al., in press).

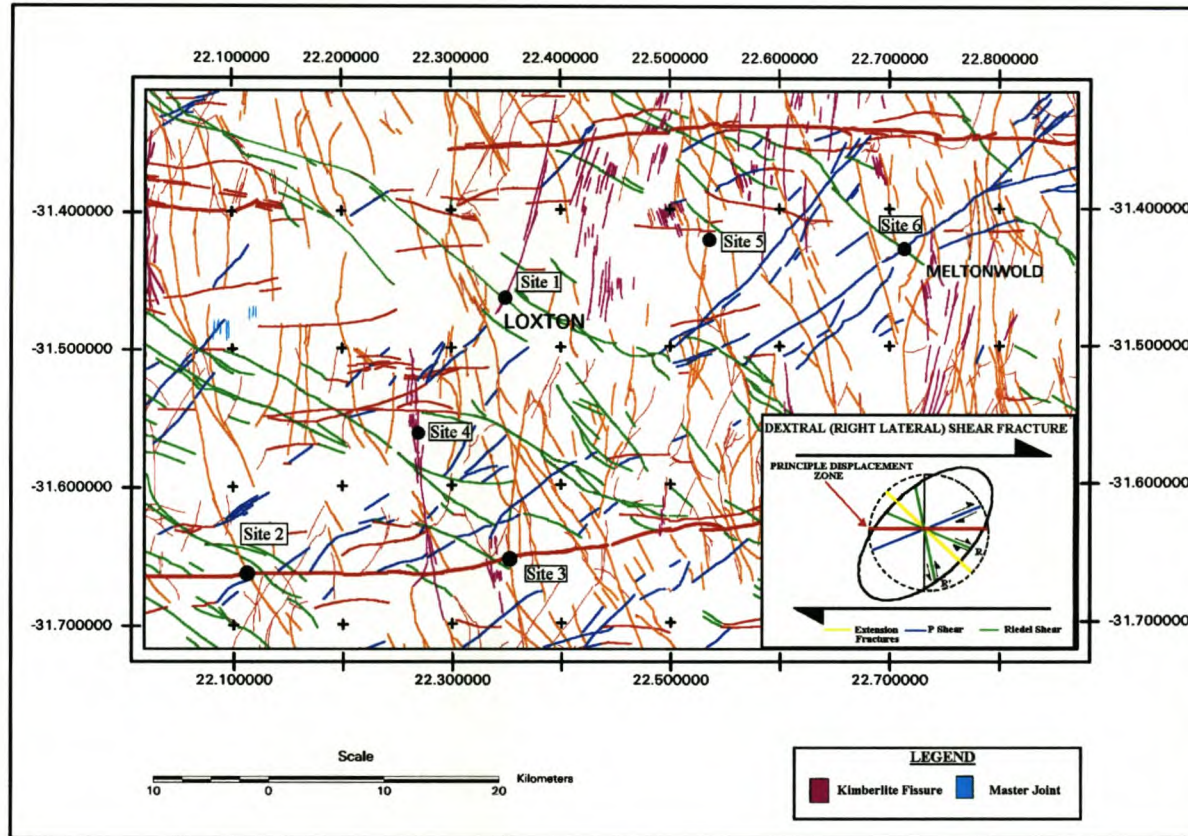


**Figure 3.6.3.C. Lineament map (from LINAIR) indicating exploration drill-sites around Loxton. The inset shows the different types of dolerite dykes that developed along the Jurassic E-W dextral shear zone: Red - E-W strike-slip fractures, Green - riedel-type fractures, Blue - P-type fractures. Orange lineaments - NNW dolerite dykes. Other lineaments are: purple - kimberlite dykes and turquoise - master-joints. Under the modern WNW compressive regional stress regime lineaments trending between  $N90^\circ$  and  $N150^\circ$  are supposed to be to most reactivated (Woodford et al., in press).**

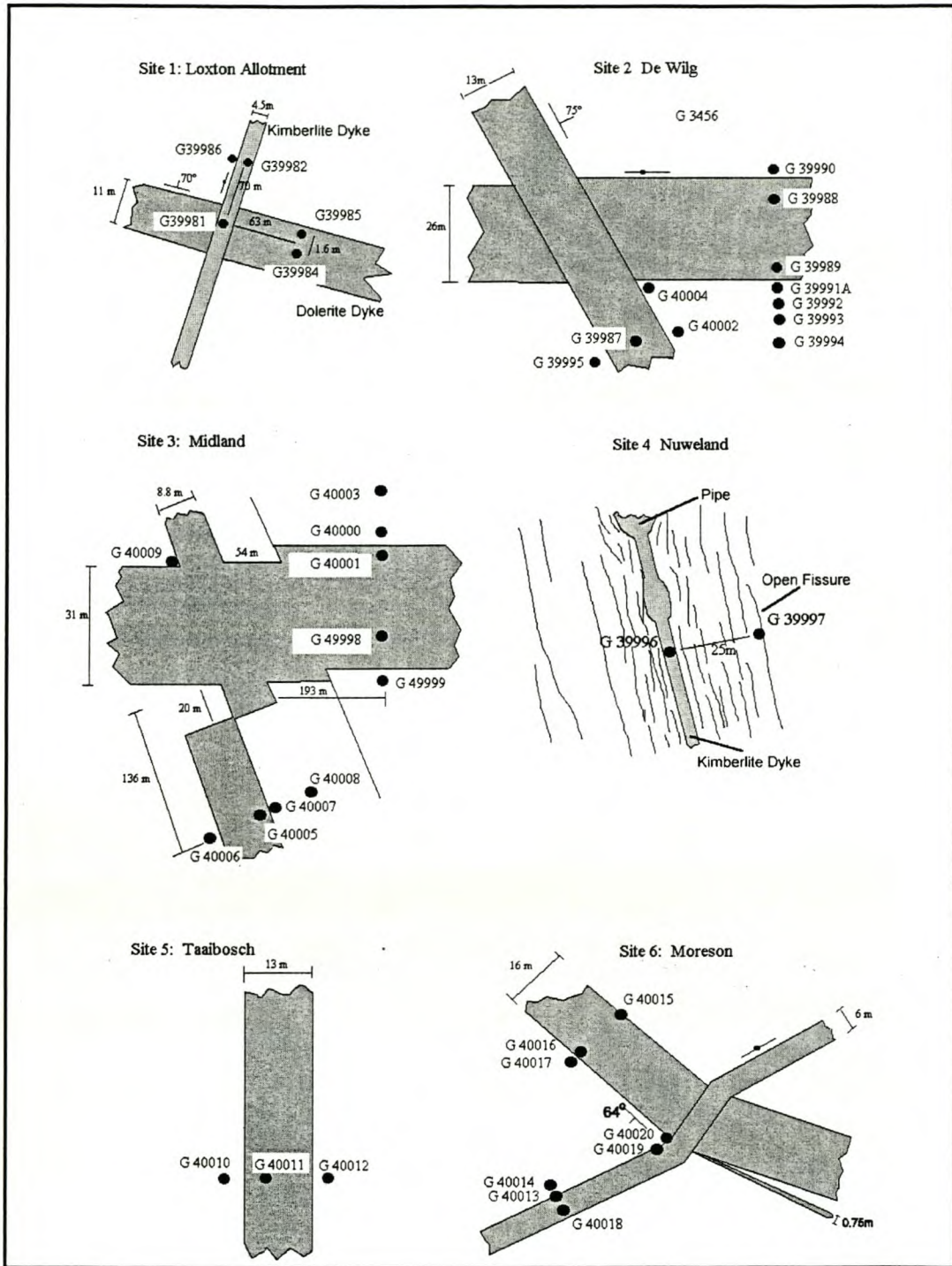


**Figure 3.6.3.D.** Detail plans of exploration drilling sites at Loxton (Woodford et al., in press).

## A) Site 1: Loxton Allotment

Is characterised by the following (*Woodford et al., in press*):

- Located at the intersection of a dolerite and a kimberlite dyke.
- It corresponds to a small structural "knot".
- The kimberlite dyke was not mapped on SPOT imagery.
- The dolerite dyke falls within the N90°- N150° range of possible modern reactivation.
- The kimberlite dyke is at right angle to the possible reactivation direction.
- The dolerite dyke forms part of a major lineament.
- The dolerite dyke is a rough lineament (segmentation).

Two boreholes were drilled into the dolerite dyke and three in the kimberlite dyke. All three boreholes in the kimberlite were dry, even the one at the intersection with the dolerite. The holes in the dolerite dyke produced moderate yields of between 3 and 4 l/s.

## B) Site 2: De Wilg

This is characterised by the following (*Woodford et al., in press*):

- At the intersection of E-W strike-slip and NNW dolerite dykes.
- Represents a small structural "knot".
- The E-W dyke falls within the N90° - N150° range of possible modern reactivation.
- The E-W dyke is 26m wide.
- The E-W dyke represents a major regional lineament composed of extensive en-échelon segments.
- The NNW dyke is also a major lineament.
- The NNW dyke is outside the N90° - N150° range of possible reactivation.
- The NNW dyke shows signs of older tectonic reactivation (fracturing and uplifting of countryrock).

A total of eleven boreholes were drilled (**Figure 3.6.3.E**). The E-W dyke gave high yields (up to 15 l/s) and the majority of water strikes occurred at depths between 100 and 230m, where the dyke displays a very complex offset pattern. The boreholes on the NNW dyke were dry.

### C) Site 3: Midland

The structural pattern is similar to Site 2, namely (*Woodford et al., in press*):

- Intersection of a E-W and a NNW dolerite dyke.
- The E-W dyke is also wider the NNW dyke.
- The E-W dyke is within the possible reactivation range, while the NNW dyke is not.
- Both features represent mega-lineaments.
- The difference from Site 2 is that it is located at a very prominent structural "knot".

A total of ten boreholes were drilled. All of them were successful and delivered moderate to high yields. The borehole drilled at the intersection of the two features delivered the highest blow-yield (32 l/s).

### D) Site 4: Nuweland

This consists of a 3m wide, north-trending kimberlite dyke with a blow and a pipe, as well as a series of parallel mega-joints and fissures. The dyke was not detected on the SPOT imagery. The borehole in the kimberlite was dry, while the borehole in one of the fissures away from the dyke yielded 4.0 l/s (*Woodford et al., in press*).

### E) Site 5: Taaiboschfontein

The target feature is a NS-NNE trending dolerite dyke that was reactivated during the emplacement of the kimberlite. Many kimberlite fissures follow the same trend in the area. It represents a mega-lineament which falls within the theoretical  $N90^{\circ}$  -  $N150^{\circ}$  trend of possible modern reactivation. The dyke is very fractured, sheared and full of calcite or calcrete-filled open fractures. Three boreholes were drilled with only one moderate yielding (4.4 l/s) successful borehole (*Woodford et al., in press*).

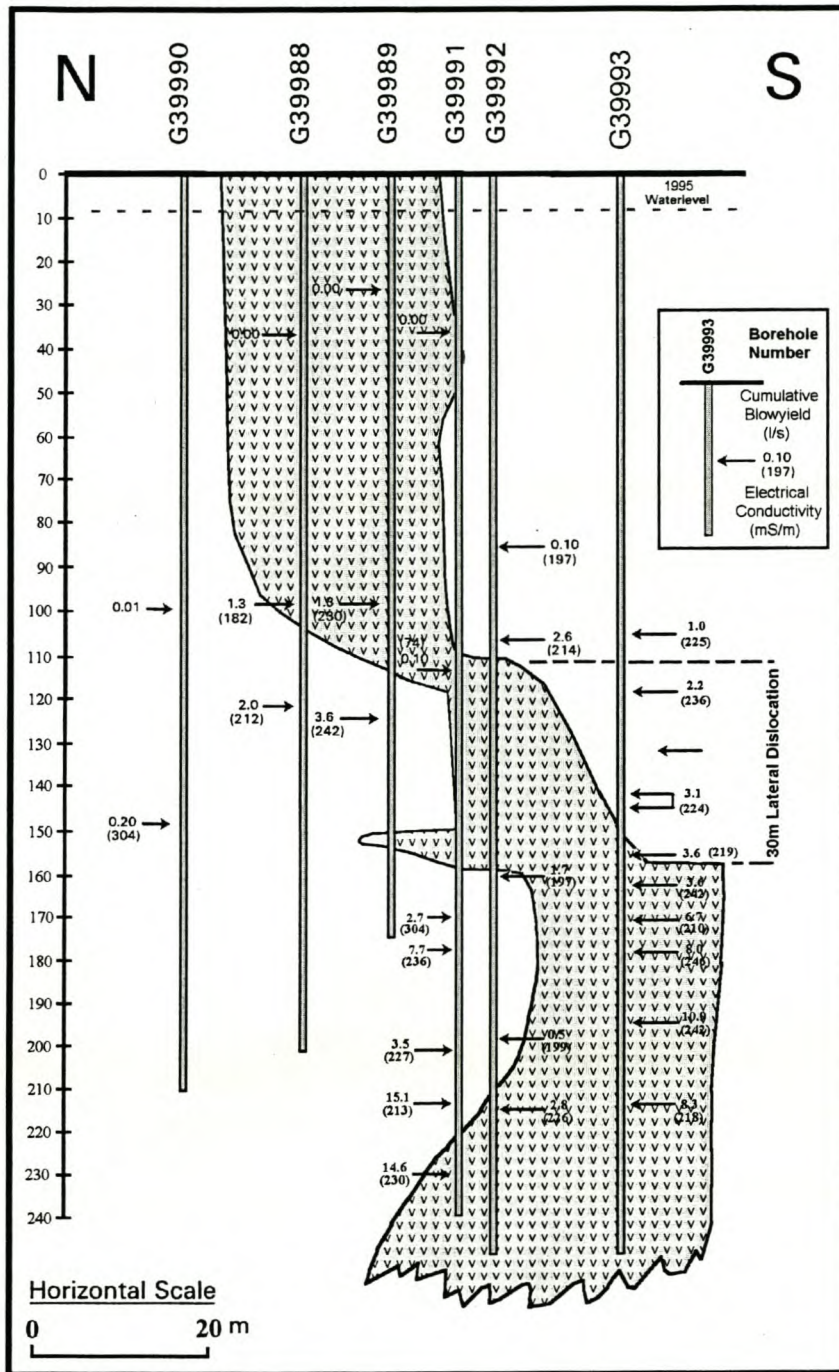


**Figure 3.6.3.E. Vertical Dislocation of the De Wilg Shear Dyke, south-west of Loxton (Woodford and Chevallier, 1998).**

## F) Site 6: Mōreson

The target features are characterised by (*Woodford et al., in press*):

- An intersection of a NE- and a NW-trending dolerite dyke.
- The NE dyke represents a mega-lineament, but is thin (6m) and orthogonal to the possible modern reactivation orientation created within a WNW compressional stress regime (P-type fracture).
- The NW “dyke” is thicker (16m), but is not a mega-lineament. It does however lie within the trend for possible modern reactivation.
- The site is not on a structural “knot”.

The thin NE-trending dyke did not, as expected, yield any significant amounts of groundwater. Boreholes drilled into the NW-orientated structure showed it to be an inclined sheet (a dipping 64° SE, curvilinear body), rather than a dyke. Moderate yields of 1.5-2.6 l/s were struck at shallow depths within and on the upper contact of the inclined sheet.

The exploratory drilling programme in the vicinity of Loxton showed (*Woodford et al., in press*):

- The E-W mega-lineaments produced high yielding boreholes. The borehole yield improves if the site is located close to a structural “knot”.
- The NNW lineaments form a second strong structural overprint in the Western Karoo. Boreholes drilled on these features at Site 2 delivered low yields, while high yields were intercepted at Site 4 near a structural “knot”.
- The NW dolerite dyke (possible recent reactivation) delivered moderate yields at Site 1 and Site 6, although the structure at Site 6 proved to be an inclined sheet.
- Boreholes drilled on the N-S and NNE lineaments, which represent kimberlite dykes, master joints or kimberlite-reactivated dolerite dykes, were moderate to low yielding. This could be ascribed to the poor hydrological properties of the kimberlitic material and / or to the unfavorable orientation of the lineaments.
- The NE-trending lineaments are supposedly “closed” under the modern WNW compressional stress regime. Only one of these lineaments was drilled at Site 6 and the boreholes were dry.

**Two important conclusions can thus be drawn (Woodford et al., in press):**

1. The E-W and NW trending lineaments are within the N90° - N150° range of possible modern reactivation. They were more productive than the NNW, NS, NNE and NE lineaments, which lie outside this orientation range.
2. It appears that structural “knots” could play a significant role in siting of successful boreholes in Karoo fractured-rock aquifers. SPOT imagery is therefore preferred for lineament and structural mapping in the Karoo Basin, when compared to Landsat TM or air-photographs.

The *Magnetic method*, (i.e. traverses across an area with a proton magnetometer to record the value of the magnetic field at, say, 5 or 10 meter intervals) has proven over the years to be a cost efficient and rapid tool for groundwater exploration alongside dolerite intrusions in the Karoo, with which a high success rate can be achieved if applied correctly. *Resistivity techniques* are the second most commonly used technique. These can be, and have been, used to identify dolerite intrusions, weathering depth of the sedimentary succession, depth to the top of the first thick dolerite sill and for the determination of unsaturated / saturated thickness of alluvium.

Standard geophysical techniques are capable of providing meaningful and cost effective results. The contrasts between the physical parameters in this instance are not great enough to produce significant and detectable geophysical variations (Woodford et al., in press).

In general, the other geophysical techniques, including the new tomographic techniques, are of only limited use under most Karoo aquifer conditions - often due to the high costs involved. However, when applied in research studies, the results can be very rewarding.

### 3.6.3.1. Sill and Ring-Complexes

Dolerite sills and ring-complexes feature prominently in the Karoo landscape. The rims of these structures are commonly exposed as topographic highs and form ring-like outcrops (Woodford et al., in press).

Karoo dolerite sills and ring-complexes have the same geographical distribution as the dykes and are by far the most common form of intrusion in the Karoo Basin, to a large extent controlling the geomorphology of the landscape. The dolerite sills and dykes form a complex intrusive network

that probably acted as a shallow magma storage system. Country-rock lithology has had a strong control on the emplacement of the sills. Du Toit (1920) pointed out the existence of preferential horizons of emplacement of dolerite sills, i.e. the Dwyka-Ecca Group contact, the Prince Albert-Whitehill Formation contact, the Upper Ecca-Lower Beaufort Group contact and other lithological boundaries within the Beaufort Group. Drilling in the Karoo has confirmed the presence of these preferential stratigraphic levels of intrusion (de la Rue Winter and Venter, 1970). The dolerite / sediment ratio decreases from west to east, reflecting the increase of sill intrusion toward the top of the Karoo sedimentary pile in the more elevated portions of the Eastern Karoo. On a regional scale, Karoo dolerite sills form large coalescing circular, oval or kidney-shaped structural units. Each unit is in itself composed of several sub-units of smaller size which in turn are made of even smaller units and so on, resulting in the so called "ring-within-ring" patterns (Woodford et al., in press).

Five major regional ring-complex units can be recognized extending from the Western to the Eastern Karoo (Figure 3.6.3.1). These are clearly defined on the topographic map of the Karoo Basin indicating the Sutherland, Victoria West, Graaff-Reinet, Cathcart and the Umtata megabasins (Woodford et al., in press).

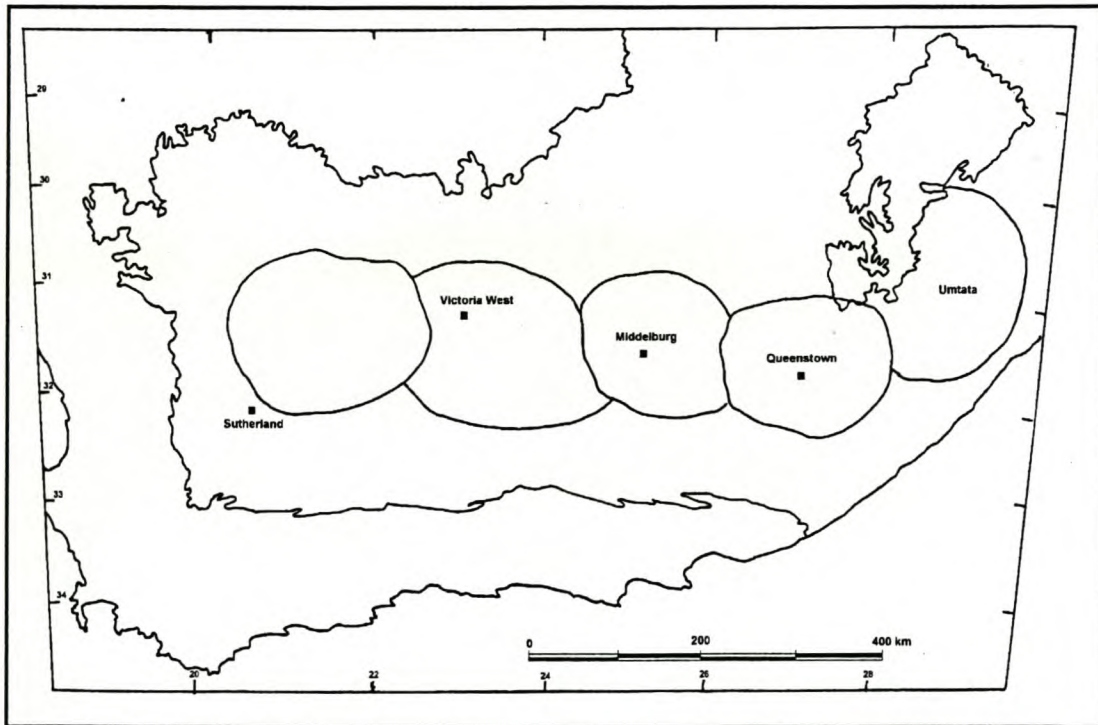


**Figure 3.6.3.1. Major Dolerite Ring Complex Systems in the Eastern and Western Karoo (after Chevallier and Woodford, in press)**

A relationship exists between the size of the dolerite basins and Karoo Supergroup stratigraphy. The more extensive sills forming these mega-structures, have been intruded near the base of the Karoo sediments, while the smaller structures (diameter of 10 km and less) have been intruded into the upper parts of the Karoo Supergroup. The shape and attitude of sills also changes from the bottom to the top of the stratigraphic sequence (*Woodford et al., in press*):

- Laterally extensive and long wave-length, undulating sills occur at the base of the Karoo sequence, i.e. along the contact of the Dwyka Group in the Prince Albert Formation and Prince Albert-Whitehill Formations,
- Well developed saucer-like structures dominate the middle portions, i.e. within the upper Ecca and Beaufort Groups, and
- Flat-lying sills reappear towards the top of the Karoo succession, i.e. directly below the Lesotho basaltic pile.

The larger Karoo dolerite sill and ring-complexes, within the 10 to 50 kilometres diameter range, have a “saucer-shaped” morphology (*Chevallier and Woodford, in press*). Each intrusion consists of four distinctive morpo-tectonic units, (*Chevallier and Woodford, in press*), namely:

- (a) A flat-lying *inner sill* forming the bottom of the saucer, (also referred as a laccolith by *Burger et al., 1981*). The thickness of the sill commonly varies between 30 and 60m. Vegter (1992) reports an average sill thickness of 30m in the De Aar area. However, very thick sills are also encountered near Lesotho (up to 1000m for Insizwa; *Maske, 1966*) and in Natal.
- (b) A flat-lying *outer sill* showing extensive fracturing and jointing. The thick sills which intruded into the base of the Karoo Basin are outer sills and can extend for hundred of kilometres. Undulation is very shallow (less than 2°), which can only be detected on large-scale maps. The thickness of these sills, usually between 50 and 100m, do not appear to be any different from that of the inner sills.
- (c) A peripheral, *inclined sheet* with a dips of up to 60° towards the centre of the basin, leaving a topographic ring after erosion (also referred as the “horn” by *Burger et al., 1981*). Vandoolaeghe (1979, 1980) reports that inclined sheets exhibit inward dips ranging from 3-70° and 10-35° in the Middelburg and Queenstown areas, respectively. The “inclined sheet” is commonly 20 to 40m in thickness, but may actually exceed that of the sills (*Chevallier and Woodford, in press*).
- (d) Abundant *feeder dykes* which branch into or out of the sill and ring complexes, or cut through them.

The relationship between the dykes and sill-ring complexes are extremely intricate. In the Western Karoo, many dolerite dykes can be observed to feed inclined sheets and thus control the shape of the ring-structure, which sometimes results in a jagged rim (*Vandoolaeghe, 1979; Chevallier and Woodford, in press*). Some dykes also branch out of one ring and coalesce with an adjacent ring.

### 3.6.3.2. Fracturing associated with Sills and Ring-Structures

*Woodford and Chevallier (1998)* identify three major types of fracturing within a dolerite sill and ring complex (**Figure 3.6.3.2.A**), namely:

- Vertical thermal columnar jointing. This is well developed within the flat-lying sill (*f1*). From air photo examination and satellite imagery it appears that the outer sill often displays a very dense system of columnar jointing.

- Fractures parallel to the strike of the intrusion are dominant within the inclined sheet. Air photo and satellite imagery show that the actual circular inclined-sheet is the most fractured part of the complex (f2).
- Well-developed, oblique or sub-horizontal open fractures develop within curved portions of the sill. In the Western Karoo, these fractures are often infilled with secondary calcite (f3). Vandoolaeghe (1980) made similar observations in the Eastern Karoo.

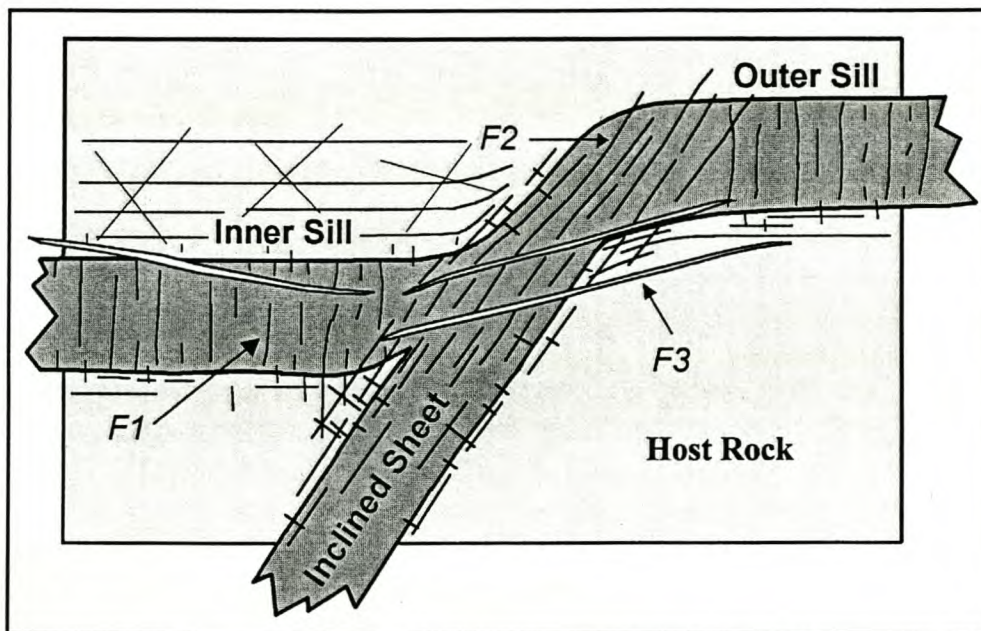


**Figure 3.6.3.2.A. Different Types of fractures associated with sill and ring complexes (after Chevallier and Woodford, in press)**

In the country-rocks, conjugated vertical jointing is often observed in the sediments above the sill or inclined sheet. Burger et al (1981) suggest that, based upon their laccolith model of intrusion, these fractures are open. Botha et al (1998) also mentioned that sills with laccolith shapes could have contributed to the existence of bedding-parallel fractures in the host rock.

Various attempts have been made in the past to develop a mechanism of emplacement for the sill and ring-structures. The following more recent tectonic interpretations are based on extensive geomorphological and geological observations and have been partly confirmed by drilling (Woodford et al., in press):

1. Burger et al. (1981), from observations made in the Northern Karoo (Free State), proposed that the sills have the form of a laccolith which thickens from the outer rim towards the centre of the structure. In this model the feeder to the laccolith is a central forming plug or dyke. The rings were envisaged as peripheral offshoots formed as a result of warping of the overlying sedimentary country-rock. Bending of the roof of the laccolith would also create open-vertical fractures that are devoid of magma (**Figure 3.6.3.2.B(b)**). In 3D this would result in a radiating fracture pattern, which is not observed in the field.
2. Chevallier and Woodford (in press) from observations made in the Western Karoo, proposed a different model and invoked a feeding system of magma along the inclined sheet or along the ring itself using a coalescing ring-dyke network. In this model, the 60° inward-dipping inclined-sheet thus changes into an upper outer sill, feeding a lower inner sill at the same time (**Figure 3.6.3.2.B(a)**).

From a geohydrological perspective, the two tectonic models propose that the rim of the ring-structure is the most tectonised unit within the sill / ring complex. These two models can vary considerably, especially concerning the development of fracturing below the ring and above the centre of the inner sill (*Woodford et al., in press*).

The dolerite ring-complexes and associated sills have to a large extent been over-looked by most geohydrologists and drillers, because of their size, thickness, hardness and structural complexity.

A large number of boreholes have been drilled into the Williston ring-complex. The boreholes penetrated the *inner-* and *outer-sill*, but missed the geohydrologically significant *inclined-sheet*. A second deeper 100m thick sill was also encountered on the northern portion of the system. Large differences in yield are observed between the *inner-sill* (low yield at the upper- and lower-contact, as well as within the sill) and the *outer sill* (high yields constrained between the upper and the lower sill contacts), because the outer-sills are more intensely fractured.

However on a local-scale of the sill itself, the *inner-sill* has not proved to be a successful groundwater exploration target, whereas the *outer-sill* has generally produced better results. The full extent of the *inclined-sheet* has yet to be fully investigated, however the sparse, detailed drilling information available shows it to be a very promising, but also challenging target that will require drilling of deeper (200-350m) boreholes. The action of weathering plays a major role in locally enhancing the permeability of incipient joints (*Woodford et al., in press*).

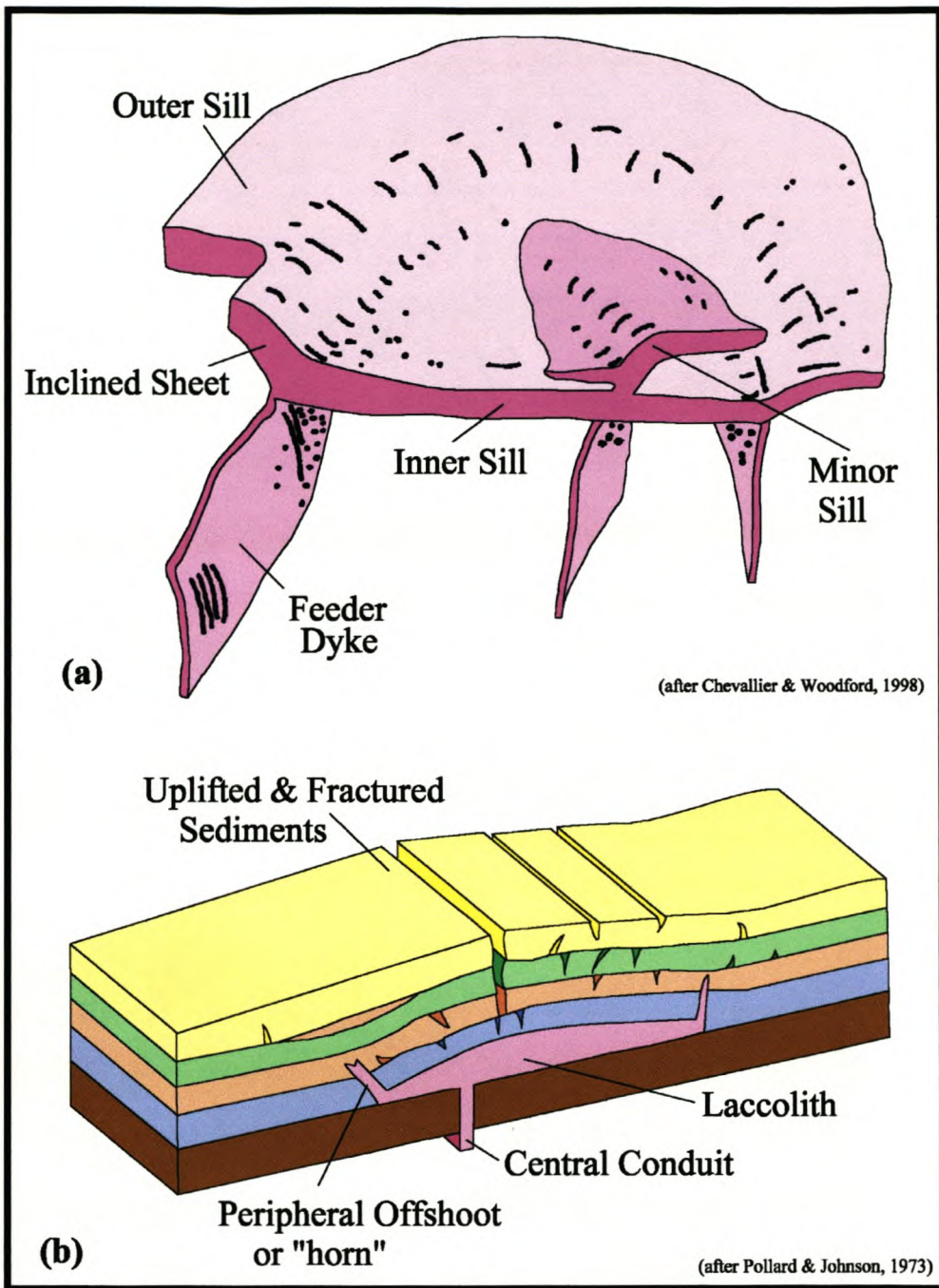


**Figure 3.6.3.2.B.** Two mechanisms of emplacement of the dolerite sill/ring systems – (a) the ring dyke model of Chevallier and Woodford (in press), (b) the laccolith model of Burger et al. (1981)

Dolerite sills and ring-complexes represent one of the least explored and most poorly understood structures in the main Karoo Basin. Consequently, very little is known about their hydrological properties. The following observations and concepts could form the basis for future research into these features (*Woodford et al., in press*):

- On a *regional scale*, the large basin structures may represent hydrogeological domains with different hydrostratigraphic units.
- On a more *local scale*, certain zones within the sill-ring complex may represent important targets for siting high-yielding production boreholes.

The fracturing associated with and the morphology of the ring-structures may result in the development of discrete hydrological units, with excellent storage and recharge conditions. Observations from KwaZulu-Natal (*KwaZulu-Natal Project Unit 8, 1995*), suggest that thinner sills tend to be more fractured and therefore have a greater yield potential. The outer ring is the most tectonically fractured portion of the system and should therefore play a prominent role in the geohydrological behavior of these Karoo aquifers. Intersections between dolerite sills and dykes are also important exploration drilling targets.

### 3.6.3.3. Breccia Plugs and Volcanic Vents

Breccia plugs and volcanic vents occur in different geographic areas and at different stratigraphic levels, displaying similarities in their size, shape, texture and hydrological properties.

Breccia plugs were thought to be of Cretaceous age, because of their proximity to the Salpeterkop Volcanic Suite (diatremes, olivine melilitite, kimberlite, etc.) and their apparent association with swarms of kimberlite fissures in the western Karoo. Until recently virtually no such research has been conducted on these features. From 1993 to 1996 the Department of Water Affairs and the Council for Geoscience conducted research into their distribution, constitution and geohydrology in the Western Karoo (*Woodford and Chevallier, in press*).

Clusters of breccia-plugs occur along the western and northern edges of the Karoo Basin. They are mostly restricted to the Ecca Formation (*Woodford et al., in press*).

Breccia plugs commonly form small, low-relief, circular hills, averaging 50 to 80 metres in diameter. They also occur as circular, negative-relief depressions of a similar dimension with characteristic calcrete development.

Two main facies are recognised (*Woodford and Chevallier, in press*):

- a) *Molten Facies* - domed, baked, molten, re-crystallised and highly contorted sediment containing xenoliths from the underlying strata. Melting is often accompanied by gas-vugs, which are commonly filled with secondary calcite, quartz and to a lesser extent grossular and vesuvianite.
- b) *Breccia Facies* - a true breccia with fractured, broken, shattered, displaced and re-cemented blocks of sediment. This facies is often accompanied by mineralization of quartz, calcite, gypsum, chlorite, apophyllite, baryte, siderite, fluorite, pyrite, pyrrhotite, sphalerite, galena, chalcopyrite, marcasite, bornite and traces of gold.

The (*a*)-type is the most frequently encountered in the field, whereas the (*b*)-type is much less common. This is probably because the (*a*)-type plug is more resistant to erosion and produces more easily detectable features of positive relief. The (*b*)-type erodes more easily, resulting in the less conspicuous features of negative relief. The core-logs show that the lithological units are locally highly disrupted, but that no major stratigraphic dislocation occurred as a result of the hydrothermal activity.

The Whitehill Formation is highly baked and leached in the vicinity of the breccia plugs. It is transformed from a pitch-black, finely bedded, pyrite-rich, carbonaceous shale to a white contorted and dislocated meta-sediment. The true breccia facies, in both cases located in the upper sections of the plugs, contain numerous openings and large cavities (up to 9m in depth) with extensive mineralization, highly-pressurised methane gas at 109m below ground level has been encountered in such a cavity.

Woodford and Chevallier (*in press*) propose that localised hydrothermal activity (often explosive), occurred when the early (lowermost) dolerite sills intruded into the partially indurated, "wet" Karoo Supergroup sediments. This resulted in the brecciation and melting of the host sediments, as well as the mobilisation and upward transport of elements from the Whitehill and Prince Albert Formations.

The breccia plugs do not contain any economic sulphide mineral deposits due to the absence of a suitable lithological trap, such as a thick carbonate-rich unit, for the concentration of chalkophile elements (*Woodford et al., in press*).

#### 3.6.3.4. Kimberlite and associated Alkaline Intrusive Complexes

Kimberlites occur as clusters of linear or arcuate swarms of dykes and fissures associated with several enlargements, blows or pipes and fractures in the Karoo (*Woodford et al., in press*).

Several swarms or tectonic provinces can be distinguished. At *Victoria West* three structural domains have been identified based upon the orientation of kimberlite fissures: NNE, NW and NS swarms. The *Postmasburg-Prieska-Britstown* swarm is a very extensive, arcuate feature that appears to follow the margin of the Kaapvaal-Namaqua craton.

Kimberlite fracture swarms consist of parallel fissures and associated joints or fractures. Each swarm can be divided into sub-swarms of smaller size. Within each sub-swarm the fissures are always closely spaced (approximately 10 to 50m apart). This tectonic style is often reported for kimberlite and was described by Nixon and Kresten (1973) for the Lesotho kimberlite swarm. The fissures are 0.5 to 4m wide and often show strong upwarping of the surrounding Karoo beds. Upwarp zones within the stable platform and fractures related to crustal tension are the main structural controls of the kimberlite intrusions (*Greeff, 1968*). In outcrop the kimberlite intrusion is often inconspicuous and only visible as stringers of highly decomposed kimberlite (green-ground) or micaceous calcrete (yellow ground). Fresh hypabyssal kimberlite is usually encountered after drilling through 12 to 60m of weathered zone. Parallel regional jointing often accompanies the fissures. They do not contain any igneous material, except for a few indicator minerals or traces of mica (*Woodford et al., in press*).

Blows and enlargements frequently occur along the fissure and can be easily recognized on aerial photographs due to the presence of well-developed calcrete. They are commonly 4 to 10m wide and consist of decomposed igneous material, containing a fair amount of crustal or mantle xenoliths and megacrysts. Kimberlite fissures are distinguished from dolerite dykes on aerial-photographs as regularly spaced, narrow, co-linear features with relatively denser vegetation growth along the fissure (*Woodford et al., in press*).

Kimberlite diatremes are unevenly distributed. They are not very common and vary in diameter from only 10 to 400m in the western Karoo, Sutherland, Victoria West, Britstown, Prieska and

East Griqualand areas. They are more numerous and extensive (200 to 1000m in diameter) on the Kaapvaal craton. Both the fresh and weathered hypabyssal kimberlite can form either positive-relief hills or negative-relief, calcrete-rich depressions. They contain a large amount and a wide variety of mantle and crustal xenolithes as well as megacrysts (*Woodford et al., in press*).

The emplacement of clusters on a *regional scale* was guided by up-welling within the mantle. Their location has been a matter of debate for many years and several theories have been put forward, i.e. hot-spot tracks, crustal tectonics, dynamics of the mantle, etc.

On a *local scale*, a common tectonic process guided the emplacement of the kimberlite swarms. The fact that swarms can be subdivided into sub-swarms points to a vertical hierarchy within the fracturing system at depth, i.e. fissures, dykes, parental dykes, larger bodies etc. The larger bodies were controlled by some deep mantle process, while the individual fractures and sub-swarms were controlled by very localised pre-existing fractures, such as dolerite dykes, master joints or faults.

The intrusion of the kimberlites did not result in the intensive thermal metamorphism of the Karoo sediments, as did the dolerites and thus they did not significantly alter the hydrological properties of the sediments. On a regional scale, however, clusters of kimberlites may represent important fractured domains (*Woodford et al., in press*).

On a local scale, the thin kimberlite dykes (< 3 m) are generally only weakly jointed and thus have a very low permeability, especially within the highly decomposed upper section of the dyke. The strong regional jointing and reactivation of existing structures that accompanies the emplacement of kimberlite swarms may be important for the occurrence and movement of groundwater. Kimberlite blows or enlargements (diameter of 4 to 10m) may represent more permeable zones along the dykes, as they are always more heterogeneous in texture, more deeply weathered and marked by dense bush growth (*Woodford et al., in press*).

Large kimberlite pipes or *diatremes* are more heterogeneous and brecciated. There is thus a possibility that high-yielding boreholes can be sited alongside these features, similar to the breccia plugs (*Woodford et al., in press*).

The Department of Water Affairs and Forestry have drilled five exploration boreholes into and alongside kimberlite dykes in the Loxton area (**Plate 3.6.3.4.(a)**) (*Woodford and Chevallier, 1998*) and one borehole into a diatreme at Carnarvon.

The NNE trending *Loxton kimberlite dyke* is situated 1km north of Loxton. The dyke is 3m wide and has a vertical attitude. Three 150m deep boreholes were drilled on this structure in the vicinity of its intersection with a NW trending dolerite dyke, as follows:

- a) In the middle of the dyke,
- b) In the kimberlite dyke at the intersection zone, and
- c) Approximately 1m from the dyke contact (150m north of the kimberlite / dolerite dyke intersection).

Boreholes (a) and (b) intercepted highly decomposed kimberlite (yellow-ground) to a depth of 11 - 12m and weathered kimberlite (green-ground) from 12 to 14m, below which depth the kimberlite was fresh (blue-ground). Only seepage was recorded at the transition zone between the weathered and fresh kimberlite.

The *Nuweland kimberlite dyke* forms part of narrow, N-S trending corridor of intense fracturing and kimberlite intrusion, some 12km south-west of Loxton. Two diatremes and a number of blow-pipes have been mapped. The fissures and blow-pipes contain kimberlitic material (mainly yellow-ground) and the diatremes contain fresher kimberlite and breccia. Most of the other fissures and parallel joints are barren or contain micaceous, calcretized material. Two exploration boreholes were drilled as follows:

- (a) in the center of the main kimberlite fissure to a depth of 162m, and
- (b) into a parallel, but barren fissure to a depth of 150m, some 22m east of borehole (a).

Borehole (a) only intercepted seepage inflow at 47m, despite the heterogeneity, textural and structural complexity of the dyke. Borehole (b) drilled into the open or "barren" fissure struck a water-bearing fracture at 65m that yielded 4 l/s (*Woodford and Chevallier, 1998*).

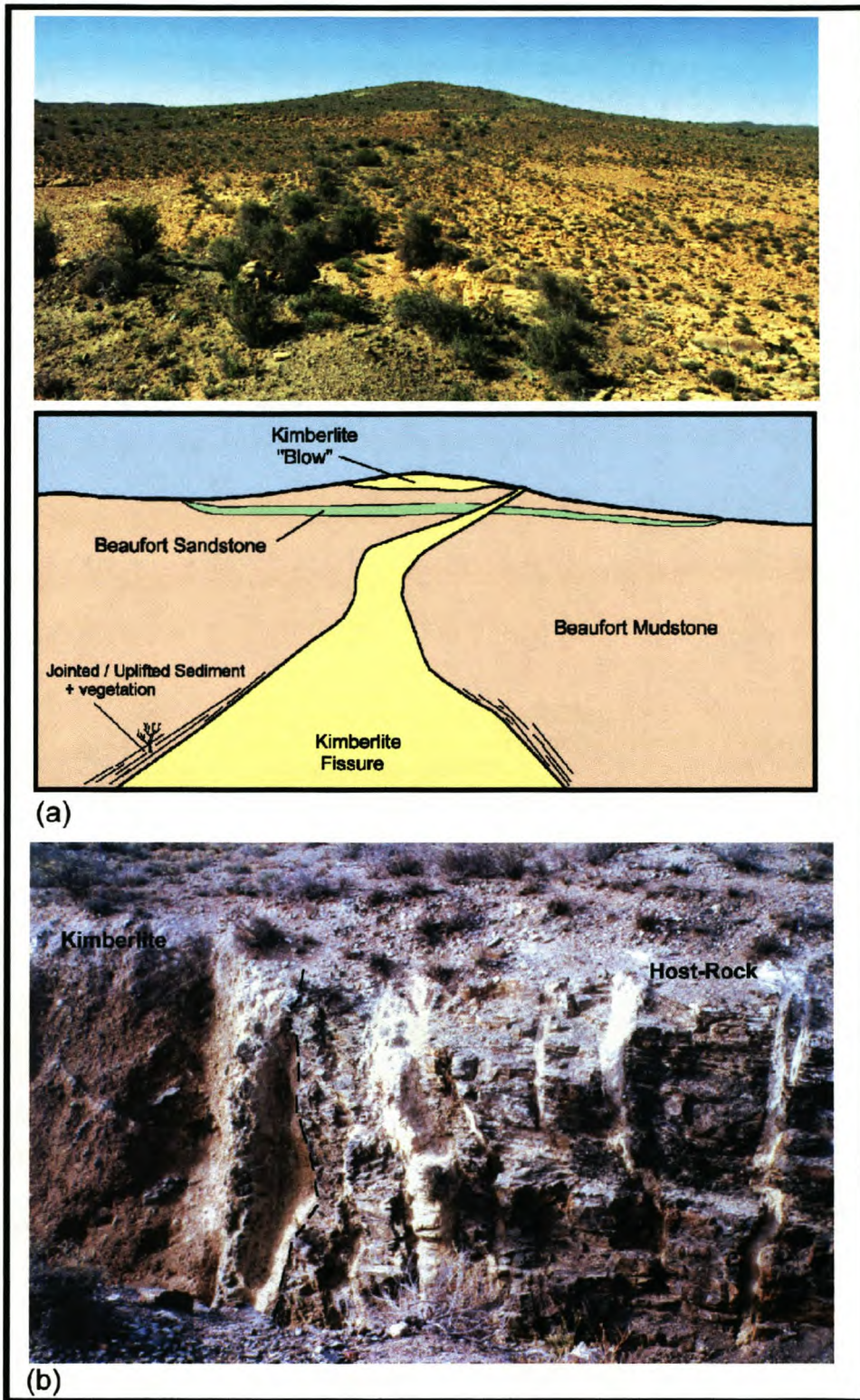


**Plate 3.6.3.4.** (a) Kimberlite fissure and pipe on the farm Nuweland (Loxton) and (b) Cross-section of kimberlite body on the farm Meltonwold (Victoria West) – Note thin kimberlite, calcite and calcrete stringers parallel to the main body.

The diamond-mining operation on Jagersfontein kimberlite diatreme in the south-western Free State extended to a depth of 750m below the surface. In order to keep the waterlevel below this depth some 64 000 m<sup>3</sup>/month of groundwater had to be abstracted continuously at a rate of 25 l/s (Woodford *et al.*, *in press*).

In 1971, De Beers Consolidated Mines (Ltd.) ceased mining and gave the Jagersfontein Municipality permission to abstract groundwater from the mine in 1980. During this time the piezometric level in open-pit and shafts recovered from 750m to 183m below ground-level (bgl). During the period January 1980 to February 1982, the Municipality abstracted a total of 497 308 m<sup>3</sup> of groundwater via a pump installed in an abandoned shaft (Kok, 1982), with a maximum waterlevel drawdown of 0.66 m. The pump inlet was installed at 220m and the pump rate was set at 17.5 l/s. The waterlevel and chemical information point to the existence of two separate aquifers, namely (Woodford *et al.*, *in press*):

- (a) A shallow, more “typical” Karoo fractured-rock aquifer (**Figure 3.6.3.4** – Well 1, showing a waterlevel of 4.8m.bgl), containing recently recharged water and,
- (b) A deeper aquifer (intercepted in the mine, piezometric level 183m.bgl) containing older water.

The occurrence of groundwater associated with *kimberlite dykes* in the Loxton – Victoria West area, was also investigated using yield information from privately drilled boreholes and field measurements of distance drilled from the dyke contact. Only three boreholes of the 71 visited were drilled into the dyke, because farmers tend to avoid drilling into the centre of these structures due to experience of low yields and problems of borehole collapse.

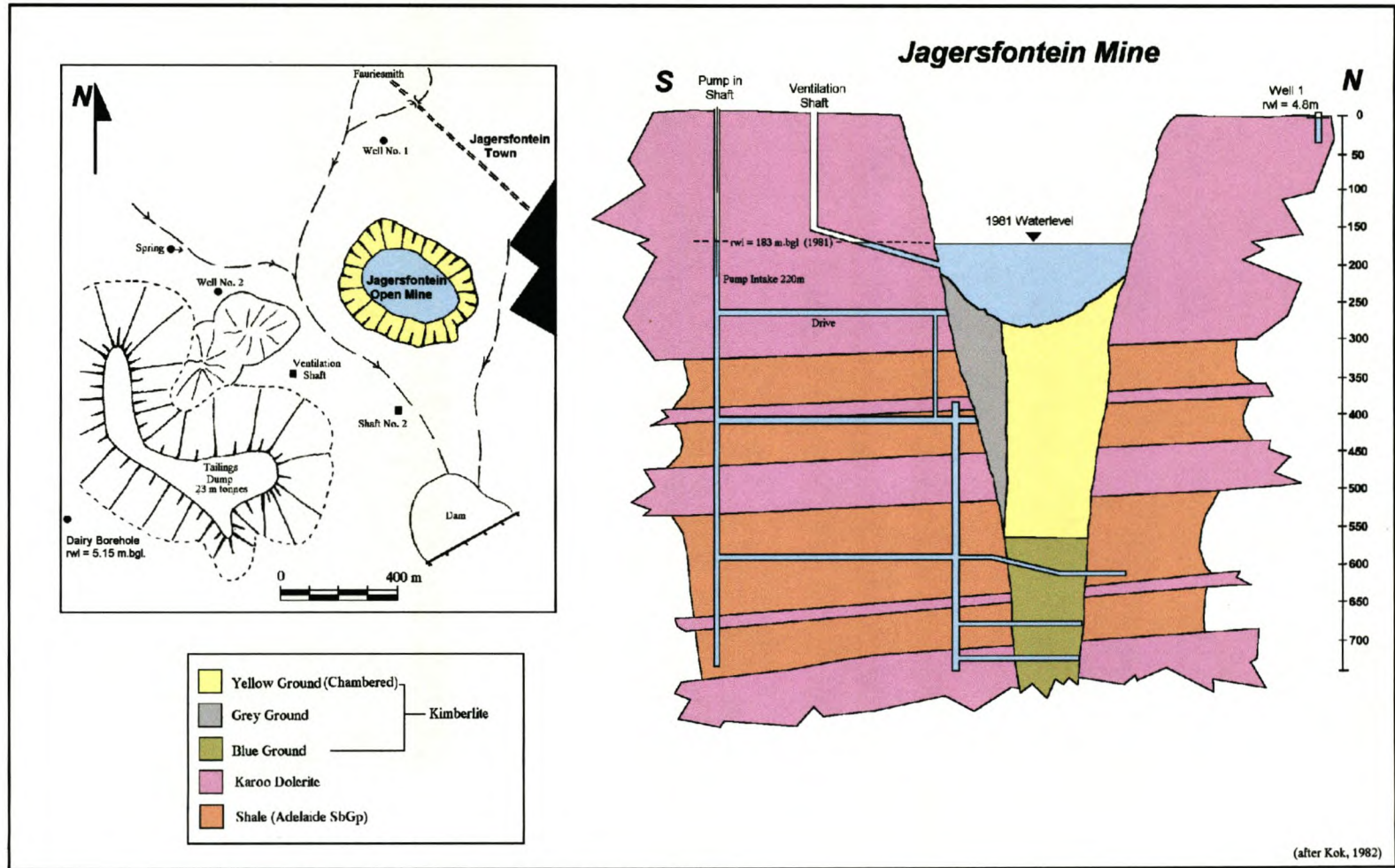
Almost half (48%) of the boreholes targeting kimberlite dykes yield 1 l/s or less, while 14 or 20% of the boreholes yielding more than 5 l/s are located further than 2m from the dyke contact. The “background” or median borehole yield for the area is 1.3 l/s (N = 827, Mean = 2.9 l/s, Standard Deviation = 4.3 l/s), which would account for the distribution within the yield classes of up to 2 l/s. The “abnormally” higher yielding boreholes appear to be located away from the dyke, where the probability (0.12) of intercepting greater than 5 l/s is highest at distances in excess of 5m from the contact (Woodford *et al.*, *in press*).

In conclusion, boreholes sited into kimberlite fissures commonly yield very small amounts of groundwater, mainly due to clogging of near-surface joints by clay produced by weathering / decomposition of the kimberlite. The transgressive, water-bearing fractures often observed on dolerite dykes, do not appear to have been developed along kimberlite fissures. Seepage is only

found in the weakly jointed transition zone between the weathered and fresh kimberlite. However, the local and regional fracturing that accompanied the emplacement of the kimberlite, mainly mega-joints, can deliver appreciable amounts of groundwater. Kimberlite diatremes, pipes and fissures have not been fully investigated and should be reassessed as potential targets (*Woodford et al., in press*).

Non-intrusive tectonic features include regional lineaments, folding, vertical jointing and faulting, bedding-plane fracturing and seismotectonic / neotectonic / unloading features (*Woodford et al., in press*).

**Figure 3.6.3.4. Geohydrology of the Jagersfontein Kimberlite Diatreme.**



### 3.6.3.5. Regional lineaments

Deep crustal and hidden geophysical features of the basement include the Beattie, Williston and Mbashe magnetic anomalies, the Kaapvaal Craton margin, the mega-fabric of the Namaqua-Natal belt (*Thomas et al., 1992*) and a magnetic high below Northern Lesotho (**Figure 3.6.3.5**). Shallow crustal mega-faults that intersect the Karoo Supergroup include the Tugela (Natal), Matatiele (Transkei) and Helspoort (Lesotho-Free State) faults.

Although no regional remote sensing studies has been done to specifically identify lineaments, the Digital Elevation Model of the Main Karoo Basin shows the following major morphological features that are apparently unrelated to dolerite intrusions (*Woodford et al., in press*):

1. The ENE-trending Transkei lineament seems to link the Williston anomaly to the Melville shear.
2. The NE-trending lineament-corridor of Western Lesotho links into the Tugela fault and the Lesotho fault. The Tugela fault brings the Vryheid Formation (Ecca Group) into contact with the Adelaide Subgroup (Beaufort Group). The Western Lesotho lineament is well defined on satellite imagery, but has no field expression - it probably comprises a zone of dense jointing not readily visible at the field-scale.
3. The Matatiele fault forms an extension of a curved morphological lineament, which cuts across southern Lesotho. It is down-thrown some 240m to the north. Nixon et al. (1983) suggested that faulting in the Quaternary was responsible for the alluvium-filled trough in the Cedarville flats.
4. Two additional major N-S trending morphological lineaments that appear unrelated to the Karoo dolerite magmatism occur in the eastern Karoo.

None of the lineaments discussed above have been described from a hydrological point of view. The Tugela fault may be of particular interest because it resulted in the juxtaposition of two different formations of different geohydrological character (*Woodford et al., in press*).

The direct influence of deep-seated pre-Karoo structures on the hydrology of the Karoo is unknown. However, the Orange-Fish River tunnel project indicated the tremendous yield

potential of these deep-seated structures, when a discrete, open east-west orientated fissure-zone was intersected and caused flooding of the tunnel (*Meyer and van Zijl, 1980*). From **Figure 3.6.3.5** it would appear that the fracturing responsible for this flooding may be related to the intersection of a number of major deep-seated lineaments which include the Kaapvaal craton margin, the Lesotho fault and lineament, and a further north-south orientated lineament.

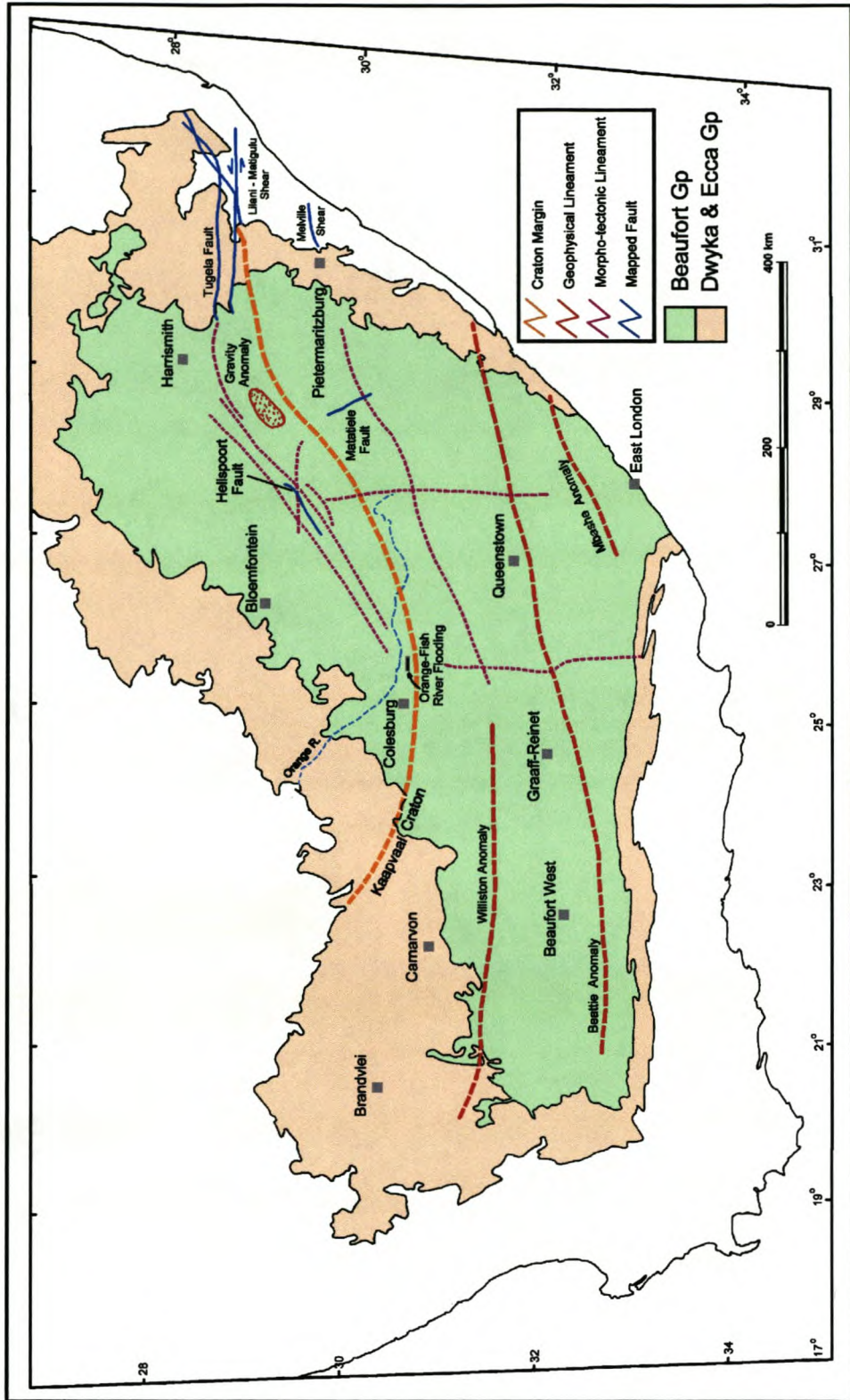


**Figure 3.6.3.5.** Deep-seated Pre-Karoo structures (geophysical anomalies), major faults (Thomas et al., 1992) and morphological lineaments.

### 3.6.3.6. Folding

The east-west-trending Cape Fold Belt developed during Permo-Triassic times (278 to 230 Ma) as a result of the closure of the Cape Basin. The uplifted mountain belt became a source for large volumes of sediment that was deposited in the Karoo foreland basin. The Cape Orogeny resulted in fairly regular E-W-trending fold axes, although arcuation commonly occurs. It has been divided into six zones with differing degrees of structural deformation (*Hälbich and Swart, 1983*). The variable style and intensity of folding that affected the Karoo Supergroup were studied in detail along two N-S cross-sections in the vicinity of Beaufort West (*Coetzee, 1983; Hälbich and Swart, 1983*; summarized by *Cole et al. 1991 and Woodford and Chevallier, 1998*).

According to Hälbich and Swart 1983, the northernmost folded sediments of the Karoo Supergroup (**Zone 1**) occur between 32°30' and 32°45', and are characteristically sinusoidal, upright mega-folds with horizontal axes, interlimb angles of about 170° and wavelengths of 2 to 3km. The sandstone beds are cut by many E-W-trending listric thrusts (fractures oblique to the bedding) filled with quartz, conjugate joints and quartz-filled shears and tension gashes. Bedding plane slip appears to have been insignificant.

Cleavage development is restricted to the shale units that have been affected by thrusting. Drill-core samples from the farm Kaffirfontein, approximately 30km southeast of Beaufort West, indicated a total absence of bedding-plane or other horizontally disposed joints in depth. In contrast, the vertical joint component is strongly developed with joint apertures of "fissure-size", lined with calcite or quartz, occurring commonly. Campbell estimated an average joint-density of 3-15 joints per m<sup>2</sup> in sandstone outcrops surveyed within a 30km radius of Beaufort West. He also noted that the joint apertures varied between 1 to 2mm (*Woodford et al., in press*).

**Zone 2** extends from 32°45' to the contact between the Beaufort and Ecca Groups. It is characterised by symmetric, upright, rounded folds with interlimb angles of 130°. Small monoclines are sometimes associated with listric thrusts in the sandstone. They are asymmetric with respect to the fold-axial planes and are probably older. Conjugate joints, shears and tension gashes are found, similar to those in *Zone 1* (*Woodford et al., in press*).

**Zone 3** includes the Ecca and Dwyka Groups. It corresponds to an abrupt transition to northward facing, asymmetric mega-folds with interlimb angles of less than 90°. Intense folding and well developed listric thrusting accounts for an estimated 30% of shortening in this zone. Well developed thrusting has been described near Laingsberg (*Newton, 1993*). Fracturing in the form

of tension gashes and bedding plane slip occurs commonly. Cleavage is very well developed in the shale and mudstones.

In addition to the E-W parallel folds described above, a number of oblique lineaments, fracture-sets and master-joints, trending NNW and NNE, occur in the Beaufort West area (*Stear, 1980; Woodford and Chevallier, 1998*). They also occur further to the north in the Western Karoo Basin and have been related to dolerite and kimberlite intrusion and neotectonic events.

The tightly folded Karoo strata should have well-developed secondary permeability because of the dense network of open fractures of different geometry, size and attitude. The development of vertical fractures is controlled by lithological boundaries with the result that the vertical hydraulic conductivities are relatively low. In addition, the high degree of connectivity between fractures should result in more extensive aquifers, when compared to the intrusive-controlled aquifers. Farmers in the southern Karoo, below the Great Escarpment, commonly site successful boreholes on the fold-axes and antithetic fracture systems. A hydrocensus carried out by the Department of Water Affairs and Forestry in the Beaufort West and Rietbron areas indicates that E-W jointing along anticlinal fold-axes are the most successful exploration targets for groundwater (*Woodford et al., in press*).

### 3.6.3.7. Vertical faulting and master jointing

The distribution of master joints and their role in the geological and structural framework of Southern Africa are not well documented. The Western Karoo has been investigated in detail (*Woodford and Chevallier, 1998*).

Master joints occur as orthogonal sets of fracturing, consisting of one orientation of systematic joints and another of non-systematic joints (*Hancock and Engelder, 1989*).

- The *systematic joint-sets* are dominant in the Karoo and often form extensive features (>1km), that are detectable with remote sensing. In general, the spacing between joints is proportional to their length. Kilometre-long mega-joints are meters apart, whereas master joints with a length of tens of metres are spaced at half a meter or less.
- *Non - systematic orthogonal-joints* are less extensive features, forming a link between the prominent joints without intersecting them, resulting in a "ladder-like" pattern. Non-systematic joints are not visible on the conventional remote sensing imagery.

Extensive mega-joints and faults have considerable vertical extension and therefore cut through different lithological units. Short joints, especially the non-systematic orthogonal joints, only affect individual competent layers (sandstone).

The systematic master-joints are regionally extensive features that occur throughout the Western Karoo Basin, and extend into the Cape Fold Belt. Two sets of systematic joints are commonly encountered in the Western Karoo (*Woodford et al., in press*):

1. Master-joints with a predominant NNW-trend, fluctuating between NS and N150°, and
2. Those with a predominant NNE-trend, fluctuating between N10° and N40°.

The NNW-trending master-joint and fracture sets appear to be more extensively developed in the area between Loxton and Middelburg, where extensive NNW-trending dolerite dykes occurs.

This fracture-system has been described in other parts of the Karoo by Parsons (1986) and Woodford (1989). Tordiffe (1978) and Vandoolaeghe (1980) also found a similar joint-pattern in the Great Fish River Basin and Queenstown area in the Eastern Cape, respectively. A comparative statistical study of jointing in the Graaff-Reinet and Beaufort West areas indicates that the non-systematic orthogonal joints are not as well developed at Beaufort West as they are at Graaff-Reinet (*Woodford et al., in press*).

The NNE-trending master-joints and fractures appear to be more pronounced in the area between Calvinia and Loxton, where they parallel the major kimberlite / carbonatite fracture-system. The emplacement of the Cretaceous Salpeterkop carbonatite complex had a strong influence on the regional distribution of NNE-trending master-joints (*Woodford et al., in press*).

Regional jointing is often related to neotectonics and erosional unloading (*Hancock and Engelder, 1989*). However, Woodford and Chevallier (1998) showed that prominent systematic master-joints and faults of the Western Karoo often show signs of reactivation and are much older than recent episodes of erosional unloading. The NNW orientated joints for instance, reflect a major stress system within the Western Karoo that has been active since the early phases of the break-up of Gondwana, until recent times. The NNE trending joint-set may be younger and linked to emplacement of the kimberlites. Both joint directions are therefore the result of regional crustal tectonics (*Woodford et al., in press*).

The less well-developed, orthogonal non-systematic joint system may be the result of uplift and thermal cooling after erosional unloading (*Woodford et al., in press*).

Vertical jointing is largely developed in the sandstone of the Beaufort Group. With the exception of the extensive mega-joints and faults, master-joints generally have limited vertical extension and poor interconnectivity. Fracture connectivity may be enhanced where two orientations of systematic joints, together with their orthogonal systems, are present which leads to a 4-fold fractured network (*Woodford et al., in press*).

The regional jointing plays a major role in determining the directional permeability (*Wending et al., 1994*) in fractured-rock aquifers, which generally is at a maximum in the direction of the principal systematic joints. On a regional scale the Beaufort Group sandstones of the Western Karoo should thus exhibit a north-south orientated tensor of maximum permeability.

Very little information has been published on the occurrence of groundwater in discrete fracture or fissure zones per se, i.e. those not directly related to magma intrusion or folding in the Karoo Basin. This is probably because they are not easily detected on aerial-photographs, by geophysical methods or by field mapping, as well as a poor understanding of their tectonic origin. A typical example of such a fissure is the widely publicized, yet poorly understood, occurrence in Shaft 2 of the Orange-Fish River Tunnel (*Woodford et al., in press*).

In general, the ubiquitous and often regularly-spaced joints visible in outcrop do not in themselves represent zones of higher permeability, where successful boreholes can be regularly sited. Well-jointed channel-sandstone of the Beaufort Group may be permeable and reportedly high-yielding boreholes have been drilled into these bodies (*Woodford et al., in press*).

Woodford and Chevallier (1998) reported higher yields in boreholes drilled within 15m of master-joints and fracture zones (**Plate 3.6.3.7**) in the Loxton-Victoria West area, but found that the overall productivity of these boreholes (Mean = 2.4 l/s, Standard Deviation = 4.1 l/s, Median = 1.0 l/s) were on average lower, than the ambient borehole yields (Mean = 2.9 l/s, Standard Deviation = 4.3 l/s, Median = 1.3 l/s) of the area.

Mega-joints and -faults showing signs of reactivation are more important from a geohydrological perspective as they are more deep-seated features and can act as conduits for groundwater flow. Unfortunately only a few boreholes have been drilled into these structures, mostly by farmers.

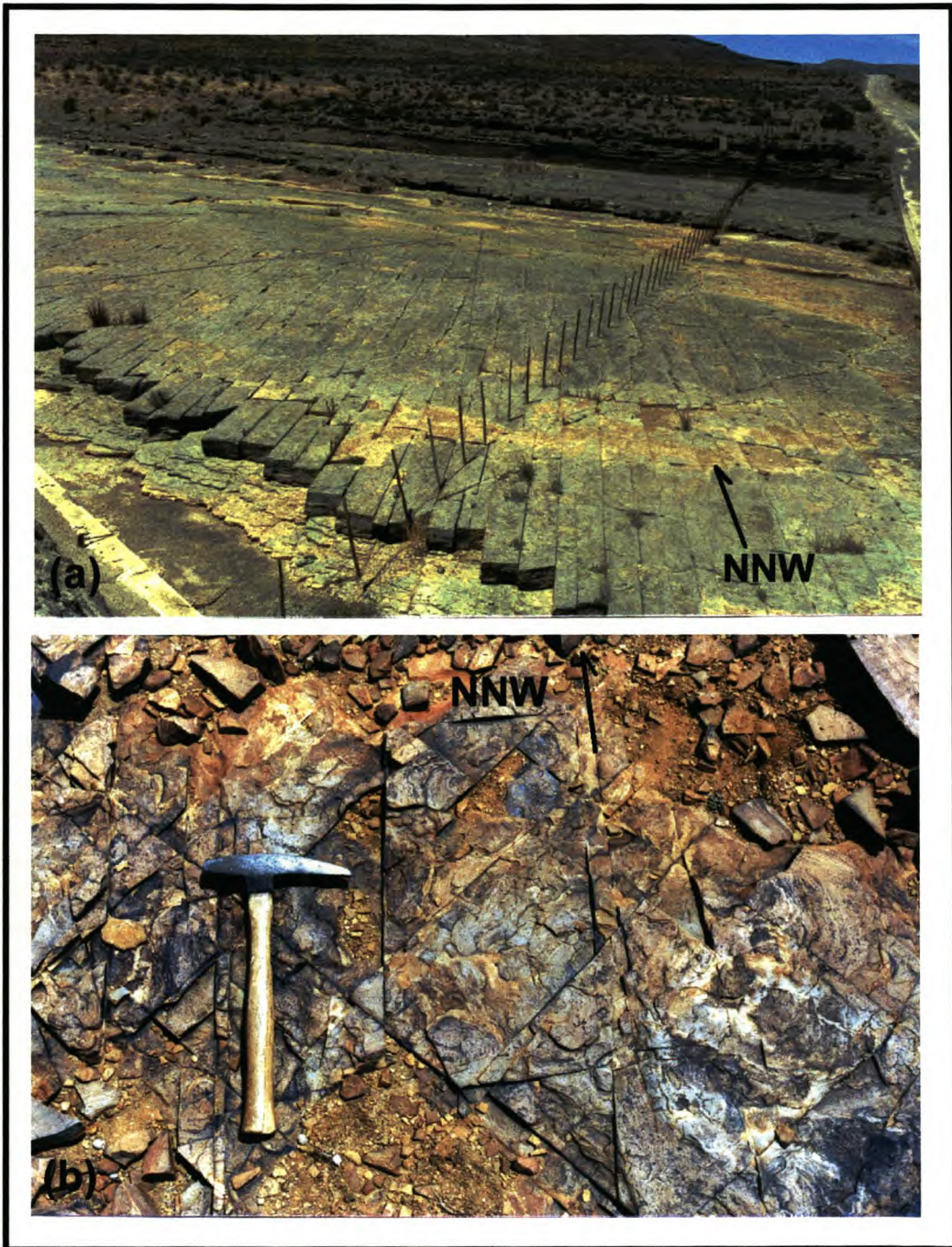


**Plate 3.6.3.7.** (a) Prominent NNW master joints with orthogonal set responsible for the “ladder” effect, Hillcrest, Sheet 3122DC (b) Superimposition of two orientations of master jointing, namely NNW and NNE at Loxton, Sheet 3122CB.

### 3.6.3.8. Bedding-Plane Fracturing

Except for the southern folded regions, there is no geological record of regional horizontal fractures in the Main Karoo Basin (*Woodford et al., in press*).

Botha et al. (1998) proposed that Karoo sediments fracture along bedding-planes episodes of isostatic rebound and erosional unloading, as a result of the difference in elasticity between the different formations. Botha states that the increasing overburden pressures have resulted in the closure of most of the deeper-seated, bedding-parallel fractures when the rate of erosion declined.

Differential gravity-loading in areas of extreme topographic contrast (i.e. the Great Escarpment) may result in the development of horizontal fracturing. Slope-creep along steep-sided valleys will result in the development of increased tensile stresses at the toe of the slope. Slope-creep usually occurs in extensively jointed rocks with a minimum slope inclination, causing existing joints on the slope to rotate and horizontal joints below the valley-floor to open and shear.

Smaller scale horizontal fractures are fairly common in the Main Karoo Basin. Bedding-plane, listric fractures occur within the overlying sedimentary rocks entrapped in dolerite ring-structures. They result from uplift and drag of the rocks above the inclined dolerite sheet. They are commonly 10 to 20m in extent and exhibit a horizontal-shear pattern. The zone affected by this shear deformation is usually in the order of 0.5m in thickness (*Woodford et al., in press*).

Drill-core from the Kopoasfontein stratigraphic borehole near Calvinia, showed that horizontal cleavage is well developed within the Eccca shales of the Tierberg, Whitehill and Prince Albert Formations, but no major horizontal fractures were intercepted. Horizontal cleavage is the most extensively developed within the Tierberg shales (*Woodford et al., in press*).

Horizontal fractures play an important role in the lateral connectivity and water circulation between vertical fractures in the near-surface, especially within the weathered zone. However, they do not seem to form large discontinuities that can act as laterally extensive aquifers.

Hydraulic tests on 24 shallow boreholes drilled into the Eccca shale on the Orange Free State University Campus Test Site, by the Institute for Ground Water, showed that the main water-strikes were associated with bedding-planes (*Botha et al., 1998*). Ten of the boreholes intersected a horizontal fracture some 100m x 10m in extent.

The existence and hydrological role of shallow, open, oblique or flat-lying fractures linked to topographic-uplift alongside steep-sided valleys, has yet to be ascertained (*Woodford et al., in press*).

### **3.7. Geohydrology**

The general hydrological characteristics of the various litho-stratigraphic units, its sedimentation processes and diagenesis, are more important when considering the longer-term sustainable utilisation of the Karoo aquifers (storativity) (*Woodford et al., in press*).

#### **3.7.1. Beaufort Group**

The main sediment source for the Beaufort rocks lay along the high-lying southern margin of the Basin. Coarser grained rocks are found near the Cape Fold Belt (alluvial fan and braided stream environments), while mudstone, shale and fine-grained sandstones dominate the more distal central and northern portion (meandering river and floodplain environment) of the Basin. The sedimentary units in the Group therefore usually have very low primary hydraulic conductivities.

The geometry of these aquifers is complicated by the lateral migration of meandering streams over a floodplain. Aquifers in the Beaufort Group will thus not only be multi-layered, but also multi-porous with variable thicknesses. The contact plane between two different sedimentary layers causes a discontinuity in the hydraulic properties of the aquifer (*Woodford et al., in press*).

Aquifers in the Beaufort Group exhibit a complex behavior, which is further complicated by the fact that many of the coarser, more permeable, sedimentary bodies are lens-shaped. High-yielding boreholes in the Beaufort Group are therefore limited and if the aquifer is not recharged frequently, it will have a short live-span (*Woodford et al., in press*).

Van Wyk (1963) and Vegter (1992) state that the porosity of Karoo sediments appears to be higher nearer the earth's surface, probably due to weathering and leaching of the rocks within the upper 30m. Similarly, the primary porosity of the sediments is expected to decrease with depth due to increasing lithostatic pressures and temperatures.

### 3.7.2. Karoo Dolerites

Dolerite intrusions represent the roots of the volcanic system and are presumed to be of the same age as the extrusive lavas. Erosion that affected the Main Karoo Basin has revealed the deep portions of the intrusive system, displaying a high degree of tectonic complexity.

The Karoo dolerite includes a wide range of petrological facies and consists of an interconnected network of dykes and sills. It is nearly impossible to single out any particular intrusive or tectonic event, however it appears that a very large number of fractures were intruded simultaneously by magma and that the dolerite intrusive network acted as a shallow stockwork-like reservoir (Woodford *et al.*, *in press*).

Van Wyk (1963) conducted a number of porosity determinations on specimens of the same rock-type obtained at different distances from dolerite intrusions. The results clearly indicate a marked decline in porosity of the host-rock within the contact metamorphic aureole of the intrusive, mainly as a result of re-crystallisation of the host-rock silicates and infiltration / cementation by magmatic silica.

It would appear that there is a lithological control on the emplacement of dykes within the Western Karoo Basin. A sharp decrease in intrusion density is noted at the boundary between the lower Ecca and the upper Ecca. This boundary corresponds to the appearance of the first sandstone units in the Karoo Basin. Even if many dykes can still be seen within the lower Ecca and Dwyka Formations, as well as the Nama basement, the bulk of the dykes are stratabound and concentrated in the Upper Ecca and Beaufort Group. This means that they propagate laterally along strike and not vertically and that their magmatic source was not everywhere under the Karoo Basin but concentrated at one spot (***the East London triple junction***) (Woodford *et al.*, *in press*).

A low primary porosity and permeability is characteristic for the Karoo rock. Yields of boreholes are increased in brittle deformation zones, associated with dolerite intrusives, faults and fold axes (Johnson *et al.*, 1997; Woodford *et al.*, 1996 and *unpub.*). This fracturing of arenaceous units and argillaceous layers, leads to the higher secondary porosity and permeability achieved. Sedimentary rock units do not constitute reliable aquifers in the absence of fractures and joint systems. Jointing is common along intrusive contacts, being of particular value on the up-slope side of the hydraulic gradient in the Karoo sediments (Robins, 1980).

Dolerite dykes develop by rapid hydraulic fracturing via the propagation of a fluid-filled open fissure, resulting in a massive magmatic intrusion with a neat and transgressive contact with the country rock. This fracturing mechanism is in contrast to the slow mode of hydraulic fracturing responsible for breccia-intrusions (i.e. kimberlite). The intrusion develops when the magma pressure at the tip of the fissure overcomes the tensile strength of the surrounding rock. Dykes can develop vertically upwards or laterally alongstrike over very long distances, as long as the magma pressure at the tip of the fissure is maintained. The intrusion of dolerite and basaltic dykes are therefore never accompanied by brecciation, deformation or shearing of the host-rock during their propagation (*Woodford et al., in press*).

The attitude of dykes often change with depth (i.e. are curved or dislocated). This phenomenon can be attributed to vertical off-setting as a result of vertical en-échelon segmentation (E-W shear dykes and their associated riedel-shears (**Figure 3.7.2.A.(a)**), or due to interconnecting of dykes between sediment layers (*Woodford et al., in press*).

The average thickness of Karoo dolerite dykes ranges between 2 and 10m (*Woodford and Chevallier, 1998*). In general, the width of a dyke is a function of its length. In other words, the wider a dyke is, the longer it will be (this probably also applies to the vertical extension of the feature). For example, the major E-W dykes of Western Karoo Domain can attain widths of up to 70m. No relationship has been found between trend and thickness.

Country rock is often fractured during and after dyke emplacement. These fractures form a set of master joints parallel to its strike over a distance that does not vary greatly with the thickness of the dyke (between 5 and 15m). The dolerite dykes are also affected by thermal- or columnar-jointing perpendicular to their margins (**Figure 3.7.2.A.(b)**). Van Wyk (1963) observed two types of jointing associated with dyke intrusions in a number of coal-mines in the Vryheid-Dundee area, namely:

- a) Three sets of pervasive-thermal, columnar joints that are approximately 120° apart, and
- b) Joints parallel to the contact, confined mainly to the host rock alongside the dyke.

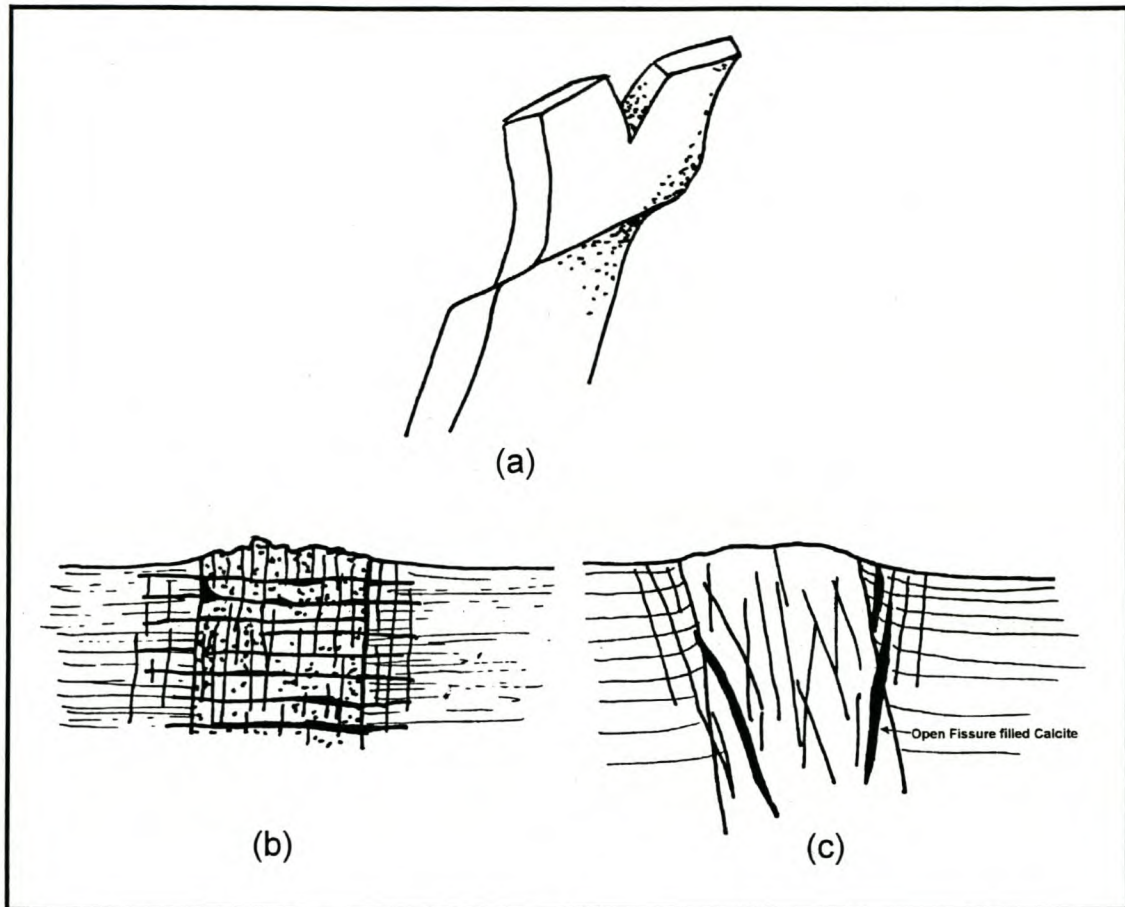


**Figure 3.7.2.A. (a) En-échelon Dolerite Dyke (b) Vertical & Horizontal Thermal Joints and (c) Tectonic Reactivation (Woodford et al., in press).**

Tectonic reactivation of the dolerite dykes have been observed in the Loxton-Victoria West area (Woodford and Chevallier, 1998), especially on the N-S dykes that have been reactivated by Cretaceous kimberlite activity or by more recent master jointing (Figure 3.7.2.A.(c)). Reactivation often results in sub-vertical fissures within the country rock and / or dyke itself, which are commonly highly weathered and filled with secondary calcite / calcrete (width of up to 150 mm). Uplifting or brecciation of the sediment along the dyke contact is also observed.

Localised upwarping of the country rock is often observed adjacent to dipping dykes (Figure 3.7.2.A.(c)), a result of later tectonic reactivation (Woodford et al., in press).

Davis and De Wiest stated in 1966 that, groundwater generally moves from levels of higher energy to levels of lower energy and that its energy is essentially the result of elevation and pressure. A piezometric level and not always a water table is the measured result as the water levels in the area do not always follow the topography and thus resemble the amount of fractures

penetrated, continuity, spacing and interconnectivity of fractures / joints in a borehole. Dykes or sills in the study area causes disruption in the groundwater flow patterns, resulting in the damming of water on the upslope side of these barriers. The bulk of the groundwater is stored in the matrices of the country rock, while the fractures serve as preferred pathways for groundwater flow (Kirchner and Van Tonder, 1995).

A wide range of intrusive igneous petrological facies, consisting of an interconnected network of dykes and sills, are included in the Karoo dolerites. The Karoo Basin contains three major structural domains (dyke swarms): a Western Domain, Eastern Domain and Transkei-Lesotho-Northern Karoo Domain (Woodford *et al.*, *in press*).

This project falls under the Western Domain, characterized by (**Figure 3.6.1.** – Woodford *et al.*, *unpub.*):

- E-W dyke intrusions which may be extensive, continuous and up to 500km in length. These intrusions were along a major right-lateral EW dislocation / shear zone, accompanied by NW Riedel shears and NE P-type fractures.
- NNW dyke intrusions with a varied trajectory, curving from WNW in the south to NS in the north. Observed in the domain are extensive, regularly spaced structures from east to west. Two specifically well developed dyke systems are:
  1. The Middelburg Dyke, delimiting the Western Karoo Domain in the east and
  2. The Loxton Fracture Zone in the center of the domain.

The E-W dextral shear zone and NNW dyking patterns are typical features found in transform fault systems that developed between two rifts. The Western Karoo dolerite shear zone might therefore represent a major offset (or step) between one of the arms of the Eastern Karoo triple-junction and another failed rift zone along the South African / Namibian West Coast (**Figure 3.7.2.B**) (Woodford *et al.*, *in press*).

Dolerite dykes have always been and still are the preferred drilling target for groundwater in the Karoo. There are a number of reasons why these features are preferred for groundwater exploration, namely (Woodford *et al.*, *in press*):

1. There exists an apparent higher probability of drilling a wet borehole in or next to a dyke than in the host rock away from the dyke,
2. They are easily detected on remotely-sensed imagery, by relatively simple geophysical techniques (the magnetometer) and are clearly visible to both the skilled and unskilled eye in the field (i.e. if not outcropping, they are often conspicuous as lines of vegetation or animal-burrows).
3. Their relatively simple and regular 3D geometry makes it easy to conceptualise and site an exploration borehole in the field, and
4. They constitute a very cost effective groundwater target.

Enslin (1950) expresses the classical hydrological conceptualisation of Karoo dykes - ***“the effect of induration and crushing of the sedimentary rock is that the permeability has been increased and the contact zone has been changed into an aquifer lying between the solid dyke and the saturated, low permeability country rock”***.

Several aspects appear to affect occurrence of groundwater and the productivity of boreholes located in or near dolerite dykes (*Woodford et al., in press*).

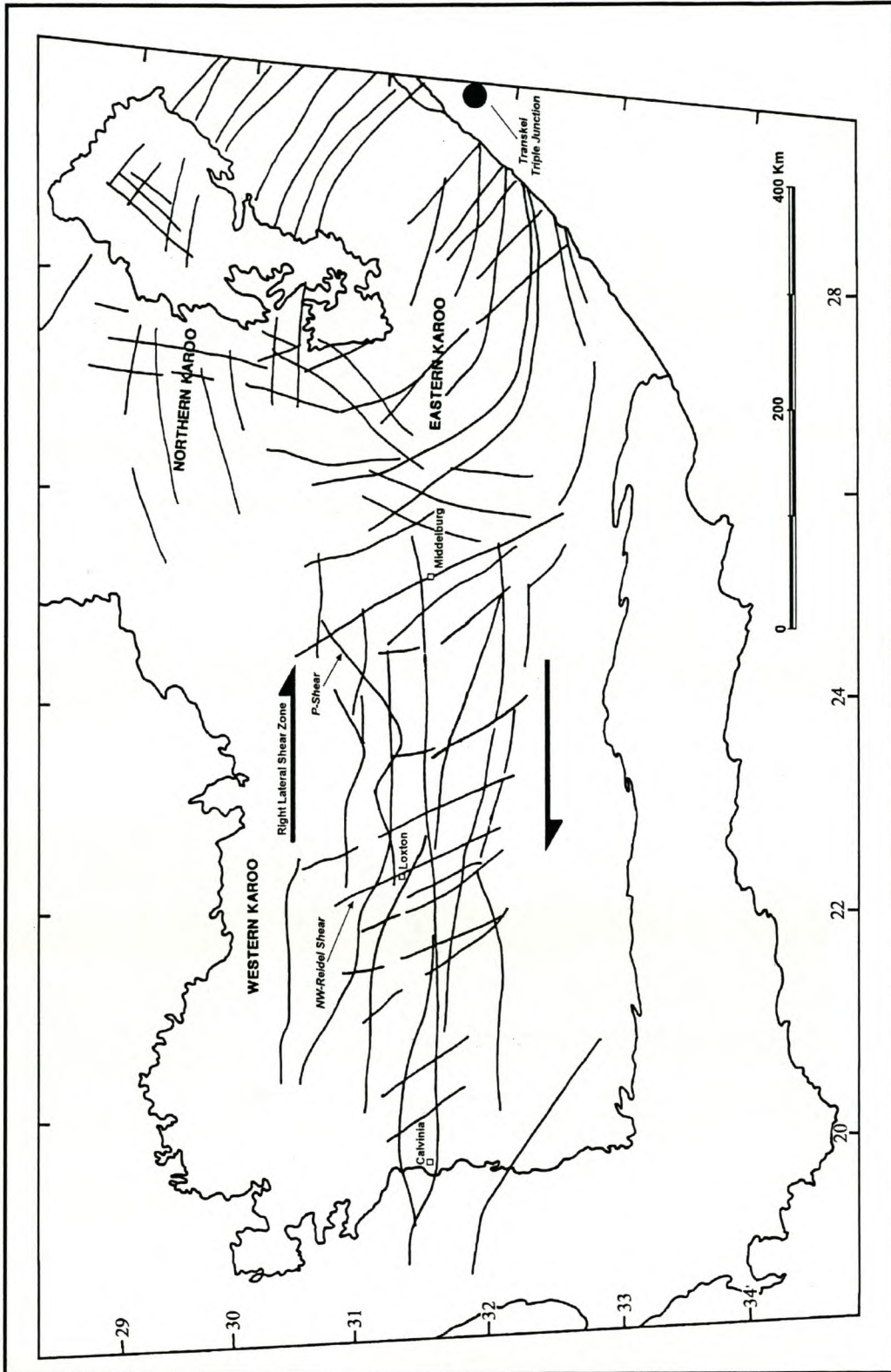


**Figure 3.7.2.B. Structural Domains and mechanism of emplacement of Dolerite Dykes (Woodford et al., in press).**

### 3.7.3. Distance from Dyke Contact

There is considerable debate concerning to what distance away from a dyke the host rock is metamorphosed and jointed, effecting the yield of a borehole drilled into this zone. Enslin (1950) illustrates this relationship, where the highest borehole yields are obtained within 1m of the dyke contact. Enslin (1950) and Van Wyk (1963) state that the jointed contact zone is less than 30 cm wide, irrespective of dyke thickness. Note that because distances from the dyke edge are measured at the surface, the dip of the dyke must also be considered. Also of importance is whether the dyke itself is water-bearing or not. Many researchers have found that drilling into the middle of solid dolerite dykes is often unsuccessful (*Enslin, 1950, Van Wyk, 1963*), while others have found that the dykes themselves are fractured (*Vegter, 1968; Woodford and Chevallier, 1998*).

Kruger and Kok (1976) analysed hydrocensus information and drilling logs from 3637 and 219 boreholes, respectively, in the Bethlehem, Ficksburg, Fouriesburg and Senekal district. Their work illustrates a number of important points, namely:

1. That the probability of a borehole striking  $> 0.14$  l/s in the Upper Beaufort sediments is extremely low,
2. Boreholes drilled alongside dykes (i.e. into the upper contact), without significantly penetrating the dyke itself, are more likely to be successful – although improvement in borehole yield is marginal,
3. The dykes themselves are almost always fractured and significantly higher yields can be obtained in these structures.

Woodford and Chevallier (1998) studied the relationship between yield data gathered from 594 privately drilled boreholes and their distance from the dyke contact, measured in the field. Only a poor statistical correlation exists between borehole yield and distance drilled from the dyke contact. Yields of up to 5-7 l/s can occur within 20m of a dyke, whereafter less than 5 l/s is more common. A similar result was obtained for 169 boreholes drilled into and alongside the Tweeling-Brandwag dyke, which indicates that borehole yields of 6-18 l/s occur within 5m of the dyke, whereafter the yields of less than 6 l/s are typically encountered.

### 3.7.4. Width of Dyke

Enslin (1950) states that Karoo dolerite dykes are seldom wider than 18.5m and generally between 2 to 8m in width. Many researchers have tried to relate the width of a dolerite dyke in the Karoo to the expected yield of a borehole sited on it. During 1964 to 1967, Kruger and Kok (1976) evaluated drilling results along dykes in the vicinity of Bethlehem, Ficksburg, Fouriesburg and Senekal, in the north-eastern Free State. They found a relationship between the width of a dyke and borehole yield, after analysing the results of 177 boreholes on drilled dykes - where dykes of between 4.5 and 14m produced yields of 2 to 5 l/s. They concluded that the highest borehole yields could be obtained on dykes of 7 to 11 metres wide. Vandoolaeghe (1980) found that higher borehole yields are obtained alongside dykes that are wider than 5m in the Queenstown area.

Woodford and Chevallier (1998), however, could not find a significant correlation between dyke width and yield of 539 privately-drilled boreholes in the Western Karoo. It is, however, apparent that thin dykes ( $\leq 2\text{m}$ ) do not deliver more than 4 l/s.

### 3.7.5. Dip of Dyke

The dip of a dolerite dyke *per se* does not appear to have a major influence on the yield of boreholes drilled on it (Enslin, 1950; Vandoolaeghe, 1980), but it is important for siting of a successful borehole. Boreholes can be sited to intersect the "upper" or "lower" dyke contact depending on its attitude. Kruger and Kok (1976) produced a schematic diagram showing where boreholes should be sited in order to maximise groundwater yield, based on a detailed analysis of dyke drilling results in the north-eastern Free State. Various authors have also expressed the need to take into account the dyke attitude in relation to the direction of the local drainage (Paver *et al.*, 1943).

Landowners have reported many successful boreholes drilled into the upper-contact of dipping dykes. The Zandwerf dyke east of Calvinia produced high yields in this contact zone. Note that the water-bearing fractures do not follow the contact of either the dyke or the sill and that they transgress both intrusions. Other examples are the Welgevonden and the Perries dyke north of Graaff-Reinet (Woodford *et al.*, *in press*).

### 3.7.6. En- échelon Dyke Segmentation

Lateral displacement or en-échelon segmentation often occurs along the major E-W dykes, such as the Tweeling-Brandwag dyke at Beaufort West. This dyke represents the southernmost extension of a major E-W dyke system within the Western Karoo and is approximately 11m wide. Note that the point of dislocation marks a change in the attitude of the dyke. Vertical offsets of the parent dyke are also observed in these structures, where intense fracturing and high groundwater yields are common (*Woodford et al., in press*).

**Figure 3.6.3.E.** is a typical example of a 20m wide, E-W shear dyke on the farm De Wilg to the south-west of Loxton (*Woodford and Chevallier, 1998*).

### 3.7.7. Transgressive Fracturing

Large volumes of groundwater are often intercepted in discrete, open-fractures or fissures that transgress the dyke, and extend some distance into the country rock (typically up to 15m away from the contact). The fractures are commonly sub-horizontal in attitude ( $< 50^\circ$ ). Vandoolaeghe (1980) concluded that horizontal- and oblique-fractures within the dolerite and adjacent sediments are the dominant water-bearing features in the Queenstown area.

These fractures occasionally extend several tens of metres away from the dyke into the country rock, i.e. a sub-horizontal, transgressive fracture in the vicinity of the 20m wide Dunblane Dyke near Middelburg, is reported to extend some 90m away from the dyke contact. The dyke forms part of an extensive NNW dyke system and can be traced from some 80km south in the Cradock district. The Dunblane dyke transgresses some of the dolerite ring-complex systems in the Middelburg area. This phenomena was at a few localities along the Tweeling-Brandwag dyke. These extensive sub-horizontal fractures are only observed in the near-surface where an advanced stage of weathering has taken place. Note that the deeper-seated transgressive, sub-horizontal open-fractures at 100-150m below surface (**Figure 3.6.3.E.**) in the De Wilg dyke do not extend more than 5m into the host rock (*Woodford et al., in press*).

### 3.7.8. Jointing Parallel to the Dyke Contact

Enslin (1950) and Boehmer (1986) proposed that Karoo dolerite dykes are jointed along a narrow zone that parallels the two contacts.

Enslin (1950) states that ***“some dolerite dykes (themselves) have vertical joints and fractures near their contacts at depth and that these zones in the dyke will then yield very large supplies of water. Owing to uncertainties of the existence of such joints at depth and technical difficulties that may be encountered if a borehole is drilled into this zone, boreholes are preferably sited to strike water in the indurated sediments alongside the dyke”***.

### 3.7.9. Effect of Dyke Attitude and Drainage

In the past, a number of authors have proposed that higher yields are obtained in boreholes sited on the upstream contact of dykes cutting drainage systems, where dykes are assumed to act as an impermeable barrier to groundwater flow. Paver et al (1943) states that boreholes should, in such cases, be sited as follows:

- a) If the dyke is vertical or near vertical then a site should be chosen on the drainage side of its outcrop and close to the contact.
- b) If the dyke dips steeply downstream a site should be chosen downstream from its outcrop, and at such a distance from it that the borehole will penetrate the dyke, and tap water trapped on the upstream side.
- c) If a dyke dips steeply upstream a site should be chosen upstream from its outcrop and such a distance from it that the borehole will reach the waterlevel before penetrating the dyke.
- d) If the dyke cuts the drainage obliquely a site should be chosen in accordance with the above and towards the side of the valley where the dyke is furthest downstream.

There are no valid grounds for such thinking, as it is the mechanisms and degree of dyke fracturing that controls the yield of the borehole. Impermeable dykes cutting across the groundwater flow path may result in elevated waterlevels on the upstream side of the dyke and the development of springs (*Woodford et al., in press*).

### 3.7.10. Dyke / Sill Intersections

Dolerite dykes (younger) that cut sills are often good targets for groundwater, especially in a valley-bottom situation where the sill material is highly weathered. The dyke-sill contact zone is generally not as wide or permeable as that of the dyke-sediment contact (*Paver et al, 1943, Van Wyk, 1963*). This may be due to the more intense development of thermal-joints along dolerite-sediment contacts as a result of differential cooling caused by the greater contrast in thermal conductance between the two rocks types. Transgressive fractures are often well developed in the vicinity of the dyke / sill contacts. For example, the Zandwerf dyke / sill intersection, where several high yielding transgressive fractures were intercepted within the weathered sill material and fresh dolerite dyke. This fracturing probably resulted during the simultaneous cooling of the dyke and the sill. The upper contact of the sill is weathered and decomposed, while the intruding finer grained dyke is not (*Woodford et al., in press*).

Jointing is common along the contact of the dyke (thermal) and within the adjacent baked, disturbed sediment. Boreholes drilled into this zone are generally higher yielding than those drilled away from the dyke in the undisturbed host rock. Syn- or post- intrusion tectonic and / or hydrothermal reactivation of the structure often results in the development of more discrete fractures or fissures that transgress the dyke and extend into the country rock. Boreholes intercepting such fractures often produce exceptionally high-yields (*Woodford et al., in press*).

On a regional scale, the structural domains have not as yet been shown to influence the regional hydrogeology. However, the wide and extensive dykes such as the E-W Victoria West dyke, the NNW Middelburg dyke and the curved "gap" dykes near East London, were major magma feeders and are accompanied by extensive fracturing (shearing and jointing). They form regional discontinuities that, although likely to have propagated laterally, extend to great depths within the crust. In theory these structures could form part of a fracture network wherein deeper-seated groundwater flows on a more regional scale. Boreholes correctly drilled into these features should also deliver high-yields, as is the case of the E-W Victoria West dyke (*Woodford et al., in press*).

On the local scale, the geometry, attitude, degree of weathering and fracturing of dykes influence the hydrological properties of individual structures. For example, thick dykes do not necessarily deform the country rocks more than do thin dykes, but the former may be more porous because of their granularity upon weathering. Emplacement of an en-échelon dyke is associated with

complex stress fields and strong deformation of the host-rock, make it a good drilling target for high-yielding boreholes. The hydrology of a particular dyke is related to a complex interplay of these parameters and can thus vary dramatically along the strike of the structure (*Woodford et al., in press*).

### **3.8. Seismicity, Neotectonics and Unloading**

A "stress province" (*Zoback and Zoback, 1980*) is formally defined as a region of "... relatively uniform upper-crustal stress field ... with consistent stress orientations and relative magnitudes ... (having) linear dimensions that range from 100 to 2000 km".

Within the upper continental crust of Southern Africa, the ambient neotectonic stress regimes differ markedly between the south-western and north-eastern portions of the subcontinent (*Zoback, 1992*), such that distinct stress provinces are recognisable. The stress province boundaries coincide with an emergent belt of earthquake activity, which in turn forms part of a larger system of relatively aseismic blocks and seismically active belts between the Nubian and Somalian plates (*Hartnady, 1990; Gordon and Stein, 1992; Gordon, 1995*).

No direct relationship has thus far been made between seismo-tectonic provinces and the occurrence of groundwater in the Karoo Basin. However, the fact that groundwater flow within Karoo aquifers is fracture dominated makes it plausible to hypothesise that fracturing created under the prevailing crustal-stress regime will significantly effect the occurrence of groundwater - but this has not yet been definitively demonstrated nor critically tested (*Hartnady and Woodford, 1996*).

*Bodmer (1994)* and *Sibson (1990)* show that orientation of reactivated faults are not only a function of the external principal stress, but also of the gradual build up of pore-fluid pressure. The greater the angle between the external stress and the fault, the greater the hydrostatic pressure must be to permit for reactivation. The build up of hydrostatic pressure will result in seismic-valving, a mechanism responsible for many earthquakes. *Bodmer (1994)* suggested that the focal mechanism could be used for predicting hydraulic overpressures and that seismicity is expected to concentrate in areas where groundwater is trapped.

In the transition zones between one stress province and another or along particular seismogenic structures within a stress province, the stress regime probably also display temporal variations, which depend on the local state of strain buildup during an earthquake cycle. That the local

earthquake cycle may have hydrogeological significance is illustrated by the (transient) groundwater phenomena encountered during and after the 29<sup>th</sup> September 1969 Tulbagh-Ceres earthquake (Olivier, 1972, Gordon-Welsh, 1974, Maclear and Woodford, 1995).

### **3.9. Geomorphology, Fluvial Terraces and Pedocretes**

#### **3.9.1. Geomorphology**

The first order morphology of the Main Karoo Basin is a result of reduced crustal tectonics, uplifting and erosion (Partridge and Maud, 1987; Burke, 1996) and consists of the African surface and the post-African surface (**Figure 3.9.1.A**).

The *African surface* is dated from around 40 Ma before the African Plate came to rest over the mantle and is mainly reflected in the topography of the central part of the basin. The Great Escarpment, which was formed during the Jurassic continental break-up, was still a prominent feature. The general course of the Orange River was established (Woodford *et al.*, *in press*).

The *post-African surface* ( $\pm 30$  Ma) and resulted from uplift centred below Lesotho. It was responsible for the reactivation of the Great Escarpment and controlled the present-day course of the Orange River. Uplift occurred in two phases, initially a phase of modest uplift of 150-300m was followed by strong uplift which raised the eastern interior of the sub-continent by 900m. The resultant surface is mainly reflected in the peripheral topography of the Karoo Basin. The lower sections of the Orange River shifted further northwards, leaving the Brandvlei paleo-terraces.

The second order features are mainly reflected by terrain variations, chiefly created by weathering and erosion of the dolerite ring-complexes. Large dolerite sill and ring-complexes, such as the Middleburg Basin, may produce strong regional topographic anomalies. The smaller ring-complexes (50 to 5km in diameter) form most of the more prominent topographic features in the Karoo. They are also reflected in the 3rd order drainage system (**Figure 3.9.1.B**) (Woodford *et al.*, *in press*).

The hydrological significance of the *first-order geomorphological features* (African and Post-African surfaces) are difficult to assess. The Post-African surface mainly affects the periphery of the Karoo Basin. These areas underwent a greater degree of erosional unloading, which resulted in surface stress relaxation - a tensional regime with slight isostatic rebound may have resulted in

the development of horizontal fractures. This may positively influence the aquifer characteristics of the Karoo rocks along the edges of the Basin, i.e. the Tierberg Formation in the north and the Beaufort Group to the south of the Great Escarpment. Vegter (1992) states that dolerite (and Karoo sediments) owe their aquifer properties to permeable fractures which are largely restricted to the shallow zone of weathering, which generally does not extend deeper than 10-15m below the waterlevel in the De Aar area.

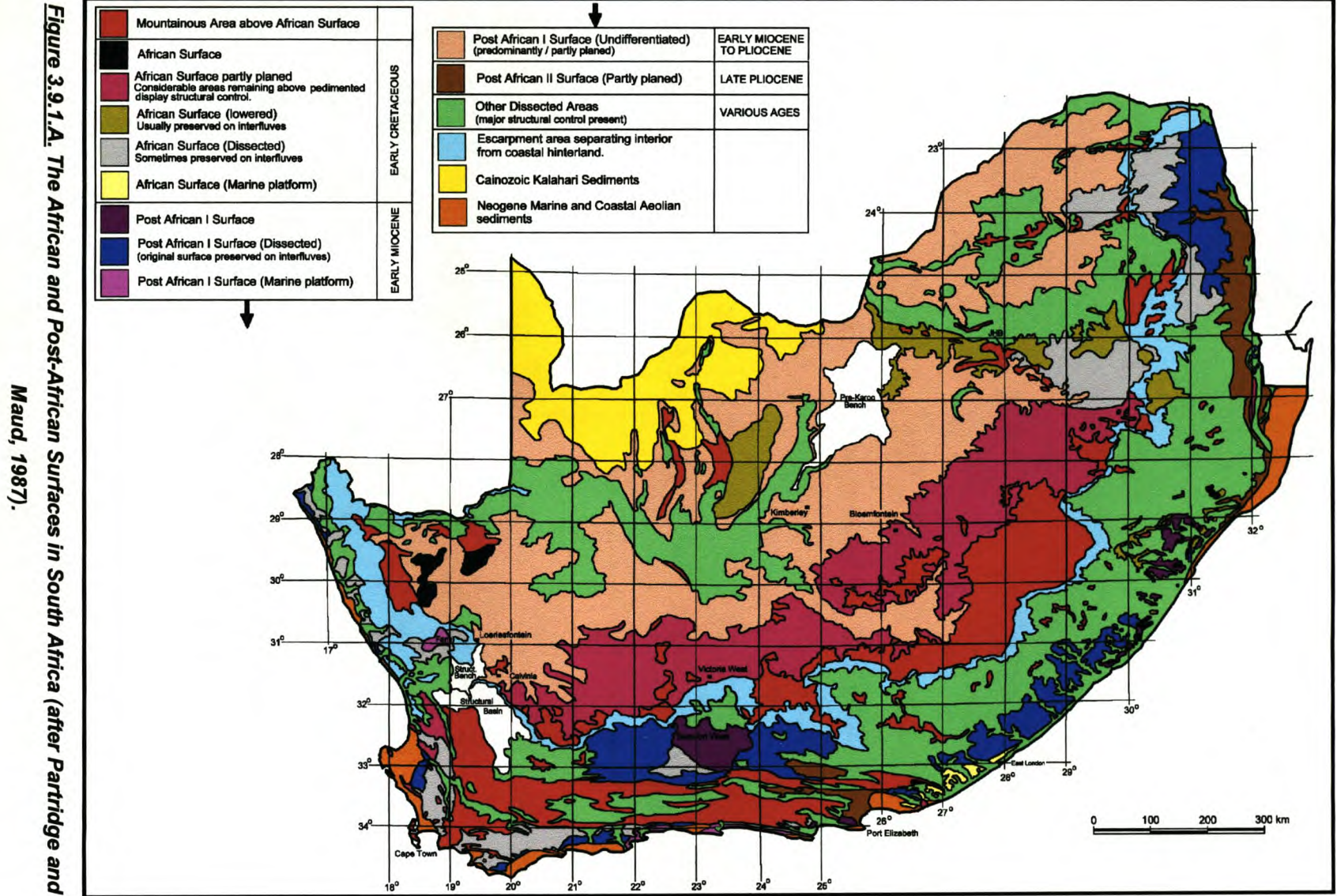
*Second-order features*, mainly the dolerite sill and ring complexes, exhibit an orderly structure, stratigraphically-bounded "rings-within-rings". These features could have influenced the broader-scale aquifer characteristics, due to variations in stratigraphic-level and density of the intrusion (Woodford *et al.*, *in press*).

### 3.9.2. Fluvial terraces

River terraces are present along most of the major rivers in the Karoo Basin. The main fluvial deposits are Miocene or Plio-Pleistocene in age (Late Tertiary - Early Quaternary) and occur from only a few meters up to 60m above the elevation of the present river courses. They consist of gravels, comprising well-rounded cobbles and boulders, sometimes cemented by calcrete (Woodford *et al.*, *in press*).

The large terrace to the south of Beaufort West is Plio-Pleistocene and lies some 10m above the general land surface, and was deposited by sheet-wash action (Woodford *et al.*, *in press*).

The Sak Rivier terraces around Brandvlei, consist of an Upper (60m) Miocene and a Lower (30m) Plio-Pleistocene terrace and result from channeling and meandering of the proto- and meso-Orange River. They are covered by windblown sand and are diamond-bearing (de Wit, 1996).



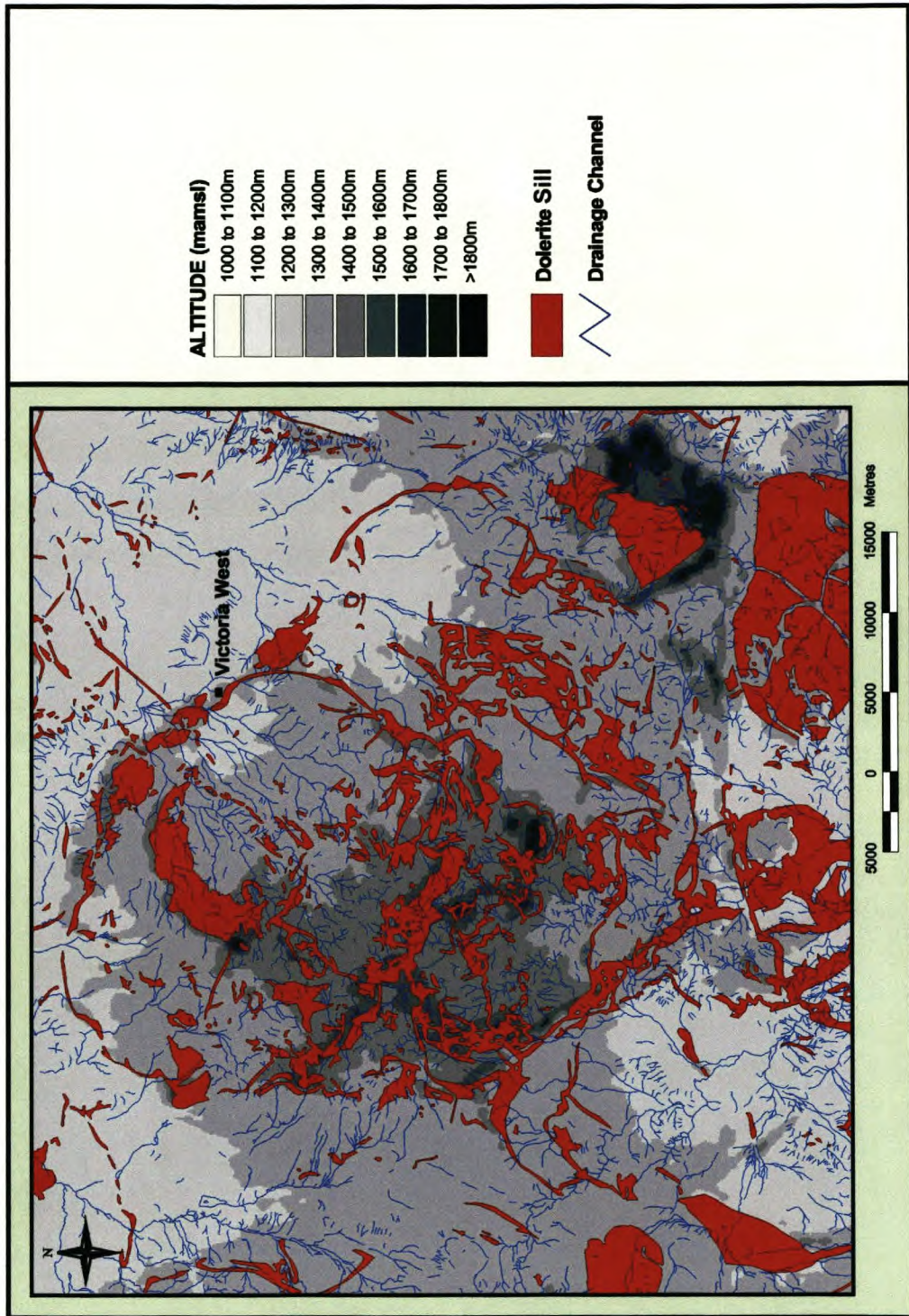


**Figure 3.9.1.B.** The influence of dolerite sill-ring complexes on the drainage system near Victoria West (Woodford et al., in press).

The Aliwal North terrace also lies between 15 and 70m above the present river and could represent different cycles of deposition (*Holmes and Reynhardt, 1989*). Diamonds have been recovered from a trap sited in the bedrock where a dolerite dyke cut at right angles across the river (*de Wit, 1991*).

The terraces of the Mzimvubu River (the Cedarville flats) are covered by dark clayey-humic sands and sometimes by lateritic soils. The deposit may reach 52m in thickness and are composed of alternating thin lenses of variable grain-size sand and clay (*Woodford et al., in press*).

Saturated alluvial deposits often form an important component of composite bedrock aquifers which are limited in extent to a thin strip along the main river courses. These aquifers supply large volumes of groundwater to many towns in the Karoo, i.e. Ficksburg obtains approximately 50% of its water from alluvial beds in the Caledon River, De Aar from deposits along the Brak River (*Kirchner et al, 1991, Vegter 1992, Woodford, 1989*).

Composite alluvial-bedrock aquifers containing significant volumes of groundwater, have been found along the Salt River at Beaufort West (*BRGM, 1979*), the Salt River at Nelspoort (*Leiscewitz, 1979*), the Carnarvonleegte River north of Carnarvon (*Smart, 1994*), the Oorlogskloof River at Calvinia (*Seward, 1982*), the Sundays River at Graaff-Reinet (*Woodford, 1989*) and Middelburg (*Vandoolaeghe, 1979*). The Masotcheni sediments, which occur as isolated deposits along the valleys of the major rivers of KwaZulu-Natal, are capable of storing significant quantities of groundwater (*KwaZulu-Natal Project, 1995*).

Productive alluvial-bedrock aquifers, such as the Caroluspoort aquifer near De Aar, commonly exhibit the following characteristics (*Woodford et al., in press*):

- The thickness of the alluvium varies between 8 and 30m, with 10 to 15m being more common.
- The upper section of the alluvium is commonly fine grained (silts and clays) and acts as a confined or leaky semi-unconfined layer.
- The basal section is generally coarse grained, consisting mainly of fine-grained sand to coarse gravel. This zone is typically 1 to 5m thick and is the most transmissive portion of the aquifer.

- The bedrock is weathered and / or jointed and also acts as a conductive layer, although to a lesser extent. The depth and degree of weathering of the rock decreases from eastern to the western Karoo, i.e. at Calvinia in the western Karoo this zone is approximately a metre in thickness, while in Graaff-Reinet it varies between 2m to 5m.
- The water level is normally very shallow (i.e. less than 5m below ground level).
- The groundwater quality is typically more saline than that of the adjoining fractured-rock aquifers.

Vandoolaeghe (1979) conducted granulometric analyses on samples of the alluvium collected during exploration drilling in the Middelburg area. The results indicate the heterogeneity and general fining-upward nature of these deposits. Alluvial aquifers capable of sustaining long term, large-scale production rarely occur east of longitude 23° in the southern Karoo Basin. This is probably because the deposits are less well developed, are thinner and finer grained, and due to continued aggradation of rivers as a result of more recent uplift in the eastern Karoo.

Vandoolaeghe (1980) found that the alluvial deposits in the Queenstown area were confined to thin strips along the major river courses, but were commonly clayey and unsaturated. Similarly, the majority of the boreholes drilled into the alluvial deposits of the Mzimvubu River in the Cedarville Flats area yielded poor results, although reasonable yields were intercepted in the underlying bedrock of the Beaufort Group (*Woodford et al., in press*).

### 3.9.3. Pedocretes

Pedocretes are soils which have been to a greater or lesser extent cemented or replaced by carbonates (*calcrete*), iron-oxides (*ferricrete*, *plinthite* or *laterite*), silica (*silcrete*), manganese-oxides (*manganocrete*), phosphate (*phoscrete*), gypsum (*gypcrete*) or magnesite (*magnesicrete*). Pedocretes appear to deposit at average rates of between about 20 and 200mm per thousand years (*Brink, 1985*).

*Calcrete* deposits may attain a thickness in excess of 30m, but are rarely homogeneous over depths exceeding 1 to 2m. They are thought to be of two basic origins (*Woodford et al., in press*):

- (1) Groundwater and
- (2) Pedogenic.

In the *groundwater type*, carbonate is precipitated above a shallow water-table or by lateral seepage of groundwater. In the *pedogenic type* the carbonate is transported downwards through the soil by rainwater. The carbonate may originate from the soil or it may be transported on dust particles or within the rainwater itself. Calcrete is usually formed in arid and semi-arid areas or as a weathering product of dolerite. The northern domain can be linked to aridity of the region, whereas the Middelburg domain is geographically bounded by the Middelburg dolerite mega-ring complex (*Woodford et al., in press*).

The term "*ferricrete*" or "*ouklip*" have been widely used in South Africa to denote indurated, iron-rich materials. Ferruginous pedocretes are formed by absolute accumulation, in which sesquioxides are added, or by relative accumulation in which sesqui-oxides are concentrated by removal of the more soluble constituents under conditions of intense weathering and free drainage (*D'Hoore, 1954*). Ferricretes appear to need at least a sub-humid climate and chemical decomposition to release the necessary iron from the parent material. Two areas of the Main Karoo Basin are affected by ferricretes, namely Kwa-Zulu Natal and the terrain below the eastern Drakensberg escarpment (*Woodford et al., in press*).

According to Ellis and Schloms (1984) duripans or dorbanks are indurated, usually reddish brown, massive or platy horizons of up to about 1.2m thick which are cemented by silica, and sometimes by calcium carbonate or iron oxides, to produce a consistency similar to that of hard rock. Duripans (*Ellis and Schloms, 1984*) are most common in the drier parts of the Cape and Namibia where the rainfall is less than 300mm. Brink's (1985) map of the distribution of duripan shows deposits in Graaff-Reinet area.

*Gypcretes* or gypsum deposit of the Karoo Basin have been formed by chemical reaction between sulphuric acid and calcareous material (*Visser et al., 1963*). The sulphuric acid is formed during the oxidation and decomposition of pyrite contained either in the White Hill Formation or in the dolerite. The gypcrete is present in the Ecca and the Upper Dwyka as either lenticular layers or nodules. An arid climate with a long-dry season is favourable for the development of gypsum deposits. Evaporation of groundwater during the long, dry seasons results in the concentration of calcium sulphate, which is then precipitated at the ground water-table interface (*Woodford et al., in press*).

Calcrete deposits often form excellent, albeit localised, sources of groundwater due to (*Woodford et al., in press*):

- An exceptionally higher rate of recharge from rainfall than the average of 2-5% for Karoo aquifers (Kirchner *et al.*, 1991), and
- Dissolution of the calcrete results in highly permeable zones within the deposits, as well as enhancing their storage capacity.

Farmers in the central Free State district of Petrusburg often tap calcrete aquifers of up to 30m thick for irrigation purposes. Weaver *et al.* (1993) targeted valley calcretes situated within a dolerite ring-complex near Strydenburg in the Northern Cape Province and delineated an extensive, thin aquifer using electrical-resistivity geophysical techniques.

### **3.10. Diagenesis, Paleo-Fluid Movements and Thermo-Metamorphism**

Diagenetic studies of the sediments were carried out during the Soekor exploration for oil and gas in the Karoo Basin (Rowse and De Swart, 1976). All the parameters (shale density and porosity, sonic velocity, vitrinite reflectance, sandstone porosity and permeability, proportion of chloroform extract), indicate a general trend of diagenesis increasing from north to south. This is related to the depth of burial, i.e. the greater the depth of burial the greater the degree of compaction and cementation.

The migration of fluids from the Cape Fold Belt in the south during the orogeny was responsible for uranium mineralization in the Karoo Basin. Most of the uraniferous occurrences are situated in the fluvial channel sandstone of the Adelaide Subgroup (Beaufort Group) and are mainly located in the Western Karoo (Fraserburg, Laingsburg, Aberdeen) (Cole *et al.*, 1991). Low temperature groundwater formed the mineralizing solutions, which migrated along geological structures and the more permeable sandstone layers.

In addition to contact metamorphism that can be seen next to major dolerite intrusions, Duane and Brown (1992) demonstrated a thermal overprint in the Karoo sediments at around 190 Ma, i.e. during the intrusion of the Jurassic dolerites. The authors suggest that the break-up of Gondwanaland may have resulted in the total rejuvenation of the Karoo aquifers. Regional hydrothermal systems were generated, the most striking result of which are the breccia plugs.

The thermal influence of the intrusion of the kimberlite was negligible and there is no evidence for any regional scale metamorphism of the Karoo sediments. The uplifting and fracturing that accompanied the intrusion of the kimberlite may have provided a mechanism whereby the

entrapped, deeper-seated groundwater could have risen to the surface and deposited secondary minerals containing carbonate and silica into the open voids, thereby reducing the porosity and permeability of the sediments even further (*Woodford et al., in press*).

A decrease in the degree of diagenesis of the Karoo sediments from south to north corresponds to an increase in porosity and permeability of the shale and sandstone towards the north portion of the basin (*Woodford et al., in press*).

The influence of the uranium province on hydrological properties has not been defined as yet (*Woodford et al., in press*).

The rejuvenation of the Karoo aquifers during the break-up of Gondwana raises the possibility that paleo-aquifers may occur within the deeper portions of the Basin (*Woodford et al., in press*).

## CHAPTER 4

### Methodology and conceptual models

#### 4.1. Introduction

The use of conceptual models is to try and define the factors that may impact on the groundwater chemistry of the studied area.

Sample collection was conducted in January 2000.

#### 4.2. Methodology

##### 4.2.1. Sample localities

All 39 new boreholes drilled by the Department of Water Affairs and Forestry (DWA&F) in the Loxton area were visited and sampled for chemical analyses which would have maximum importance to the study, based on the type of structure drilled on, its depth and yield. Initially twelve boreholes were selected for isotope analysis. A total of 34 samples were sent to the Earth Sciences Department at the University of Cape Town for isotope analysis. Samples were collected by bailer as well as by the sun-powered submersible pump (A complete table of sites and borehole sample information is available in **Appendix A**, as well as on site maps in *Chapter 3 & 5*).

##### 4.2.2. Sampling methods

Procedures for sampling were according to Weaver (1992). Some of the boreholes were sampled by means of a bailer, operating on a "messenger" system, while others were sampled by the use of the sun powered submersible pump. Water from the pumped samples flowed through a filter and was collected at the outflow of a flow-through-cell. Samples were collected in 250ml polyethylene bottles. Bottles were washed with the sampled water. Samples were kept as cool as possible.

pH, temperature and electric conductivity (EC) were immediately measured in the field (in the flow-through-cell) by means of an Orion analyzing system. These parameters are measured at the time sampling commences, as it may alter as the result of aeration and degassing (Parker, 1994). Extent of sample collection is also provided with this preliminary overview of water quality (Weaver *et al.*, 1996). The measuring instrumentation was calibrated before work commenced each day. Determinants required for the study are outlined in **Table 4.2.2.1**.

A total of 34 samples were taken for isotope analysis as some of the boreholes were sampled at different depths. Forty-six samples were taken to INFRUITECH in Stellenbosch for cation and anion analysis, as well as for trace elements. Samples were collected in two 250ml polyethylene bottles, one was acidified with HNO<sub>3</sub>.

Another 14 samples, which were obtained by means of the "plastic bag method", were sent for <sup>14</sup>C analysis to the Schönland Research Centre of the University of the Witwatersrand.

**Table 4.2.2.1. Physical and chemical determinants.**

Group	Determinants
Physical determinants	EC, pH, Temperature
Major cations	Na, Mg, Ca, K
Major anions	Cl, SO <sub>4</sub> , NO <sub>3</sub> , F, HCO <sub>3</sub>
Trace elements	Al, Ba, Ni, P, Sr, B, U, Cu, Mn, Zn
Isotopes	<sup>18</sup> O, D, T

#### 4.2.3. Laboratory analysis

Chemical analysis of the water samples were undertaken by the Soil Science Section of INFRUITECH in Stellenbosch. Analysis of the stable environmental isotopes (D or <sup>2</sup>H and <sup>18</sup>O) were done by the Earth Sciences Department of the University of Cape Town. The Schönland Research Centre of the University of the Witwatersrand performed the <sup>14</sup>C dating and tritium analyses. All laboratory results are available in **Appendix B**.

Quality control was ensured by comparing the field data with the data obtained by the different laboratories.

### 4.3. Conceptual models

From a hydrogeological point of view, a fractured rock mass can be considered a multi-porous medium, conceptually consisting of two major components: matrix rock blocks and fractures. Fractures serve as higher conductivity conduits for flow if the apertures are large enough, whereas the matrix blocks may be permeable or impermeable, with most of the storage usually contained within the matrix. Actually, a rock mass may contain many fractures at different scales. The permeability of the matrix blocks is in most cases of practical interest a function of the presence of micro-fractures. In the case where the domain is a micro-scaled fractured medium intersected by a network of interconnected fractures, the rock is termed a fractured porous rock and the domain is therefore characterized by at least two subsystems, each having a different scale of inhomogeneity (*called scale-effect*) (Woodford *et al.*, *in press*).

The simplest conceptual model for Karoo aquifers consist of two separate systems, in which groundwater flow takes place (**Figure 4.3.A**). The fracture and aquifer matrix have different hydraulic properties. As mentioned, the fracture has a high transmissivity and a low storativity and the matrix has a low transmissivity and a high storativity. When water is pumped from a borehole that intersects a fracture, the dominant flow would be from the fracture to the borehole during early pumping times, with some leakage from the matrix. In the matrix, the flow is perpendicular to the fracture at early times and the shape of the cone of depression and extent of its influence are thus determined by the direction and extent of the fracture (Woodford *et al.*, *in press*).

The fracture acts as a sink that pumps from the matrix. The flow from the matrix to the fracture will depend on the transmissivity of the matrix and the piezometric gradient, according to Darcy's law (Water will flow from an area of highest piezometric level to an area of lower piezometric level). The highest flow rate from the matrix will be in the vicinity of the fracture (Woodford *et al.*, *in press*).

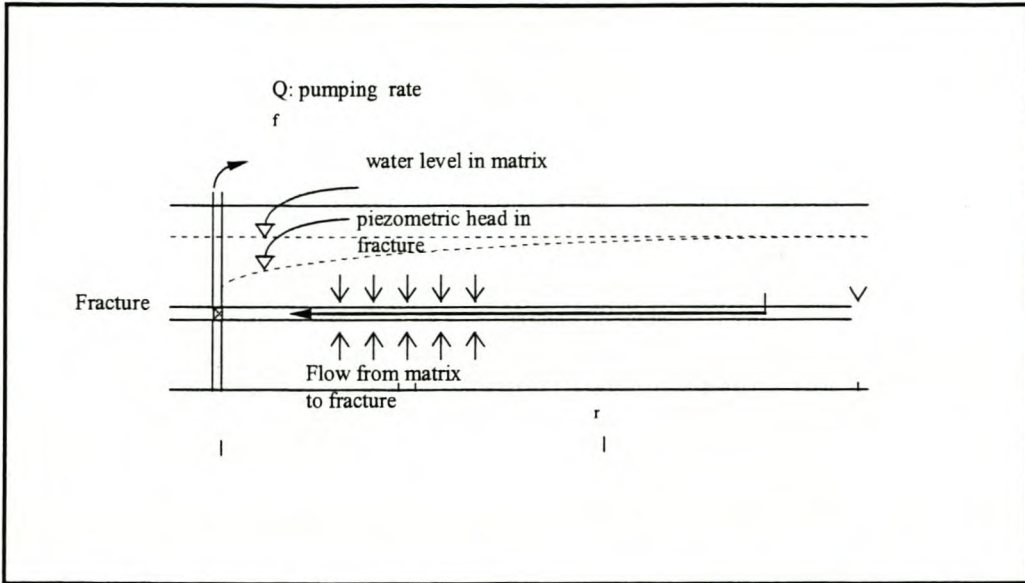


**Figure 4.3.A. Typical conceptual model of Karoo aquifers (Woodford et al., in press). (Vertical Section)**

A very important concept in Karoo aquifers, is that we are dealing with at least two piezometric levels in one borehole if a fracture was intersected in the borehole. The fracture displays semi-confined properties (i.e. piezometric level of the fracture) and the matrix also has a piezometric level (or just waterlevel) if situated above the fracture. Under natural conditions these two levels have the same height (usually the piezometric level is a bit lower than the water level in the matrix, due to small amounts of flow from the matrix to the fracture). Under pumping conditions, however, a noticeable pressure difference exists between these two levels. Close to the abstraction borehole a large pressure gradient exists between the fracture and matrix (thus the flow from the matrix to the fracture is large) and further away the pressure gradient becomes smaller and smaller (less flow to fracture) and a cone of depression is established (Woodford et al., in press).

The same reasoning could be followed if a borehole is drilled in the contact zone of a dolerite dyke (Figure 4.3.B). In this case the conceptual model is a vertical fracture zone with water leaking from the country rock (matrix) to the fracture – again the simple case of two flow systems (double porosity concept) (Woodford et al., in press).

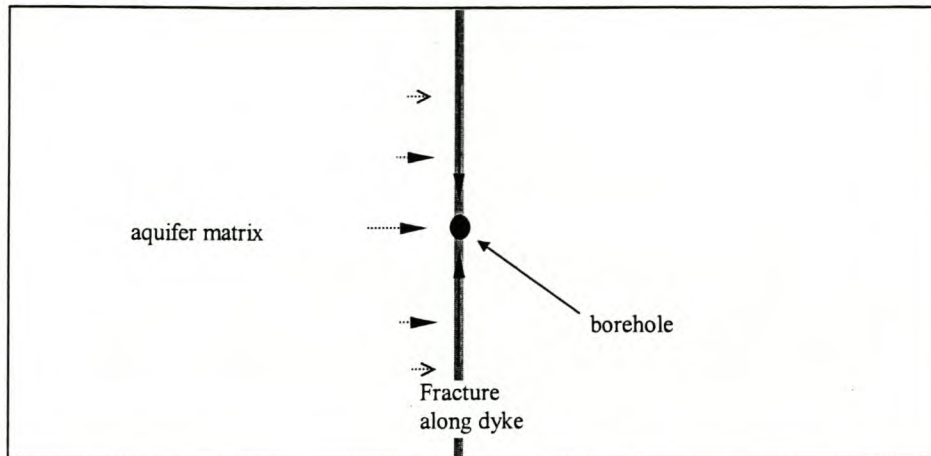


**Figure 4.3.B.** Borehole located on the axis of a vertical fracture (along dyke) with the flow perpendicular to the fracture (Woodford et al., in press). (Plan View)

#### 4.3.1. Model I - Geology

##### 4.3.1.1. Influence of the lithology on the groundwater chemistry

Weathering entails the interaction of an aqueous solution with rock material to produce a solution of different composition from the reactant (Henderson, 1986). Carbonic acid forms from biological processes in the soil and precipitation, to attack minerals and release dissolved components to the water (Katz and Choquette, 1991). Thus it is safe to say that the weathering process is both a chemical and a mechanical process.

Fractures and joints form the percolation system in the Karoo rock. As porous rock is more penetrable by water, the degree of chemical attack is higher and thus determined by the porosity of rock. Tordiffe (1978) stated that finer grained minerals are more susceptible to chemical weathering than coarser grained minerals, due to the larger surface area exposed and because of the protective residual coating that develops around coarser grains, preventing further chemical reaction between the unaltered surface of the grain and the water.

The main outcrops observed during the study are sandstone, dolerite and mudstone. Rock forming minerals contribute to the chemical composition of the subsurface water, based on their reactivity to the hydrosphere. The geology of the area and the reaction of rock forming minerals to natural water are the major geological controls on groundwater chemistry. The weathering of minerals is of importance for two reasons (Bricker and Jones, 1995):

1. The weathering reactions determine the major dissolved species that occur in natural water, and
2. Trace elements commonly occur in solid solution in rock forming minerals and are released when these minerals are exposed to weathering.

Saturation indices (SI) show the degree to which a mineral has dissolved in water (*Plummer et al., 1992*). A SI equal to zero in the logarithmic form, is at equilibrium and the water is thus saturated with the specific mineral (*Freeze and Cherry, 1979*). A negative SI value indicates unsaturated water and a positive value oversaturation, with respect to any specific mineral.

The selected trace element composition of various rock types examined in this study are tabulated in **Table 4.3.1.1**. A general picture of element distribution among major rock types found in the Karoo is indicated by these values (*Adams, 1998*).

**Table 4.3.1.1. Average trace element composition (ppm) of the major rock types (Adams, 1998).**

Element <sup>1</sup>	Dolerite	Carbonatitic breccia / dyke	Sediments
Ba	1154	6377 / 3135 <sup>2</sup>	838
Cu	70	27	5.2
Ni	55	91	32.4
Sr	249	1674 / 613 <sup>2</sup>	368
U	0.8	Not detected	2.6

<sup>1</sup> Elements available and used in this study. <sup>2</sup> Values for dykes.

Fractures are usually associated with a certain tectonic event, such as dolerite, carbonatites and kimberlites intrusions in the Karoo. The major joints are also observable, due to the Cape Orogeny. Farmers usually target these fracture patterns for borehole siting, as the linear structures are easily observable in the field due to linear growth of greener and larger vegetation. Fracture intersection is common and the length of fractures may vary from a few meters to several kilometers, as postulated by Newton (1987).

If water chemistry is characterised by the fracture drilled, then the same chemistry would be expected at different points along the same fracture. If no correlation is found between the groundwater chemistry and the fractured bedrock, than the fracture serves only as a water

conduit, significant only in relation to the quantitative aspect of groundwater. Dolerite and carbonatite intrusions act as significant groundwater conduits, as these intrusions occur along fractures (*Adams, 1998*).

#### 4.3.2. Model II - Recharge

Precipitation is mainly derived from the Atlantic ocean, in the form of rain, mist and snow. Recharge of groundwater occurs at intrusive contacts of dolerites or where the fracture and joint systems are exposed to the surface, during these precipitation events (*Adams, 1998*).

Precipitation is the initial water source for recharge, undergoing chemical changes due to various processes, as the water moves through the air and reaches the soil surface. The infiltrating meteoric water is charged with CO<sub>2</sub> and causes chemical reactions between the soil / rock and water, resulting in a solution of cations and anions (*Tordiffe, 1978*). Precipitation of salts may occur in the unsaturated zone, above the groundwater table. After the infiltration capacity of the soil has been reached, overland flow and ponding occurs (*Adams, 1998*).

Groundwater quality studies are recognising the importance of the use of environmental isotopes <sup>18</sup>O (oxygen - 18) and D (deuterium). Depletion of these stable isotopes in rain water as it moves away from its source (oceans) can define several processes that determine the groundwater composition. The <sup>18</sup>O and D values of the area are plotted relative to the Global Meteoric Water Line (GMWL) or Local Meteoric Line (LML). If the isotope ratio of the groundwater plots on the GMWL, it is assumed that the water has originated from the atmosphere and that it is unaffected by other isotopic processes (*Domenico and Schwartz, 1990*). Deviations from the GMWL indicate different processes affecting the <sup>18</sup>O and D ratio, as depicted by **Figure 4.3.2**. (*Adams, 1998*).

Recharge of subsurface water would ideally start with a young Ca-HCO<sub>3</sub> type water. As the water interacts with its physical environment, it will change signature to that of a Na-Cl type water. Areas of higher topography will tend to have a more recent recharged Ca-HCO<sub>3</sub> type water due to low reactivity with the environment and where these water are discharged or become more static, the chemistry of the water would evolve to a stagnant Na-Cl type water (*Adams, 1998*).

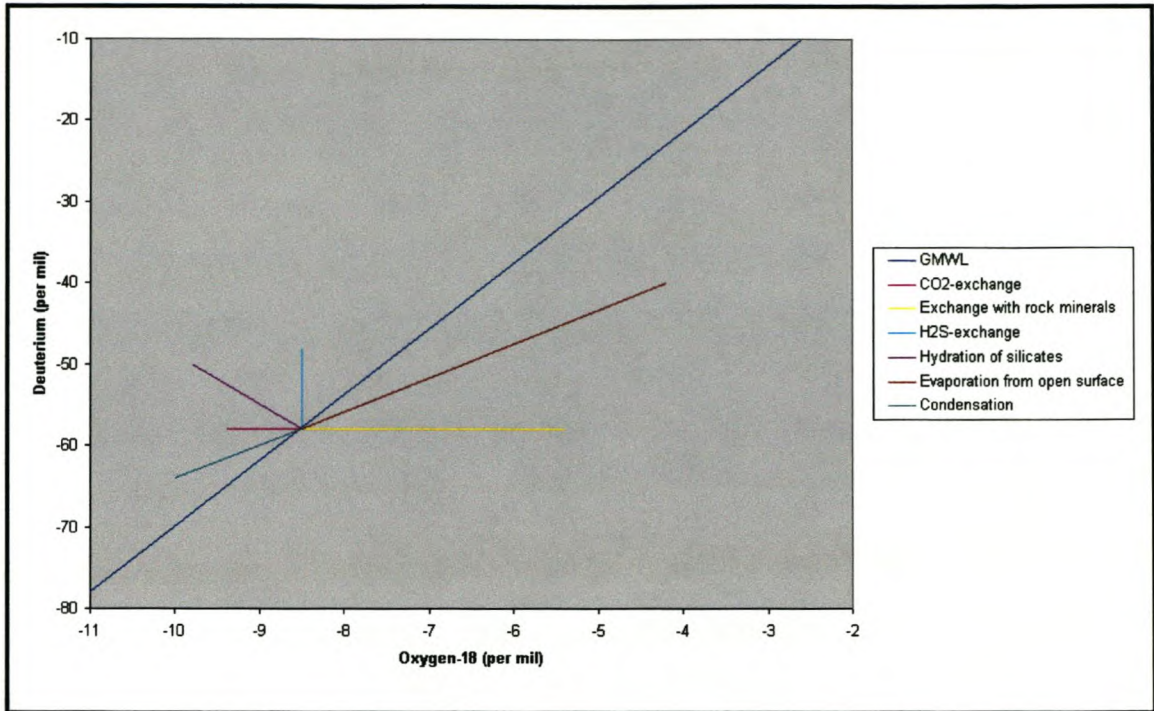


**Figure 4.3.2. D vs. <sup>18</sup>O diagram, indicating processes that may affect the stable isotope ratios (modified after Domenico and Schwartz, 1990)**

The recharge rate (R) can be estimated from the mean residence time by assuming that a pumped borehole produces a well-mixed sample of all the water flowing into it:

$$R = \frac{\sum_i H_i \cdot p_i}{T}$$

where  $H_i$  = the thickness of individual saturated aquifer zones intersected by the borehole, and  $p_i$  = their porosity.

For radiocarbon values less than 80 pMC and tritium at less than 0.5 TU it can be assumed to a good approximation that there is no bomb-produced input.  $A_0$  is therefore essentially constant and

$$R = \frac{\sum_i p_i H_i}{8270[(A_0/A) - 1]}$$

Aquifer porosity is a critical parameter in these calculations. Values may be measured directly from drill cores. At best the porosity can only be estimated. This implies at least a good knowledge of the borehole log and the nature of the local rock formations. In addition, borehole depth and rest-water level should be known (*Woodford et al., in press*).

**Note:**

- Given enough time, an environmental tracer will “label” by advection and diffusion all the water held within interconnected aquifer openings, in a manner similar to other chemical species.
- Porosity is the relevant parameter for all aquifer types. Storativity is a hydraulic parameter sometimes orders of magnitude lower than the porosity.
- Effective porosity may be assessed using artificial tracers. This factor is time-scale dependent and relevant to short-lived tracer or transient responses. The time scales assessed with environmental tritium and even more so, radiocarbon, are such that they effectively label the entire water body (*Bredenkamp et al., 1998*).
- In one of the case studies presented, reasonable correspondence has been achieved between recharge assessment using the above approach and other independent methods. Although most aquifers deviate substantially from the idealised phreatic case, the exponential mixing concept gives a fair approximation.

#### 4.3.3. Model III - Topography

Elevation changes of land surface have a marked influence on the chemical quality of water. Changes in water chemistry along a flow path depend on the initial water added to the aquifer at a given point. This water is predominantly  $\text{HCO}_3^-$  rich and as it will flow toward the area of discharge it will acquire a more  $\text{Cl}^-$ -rich character (*Adams, 1998*).

As water moves towards discharge area, the rate of  $\text{CO}_3^{2-} + \text{HCO}_3^-$  dissolution decreases and an increase of  $\text{SO}_4^{2-}$  is noticed, being readily acquired from bedrock strata. This sequence is known as the ***Chebotarev sequence*** (*Freeze and Cherry, 1979*). Changes in dominant anion concentration along a flow path / line, are as follow:



This sequence is dependent on the residence time of the recharged water (i.e. the rate at which it flows away from the recharge area). Generally recharge occurs in flat areas, on slopes, in valleys, rivers and hills. The amount of time that water is in contact with its surroundings will determine the amount of chemical constituents added to the groundwater (*Adams, 1998*).

Water will flow from a topographic high to a lower area, due to the hydraulic gradient. Water in an elevated area has very low  $Cl^-$  values, opposed to flatter lying areas or areas acting as discharge points.

The major factor influencing the accumulation of salts is evaporation. The accumulation of salts is pronounced in flat areas, where the precipitated water is allowed to pond. High evapotranspiration is therefore the main contributor to salt accumulation (*Adams, 1998*). Sami (1992) states that if evaporation exceeds precipitation throughout the year, that leaching will be limited and the soluble salts tend to accumulate near the soil surface. After periodic large rainfall events, these salts will be flushed into streams and the subsurface.

These phenomena are described by looking at specific flow lines in some specific areas or grouping of boreholes in different topographic settings. Major cations and anions, as well as EC / TDS indicate the relationship between topography and water quality. Groundwater flow (from high to low lying areas) can be identified by the chemical changes occurring over time and space, along a flow path. High lying areas will have a more bicarbonate type water than, low lying, flatter areas where more salty (i.e. sodium chloride) type water occurs. The effect of mixing must also be incorporated in data interpretation, as areas of recharge will have a bicarbonate overprint within the chloride rich water in flat areas (*Adams, 1998*).

#### 4.4. Groundwater Flow Models

Models of groundwater movement are required in order to interpret radioactive environmental tracer data in terms of parameters useful for practical geohydrology. Amongst these are the piston-flow, dispersion and exponential models. For a more complete discussion of models see e.g. Verhagen et al. (1991). In these models, it is assumed that at recharge small volume elements or "parcels" of water enter the ground from the surface and then move unaltered through the sub-surface along smooth flow paths (i.e. isotropic, homogeneous aquifer) to a discharge point.

The convolution integral governing the concentration of the tracer  $A(t)$  at time  $t$  is:

$$A(t) = \int_0^{\infty} A_0(t - \tau) e^{-\lambda\tau} f(\tau) d\tau$$

where  $A_0$  = the tracer concentrations at recharge;

$\tau$  = the individual parcel transit time;

$A_0(t - \tau)$  = the input function;

$e^{-\lambda\tau}$  = the radioactive decay function; and

$f(\tau)$  = the transit time function or "model" of the movement of ground water through the aquifer.

There are two extreme idealised groundwater regimes (*Woodford et al., in press*):

1. A confined, flowing system, in which water moves from a defined recharge area and is then isolated from further contact with the surface (**Figure 4.4.A**). At the point of extraction (borehole) all flow lines are of equal length and all parcels will have traveled for the same time  $\tau$ . This is known as the *piston flow model*. Here, the transit time function = 1, and for a constant tracer input concentration, the ground water residence time is:

$$A(t) = A_0 e^{-\lambda\tau}$$

which is the equivalent of "dating" the ground water.

2. An isotropic, phreatic aquifer, receiving uniform diffuse recharge (**Figure 4.4.B**). At the point of extraction, the deeper flow lines have a longer transit time than the shallower ones. The water pumped from the borehole will contain a well-mixed sample of components of different transit times or ages. Therefore a mean residence time (MRT)  $T$  is introduced. The transit time function is here taken to be:

$$f(\tau) = \frac{e^{-\tau/T}}{T}$$

known as the *exponential model*.

These are "lumped-parameter" or "black-box" models, in which spatial variations are ignored (they are usually not, or only poorly, known) and the various properties are considered homogenous throughout the system (*Woodford et al., in press*).

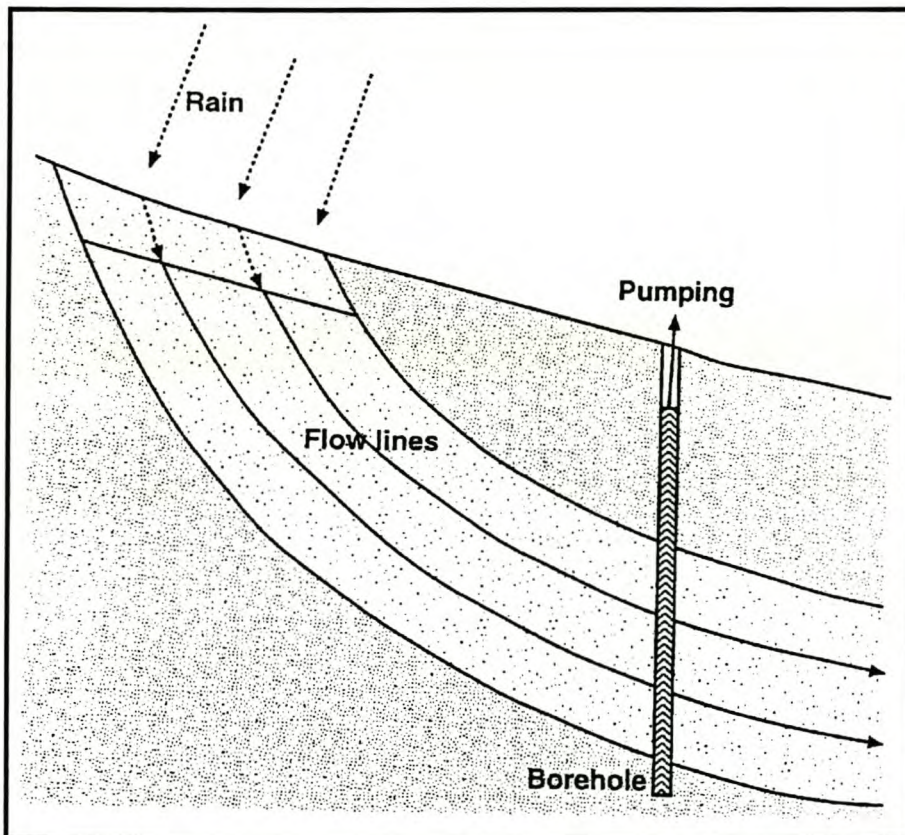


**Figure 4.4.A.** Idealised flow-lines for a confined aquifer receiving recharge only in the outcrop area. (*Woodford et al., in press*)

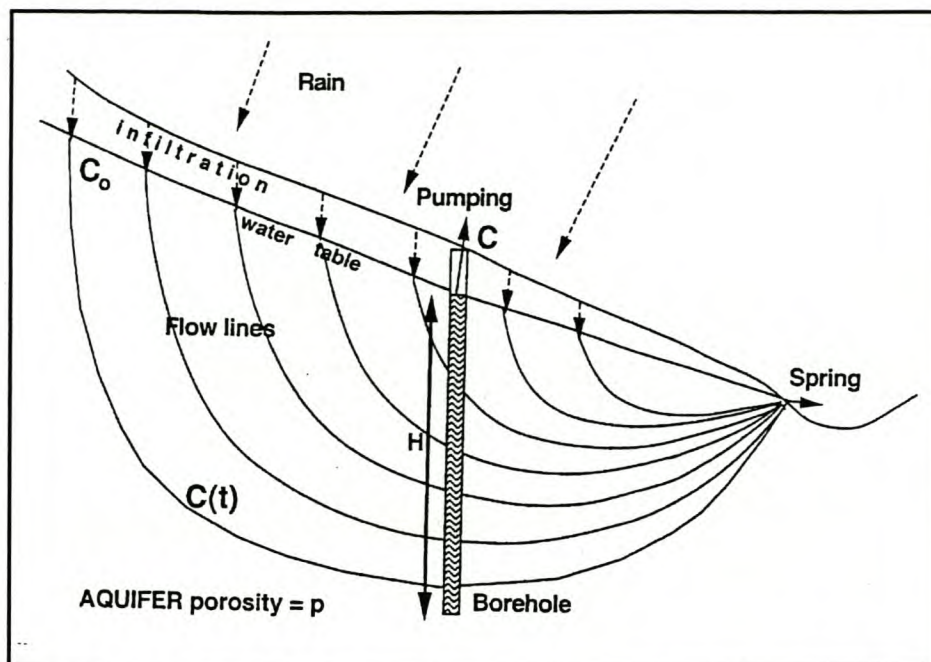


**Figure 4.4.B. Idealised flow-lines for an isotropic, unconfined, phreatic aquifer receiving uniform diffuse recharge. (Woodford et al., in press)**

Both  $^{14}\text{C}$  and  $^3\text{H}$  input concentrations underwent considerable changes over the past 40 years and therefore are functions of time or  $A_0(t - \tau)$ . These values are input into the convolution integral. The integral is then evaluated for increasing mean residence times  $T$  from the present (time of observation) for each isotope, using the exponential transit time function. Typical results for Southern Africa are available in curves and can now be used to estimate MRT values for either the observed  $^3\text{H}$  or  $^{14}\text{C}$  concentrations. With the bomb peak still measurable in the environment, ambiguous MRT values in the range 10 - 60 years are produced at values  $> 2$  TU and  $> 100$  pMC. This can often be overcome by considering both  $^3\text{H}$  and  $^{14}\text{C}$  in evaluating the most likely value of MRT, as well as the geohydrological conditions. A plot of  $^{14}\text{C}$  against  $^3\text{H}$  for different MRT values calculated by the exponential-mixing model can be drawn to observe if values plot on or close to this line. This implies that conditions conform reasonably to the assumption of an isotropic, diffusely recharged, aquifer (Woodford et al., in press).

In addition, CFC (chloro-fluoro-carbon) measurements can potentially assist to remove ambiguity in this MRT range, as the atmospheric concentration of these dissolved gas tracers have not undergone a transient, but are monotonously increasing or are leveling off (Woodford et al., in press).

#### 4.5. Groundwater Flow Modeling

The flow in fractured aquifers can be explained by various theoretical models. Three main types of approaches to the problem are used (*Woodford et al., in press*):

- The deterministic approach, which is based on an accurate and detailed description of individual fracture systems, and is mainly used for small-scale problems in geotechnical engineering;
- The double-porosity medium approach, which assumes a uniform distribution of matrix blocks and fissures throughout the aquifer (including single-fractured models and multi-porosity / multi-permeability models);
- The equivalent homogeneous aquifer approach, which considers only main trends of the pressure behavior of the fissured aquifer and tries to relate them to a known model of lower complexity.

These theoretical models form the basis of the type curve methods derived by various researchers for the analysis of pumping test data in fractured aquifers. For a complete description of all the different models, the reader is referred to Kruseman and De Ridder (1990).

The double-porosity concept has been used extensively in the petroleum field. Two approaches that differ in the manner by which flow from a block to a fissure occurs, have been taken. The first approach assumes that flow occurs under pseudo-steady state conditions; in the other approach, the flow occurs under transient conditions from the block to the fracture. Although the pseudo steady- state approach simplifies the mathematical computations, it ignores some of the physics of the problem. This implies that the transient approach is clearly superior from a theoretical standpoint. The effect of fracture skin (a thin skin of low-permeability material deposited on the surfaces of the blocks that serves to impede the free exchange of fluid between the blocks and the fracture) in double-porosity systems is to delay flow from the blocks to the fractures and gives rise to pressure responses that are similar to those predicted under conditions of pseudo-steady state flow. By reducing gradients of hydraulic head in the compressible blocks, fracture skin provides theoretical justification for the pseudo-steady state flow approximations (*Woodford et al., in press*).

The effective management of an aquifer is primarily dependent on how well the aquifer parameters are known. Most interpretation methods are all using analytical solutions of the

groundwater flow equation, dependent on certain assumptions, including homogeneity. However, in a fractured porous medium, especially on the scale of a pumping test, this assumption is violated. The mixture of horizontal movement in the fractures and vertical leakage in the surrounding matrix cannot be accounted for in the analytical solutions. Therefore incorrect and unrealistic values for especially the storativity of the aquifer are calculated (*Woodford et al., in press*).

Predictive tools and techniques in geohydrology and hydrology have developed rapidly since 1970, when the use of computers for this purpose became common. Numerous models, all based on the same or similar mathematical, chemical and hydraulic principles, were developed by many researchers in the field of geohydrology. The field of hydrology distinguishes itself from geohydrology in the sense that hydrological models are usually of a stochastic nature. Numerous hydrological models are currently also available and in use for the simulation and prediction of a vast array of circumstances (*Woodford et al., in press*).

In contrast to the rather precise development of predictive tools, data sets are often lacking. The reason for this discrepancy lies in (*Woodford et al., in press*):

- The inaccessibility of systems to measure values,
- The lack of time to measure, and
- The high cost of measurement.

Of these and particularly in the case of groundwater, the inaccessibility of the aquifer to measure parameters is probably the biggest constraint. This goes hand in hand with time and cost. In most instances, geohydrological systems can only be probed by a very limited number of boreholes. This usually requires input from a very experienced geohydrologist and interpretation of geohydrological systems is mostly very complex. Within the mining situation, geohydrological systems become even more complex because they are usually of a dynamic nature, with flow regimes changing as mining progresses (*Woodford et al., in press*).

Various possibilities for the classification of these predictive tools exist. These are, for instance (Woodford *et al.*, *in press*):

- Geochemical / hydrochemical / kinetic models.
- Pathway models.
- Water / salt balance models.
- Flow models.
- Acid-base accounting.

A large number of computer models are available, but usually the following two models are used in South Africa for groundwater flow and mass transport modeling (Woodford *et al.*, *in press*):

- MODFLOW 3D finite difference model (various pre-processors exist e.g. Modime, Pmwin)
- AQUAWIN (2D finite element model, including options for management, risk analysis and pump/test analysis)

Three-dimensional models have the difficulty of assigning parameter values to each of the layers as well as spatially in the x-y directions. A lack of information usually necessitates researchers to abandon efforts for three-dimensional modeling and use 2D codes.

Up to date no Karoo aquifers in South Africa are managed with the aid of 2D or 3D numerical models (Woodford *et al.*, *in press*).

#### **4.6. Groundwater Management Principles**

For proper management of a borehole or an aquifer, the following two principles are important (Kirchner and Van Tonder, 1995):

- The total amount of abstraction from an aquifer must be less than the sustainable yield of the aquifer.
- A borehole must be operated in such a way, that the water level never reaches the position of the main water strike in the borehole. This will lead to a drastic decrease in the yield of the borehole and even drying up of a borehole if too much water is abstracted from a borehole.

The following important issues will be addressed in this section (*Woodford et al., in press*):

- Many times in practice the complaint "*my borehole has dried up*" is heard. Usually this is due to too high an abstraction rate in the abstraction borehole (and not to a general lowering of the water level in the aquifer), although enough water is still present in the aquifer just tens of meters from this borehole.
- For a first estimation of a sustainable daily abstraction rate for an abstraction borehole, the late T-method, distance-to-boundary method or drawdown-to-boundary method could be used. In the case of deep water strikes (more than 20m below RWL), the late T-method will give an over estimation of the sustainable daily abstraction rate.

The two-layered radial pump test program RPTSOLV, will yield a more reliable sustainable daily abstraction rate. When a no-flow boundary is used in this model, a minimum sustainable abstraction rate will be obtained with this model (*Kirchner and Van Tonder, 1995*).

Up to now no perfect method has been developed for management purposes. The most reliable method is the use of a 3D groundwater flow model. However, for the use of such a 3D model, very good field data are required which could be very costly.

The discovery that horizontally orientated meso-fractures are the main conduits of water to a borehole in a Karoo aquifer signals a danger flag. Dewatered fractures may be deformed by the weight of the overburden and the borehole may be lost. It may well be that the deformation of the water-bearing fracture in the borehole's vicinity is irreversible and the borehole dries up (*Kirchner and Van Tonder, 1995*).

It is thus imperative that these boreholes must not be pumped to an extent that their water-bearing fractures are dewatered. It is very important that the water level in the abstraction borehole never reaches the position of the main fracture, because the yield of the borehole will

decrease drastically. Moreover, if the hydraulic head gradient is very steep in the vicinity of the borehole,  $\text{CaCO}_3$  can deposit due to the change in partial  $\text{CO}_2$  pressure. This calcification in turn can block the borehole and decrease the water yield. The *uncertainty in drawdown* therefore is of major importance. A sustainable pumping strategy in terms of probability must ensure that the probability of drawing piezometric head in the pumping well down to the depth of the main water bearing fracture should be less than e.g. 5% (Kirchner and Van Tonder, 1995).

Major flow in Karoo aquifers occurs from the rock matrix to the fracture, which supplies the borehole with water. A highly permeable fracture quickly dewateres when pumped, unless recharged through its surfaces. The recharge rate depends on the rate at which water can be transported from the surrounding rock matrix to the fracture. A point can be reached when the aquifer cannot supply water fast enough to the fracture, to compensate for the loss through pumping. There is thus a limit to the rate at which the rock-fracture system can supply water to a borehole (Kirchner and Van Tonder, 1995).

The limited yield of a borehole is therefore caused by the finite rate at which water can leak through the matrix to the fracture system rather than by the limited amount of water stored in the aquifer. *The uncertainty in the leakage rate* (hydraulic conductivity) therefore must be investigated. In conjunction to that *an overall optimized pumping strategy* must be determined that ensures a *reliable long-term water yield* of a pumping well group. The optimized pumping strategy must include the optimization of *single well pumping rates, their recovery times*, as well as the *number and location* of pumping wells. A better sustainable management strategy is to use more boreholes but pumped at lower abstraction rates (Kirchner and Van Tonder, 1995).

## CHAPTER 5

### Hydrochemistry

#### 5.1. Introduction

Statistical data analysis will determine the major factors and processes, characterising the groundwater in the study area of Loxton. The chemical data will be presented, analysed and interpreted in this chapter. All necessary data-tables and chemistry are provided in **Appendix A & B** respectively.

#### 5.2. Precipitation Chemistry

Analysis of the rainwater sample collected in the area of Loxton, is presented in **Appendix B**.

The rainwater sample was moderately acidic, with a pH of 6.2. This low pH could be attributed to the dissolution of atmospheric CO<sub>2</sub> in the water. The concentration of the total dissolved solids (TDS) was 16 mg/l and this rainwater sample had a high ionic balance error (47.3%). This phenomena of low TDS and high ionic charge errors is also common in diluted groundwater (*Katz and Choquette, 1991*).

This precipitation sample was classified as a Cl<sup>-</sup> and Na<sup>+</sup> dominated water, indicating an end point in the evolution sequence (stagnant water, discharge zone). This is not acceptable as Piper and Durov diagrams can't be used to classify rain or surface water.

It is stated that rain is an extremely diluted, slightly to moderately acidic, oxidising solution, that can quickly cause chemical alterations in soils or in geologic materials, into which it infiltrates (*Woodford et al., in press*).

#### 5.3. Surface Water Chemistry

No surface water samples were collected in the study area, as no surface water was observed in streams, rivers or natural depressions.

## 5.4. Groundwater Chemistry

### 5.4.1. Statistical Analysis

#### 5.4.1.1. Introduction

Ion balance errors are calculated in the database (HYDROBASE) created for this study. A complete hydrochemical data set appears in **Appendix B**. The whole data set falls in the 5% ion balance error range.

Understanding of the basic chemical determinants or parameters is needed in order to understand the groundwater chemical behavior in the study area. Large data sets are interpreted by statistical analysis, commonly used in geohydrological studies (*Ashley and Lloyed, 1978; Dawdy and Feth, 1967; Usunoff and Guzman-Guzman, 1989*). Correlation matrices were used to identify the relationship between various chemical parameters. Factor analysis was used to classify and reduce the data set. All statistical analysis was calculated using the STATISTICA software package.

The statistical approaches applied:

1. Descriptive statistics give an overview of the average groundwater composition. Ranges and means of the groundwater are compared with the mean composition of the rain water sample in the area.
2. Correlation matrices in order to find any relationship between variables in the data set. A correlation coefficient matrix was produced as a measure of which the variance of each variable can be expressed, by its relationship with each of the other variables. The degree of linear correlation is termed the correlation coefficient, as the variances are the measure of values scattered around the mean.
3. Factor analysis (R-Mode) to find the main factors or processes responsible for the groundwater chemistry in the area. Factor analysis rearranges data to be presented in a manner better explaining the structure of the underlying system that produced the data (*Dawdy and Feth, 1967*). The interrelationship of the chemical parameters is explained in a simple structure, with a set of factors created.

#### 5.4.1.2. Descriptive Statistics

The groundwater pH range between 6.1 and 8.9 indicates that most of the dissolved carbonates are in the  $\text{HCO}_3$  form (*Domenico and Schwartz, 1990*). Electrical conductivity (EC) and total dissolved solids (TDS) values vary between 35.5 to 316 mS/m and 249 to 2212 mg/l for the study area, respectively. It is evident that the groundwater in the area differs considerably, when looking at the average composition. Groundwater salinity is also possible to change over short distances in the area (*Adams, 1998*).

Rainwater and groundwater chemistry vary considerably (**Table 5.4.1.2**), indicating chemical processes occurring in the initial rainwater chemistry and the chemistry of the final groundwater. The higher pH of groundwater can be explained by the dissolution of carbonate minerals in the subsurface and a concurrent increase in the groundwater pH (*Adams, 1998*).

**Table 5.4.1.2. Univariate statistical overview of the data set (rain & groundwater) (Adams, 1998)**

RAINWATER			GROUNDWATER				
Variable	Mean	Rain	Mean	Median	Min.	Max.	Std.Dev.
pH	5.16	6.2	7.229	7.200	6.100	8.900	0.544
EC (mS/m)	1.49	2.3	88.371	115.00	35.500	316.000	72.122
Temp. (°C)	12.75	25	22.357	21.800	19.000	36.70	3.853
Eh (mV)	N.D.	N.D.	N.D.	N.D.	N.D.	N.D.	N.D.
pCO <sub>2</sub> (atm.)	N.D.	N.D.	N.D.	N.D.	N.D.	N.D.	N.D.
Alkalinity	0.6	23	128.145	210.000	38.000	419.000	105.362
TDS	16.65	16	618.809	805.000	249.000	2212.000	504.804
HCO <sub>3</sub>	8.65	28	151.268	256.000	40.000	510.000	128.779
K	0.24	1.7	2.686	5.300	0.600	33.700	7.804
F	0	0	0.669	0.850	0.100	2.200	0.536
Cl	6.07	87	113.815	125.000	54.000	267.000	63.681
Ca	0.26	2	52.047	72.000	8.000	679.000	160.709
SO <sub>4</sub>	0.57	22	21.261	231.500	2.000	2332.000	566.244
NO <sub>3</sub> as N	0	0.190	0.009	0.024	0.002	0.793	0.194
Mg	0.16	1	5.810	16.000	1.000	77.000	24.104
Na	0.2	68	121.975	137.000	48.000	357.000	95.074
Sr	0.01	0.615	0.426	1.475	0.021	10.718	2.515
Al	0	0.08	0.033	0.100	0.010	0.290	0.076
Ba	0.002	0.005	0.004	0.008	0.001	0.050	0.009
Ni	0.02	0.004	0.006	0.010	0.001	0.219	0.036
PO <sub>4</sub>	0.08	0	0.025	0.064	0.003	0.175	0.051
B	0.003	0.807	0.289	0.522	0.020	1.640	0.423
U	0	0	0.009	0.039	0.001	0.095	0.025
Cu	0.004	0.013	0.008	0.010	0.003	0.015	0.003
Mn	0	0.02	0.008	0.023	0.002	0.181	0.062
Zn	0	0	0.004	0.006	0.001	1.085	0.491

All values in mg/l, unless indicated otherwise. N.D. was not determined. Standard deviation (Std. Dev.)

### 5.4.1.3. Correlation Matrices

To find any correlation between the different chemical constituents of the subsurface water, multivariable statistics (Pearson's correlation matrices), were used. Correlation is the measure of the relation between two or more variables (*Levinson, 1980*). The usefulness of correlation matrices is in finding a relationship between two or more chemical constituents in a large data set. Correlation coefficients ( $r$ ) range from +1.00 (perfect positive correlation) to -1.00 (perfect negative correlation). A correlation coefficient of 0.00 would lack any correlation. Only correlation with  $r > |0.4|$  are used. Samples with correlation coefficients of  $\geq |0.7|$  shows strong correlation whilst correlation of  $r = |0.5 - 0.7|$  has moderate correlation at a significant level of  $< 0.05$ . Hydrochemical parameters with significant correlation are presented in **Table 5.4.1.3**.

A strong correlation exists between Na and a moderate correlation between  $\text{SO}_4$ , with electrical conductivity (EC). These relationships are a clear indication of the main contributing elements to groundwater salinity. The moderate correlation between Pb, Li and strong correlation of Sr with EC, indicate the concentration increase of these elements, as the salinity of the water increases.

The groundwater salinization increase may be the result of dissolved solid concentration increasing due to evaporation and interaction between the geological materials and groundwater. The amount of cations released from the aquifer matrix is proportional to that of chloride. High salinity water may be added to the subsurface before and during events of recharge (*Adams, 1998*).

The positive correlation between Ca- $\text{SO}_4$  and Na- $\text{SO}_4$ , possibly shows the contribution of evaporitic salts (Gypsum -  $\text{CaSO}_4 \cdot 2\text{H}_2\text{O}$ ) in the geological material.

The major exchangeable ions Na-Ca, Sr-Ca and Sr-Na, all correlate positively. The elemental concentrations in the groundwater may be due to cation exchange processes.

**Table 5.4.1.3. Pearson's correlation matrix for Loxton data**

	NH <sub>4</sub> -N	Sb	Ba	HCO <sub>3</sub>		d	Ca	CO <sub>3</sub>	Cl	EC	F	Pb	Li	PO <sub>4</sub>	Na	Sr	SO <sub>4</sub>	
NH <sub>4</sub> -N	1																	
Sb		1																
Ba	0.45		1															
HCO <sub>3</sub>		-0.44		1														
B					1													
Cd						1												
Ca		0.47			0.67		1											
CO <sub>3</sub>	0.50							1										
Cl				0.41					1									
EC					0.44		0.63		0.46	1								
F			-0.48								1							
Pb										0.57		1						
Li		0.41		-0.49	0.50					0.62	0.49	0.46	1					
PO <sub>4</sub>						0.41								1				
Na					0.66		0.66	0.43	0.45	0.71			0.50		1			
Sr		0.44			0.54		0.49			0.82		0.43	0.70	0.47	0.68	1		
SO <sub>4</sub>		0.53			0.72		0.96			0.66			0.42		0.79	0.55	1	

The mobility of metals in groundwater is determined by the use of redox potential (Eh) and pH diagrams (Appelo and Postma, 1994; Hem, 1989). The correlation between pH, Eh and pCO<sub>2</sub> exists in natural groundwater and can be a measure of validity of correlation matrices in the groundwater data interpretation (Adams, 1998).

#### 5.4.1.4. Factor Analysis

Factor analysis shows the relationship between variables, to be used to target specific correlation or relationships evident from statistical analysis.

Factor extraction was carried out on the data set by means of principal components, using the STATISTICA computer software. Varimax rotation was used to obtain uncorrelated components (Schot and Van Der Waal, 1992), as well as to find the maximum amount of factors (Drever, 1988).

Factor analysis results are outlined in **Table 5.4.1.4**. Component loadings  $\geq |4|$  are included in the results.

Factor 1 relates to the largest eigenvalue and is able to explain the greatest amount of variance in the data, while factor 2 will explain the greatest of the remaining variance and so forth (Usunoff and Guzman-Guzman, 1989).

Eight factors (8) account for 69.19% of variance, which is small, but understandable in a complex system, where the variance is not systematic (**Table 5.4.1.4**).

Factor 1 is interpreted as the salinization of groundwater due to evaporated surface water infiltration. The main salinity contributors are EC, Na, Ca, Sr and SO<sub>4</sub>, the main cation exchange elements are Sr, Na and Ca, which are positively correlated and indicate the influence of geological matrices and the presence of gypsum. The processes of dissolution or precipitation of evaporitic and sulphate minerals are indicated by a significant correlation between Ca, Sr and SO<sub>4</sub>. Redox reactions and land use practices may also be a source of SO<sub>4</sub>. Salinization of groundwater masks the influence of other hydrochemical processes and may be the reason for the pronounced TDS.

Factor 2 relates to the alkalinity of the groundwater,  $\text{HCO}_3$ , Mg and Cl correlating positively and indicating the occurrence of cation exchange reactions. Flushing and leaching of these elements to the groundwater system may be caused by recently recharged water, indicated by the presence of  $\text{HCO}_3$ . Antimony (Sb) and manganese (Mn) are related to the weathering of Sb (pyrite) and Mn containing minerals and Sb is negatively correlated to alkalinity.

Factor 3 indicates the known relationship between pH and redox potential of groundwater, as Cl is also positively correlated. The mobility and solubility of trace elements selenium (Se), barium (Ba - barite) and nickel (Ni - carbonates) are influenced or regulated by these determinants. This factor also correlates negatively to  $\text{NH}_4$  (from nitrates),  $\text{CO}_3$  (sand- and mudstone) in groundwater, due to the geology and the acidity of the environment.

Factor 4 indicates the presence of kimberlite intrusives, due to the presence of phosphate ( $\text{PO}_4$  - calcite) and other heavy metals such as copper (Cu), cobalt (Co), vanadium (V - apatite) and zinc (Zn). pH,  $\text{PO}_4$ , Co and Zn is all positively correlated to each other, but negatively correlated to Cu (dolerites) and V.

Factor 5 is the result of interaction in the subsurface between water and the surrounding geology of the area. The positive correlation of the heavy metals aluminium (Al), cadmium (Cd) and iron (Fe - clay and mudstone) must be from the local geology.

Factor 6 indicates the interaction between kimberlite and water in the subsurface, as chromium (Cr) can be obtained from chrome-spinel. Uranium (U - apatite) and arsenic (As) is positively correlated, with silica (Si) indicating a negative correlation.

Factor 7 is the result of pollution related factors. The nitrate ( $\text{NO}_3$ ) must be the result of pollution sources like fertilisers and animal waste products in the area.

Factor 8 indicates the influence of carbonate intrusives on the chemistry of groundwater in the study area. Potassium (K), carbonate ( $\text{CO}_3$  - calcite) and pH, all correlate positively and show that the carbonates control the alkalinity of groundwater, which may be due to the presence of kimberlite.

**Table 5.4.1.4. Factor analysis of Loxton data with Varimax rotation.**

VARIABLES	Factor 1	Factor 2	Factor 3	Factor 4	Factor 5	Factor 6	Factor 7	Factor 8
Al					-0.634			
NH <sub>4</sub> -N			-0.776					
Sb	0.549	-0.434						
As						0.607		
Ba			-0.761					
HCO <sub>3</sub>		0.870						
B	0.662							
Cd					-0.660			
Ca	0.784							
CO <sub>3</sub>			-0.506					0.428
Cl		0.708						
Cr						0.608		
Co				-0.748				
Cu				0.550				
EC (mS/m)	0.917							
F	0.428							
Fe					-0.601			
Pb	0.587							
Li	0.662							
Mg		0.916						
Mn		0.553						
Mo								
Ni			-0.935					
NO <sub>3</sub> -N							-0.553	
pH			-0.511	-0.422				0.530
PO <sub>4</sub>				-0.582				
K								0.671
Se			-0.724					
Si						-0.530		
Na	0.829							
Sr	0.829							
SO <sub>4</sub>	0.836							
T-Alk.		0.871						
TDS (EC)	0.917							
U			-0.437			0.595		
V				0.687				
Zn				-0.747				
Expl. Var.	6.959	4.394	3.659	3.237	2.087	1.878	1.663	1.722
Eigenvalues	7.501	4.349	3.920	3.040	2.040	1.742	1.573	1.435
Cumulative %	20.272	32.026	42.621	50.836	56.350	61.059	65.312	69.189

All values in ppm, unless otherwise indicated.

## 5.4.2. Groundwater Types of the Study area

### 5.4.2.1. Introduction

All the chemical data was stored in a data base (HYDROBASE) and imported into WISH, to generate stiff diagrams (histograms) in determining the water types of the study area, as the main cations and anions determine the dominant water type.

### 5.4.2.2. Groundwater Types

The main water type found in the area is a water type not dominated by any an- or cations in particular. Secondly a Na-SO<sub>4</sub> type water is dominant, followed by a Na-HCO<sub>3</sub> dominated water and to a lesser extent a Ca-SO<sub>4</sub> type water. **Figure 5.4.2.2.A** depicts the different water types graphically, indicating the dominance (91%) of the four water types mentioned above in the Loxton area. The other nine percent of groundwater in the area is represented by NaCl and Ca/Mg-HCO<sub>3</sub> type water.

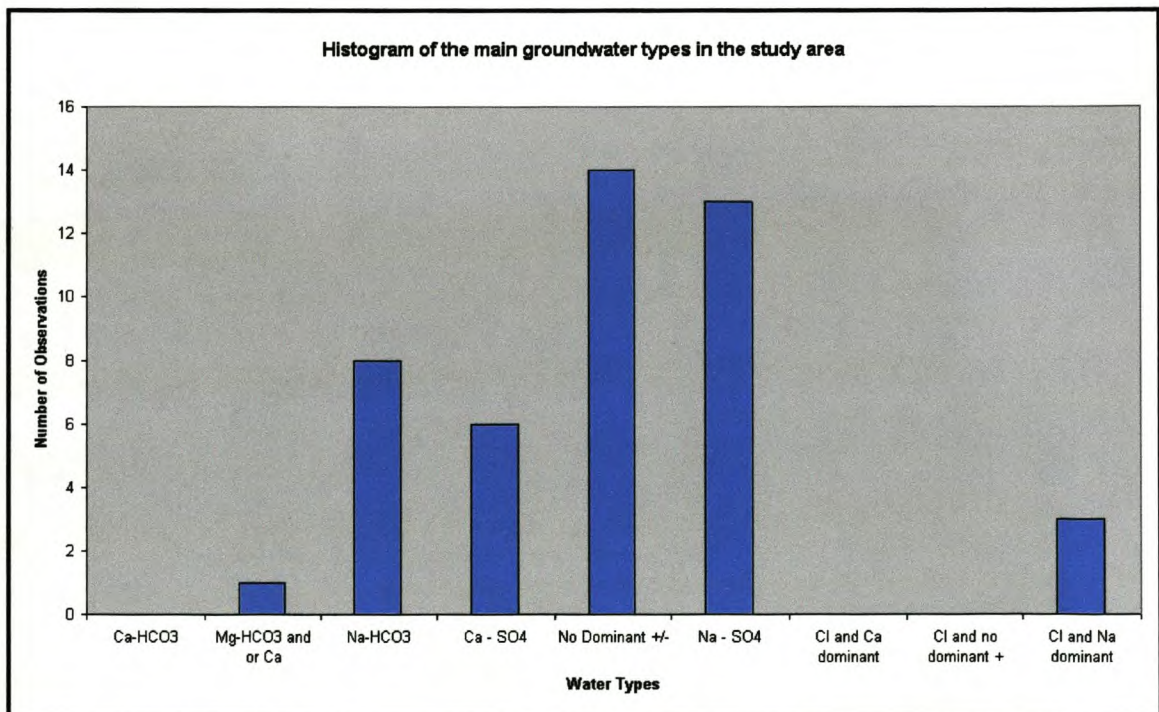


**Figure 5.4.2.2.A. Histogram of the main water types in the area**

A composite Piper diagram (**Figure 5.4.2.2.B**) depicting subdivisions on the basis of water types plotting in different clusters and in terms of regime, as well as recharge / discharge zones, was accomplished (Kirchner, 1994; Ophori and Toth, 1988; Piper, 1944). The Piper diagram correlates to recharge (sloping topography) and discharge (flat topography) areas of the study at Loxton.

The nine different water types in the study area are described in terms of their relative position on the nine zones of an Expanded Durov diagram (**Figure 5.4.2.2.C**):

1.  $\text{HCO}_3^-$  and  $\text{Ca}^{2+}$  water. This water type is often a recently recharged or recharging water.
2.  $\text{HCO}_3^-$  and  $\text{Mg}^{2+}$  dominant or  $\text{HCO}_3^-$  and  $\text{Ca}^{2+}$  and  $\text{Mg}^{2+}$  important. This type of water is often associated with dolomite or mafic igneous rocks.
3.  $\text{HCO}_3^-$  and  $\text{Na}^+$  dominated water, often indicating ion exchange reactions.
4.  $\text{SO}_4^{2-}$  (or anions indiscriminate) and  $\text{Ca}^{2+}$  dominated water, associated with recharge water in lavas or gypsum deposits.
5. No dominant an- or cations in the water, resulting from dissolution or mixing.
6.  $\text{SO}_4^{2-}$  (or anions indiscriminate) and  $\text{Na}^{2+}$  dominated water, not frequently found and may be due to mixing.
7.  $\text{Cl}^-$  and  $\text{Ca}^{2+}$  dominated water, not common unless reverse ion exchange is taking place.
8.  $\text{Cl}^-$  and no dominant cations, suggest that reverse ion exchange is taking place.
9.  $\text{Cl}^-$  and  $\text{Na}^+$  dominated water, frequently indicates an end point in a water evolution sequence.

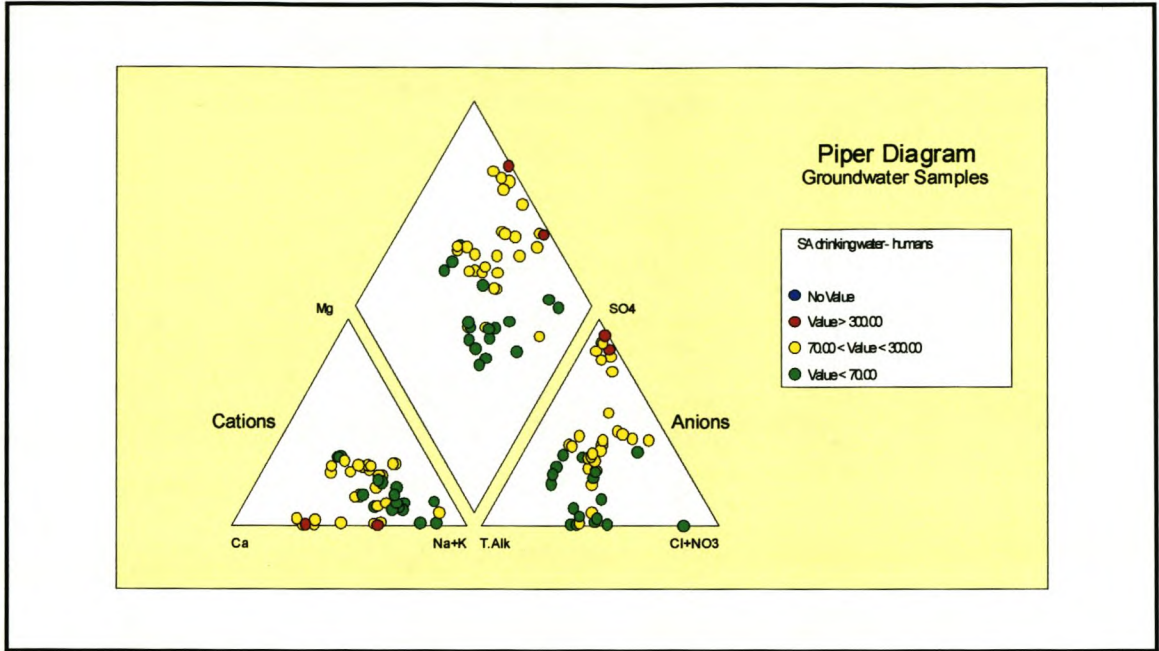


**Figure 5.4.2.2.B.** Piper diagram of all groundwater samples at Loxton

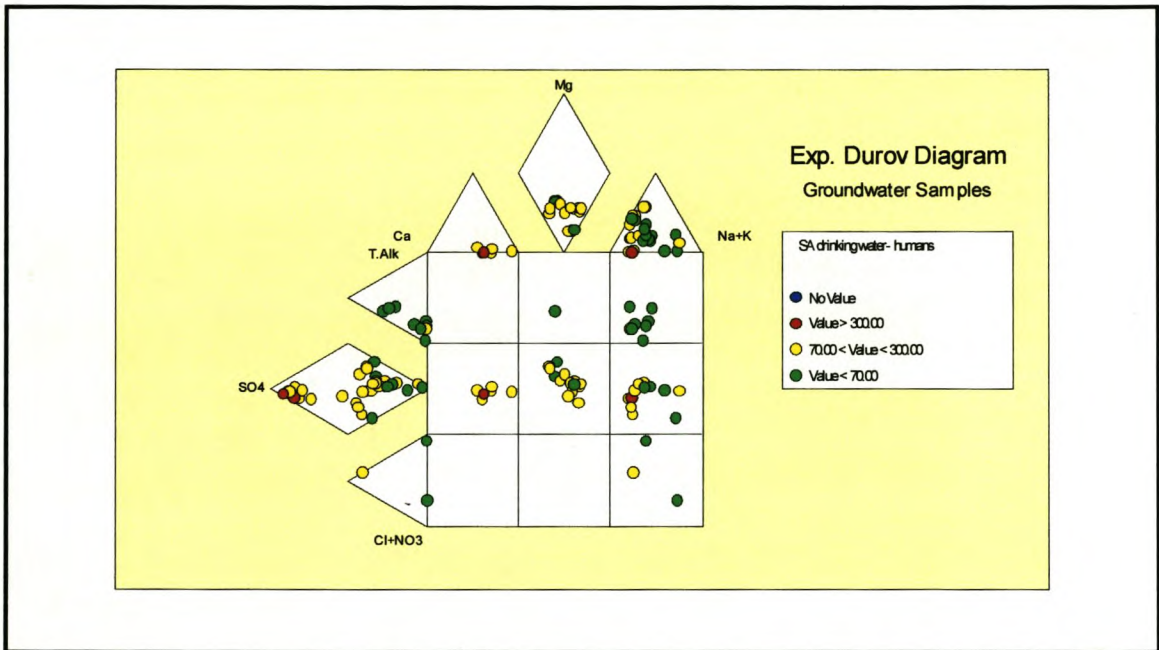


**Figure 5.4.2.2.C.** Expanded Durov diagram of all the groundwater samples at Loxton

### 5.4.2.3. Description of the Chemical Constituents

Karoo formations due to their ubiquity throughout Southern Africa display variable water quality properties. Lateral changes in climatic patterns seem to be the main factor controlling the diversity of the mineralization and water types occurring in Karoo rocks. This variability is caused by differences in rainfall, recharge, evaporation, topography, soil type and thickness, vegetation cover and human activities (*Woodford et al., in press*).

Due to the nature of groundwater flow, which varies significantly from area to area, local groundwater quality variations are significant and anomalies to the large-scale generalizations are prevalent. Micro-scale differences occur due to the nature of groundwater flow in Karoo rocks, namely the resulting variations within matrix and fracture components of the groundwater flux. The residence times are often different for these two main components and give rise to the differences in mineralization and solute proportion in passing groundwater (*Woodford et al., in press*).

Local topography (**Figure 5.4.2.3.K - see page 146**) has an influence on the local groundwater quality. Flat laying areas act as sinks (i.e. rivers and valleys) for groundwater, which is usually of a much poorer quality (> 149 mS/m) than groundwater in sloping areas (i.e. hills and foothills), which tend to be fresher (*Adams, 1998*).

As groundwater drains towards the lower lying areas, where it becomes static or stagnant, there is a concurrent increase in EC (**Figure 5.4.2.3.A**).

Tredoux and Kirchner (1981) have applied sodium percentage maps to indicate and interpret the direction in which discharge occurs, as the percentage of sodium (Na%) of the total cations can indicate where recharge and discharge areas are situated (**Figure 5.4.2.3.B**). Areas of discharge tend to have a relatively higher Na% in the water, as opposed to recharge areas, indicating that lower lying areas (i.e. flat plains, valleys and rivers) act as sinks to groundwater discharge.

Ions like calcium (Ca), sulphate (SO<sub>4</sub>) and chloride (Cl), all tend to increase in discharge regions (**Figures 5.4.2.3.C-E**). Potassium (K) shows an increase to the west of the topographic high (**Figure 5.4.2.3.F**), but is not controlled by the salinity of water, but sourced from the geological material in the area.

Nitrate ( $\text{NO}_3$ ) shows the effect of land use practices (**Figure 5.4.2.3.G**), as isolated occurrences (Site 6 & 2) of high levels of nitrate are indicative of anthropogenic sources, for no nitrogen containing geological material exists within the study area.

There are noticeable differences in the concentrations of K,  $\text{HCO}_3$  (**Figure 5.4.2.3.H**), Cl, Na, Ca,  $\text{SO}_4^{2-}$ , Li, B and Sr (**Figure 5.4.2.3.I**), with depth. Sr, B, Al and Li concentrations all tend to decrease with depth. In a paper by Arad et al (1986) B, Cl, Ca, F (**Figure 5.4.2.3.J**) and Na values were used in defining water groups. In Israel Sr, B and F concentrations increased with an increase in salinity. The same trend is observed in the Loxton study area.

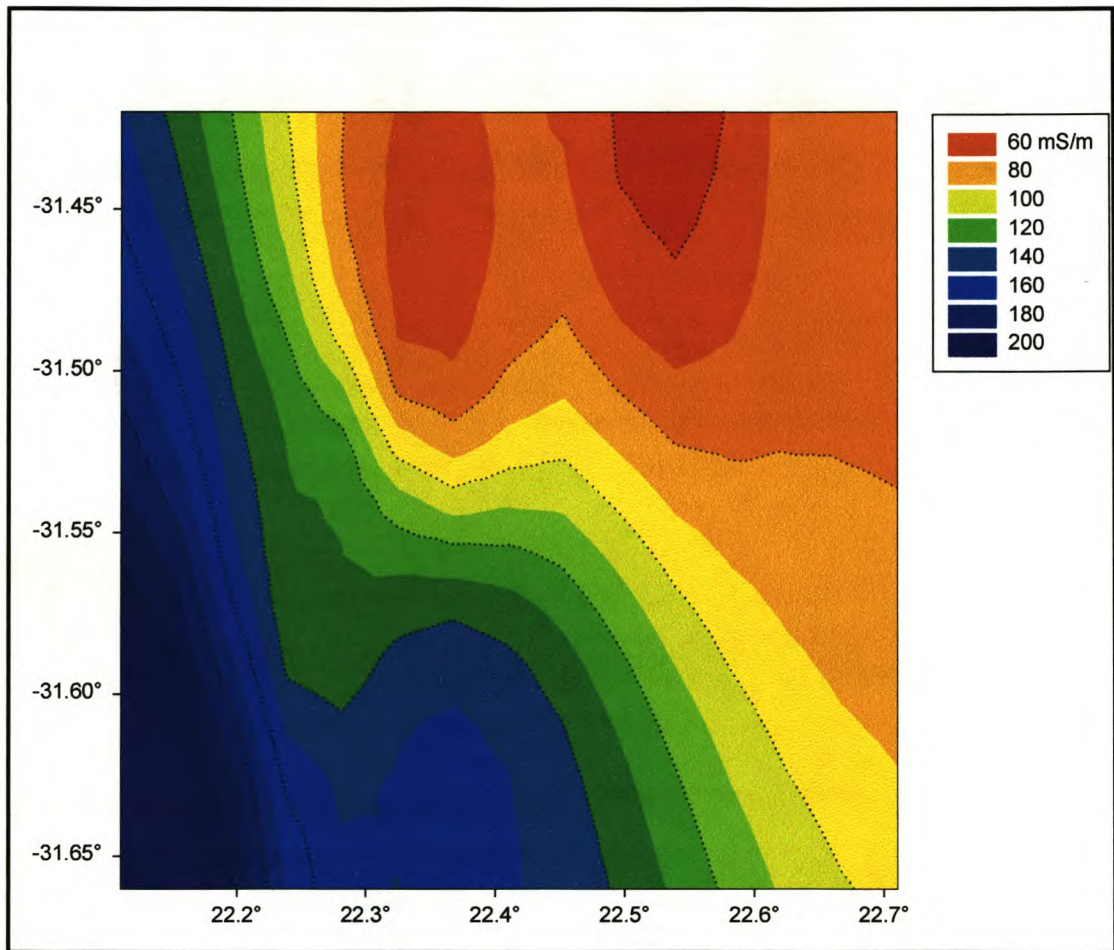


**Figure 5.4.2.3.A. Electric conductivity map for the study area.**

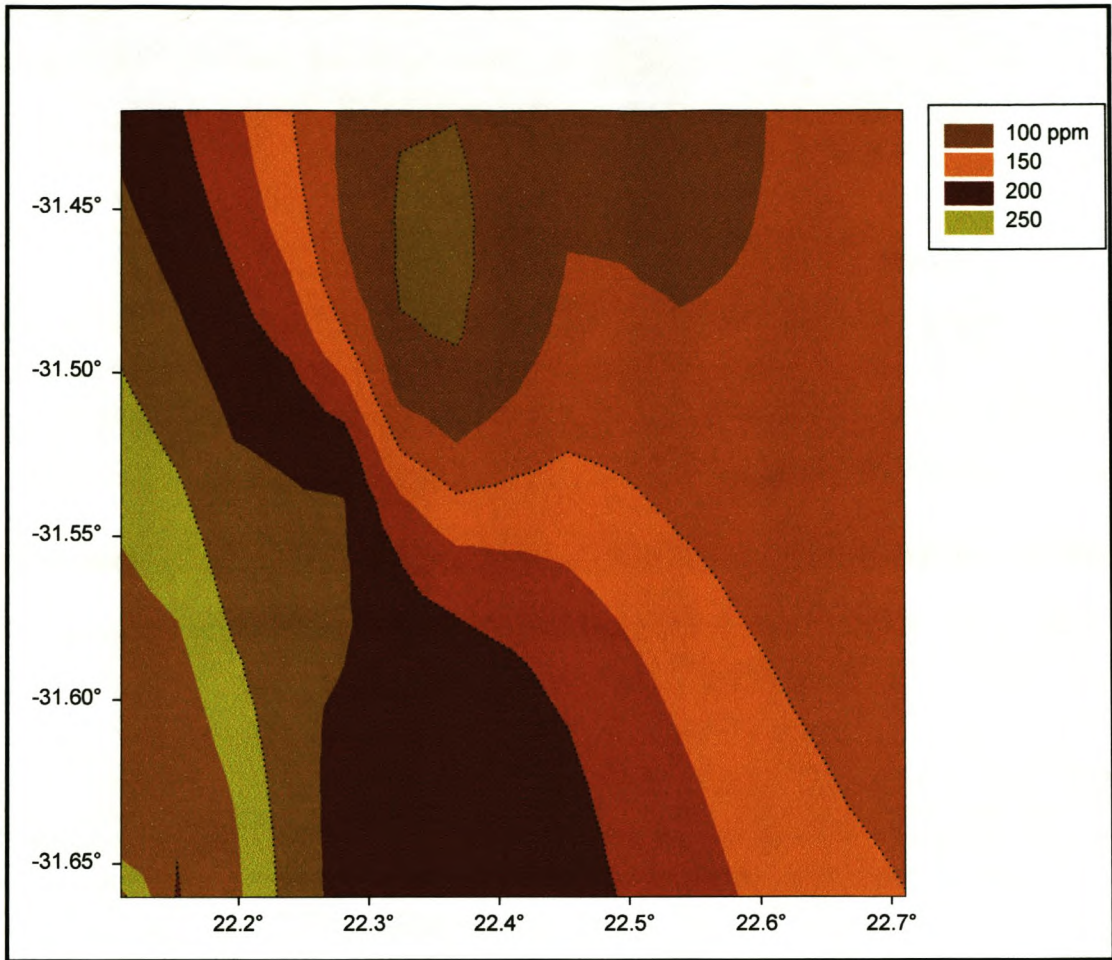


***Figure 5.4.2.3.B. Sodium (ppm) map for the study area.***

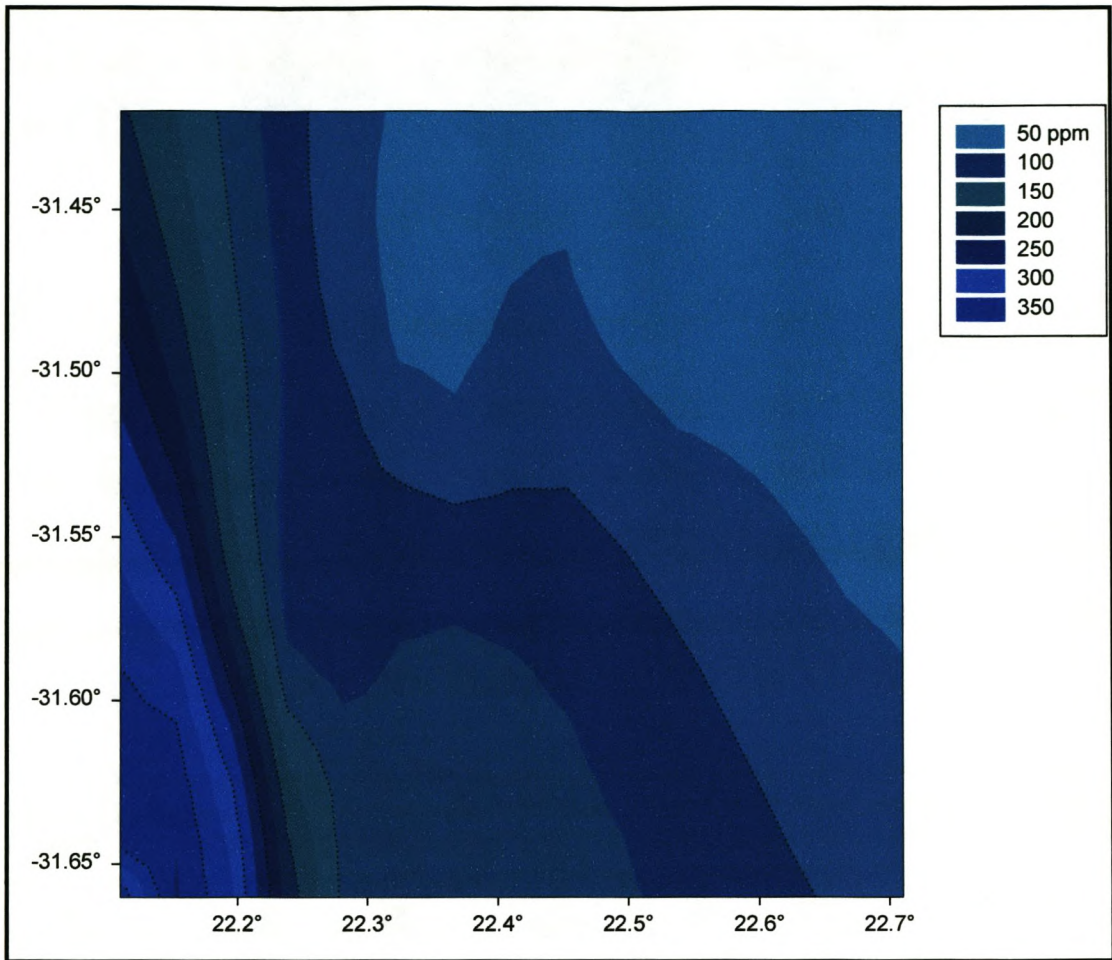


***Figure 5.4.2.3.C. Calcium map for the study area.***

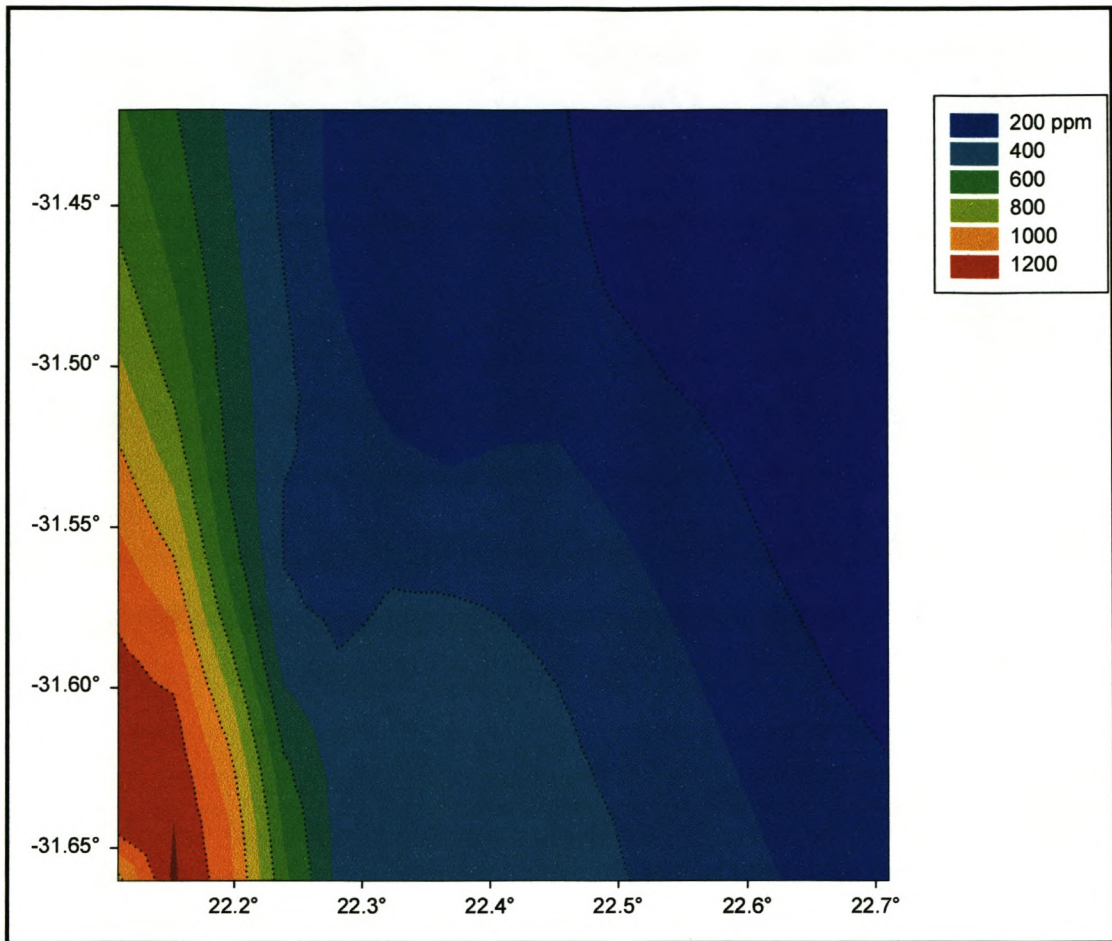


***Figure 5.4.2.3.D. Sulphate map for the study area.***

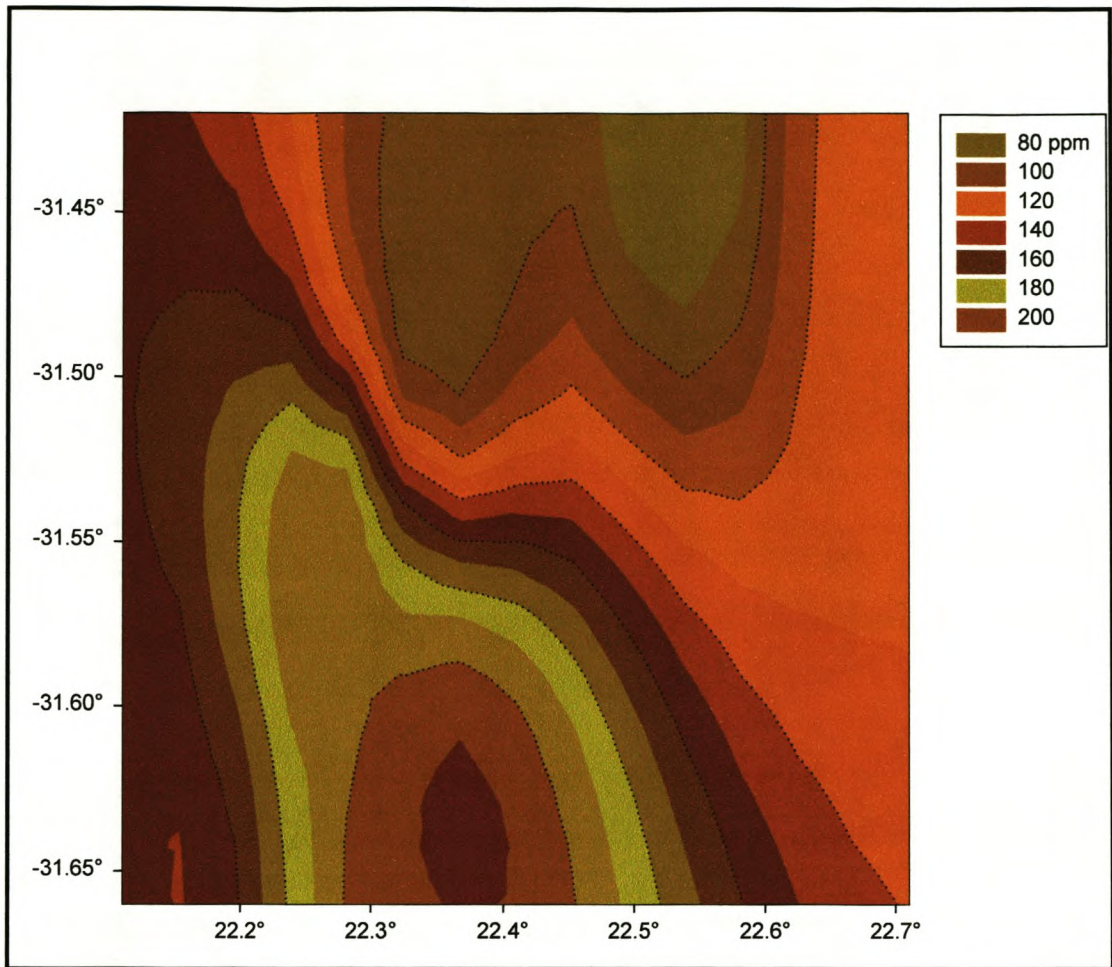


***Figure 5.4.2.3.E. Chloride map for the study area.***

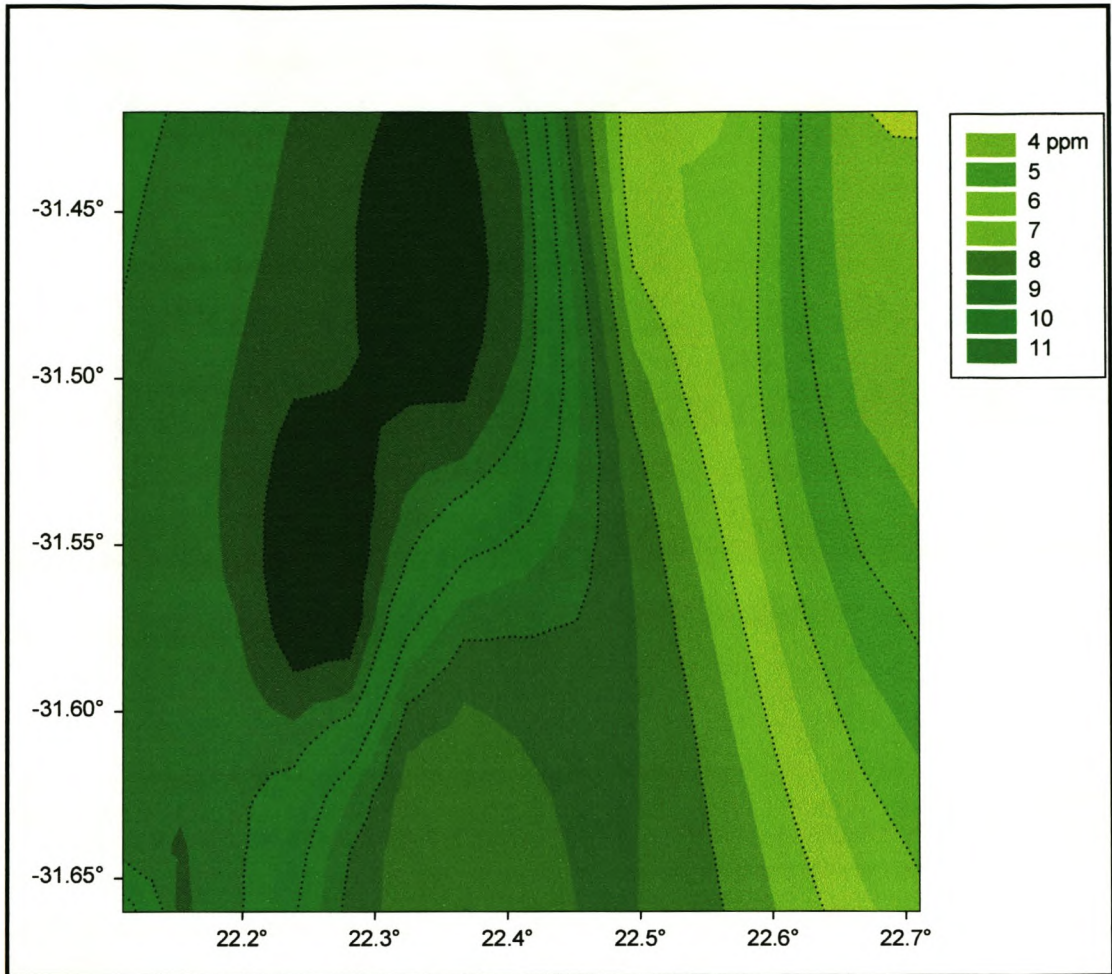


***Figure 5.4.2.3.F. Potassium map for the study area.***

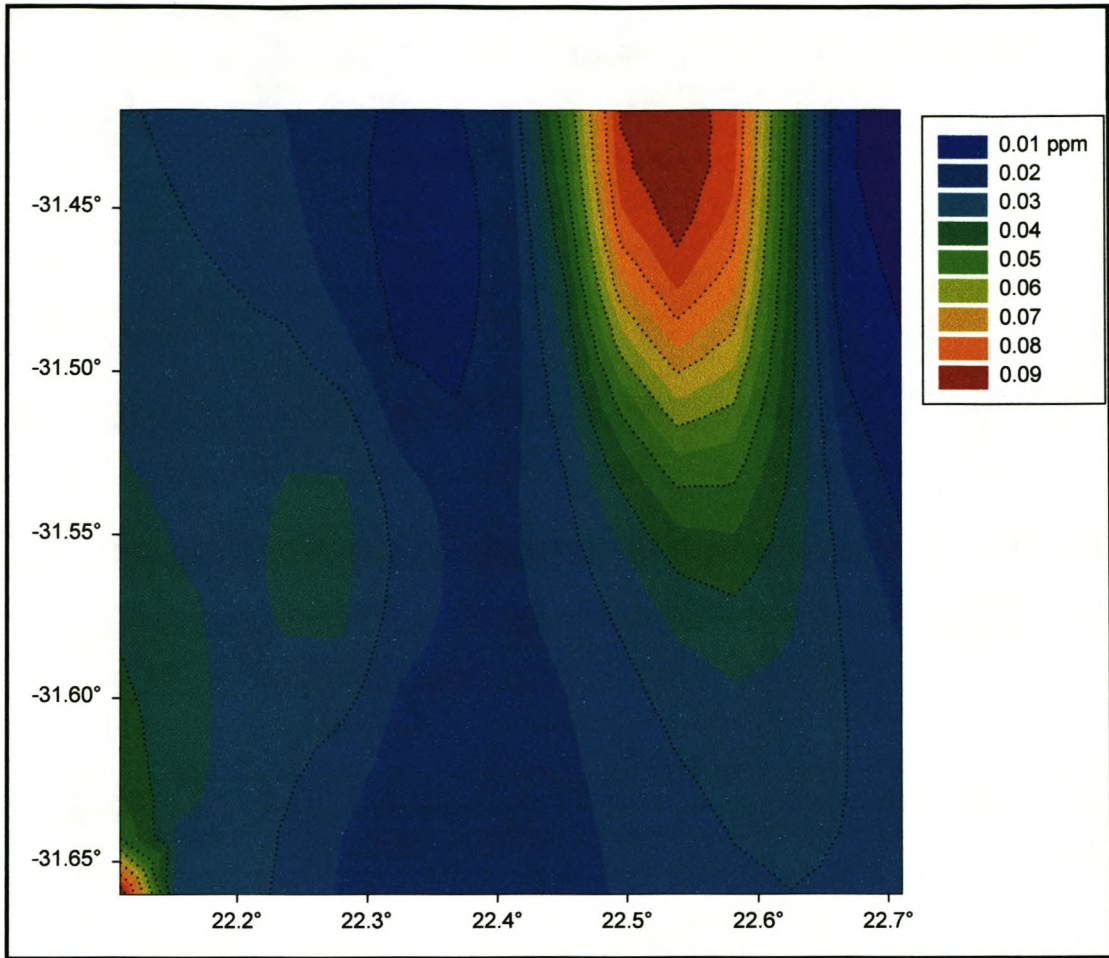


***Figure 5.4.2.3.G. Nitrate map for the study area.***

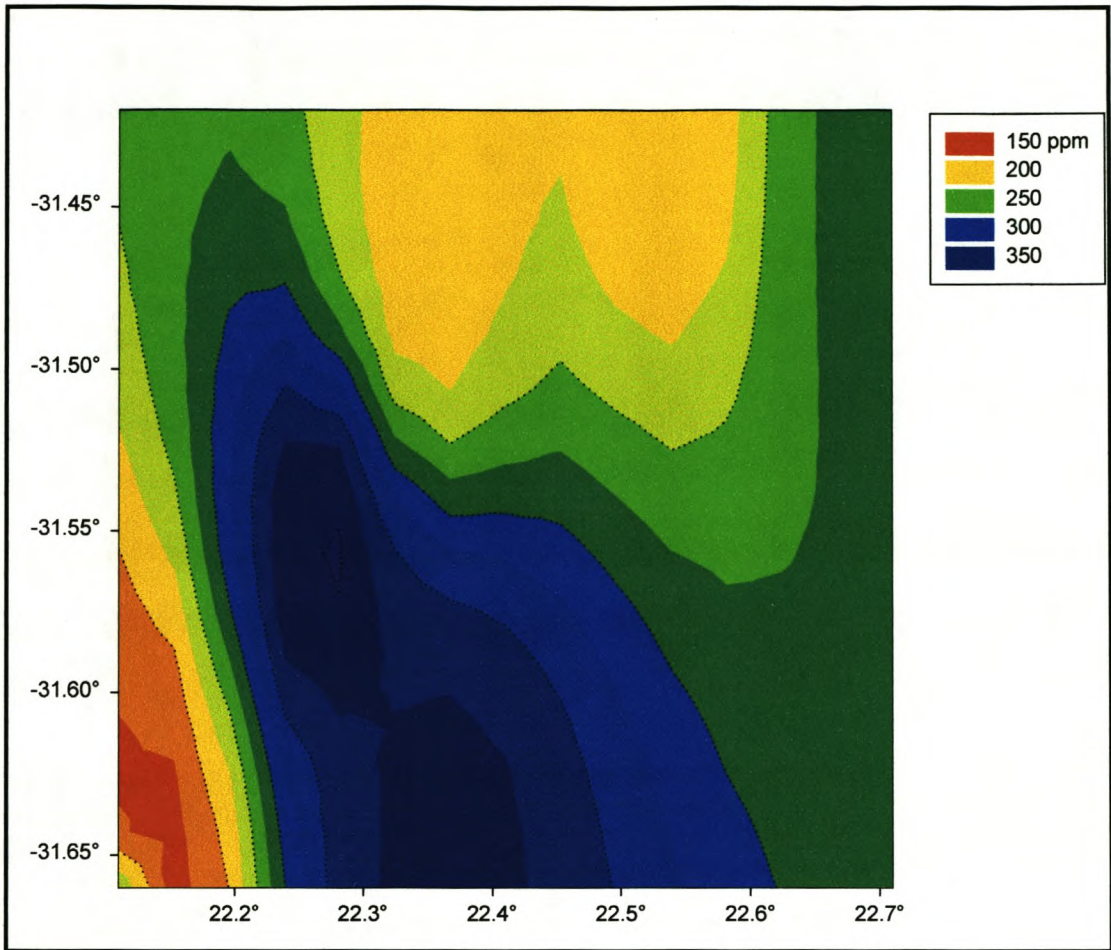


***Figure 5.4.2.3.H. Bicarbonate map for the study area.***

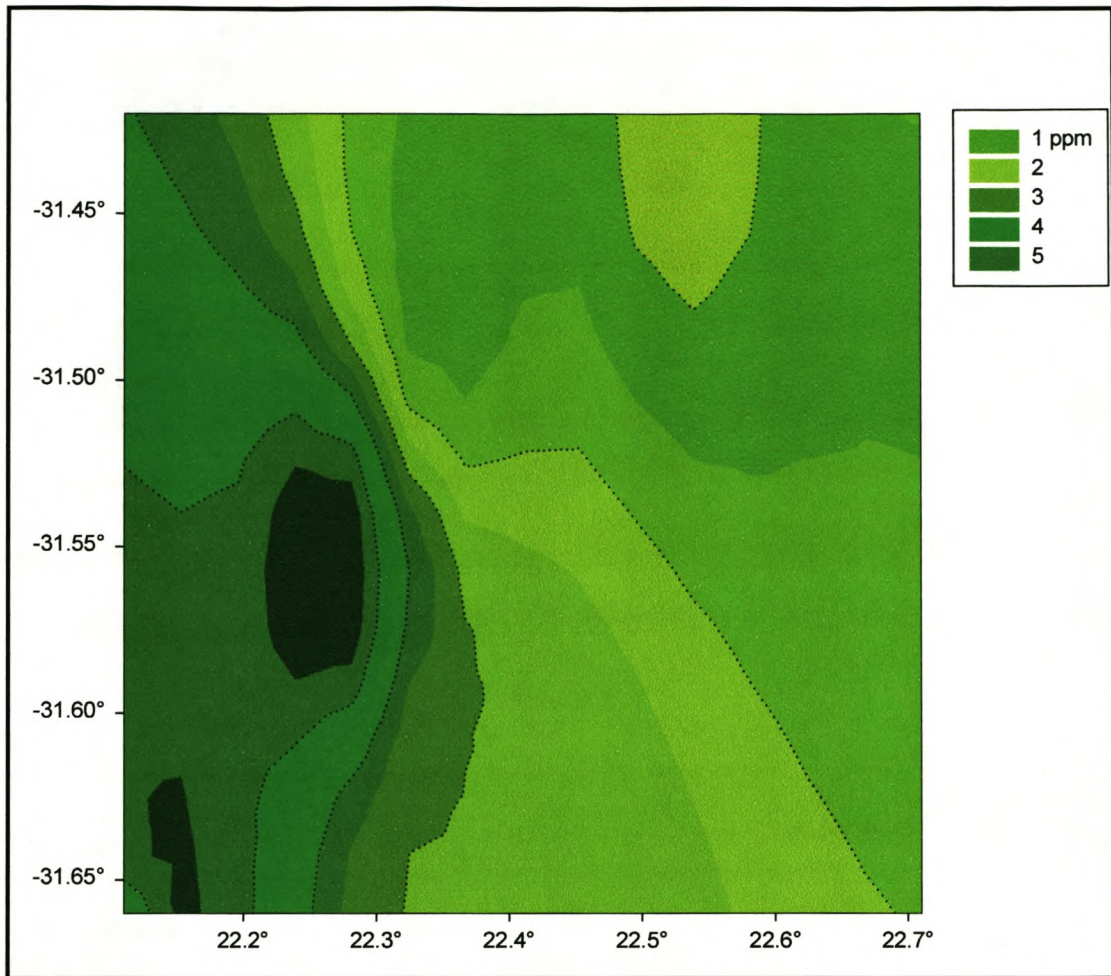


***Figure 5.4.2.3.I. Strontium map for the study area.***

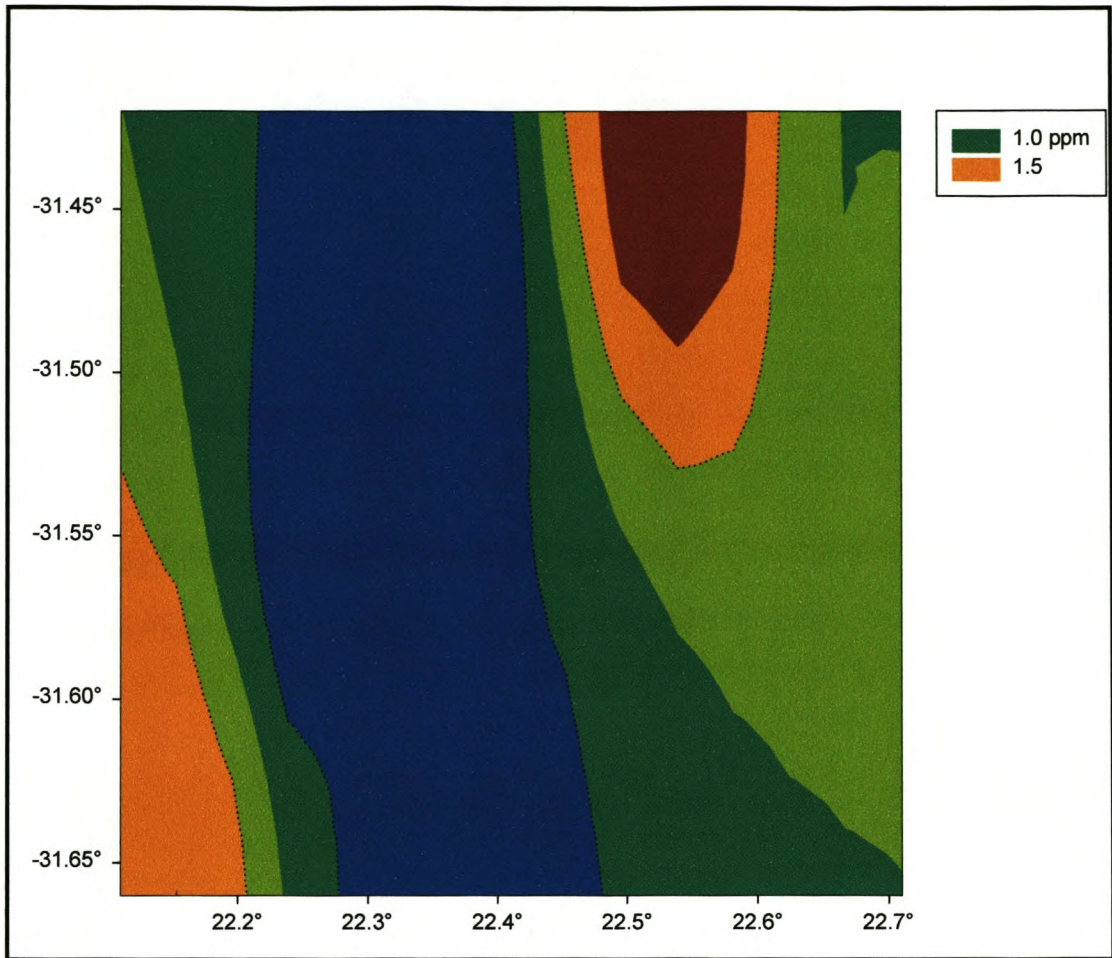


***Figure 5.4.2.3.J. Fluoride map for the study area.***

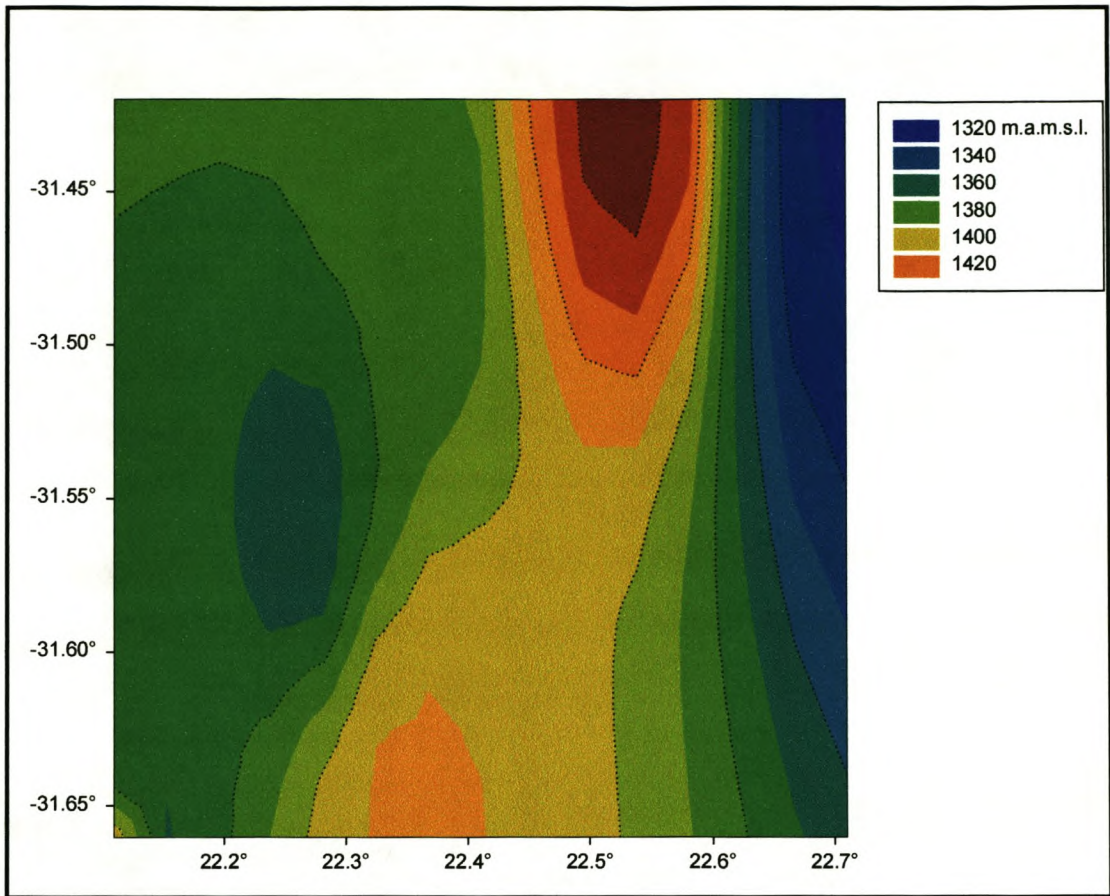


***Figure 5.4.2.3.K. Topographical map for the study area.***

#### 5.4.2.4. Groundwater Evolution

The evolution of groundwater possibly follows the sequence in **Table 5.4.2.4.A**, with an increase in mean TDS concentration in the sequence (*Adams, 1998*). An assumption is made that facies 1 type water would occur in recharge areas and be more recent water, whereas facies 9 type water would be from discharge zones. This assumption is not supported by the results from this study area (**Table 5.4.2.4.B**).

**Table 5.4.2.4.A. Assumed hydrochemical facies and regimes of the groundwater**

Facies	Water Type	Regime	Mean TDS (mg/l)	Occurrence
1	Ca - HCO <sub>3</sub>	Recharge + static and discordinate		
2	Mg - HCO <sub>3</sub> and or Ca	Recharge + static and discordinate	446	1
3	Na - HCO <sub>3</sub>	Static + dynamic and coordinated	443	8
4	Ca - SO <sub>4</sub>	Static and discordinate	1322	6
5	No Dominant +/-	Discharge + stagnant water	687	14
6	Na - SO <sub>4</sub>	Stagnant water	605	13
7	Cl and Ca dominant	Static and discordinate + Ca - SO <sub>4</sub>		
8	Cl and no dominant +	Static discordinate + Ca - SO <sub>4</sub>		
9	Cl and Na Dominant	Static discordinate + Ca - SO <sub>4</sub>	498	3

**Table 5.4.2.4.B. Hydrochemical facies and regimes of the groundwater, according to mean TDS.**

Facies	Water Type	Regime	Mean TDS (mg/l)	Occurrence
3	Na - HCO <sub>3</sub>	Static + dynamic and coordinated	443	8
2	Mg - HCO <sub>3</sub> and or Ca	Recharge + static and discordinate	446	1
9	Cl and Na Dominant	Static discordinate + Ca - SO <sub>4</sub>	498	3
6	Na - SO <sub>4</sub>	Stagnant water	605	13
5	No Dominant +/-	Discharge + stagnant water	687	14
4	Ca - SO <sub>4</sub>	Static and discordinate	1322	6

*Statements like:* HCO<sub>3</sub> dominated groundwater (among the anions) is an indication of much younger water with a relatively short flow path (*Sowayan and Allayla, 1989*), and water with a high salt content were relatively older than fresher water, found in the Beaufort sediments (*Talma, 1981*), are questioned.

Although groundwater type development may occur simultaneously within the fractured aquifer, no definite trend can be identified in terms of the groundwater type distribution (evolution) for the

study area and no regional patterns could be identified. There seem to be a separation between Sites 1-4 (A) and Sites 5-6 (B), as indicated by the maps in *Section 5.4.2.3*, with evolution continuing west at (A) and to the east at (B). Fractured aquifers in the area must be made up of groundwater compartments, as a result of geological structures. Changes in groundwater chemistry could be the result of topography, vertical heterogeneity in lithology and localised recharge and discharge zones along structures.

The chemical character of the groundwater is predominantly controlled by the infiltration of evaporated surface and subsurface water, the topographical nature of the catchments, geological influences (i.e. the process of dissolution, precipitation and ion exchange) and the influence of man (*Adams, 1998*). The effects of these factors must be ascertained by hydrochemical techniques, as this is a complex area with different systems and processes at the six sites of the study.

## **5.5. Factors Affecting Groundwater Chemistry**

### **5.5.1. Influence of Topography on the Groundwater Chemistry**

Flat areas are usually associated with areas of discharge, where the flow of water becomes more sluggish or static and evaporation is more pronounced, relating to higher salinity. The residence time of water in higher lying regions is low as water tends to flow from these areas due to the hydraulic gradient that exists and the effect of evapotranspiration is therefore less pronounced (*Adams, 1998*). In the flatter areas a third of the water is Na-SO<sub>4</sub> type water, with respect to an Na-HCO<sub>3</sub> dominated water in the higher lying areas.

Topography has a definite influence on water chemistry as seen from **Figure 5.5.1**. Points with low Cl and TDS values (slopes and terraces) plot in the lower left hand corner of the diagram and groundwater from flat areas shows a increase in Cl content, with a subsequent increase in TDS, plotting toward the right hand corner of the diagram. The riverbeds plot between the high and low lying areas. As the plot of flat areas is spread over the diagram, they indicate that topography does not absolutely determine chemical composition, which may be due to factors other than residence time and evapotranspiration (*Adams, 1998*).

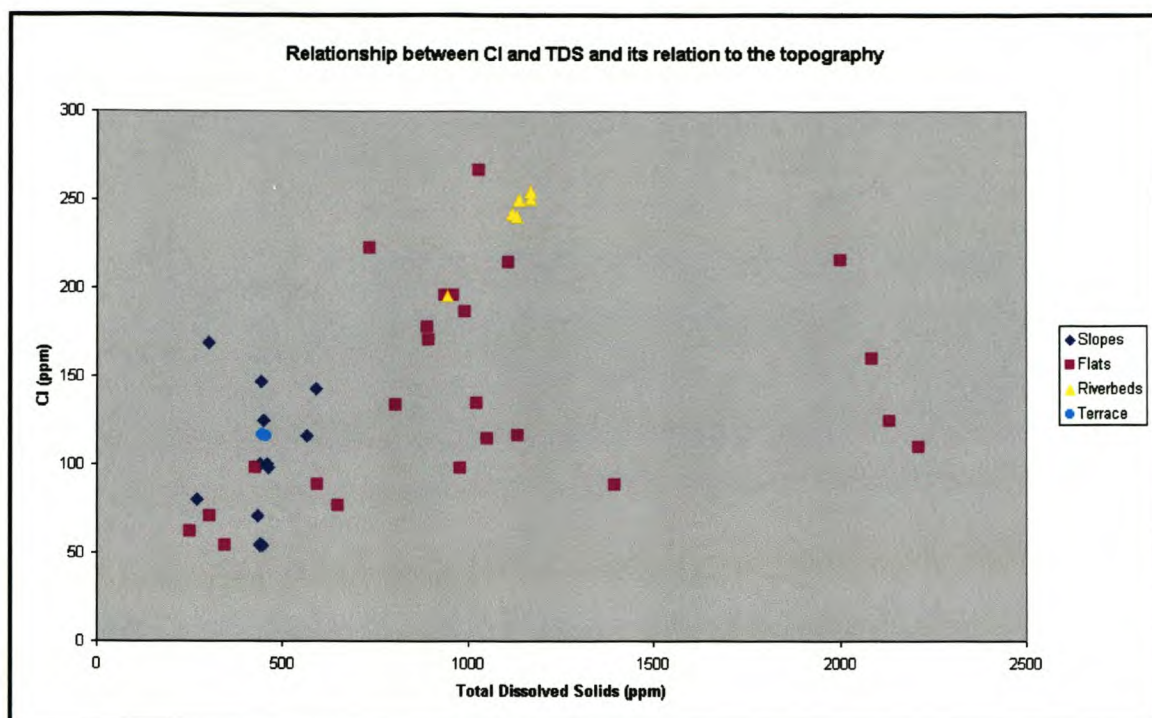


**Figure 5.5.1. Relationship between Cl & TDS and its relation to topography.**

Groundwater flow is determined by the topography, but groundwater will also flow along joints and fracture zones caused by dolerite intrusions prevalent in the study area. Dykes and sills may form impermeable barriers to groundwater flow, but also form permeable zones, causing mixing between the components. Orientation of these structures would control the local flow regime (Adams, 1998). Mean TDS values increase from topographically high areas, to topographically flat laying areas, as depicted in **Table 5.5.1**.

**Table 5.5.1. Average groundwater chemistry for various topographical settings.**

Topo - Setting	EC (mS/m)	pH	Cl	Na	Ca	HCO <sub>3</sub>
Slopes	62.95	7.42	100.92	89.54	42.08	225.62
Terraces	94.30	7.15	116.50	90.00	35.50	247.50
Flats	148.38	7.22	140.96	200.63	201.50	226.46
Riverbeds	158.65	7.17	239.17	229.83	95.17	378.17

Lower Ca and HCO<sub>3</sub> values are evident in the higher lying areas, suggesting that direct recharge and subsequent dissolution of carbonate minerals are limited to the higher laying areas. Fracture zones will favor recharge. The content of Na and Cl increases from topographic highs to lows, indicated also by the fresher water from high lying areas where its not subjected to concentration as in the low laying areas (Adams, 1998).

Local topography will determine the location and amount of salt accumulated due to evaporation, such as sinks (flatter areas and localised depressions) acting as ponding localities for water. The relation between topography and drainage is the major factor influencing the local accumulation of salts (*Adams, 1998*). Black, micaceous shales appear to be the main source of salinity in the Breë River Valley (*Greeff, 1991, 1994*).

### 5.5.2. Influence of Evapotranspiration on the Groundwater Chemistry

The annual mean precipitation in the study area is less than 200 mm/year, while the annual potential evaporation is 3 000 mm/year, which has a marked effect on groundwater composition.

Surface water flows from topographic highs to lows and accumulates in flat areas or depressions, where ponding, evaporation and salt accumulation occurs. This salt is dissolved and transported to the subsurface (i.e. the unsaturated and saturated zones), during rain events, with the cycle repeating. Thus the phenomena of high TDS and salinity water found in flatter areas (*Adams, 1998*).

The high salinity of water in flatter areas is confirmed by the behavior of  $\delta^{18}\text{O}$  and  $\delta^2\text{H}$  isotopes. There is an enrichment of both  $\delta^{18}\text{O}$  and  $\delta^2\text{H}$  isotopes in the residual liquid of evaporated water from surface water bodies or saturated soils. The isotopes with smaller atomic mass ( $^1\text{H}$  and  $^{16}\text{O}$ ) are preferentially transformed into the gas phase, thereby distinguishing evaporated water with its relative enrichment of  $\delta^{18}\text{O}$  and its deviation from the global meteoric water line (GMWL) (**Figure 5.5.2.A**). Sampling points do not plot in a cluster, indicating that the groundwater is not uniform and does not have the same origin. This important phenomena shows that a common recharge source is unlikely, due to  $\delta^{18}\text{O}$  variability in the different localities (*Adams, 1998*).

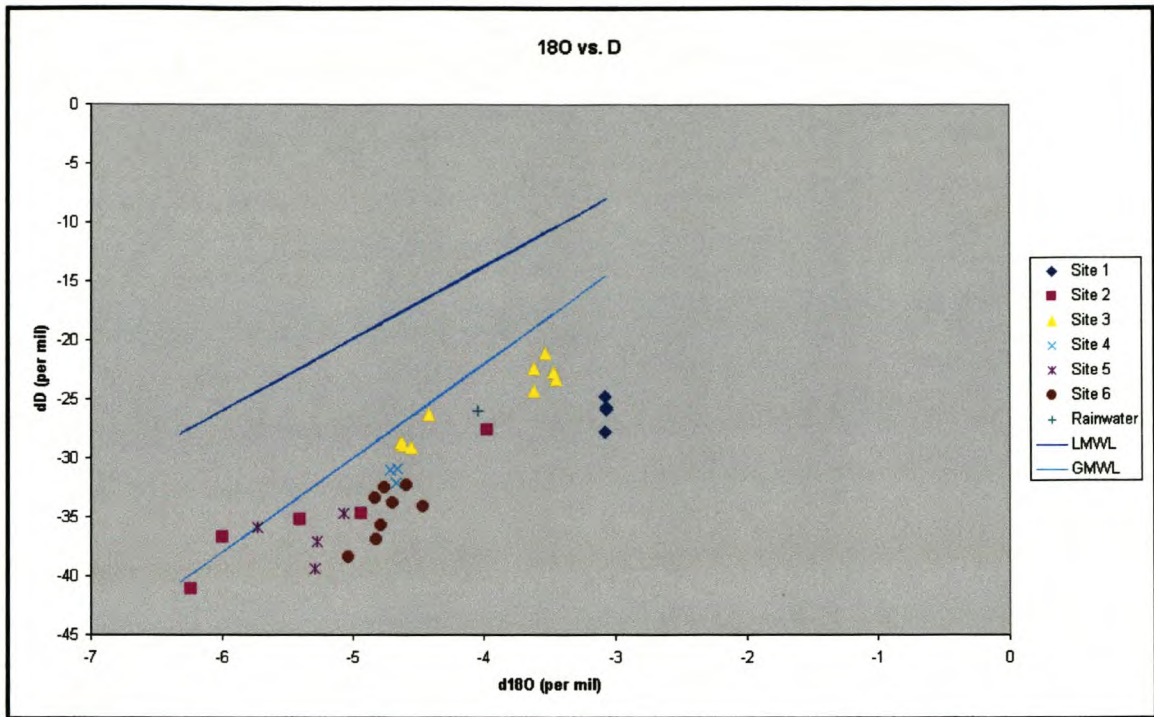


**Figure 5.5.2.A. Deuterium vs. Oxygen-18 for all samples at Loxton**

One point plots to the left of the GMWL may suggest other processes than evaporation. The local rainwater line (LMWL) is located above the GMWL. The main cause of groundwater salinity, is the infiltration of evaporated water to the subsurface, suggested by the isotopic enrichment of  $\delta^{18}\text{O}$  and  $\delta^2\text{H}$  (**Figure 5.5.2.A**), indicating very slow recharge from ponded water during excessive rainfall events. This evaporated water infiltrates the subsurface through preferential pathways. Points on or very close to the GMWL indicate rapid infiltration, before evaporation took place (*Adams, 1998*).

**Figure 5.5.2.B** exhibits no correlation between Cl concentrations and  $\delta^{18}\text{O}$ , thus no relationship exists between isotopic enrichment and groundwater salinity, as a result of evaporation effects. Difference in Cl and  $\delta^{18}\text{O}$  indicate different infiltration conditions and that the water may be unrelated, probably due to mixing of different water bodies (*Adams, 1998*).

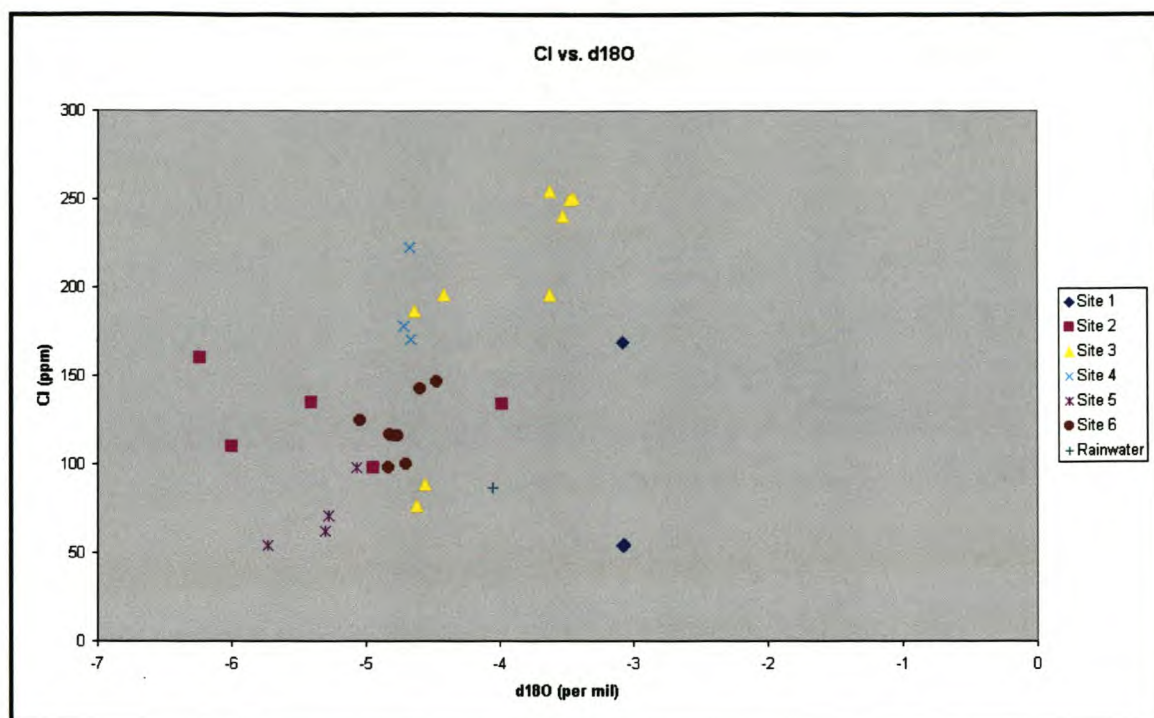


**Figure 5.5.2.B. Chloride vs. Oxygen-18 for all samples at Loxton.**

Depletion of heavier stable isotopes occurs as water vapor condenses in an air mass, which is forced upward by changes in topography (Mook, 1994). Lighter stable isotope concentrations are observed in intense rainfall events occurring at high altitude. **Figure 5.5.2.C**, indicates a trend of altitude against  $\delta^{18}\text{O}$  content, where water from higher elevated precipitation is considerably depleted in stable isotopes ( $\delta^{18}\text{O}$ ) (Sites 1 & 3), relative to water originating from lower altitudes (Sites 2, 4 & 6). Points plotting away from the regression line indicate other control processes, like seasonality and temperature effects (Adams, 1998).

It is not surprising that recharge and evaporation patterns have a solute-shaping influence on the groundwater chemistry of the Karoo rocks when considering the highly variable climatic conditions within the Basin. The contrast in groundwater solute concentration and type between the eastern and western Karoo Basin is most significant. The global climatic effects are very different along the edges of the Karoo Basin. The regular and relatively high rainfall in the eastern Karoo results in continuous dilution, leaching and further transport of leached constituents, thereby maintaining a relatively low overall concentration of constituents. Groundwater is under-saturated with respect to most of the minerals, which do not attain their solubility limits (Woodford *et al.*, *in press*).

On the other hand, erratic and sparse rainfall, combined with high evaporation rates in the Western Karoo induces a continuous concentration of solutes as the flushing-effect is at a minimum. The combination of a long groundwater residence times and evapotranspiration results in the reported high salt concentrations of groundwater in the Western Karoo (Woodford *et al.*, *in press*).

The high concentration of anions in groundwater is often the result of rainfall-originated constituents being concentrated many times over by evaporated water leaving its salt content behind (Woodford *et al.*, *in press*).

The concentration effect is further exacerbated by the lack of organic matter due to the thin soil cover. Unfavorable denitrification conditions thus may result in elevated nitrate concentrations. As some minerals reach their solubility limits they tend to precipitate forming rejuvenated calcite and ferric incrustations (Woodford *et al.*, *in press*).

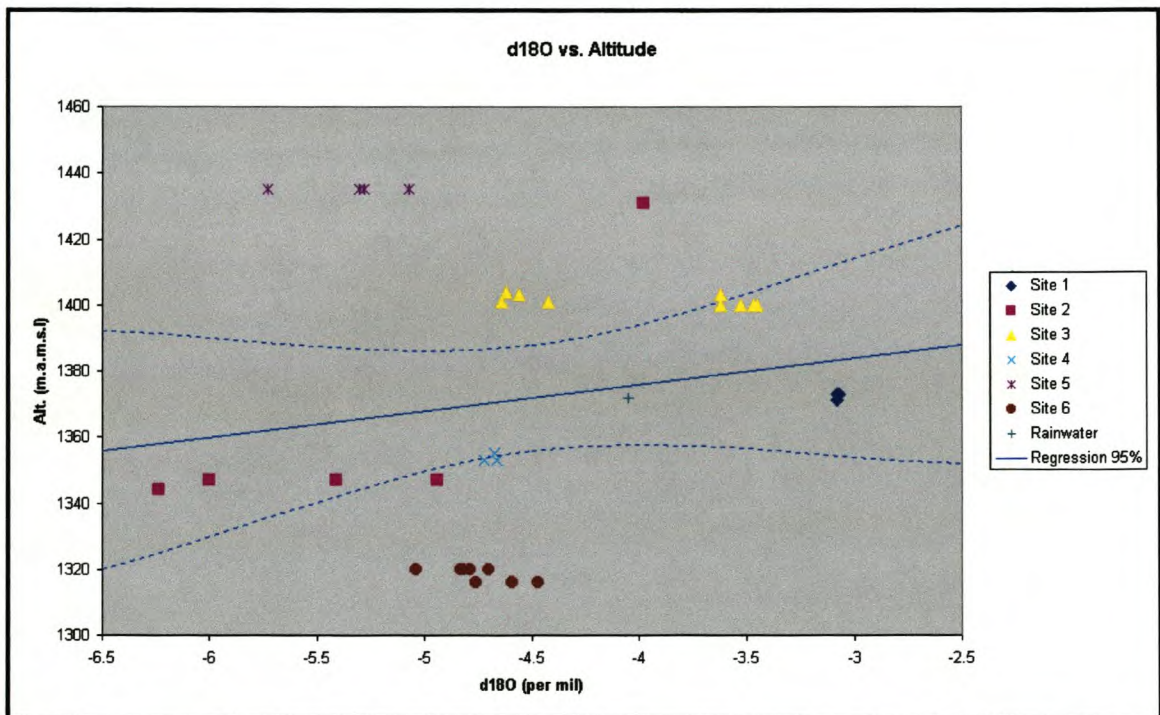


**Figure 5.5.2.C. Altitude vs. Oxygen-18 for all samples at Loxton.**

### 5.5.3. Influence of Geology on the Groundwater Chemistry

#### 5.5.3.1 Introduction

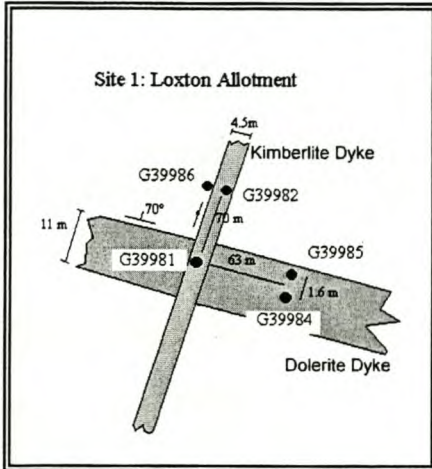
The geological materials that constitutes the earth's crust are the primary reservoir and ultimate source of most major elements and trace elements in soils and in natural water (*Bricker and Jones, 1995*). The main factors responsible for the variability of groundwater chemistry is dissolution, precipitation and cation exchange. Water incorporates major and trace elements on encountering soil and rock, released by decomposing and dissolving rock minerals (*Adams, 1998*).

Geology of the study area is described in *Chapter 3 (Figure 3.6.3.C. p.52)*. Fluvial sandstone and mudstone of the Beaufort Group is the dominant geological components in the area. The main structural domains of the study area are the Jurassic dolerite dykes and or sills & the Cretaceous kimberlite fissures and or pipes, as well as E-W trending sinusoidal megafolds and antithetic monoclines of the Cape Fold Belt (*Visser and Botha, 1980*). The lithological units are near horizontal with a regional dip of 4° southward. Geological information from all the boreholes drilled in the area was made available by the Department of Water Affairs and Forestry (*Appendix C*). Site information tables is available in *Appendix A*.

Numerous hydro-geochemical processes have major or minor effects on the quality of groundwater in aquifers in the Karoo Basin. Different processes dominate the quality of water in the parts of the aquifers deposited within different sedimentary environments (*Woodford et al., in press*).

The major hydro-geochemical processes and their interrelations are discussed in this section. The processes that occur in aquifers, the effect of these processes on the quality of groundwater and the relations of the processes to the sedimentary environment will be discussed. A locality map of Loxton, indicating the layout of the six sites is represented in *Figure 3.6.3.C. p. 52*.

### 5.5.3.1.1. Site 1: Loxton Allotment



This site (**Figure A**) is located at the intersection of a dolerite and kimberlite dyke (structural "knot"). The dolerite dyke form part of a major lineament ("open" reidel shear). Boreholes in the dolerite dyke produced moderate yields of between 3 and 4 l/s, while the boreholes in the kimberlite dyke were dry.

The figure is north-south orientated, with a local slope direction of NW-SE on surface.

**Figure A. Loxton Allotment.**

Analysis indicate that groundwater type is mainly controlled by the lithology of the area. The sloping topography facilitates run-off expressed in the early stages of evolution displayed by the groundwater encountered in the boreholes drilled into the dolerite. Interesting is the evolved water associated with the kimberlite dyke. The distances from the structures have no apparent influence on groundwater at this site.

Calcium, magnesium and sodium bicarbonate water is dominant and controlled by dolerite, while sodium and to a lesser extent sulphate dominated occurs in the kimberlite in the site area. The water is associated with mafic igneous rocks and mixed water. The sodium and sulphate dominated water is representative of water at a late stage of evolution, controlled by kimberlite and the shallow depth of sampling.

Isotope analysis and interpretation indicated that the water of borehole G 39984 is of the same age and origin, although it is classified as different types at depth. Dating indicates a relationship of the geological structures with groundwater recharge, as G 39984 indicated water of only decades due to its position on a major lineament, opposed to G 39981 which indicated water of century age in the kimberlite. A possible recharge mechanism might be a catchment deeper inland, receiving isotopically lighter water and transporting the groundwater in preferred pathways like fractures, joints and faults, which leads to mixing of water at depth.

### 5.5.3.1.2. Site 2: De Wilg

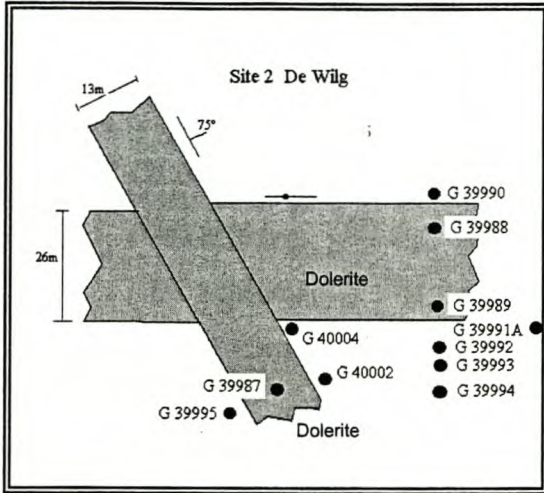


**Figure B. De Wilg.**

This site (**Figure B**) is located at the intersection of an E-W strike slip and NNW dolerite dyke (a dolerite dyke on a small structural "knot"), with a lot of calcrete present on surface. The E-W dyke represents a major regional lineament composed of extensive en-échelon segments. The NNW dyke shows signs of older tectonic reactivation (ring-structure feeder). The E-W dyke gave high yields (up to 15 l/s) and the majority of water strikes occurred at depths between 100 and 230m, while the boreholes on the NNW dyke were dry.

This figure is north-south orientated, with a local surface slope direction of E-W.

The importance of lithology on groundwater type is illustrated at this site. The flat topography in the area might be instrumental in the evolution of the groundwater. All the boreholes are on or close to the structures; the water from all the boreholes drilled in a line over the dolerite dyke is classified as the same type of groundwater (Ca / Na - SO<sub>4</sub>). This site indicates that the groundwater classification is controlled by the structural geology.

The site is dominated by calcium sulphate and sodium / sulphate dominated water, indicating recharged water in lavas (in this instance dolerite) and water due to mixing influences, respectively. Borehole G 39987 is an endpoint water in an evolution sequence, confirming the role of geological structures on groundwater recharge.

Dating of borehole G 39992 indicated water of century age. Isotope analysis reflects the process of intense evaporation, facilitated by the flat topography. Isotopes also indicated that the recharge mechanism at G 40004 might be direct recharge, due to a shallow sampling depth. Boreholes associated with the NNW dyke were dry, confirmed by the more evolved character of groundwater at these holes, representing very low transmissivity.

### 5.5.3.1.3. Site 3: Midland

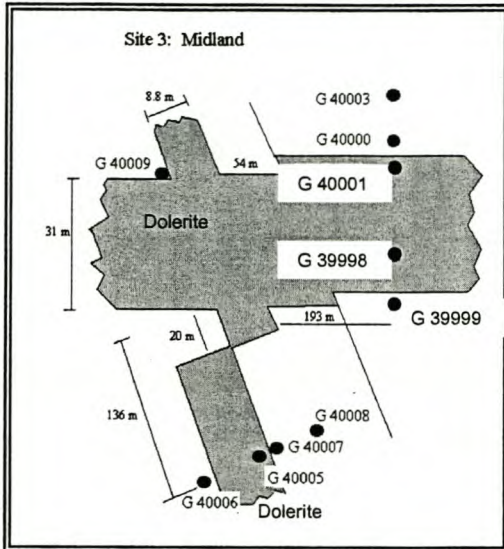


**Figure C. Midland.**

This site (**Figure C**) is located at the intersection of an E-W and NNW dolerite dyke (prominent structural "knot"). Both features represent mega-lineaments. The E-W dyke is within the possible reactivation range. All of the boreholes drilled delivered moderate to high yields. The borehole (G 40009) drilled at the intersection of the two features delivered the highest blow-yield (32 l/s).

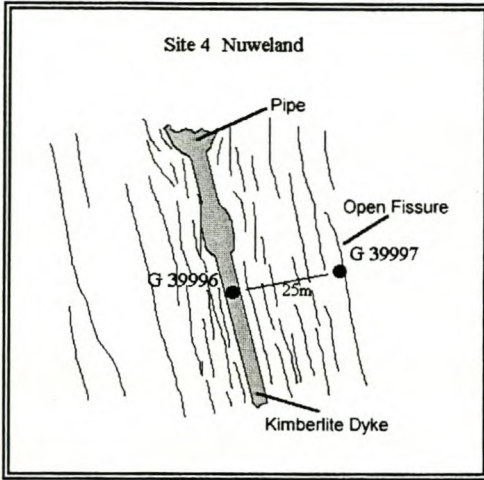
This north south orientated figure has a local S-N surface slope.

Groundwater at this site is dominated by geological influences, associated with the prominent structural "knot".

It is mainly evolved water (water with no ion dominance or  $\text{NaSO}_4$ -type water) is present on the E-W dyke in the riverbed, linking this site to *Site 2*. The change in water type at 90m from borehole G 39998 can be due to mixing. The three boreholes drilled close to the NNW dyke are representative of recharged water in lavas (in this instance dolerite) and indicating no structural or distance effects.

The isotope analysis indicates a distant source recharge mechanism for the E-W structure and intense evaporation for the water in the NNW dolerite dyke. All the dating analyses show water with an age reaching to decades. Isotopes indicated a direct recharge of water at 23m for borehole G 40009. The flat areas are dominated by intense evaporation, while the river beds seems to act as a preferred pathway to isotopic lighter water from a catchment situated more inland, indicating the influence of topography at this site. This site represents younger water than *Site 2* (century) and may indicate an E-W flow path along this E-W strike-slip fracture.

#### 5.5.3.1.4. Site 4: Nuweland



This site (**Figure D**) is located at a 3m wide, N-S kimberlite dyke with a blow and a pipe, as well as a series of parallel mega-joints and fissures. The borehole in the kimberlite was dry, while the borehole in one of the fissures away from the dyke yielded 4.0 l/s.

A local WSW-ENE surface slope is observed at this site, with this figure being orientated north to south.

**Figure D. Nuweland.**

This site indicates the dominance of lithology on groundwater character. Recharge is affected by the flat topography, which facilitates ponding and evaporation. There is a definite difference in groundwater type due to the different structures drilled. The water ( $\text{NaSO}_4$ ) of the kimberlite is associated with mixing influences. The mega joint contains water resulting from dissolution or mixing, as it is not dominated by any cations or anions.

The isotope analysis of the water from borehole G 39997 is the same (age and origin), as indicated by the chemical analysis. The recharge at this site is dominated by intense evaporation, facilitated by the flat topography. The water in the open fissure is decades old, indicating a faster recharge mechanism for water with regard to the kimberlite.

#### 5.5.3.1.5. Site 5: Taaibosch

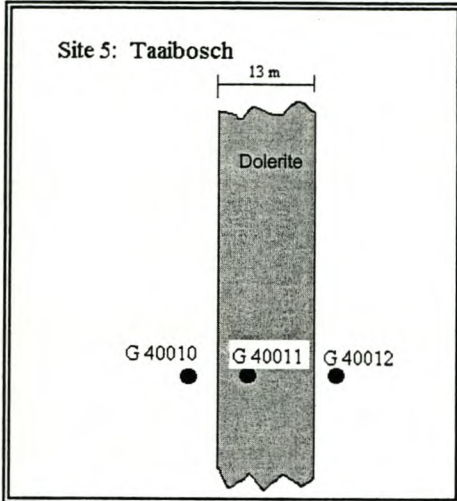


**Figure E. Taaibosch.**

The target feature at this site (**Figure E**) is a 13m wide, NS-NNE trending dolerite dyke (mega-lineament) that was reactivated during the emplacement of the kimberlite. The dyke is very fractured, sheared and full of calcite or calcrete-filled open fractures. Three boreholes were drilled with only one moderate yielding (4.4 l/s) successful borehole (G 40012).

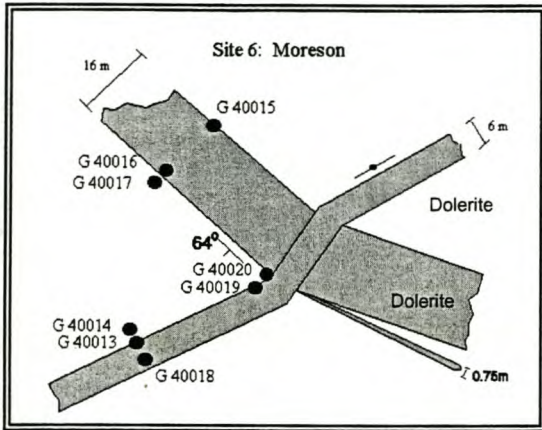
This figure is north to south orientated and indicates a surface sloping gently from west to east.

The influence of lithology on the water at this site is indicated by the data in **Appendix A**. An evolution sequence of groundwater is displayed along the topographical W-E slope.

The change in water type with depth at borehole G 40011 can be explained by mixing at 90m, as well as dissolution at 68m. Borehole G 40010 is associated with ion exchanged water, due to the dolerite dykes which act as conduits of preferred groundwater flow within the aquifer, having a higher permeability than the country rock.

Isotope analysis indicated that water at G 40011 is from the same origin and it also indicated the dating as reaching century age. Recharge occurred after intense evaporation, facilitated by the flat topography at the site.

### 5.5.3.1.6. Site 6: Môreson



This site (**Figure F** - NS orientated) is located at an intersection of a NE- and a NW-trending dolerite dyke. The NE dyke represents a mega-lineament, but is thin (6m) and orthogonal to the possible modern reactivation orientation created within a WNW compressional stress regime (P-type fracture). The NW "dyke" is thicker (16m), but is not a mega-lineament (inclined sheet). It does however lie within the trend for possible modern reactivation ("open" reidel shear).

**Figure F. Môreson.**

Moderate yields of 1.5-2.6 //s were struck at shallow depths within and on the upper contact of the inclined sheet.

A local SE-NW surface slope prevails at this site.

The data indicates the dominance of geology on groundwater characteristics, as well as a possible structural control. The topography also plays its part in groundwater evolution, as to promote run-off at this site.

Sodium bicarbonate water is dominant at this site, associated with ion exchange water in this P-type fracture. Borehole G 40018 is located in the NE dolerite dyke and displays water at the end point of a evolution sequence, indicating low transmissivity. G 40020 shows water with a chemical character due to mixing.

Data also suggests that intense evaporation of water is taking place at the site before recharge of groundwater commences. The water at this site dates at century age, although the water is quite young in an evolutionary sense. This may be the result of a "deeper seated" aquifer, with a younger water of better quality.

### 5.5.3.2. Physical Weathering

Apart from mineralogical composition of the parent rock, hydraulic and hydrological factors greatly influence groundwater quality. Dolerite dykes and sills on one hand and fracture / fault sets on the other often control the mode of groundwater flow, availability of rainfall recharge and groundwater velocity and hence the residence time of water in the subsurface. Openness of groundwater systems is important in terms of availability of electron acceptors and carbon dioxide (*Woodford et al., in press*).

Mechanical processes close to the surface also influence the weathering patterns. Ice expansion, experienced on freezing of water, growth of the plant roots, animal holes etc. are activities that contribute to the development of the weathering process. Interestingly enough termite mounds were reported in Australia as being responsible for elevated nitrate concentrations on regional basis (*Barnes et al, 1992*).

Changes in dynamic equilibrium – be it hydrological or hydrochemical reflect themselves as changes in groundwater quality. The minerals become unstable and react in a way that thermodynamically allows for a development of a new equilibrium (*Woodford et al., in press*).

Certain minerals and rocks are more vulnerable to the chemical reaction than the others. This is reflected morphologically where more resistant rocks form the elevated areas, while the less resistant rocks are eroded away. Most of the boreholes in the Karoo are sited on dolerite dykes, either on a contact between the dyke and other rocks or directly into the dyke. Weathering of these intrusive rocks ("trap rock") will therefore have definite impact on groundwater chemistry (*Woodford et al., in press*).

### 5.5.3.3. Weathering of Dolerite

Weathering of the main Karoo rock types was described by Tordjiffe (1980). The weathering sequence for igneous rocks is as follows:

anorthite → augite, hornblende, biotite or albite → K-feldspar, muscovite → quartz.

The minerals that form dolerite are susceptible to chemical weathering. In this process certain amounts of the cations calcium, magnesium and sodium are released into passing groundwater. Major anions are most probably not derived from the parent rock (with exception of fluoride). Bicarbonate, chloride and sulphate are derived from processes that will be discussed below.

#### 5.5.3.4. Weathering of Sedimentary Rocks

The Karoo sedimentary sequence is composed mainly of sandstone, mudstone and shale. Mudstone is by far the most ubiquitous rock in the Karoo. This is the reason why parent sedimentary rocks are prone to contain high concentrations of salts when compared to groundwater associated with dolerite structures (*Woodford et al., in press*).

In addition to silicates the sedimentary sequence contains minerals important to groundwater chemistry such as calcite and pyrite, largely in the form of incrustations between detrital grains. Calcite is a common secondary mineral in basin sediments of dry climates. Sandstone in particular contains K-feldspar in addition to quartz and also minor amounts of Na-plagioclase. Most of the intergranular cement material is calcite, although silica is not uncommon (*Woodford et al., in press*).

Gypsum is also commonly found in arid soils. The correlation between known gypsum deposits in the Karoo Basin and the high sulphate content of groundwater in the western part of the Karoo is documented (*Visser et al., 1963*).

#### 5.5.3.5. Role of Carbon Dioxide

Karoo aquifers are known for their relatively poor soil cover, especially in the western parts of the Karoo Basin. Although this encourages the free flux of oxygen into the subsurface, the important weathering agent - carbon dioxide, is in low supply. Weathering of the sedimentary sequence by carbon dioxide is the most important decomposition process in unconfined aquifers and in the recharge zone of the confined aquifers (*Woodford et al., in press*).

Both the availability of carbon dioxide (and dissolved oxygen) and the distinctive climatic patterns are responsible for the groundwater quality variations between the rainfall-rich eastern portion and the rainfall-deficient western portion of the Karoo basin. These variations even effect the hydraulic properties of the aquifer matrix. Decomposed residues formed as a result of soil-

generated carbon-dioxide in the eastern part of the Karoo Basin provide material for a thicker soil profile and may completely or partially fill in fracture sets in the parent rock (*Woodford et al., in press*).

Weathering of silicates results in appreciable concentrations of bicarbonate, which is typical for the eastern part of the Karoo Basin. Weathering of plagioclase results in the release of cations such as calcium and sodium (*Woodford et al., in press*).

When the availability of carbon dioxide is greatly reduced, hydrolytic decomposition of the silicates takes over and adds solutes into passing groundwater. The result is that major ions are removed slowly, leaving clay minerals and amorphous iron oxides. The general rainfall conditions and residence times determine what type of clay mineral is formed. Montmorillonite should be formed under relatively dry conditions (western Karoo) and kaolinite in the wetter environments (eastern Karoo) (*Woodford et al., in press*).

#### 5.5.3.6. Mineralogy

Freeze and Cherry (1979) postulated a theory that the order in which groundwater encounters strata of different mineralogical composition, can exert an important control on the final water chemistry. They showed that the groundwater chemistry can be influenced by different lithological units, due to different thermodynamic constraints. An approximate composition of the dominant rocktypes found in the study area is given in **Table 5.5.3.6**.

Hem (1989) compiled a list of elements illustrating an estimate of the crustal abundance of 93 elements for both igneous and sedimentary rocks. Although the uncertainties of the values are high (*Bricker and Jones, 1995*), these estimates give a general indication of element distribution among the major rocktypes.

Trace silicate and oxide minerals, as well as quartz minerals, do not have a significant effect on the groundwater, as the minerals are normally unreactive or react very slowly under the average groundwater pH and temperature conditions. The groundwater chemistry of an aquifer is usually determined or dominated by the faster reacting minerals (*Katz and Choquette, 1991*). Mineral contribution to groundwater chemistry is a complex and often difficult task to quantify, as the influences exerted by background chemistry on the water chemistry are often difficult to compute with balance equations and modeling techniques (*Adams, 1998*).

Relationships between ionic species may indicate the elements contributing to the groundwater chemistry due to various hydrochemical processes at increasing salinities. Chloride is a conservative ion, used as an excellent indicator of increasing salinities in an area, as well as to determine concentration effects proven by statistical analysis. Addition of elements to the groundwater due to mineral weathering would not show a correlation with Cl<sup>-</sup>. Ionic species showing no relationship with Cl<sup>-</sup> in the data set are (**Table 5.4.1.3**): Ba, K, Mn, F and B, these elements are unaffected by salinization of the groundwater. The contribution due to mineral weathering decreases with an increase in salinity, due to an increase of cation exchange (*Adams, 1998*).

Barite could be the source for barium in the feldspar (e.g. celsian Ba[Al<sub>2</sub>Si<sub>2</sub>O<sub>8</sub>]) and biotite, of the geological material. Biotite, K-feldspars, plagioclase, muscovite and orthoclase may be source for potassium. Pyroxenes, biotite, magnetite and olivine may be the source of manganese. Fluoride ions in the groundwater may be derived from the apatite and fluorite minerals in the area (*Adams, 1998*).

A particular rock type may be the cause of elevated trace element levels in groundwater chemistry at any particular site. These elevated levels can be used to define the predominant type of rock at the specific site. Areas underlain by carbonatite and associated rocks, will have elevated barium and strontium levels and manganese would be elevated in dolerite rock areas (*Adams, 1998*).

The influence of geology on groundwater chemistry is hidden by the effect of groundwater salinity concentration as a result of evaporation (*Adams, 1998*).

**Table 5.5.3.6. Mineralogy of major rock types in Loxton (Bricker & Jones, 1995; De Wet, 1975; Deer et al., 1992).**

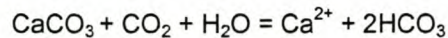
Rocktype	Mineralogy	Mineral Composition	Trace Element Contents
<b>Sandstone</b>	Quartz	SiO <sub>2</sub>	Si
	Biotite	K(Mg,Fe) <sub>3</sub> AlSi <sub>3</sub> O <sub>10</sub> (OH) <sub>2</sub>	F, Ca, Na, Ba, Mn, Mg, Fe, Al, Si, Rb, Cs, K
	Feldspars	K,Na(AlSi <sub>3</sub> O <sub>8</sub> ) and Ca,Ba(Al <sub>2</sub> Si <sub>2</sub> O <sub>8</sub> )	K, Na, Ca, Ba, Al, Si
	Plagioclase	(Na,Ca)Al(Al,Si)Si <sub>2</sub> O <sub>8</sub>	K, Sr, Ba, Mn, Na, Si, Ca, Al
	Chlorite	(Mg,Fe) <sub>2</sub> (Al,Fe) <sub>2</sub> Si <sub>3</sub> O <sub>10</sub> (OH) <sub>8</sub>	Mg, Fe, Al, Si, Li, Mg, Mn, Ni
	Muscovite	KAl <sub>3</sub> Si <sub>3</sub> O <sub>10</sub> (OH) <sub>2</sub>	K, Al, Si, Na
	Calcite	CaCO <sub>3</sub>	Sr, Ba, F, Cl, PO <sub>4</sub> , SO <sub>4</sub> , Ca, Mg, Fe, Zn, Mn, Co, Cu
	Orthoclase	K <sub>2</sub> O.Al <sub>2</sub> O <sub>3</sub> .6SiO <sub>2</sub>	K, Na, Al
Illite matrix	K <sub>0.7</sub> <sup>xii</sup> [Si <sub>3.3</sub> Al <sub>0.7</sub> ] <sup>iv</sup> [Al <sub>2</sub> ] <sup>vi</sup> O <sub>10</sub> (OH) <sub>2</sub>	K, Na, Al, B	
<b>Mudstone</b>	Quartz	SiO <sub>2</sub>	Si
	Calcite	CaCO <sub>3</sub>	Sr, Ba, F, Cl, PO <sub>4</sub> , SO <sub>4</sub> , Ca, Mg, Fe, Zn, Mn, Co, Cu
	Chlorite	(Mg,Fe) <sub>2</sub> (Al,Fe) <sub>2</sub> Si <sub>3</sub> O <sub>10</sub> (OH) <sub>8</sub>	Mg, Fe, Al, Si, Li, Mg, Mn, Ni
<b>Shale</b>	Quartz	SiO <sub>2</sub>	Si
	Illite	K <sub>0.7</sub> <sup>xii</sup> [Si <sub>3.3</sub> Al <sub>0.7</sub> ] <sup>iv</sup> [Al <sub>2</sub> ] <sup>vi</sup> O <sub>10</sub> (OH) <sub>2</sub>	K, Na, Al, B
<b>Dolerite</b>	Quartz	SiO <sub>2</sub>	Si
	Pyroxene	(Na, Ca, Mg)SiO <sub>3</sub>	Al, Na, Mn, K, Ni, Sr, Fe, Mg, Ti, Li, Ca, Cr
	Magnetite	Fe <sub>3</sub> O <sub>4</sub>	Al, Mg, Mn, Zn, Cu, Fe, Cr, Ti
	Biotite	K(Mg,Fe) <sub>3</sub> AlSi <sub>3</sub> O <sub>10</sub> (OH) <sub>2</sub>	F, Ca, Na, Ba, Mn, Mg, Fe, Al, Si, Rb, Cs, K
	Plagioclase	(Na,Ca)Al(Al,Si)Si <sub>2</sub> O <sub>8</sub>	K, Sr, Ba, Mn, Na, Si, Ca, Al
	Olivine	2(Mg,Fe)O.SiO <sub>2</sub>	Mg, Fe, Ca, Mn
	Ilmenite	FeO.TiO <sub>2</sub>	Fe, Ti, Mg, Mn
<b>Carbonate</b>	Pyrite	FeS <sub>2</sub>	Fe, S, Ni, Co, Pt, As, Mn, Sb
<b>Intrusives</b>	Ilmenite	FeO.TiO <sub>2</sub>	Fe, Ti, Mg, Mn
	K-Feldspar	K,Na(AlSi <sub>3</sub> O <sub>8</sub> )	Na, Ca, Ba, Sr
	Biotite	K(Mg,Fe) <sub>3</sub> AlSi <sub>3</sub> O <sub>10</sub> (OH) <sub>2</sub>	F, Ca, Na, Ba, Mn, Mg, Fe, Al, Si, Rb, Cs, K
	Barite	BaSO <sub>4</sub>	Ba, Sr, Ca, Pb, Cr
	Calcite	CaCO <sub>3</sub>	Sr, Ba, F, Cl, PO <sub>4</sub> , SO <sub>4</sub> , Ca, Mg, Fe, Zn, Mn, Co, Cu
	<b>Kimberlites</b>	Olivine	2(Mg,Fe)O.SiO <sub>2</sub>
Garnet		(Mg, Fe, Mn, Ca) <sub>3</sub> Al <sub>2</sub> Si <sub>5</sub> O <sub>12</sub>	Mg, Fe, Mn, Ca, Cr, Al
Pyroxene		(Na, Ca, Mg)SiO <sub>3</sub>	Al, Na, Mn, K, Ni, Sr, Fe, Mg, Ti, Li, Ca, Cr
Phlogopite		K <sub>2</sub> (Mg,Fe) <sub>6-4</sub> (Fe, Al, Ti) <sub>0-2</sub> [Si <sub>16-8</sub> Al <sub>2-3</sub> O <sub>20</sub> ](OH,F) <sub>4</sub>	K, Mg, Fe, Al, Ti, F
Ilmenite		FeO.TiO <sub>2</sub>	Fe, Ti, Mg, Mn
Serpentine		Mg <sub>3</sub> [Si <sub>2</sub> O <sub>5</sub> ](OH) <sub>4</sub>	Mg
Meliilite		(Ca,Na) <sub>2</sub> [(Mg,Fe,Al,Si) <sub>3</sub> O <sub>7</sub> ]	Ca, Mg, Al, Na, Fe
Monticellite		Ca(Mg,Fe)[SiO <sub>4</sub> ]	Ca, Mg, Fe, F
Zeolites		(Na <sub>2</sub> , K <sub>2</sub> , Ca, Ba)[(Al,Si) <sub>2</sub> ] <sub>n-x</sub> .H <sub>2</sub> O	Na, K, Ca, Ba, Al, F, CO <sub>3</sub> , SO <sub>4</sub> , Cl
Calcite		CaCO <sub>3</sub>	Sr, Ba, F, Cl, PO <sub>4</sub> , SO <sub>4</sub> , Ca, Mg, Fe, Zn, Mn, Co, Cu
Magnetite		Fe <sub>3</sub> O <sub>4</sub>	Al, Mg, Mn, Zn, Cu, Fe, Cr, Ti
Chrome-Spinel		(Fe, Mg)Cr <sub>2</sub> O <sub>4</sub>	Cr, Fe, Mg, Zn, Mn, Ni, Ti, Al, Be, Nb, Ta
Apatite		Ca <sub>5</sub> (PO <sub>4</sub> ) <sub>3</sub> (OH,F,Cl)	Ca, F, Cl, PO <sub>4</sub> , OH, Pb, As, V, Cu, Al, Fe, U, K, Li, Co, Si, Mn, Sr, P, S, Ba, Mg, Cu
Perovskite		(Ca,Na,Fe,Ce,Sr)(Ti,Nd)O <sub>3</sub>	Ca, Ti, Na, Fe, Ce, Sr, Nd, Y, La, Ta, Ba, Zr, La, Cr, Al

### 5.5.3.7. Dissolution

A mild carbonic acid (H<sub>2</sub>CO<sub>3</sub>) forms, as the initial precipitation is charged with CO<sub>2</sub> in the atmosphere. During infiltration of precipitation the groundwater in the area gets charged with CO<sub>2</sub>, proven by the higher partial pressure of CO<sub>2</sub> (p CO<sub>2</sub>) in groundwater, than the p CO<sub>2</sub> of the earth's atmosphere (i.e. 0.0003 atm) (Freeze and Cherry, 1979). This is the result from root respiration and organic matter decomposition (Schot and Wassen, 1993).

Higher Ca, Mg, Na and K concentrations in the groundwater, relative to the precipitation chemistry, are indicative of the weathering of minerals containing these cations (*Katz, 1989*).

The dissolution of carbonate (calcite) in the study area seems to be common. Ca-HCO<sub>3</sub> type water dominate in areas of recharge, by assuming this simplified reaction (*Adams, 1998*):



Calcium is liberated from the carbonate minerals common in the rock matrix of the aquifer material (i.e. calcite in the rock matrices of sandstone and mudrock). Mg-carbonates (dolomite) are not favored above calcite, as the Ca / Mg ratio for groundwater in the area is large, due to low amounts of Mg in the groundwater relative to the Ca ion.

#### 5.5.3.8. Precipitation and Saturation States

Saturation indices (SI) were calculated with the NETPATH computer program, through a WATEQF subroutine (*Plummer et al., 1992*). Set limits range between -1 for the lower limit for all unsaturated water and +1 for oversaturated water. A log scale is used to adapt large deviations from equilibrium. Undersaturation (SI < -0.1) would result in dissolution of a specific mineral, while oversaturation (SI > 0.1) result in the precipitation of minerals. The uncertainty in the pH measurement in this study, is the reason for not taking SI = 0 as equilibrium. An error of ±0.05 pH units leads to an uncertainty of ±0.05 units in SI of minerals and in view of uncertainties in Ca<sup>+</sup>, Mg<sup>2+</sup> and HCO<sub>3</sub><sup>-</sup> analysis. The total uncertainties are in the order of ±0.1 units of SI (*Langmuir, 1971*).

Saturation indices are useful in the determination of any ion's saturation state in a water sample. Activity-activity diagrams (**Figures 5.5.3.8.A-E**) indicate the saturation state of groundwater, with respect to various mineral phases like calcite, gypsum, strontianite, barite and fluoride in this study. The log activities are also available in **Appendix D**.

Saturation lines in the figures were derived from the solubility products of the various mineral phases (*Adams, 1998*). Points below the saturation line indicate unsaturated groundwater to the specific mineral, as all point above the line indicate oversaturation. Points on or near the saturation line indicate groundwater saturation to the specific mineral phase. The various mineral phases solubility products are outlined in **Table 5.5.3.8**.

**Table 5.5.3.8. Mineral solubility products (Appelo and Postma, 1994).**

Mineral	Reaction	Solubility Product
Calcite	$\text{CaCO}_3 \leftrightarrow \text{Ca}^{2+} + \text{CO}_3^{-}$	$10^{-8.48}$
Strontianite	$\text{SrCO}_3 \leftrightarrow \text{Sr}^{2+} + \text{CO}_3^{-}$	$10^{-9.271}$
Fluorite	$\text{CaF}_2 \leftrightarrow \text{Ca}^{2+} + 2\text{F}^{-}$	$10^{-10.6}$
Gypsum	$\text{CaSO}_4 \leftrightarrow \text{Ca}^{2+} + \text{SO}_4^{-}$	$10^{-4.58}$
Barite	$\text{BaSO}_4 \leftrightarrow \text{Ba}^{2+} + \text{SO}_4^{-}$	$10^{-9.97}$

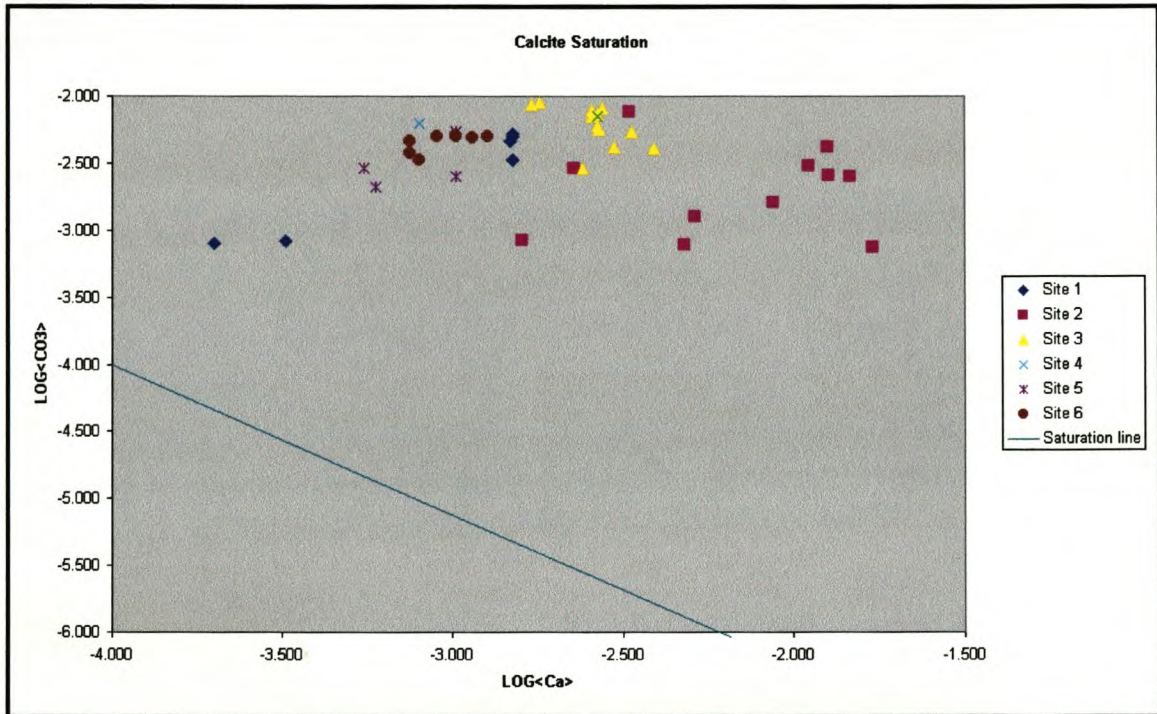


**Figure 5.5.3.8.A. Activity-activity diagram for calcite saturation.**

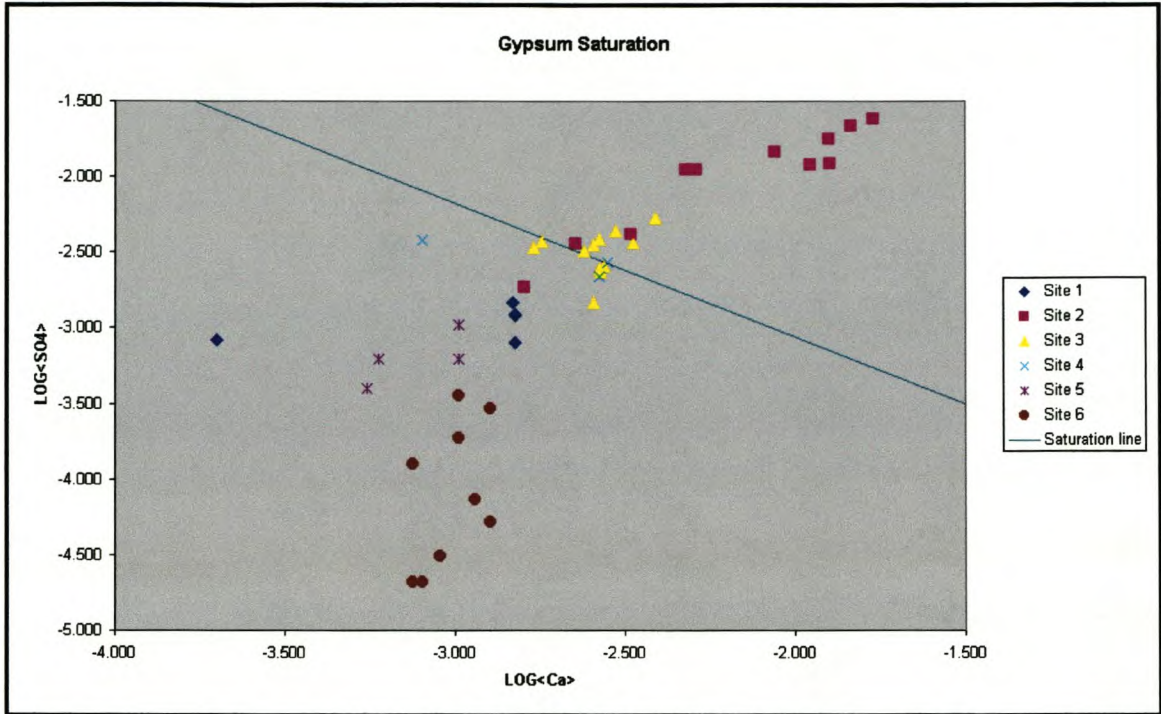


**Figure 5.5.3.8.B.** Activity-activity diagram for gypsum saturation.

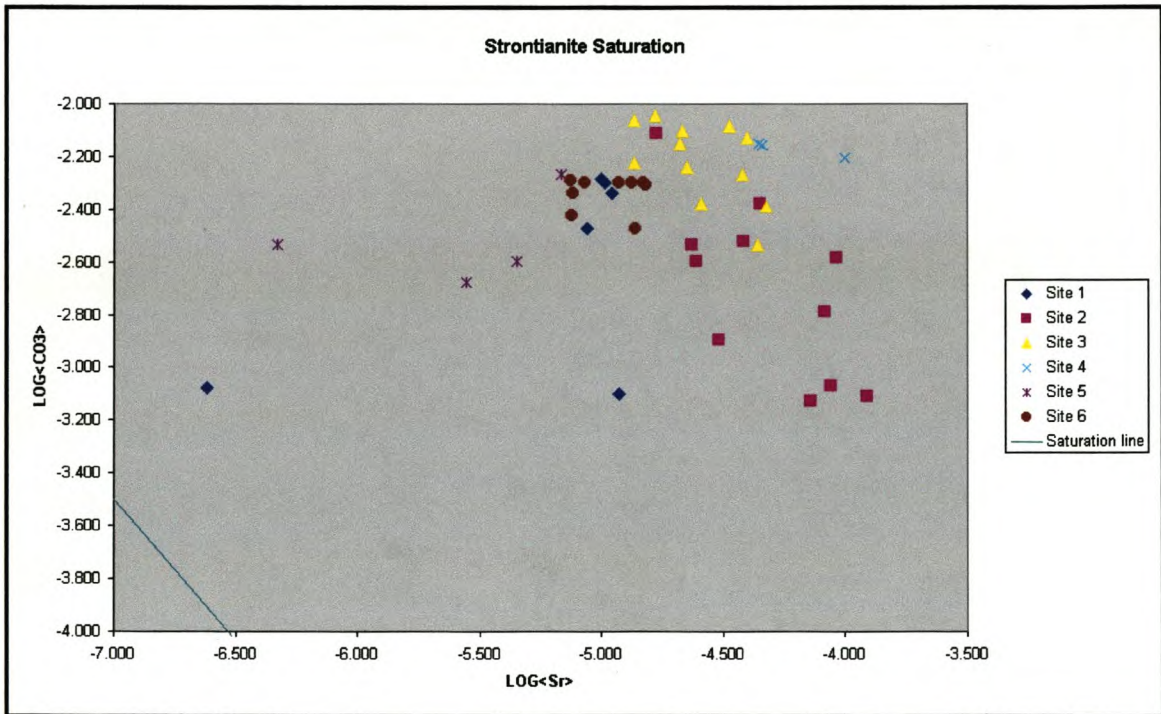


**Figure 5.5.3.8.C.** Activity-activity diagram for strontianite saturation.

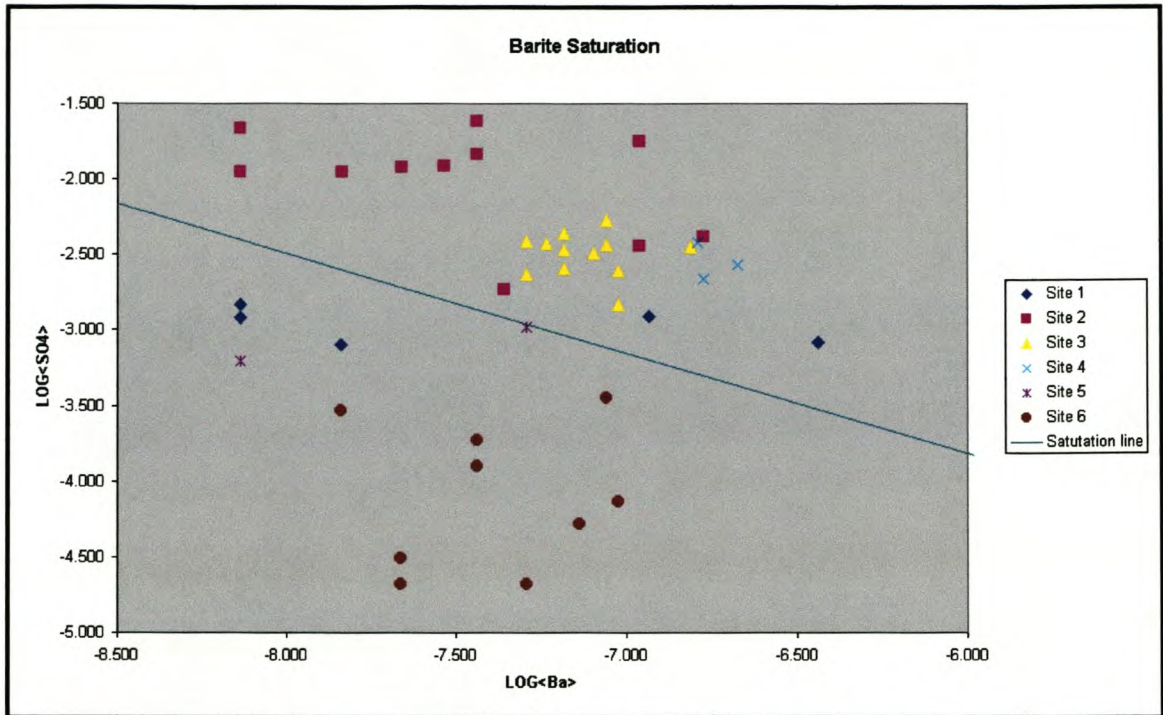


**Figure 5.5.3.8.D. Activity-activity diagram for barite saturation.**

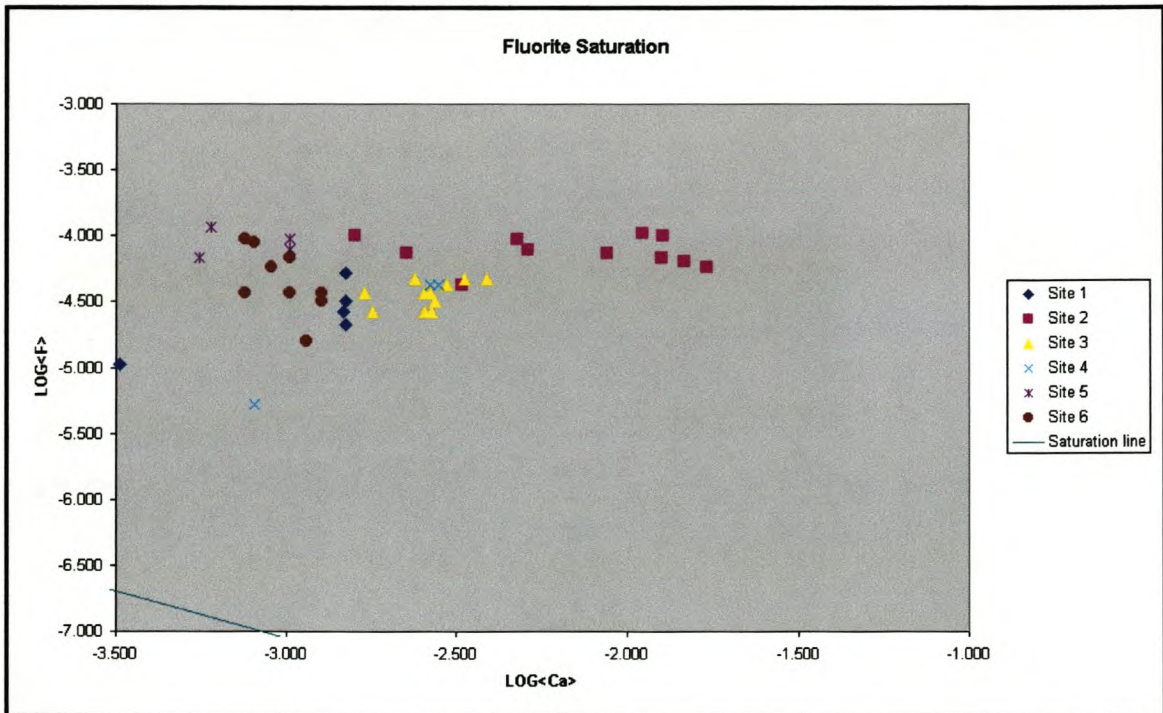


**Figure 5.5.3.8.E. Activity-activity diagram for fluoride saturation.**

Groundwater in Loxton is oversaturated with calcite, strontianite & fluorite, with equal distribution between over- and undersaturation, with respect to the minerals barite and gypsum (**Figures 5.5.3.8.A-E**). Some three sample points for Site 1 and Sites 5 & 6 is undersaturated to barite and one sample from Site 2,3 & 4 as well as Site 5 & 6 is undersaturated to gypsum (**Figures 5.5.3.8.B & D**).

Calcite saturation controls the calcium concentration in the groundwater, as Ca ions are consumed by calcite saturation. The dissolution of gypsum, with a consequent increase in Ca concentration, causes calcite precipitation (*Appelo and Postma, 1994*). The removal or addition of Ca in solution, is also controlled by cation exchange processes. The undersaturation of gypsum is due to its high solubility and because it's a major source of Ca for calcite saturation (*Adams, 1998*).

Gypsum ( $\text{CaSO}_4$ ) is also a major source of  $\text{SO}_4$  in the groundwater of the area.  $\text{SO}_4$  is then reduced to  $\text{H}_2\text{S}$ , the "rotten egg" odour of groundwater in the area. Gypsum undersaturation may be a result of Ca loss, due to cation exchange and common ion effects, whereby barium is the preferred ion to attach to  $\text{SO}_4$ , forming barite. Barite ( $\text{BaSO}_4$ ) equilibrium controls barium concentrations and could also be less soluble than gypsum (*Adams, 1998*).

The precipitation of calcite results in a decrease in  $\text{CO}_3$ , causing the dissolution of other carbonate minerals (i.e. strontianite). This and cation exchange processes are probably the cause of strontianite oversaturation (*Adams, 1998*).

The oversaturation of fluoride in groundwater is achieved as fluoride dissolution may be caused by complexing effects, reducing free Ca and fluoride activities (*Nordstrom and Jenne, 1977*). Oversaturation of most of the mineral phases is probably due to an increase of ions, as a result of cation exchange and dissolution of minerals in the water rock interaction.

#### 5.5.3.9. Cation Exchange

Ion exchange and sorption are processes that change the proportions of ions in the solution. The better known reaction is the exchange of calcium for sodium on the exchange sites of sodium-rich minerals. This reaction depends on the concentrations of exchangeable ions in solution.

If availability of carbon dioxide is limited, hydrolysis of calcite (and silicates) occurs and the resulting hydroxyl ion may be involved in further reactions. In this way iron present in clay

minerals may be leached out to form ferric hydroxide. This mineral commonly forms a coating on Karoo rocks (*Woodford et al., in press*).

The exchange capacity of clay minerals allows for the dissolution of more calcite than would otherwise dissolve. The process also mobilizes significant amounts of sodium into solution and can lead to excessively alkaline solutions, i.e. at some coal-mines in the northern part of the Karoo (*Woodford et al., in press*).

Groundwater in the study area evolves from a Ca / Mg -HCO<sub>3</sub> type water, towards a Ca-SO<sub>4</sub> type water, indicating that several processes are occurring in the evolution sequence on the way to the much older water at the end.

Ions would combine and precipitate as minerals when saturation is reached, while others will enter into exchange reactions (*Sowayan and Allayla, 1989*). Chloride is the only ion not affected by these processes, because of its conservative nature (*Adams, 1998*).

Different groundwater types in the area are indicative of the changes in major cat- and anions in groundwater. Replacement of Na with Ca to form Ca-HCO<sub>3</sub> type water from Na-HCO<sub>3</sub> water, as well as Na-SO<sub>4</sub> type water from Ca-SO<sub>4</sub> water types, are processes indicative of a natural groundwater evolution sequence. At the end of the sequence Na-Cl type water (saline water) is dominant and is refreshed by the replacement of Na for Ca, due to reversal of ion exchange processes, to form Ca-Cl type water. Refreshing may occur as a result of mixing with fresher Ca-type recharging water (*Adams, 1998*).

Statistical analysis showed that the main ions involved in cation exchange reactions are (*Adams, 1998*):

Na-Ca; Na-Mg; Sr-Ca; Sr-Mg; Sr-Na and K-Na.

The Loxton study only indicated the following reactions:

Na-Ca; Sr-Ca and Sr-Na.

The positive correlation of some of the cations is indicated by the correlation matrix, produced for the data set (**Table 5.4.1.3**), however cation exchange processes require that the major exchangeable ions are negatively correlated (i.e. an ion should increase at the expense of another cation). Evapotranspiration masks the signature of various chemical processes like

cation exchange reactions and should therefore not be sought after in a data set of a complex area, due to aquifer heterogeneity (*Adams, 1998*).

The chemical character of water changes with depth, due to the effects of cation exchange reactions, where ions are adsorbed by the matrix of the aquifer and replaced by subsurface water at different depths (more pronounced) and over different periods of time. These reactions disturb the natural equilibrium, with the subsequent dissolution of other minerals in the geological environment and an increase or decrease in pH and the number of ions dissolved in the groundwater, accompanied by EC increases with depth (*Woodford et al., in press*).

#### 5.5.3.10. Isotopes

Groundwater chemistry alone is not acceptable for the interpretation of water residence time, as water trapped in depressions where ponding occurs and evaporation concentrates the salts, would not give an accurate indication of the residence time of the water. Tritium is a stable isotope and hence it's usability in the study of dynamic water systems. **Figure 5.5.3.10** is a plot of the  $^{14}\text{C}$  (pMC) versus  $^3\text{H}$  (T.U.) content, indicating the expected trend of older water found at deeper sampling positions within a borehole. Borehole G 40009 is the exception and may be due to a sampling or analysis error.

There is a fair difference in isotopic values between surface measurements and measurements taken at depth, enforcing the possibility of a "second deeper seated aquifer". The water with the lower  $^{18}\text{O}$  values, for samples at depth suggest that the water has a source further inland, from rainfall on the range to the NE, the Hexrivierberge or Pramberge, which has greatly depleted  $^{18}\text{O}$  values relative to SMOW.

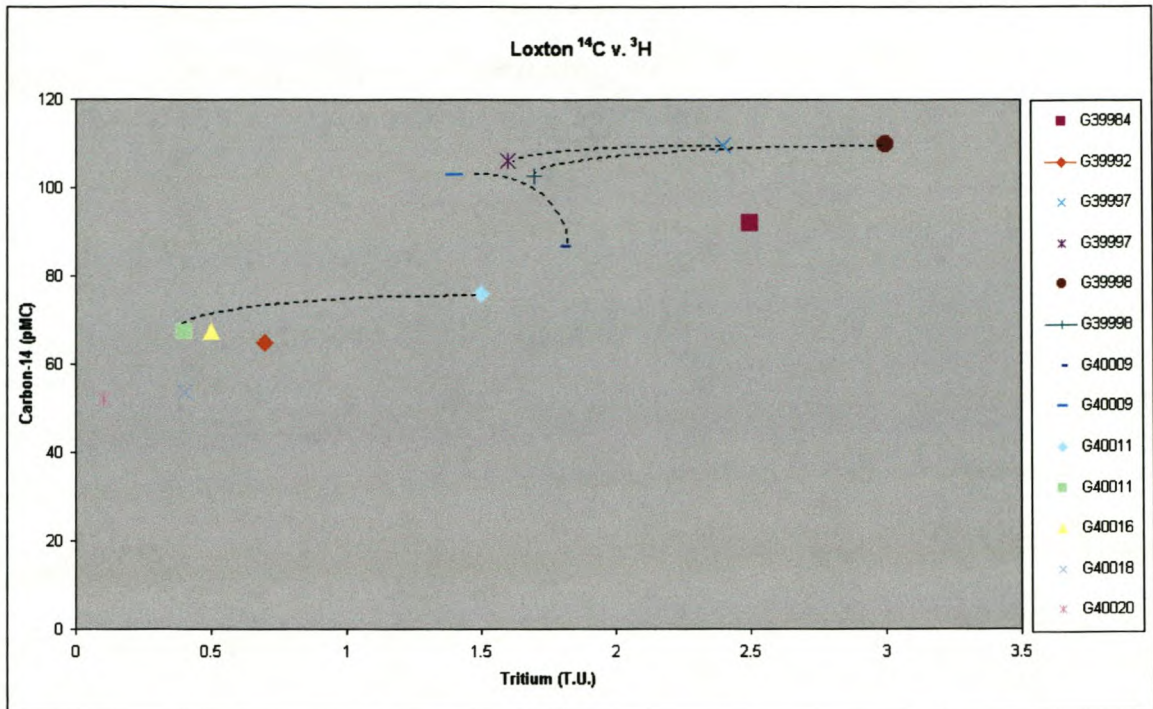


**Figure 5.5.3.10. Carbon-14 vs. Tritium plot for Loxton groundwater.**

### 5.5.3.11. Redox Controlled Reactions

Chemical reduction and oxidation induced by various factors can lead to dissolution of certain oxides, oxidation of sulphides and conversion of nitrogen forms. A commonly described sequence involving the presence of sedimentary organic matter from a more oxidized to a more reduced state is (Woodford *et al.*, *in press*):

- Consumption of dissolved oxygen.
- Reduction of nitrate to nitrogen gas (denitrification).
- Dissolution of manganese.
- Dissolution of iron.
- Reduction of sulphate to sulphide.
- Conversion of dissolved nitrogen gas to ammonia.

These reactions can occur in the reverse sequence depending on the redox-state of the aquifer system and how “open” or “closed” the system is towards influencing environmental impacts.

One of the more important reactions to occur in Karoo rocks is oxidation of pyrite. When oxygen-enriched water reaches these pyrite-mineralized rocks the sulphate concentrations increase and a low pH (acidic) water is produced if there is insufficient buffering capacity present in the aquifer, which may mobilize an array of trace metals into solution. The oxidation of pyrite causes a major environmental problem in mines operating in the Karoo environment. Coal and gold mines in the northern part of the Karoo Basin can produce effluents with sulphate concentrations measured in thousands of mg/l (*Woodford et al., in press*).

Redox controlled reactions also influence the status of nitrates in groundwater. The rates of nitrification and denitrification are affected by the prevailing redox conditions, and more specifically any changes in these conditions. Spatial analysis of observed nitrate concentrations often shows poor correlation with other chemical constituents due to redox conditions that vary rapidly over short distances within the aquifer (*Woodford et al., in press*).

#### **5.5.4. Influence of Human Activities and Land Use on the Groundwater Chemistry**

The quality of groundwater will change due to natural processes or through the influence of man. The predominant agricultural activity in the area is livestock farming. Livestock watering points are usually situated near boreholes, where it is susceptible to pollution, due to the absence of buffer zones. Occurrences of high nitrate levels are a possible indication of point source pollution. The source of nitrate in the area may be due to nitrogen in the soils and animal wastes, containing more or less 5% nitrogen of its dry mass (urea), which is hydrolysed and decomposed to ammonia (*Alexander, 1961*). Tillage of fields may act as a nitrogen source (*Adams, 1998*).

Evaporation is the main process that may concentrate  $\text{NO}_x\text{-N}$ , which is easily leached out of surface soil mixing zone by water, due to its negative ionic charge and low adsorption potential (*Shirmohammadi et al, 1991*). Nitrate concentrations vary between 0.002 - 0.793 mg/l (mean 0.009 mg/l) even though there is no geological source of nitrate possible within the rock formations (*Tredoux, 1993*).

High B concentrations (in illite) tend to be a sign of pollution. Given that the area is mainly used for agricultural purposes, pesticides could be a probable cause of contamination. Li is usually found as an impurity of sodium and potassium minerals (chlorite, apatite, pyroxene) (Galvin 1996).

#### **5.5.5. Spatial Distribution of Major Constituents**

The spatial distribution of the major chemical constituents of groundwater in the Karoo was evaluated on a regional basis. Although small-scale variations may be of importance for a local development of groundwater resources, the emphasis was placed on identifying broad, macro-scale trends in groundwater quality (Woodford *et al.*, *in press*).

No special groundwater study has yet been conducted to identify groundwater quality trends on such a basin-wide scale. There were, however, two attempts to describe the groundwater quality in Karoo aquifers (Woodford *et al.*, *in press*):

- Bond in 1946 presented a national account of groundwater quality in South Africa. This pioneer work is however outdated and is based on very few sampling points with a limited scope of analyzed constituents.
- The regional characterization program conducted by DWA&F. This is a relatively new initiative that is focused on the description of groundwater resources of South Africa, on map-sheet (1:50 000) basis. The groundwater quality section is however not described in any depth, authors limiting their description to electrical conductivity and identification of the most salient problems. Only one sheet has thus far been completed (Queenstown). The characterization program generates a valuable database of boreholes, springs and groundwater quality, which should not be left without a detailed analysis as soon as the database is updated.

The groundwater quality database used in this analysis is based on the available dataset housed at the QualDB (DWA&F). This database is the most representative source of groundwater quality nation-wide (Woodford *et al.*, *in press*).

The main Karoo Basin was evaluated by DWA&F (*after Woodford and Chevallier, in press*) using analyses from over 11 000 sites. At sites where more than one analysis was available the most recent analysis was considered for further evaluation. No consideration was given to vertical

variations in groundwater quality within the aquifers. The available dataset does not really allow for such an examination. It goes without saying that it may be of importance to examine vertical variations of groundwater quality when installing a groundwater abstraction system under site-specific circumstances (*Woodford et al., in press*).

The data records do not reflect a snapshot of a single representative period. All available data have to be used in order to obtain acceptable coverage of the entire study area. The temporal changes in groundwater quality could thus not be screened out and units are compared using data records from different time periods. All records fall within the 1970-1997 period. A map was compiled showing the percentage of data records for the period 1990-1997 out of the total number of records used for this analysis (*Woodford et al., in press*).

The groundwater quality data were evaluated statistically using the approach that was applied for mapping of Groundwater Resources of South Africa (1995). The major lithological units within the Karoo Basin were subdivided into smaller domains by considering their hydraulic properties. The groundwater chemistry within each of the domains was characterized using the water chemistry data falling within the geographic area of the domain. This approach inherently assumes that aquifers can be defined on the basis of geological units. The log-transformed groundwater quality data (to improve statistical distribution properties) of a specific domain was summarized using the geometric mean. The variability of the data was portrayed as a range defined by standard deviation space. The standard deviation was also determined from the log-transformed data (*Woodford et al., in press*).

This approach therefore gives a probability range of values of solute concentrations that may be expected within a certain domain. Hence all anomalies are more or less smoothed-out. As with any other method the evaluation is biased, the main sources include the following :

- Temporal variation – groundwater quality in the borehole may change with time.
- Uncertainty resulting from different sampling methods.
- Uneven spatial distribution of sampled boreholes.
- Uncertain information on the status of the sampled borehole – whether it reflects “ambient” or “polluted” conditions.
- Vertical variations in groundwater quality along the borehole profile are not taken into account.

Virtually all the chemical parameters were analyzed for in the laboratory. The sensitive parameters such as pH and alkalinity are thus not always representative of the field conditions. Other parameters such as dissolved oxygen, redox potential and temperature have only been recently added to the National Groundwater Quality Monitoring Program's protocol and their regional analysis is not as yet feasible (*Woodford et al., in press*).

*Trace element* and data other than the major constituents are not available for the entire Basin. Only very few analyses exist where trace elements were determined and these do not allow for any regional generalizations. Trace element data – which include iron and manganese – have mainly been collected for pollution studies and thus do not represent natural conditions.

Groundwater domains with similar chemistry (statistical parameters) were grouped together according to the ranges defined by the DWA&F drinking water quality standards. The colour scheme representing drinking quality classes was used whenever appropriate.

The information was analysed on a national scale and is discussed below (*Woodford et al., in press*).

#### 5.5.5.1. Summary of the Chemical Parameters

Water is often judged on its “salt content”, i.e. the amount of total dissolved solids (TDS) within a unit volume (mg/l). In South Africa another indirect parameter for water mineralization is often used – electrical conductivity (EC) measured in mS/m. The effect of dissolved solids is not, however, affected by concentration alone. In highly mineralized water the concentration has to be replaced by *ion activity*, which is a transformed portion of concentration that is active in chemical processes. The equivalent of the ‘activity’ characterized to TDS is *ionic strength*.

Ionic strength is an important parameter for more sophisticated hydrogeochemical analyses and it is used for the determination of saturation indices and hydrogeochemical modeling. The assumptions for Davies equation and / or Debye-Huckel equation are applicable to solutions with ionic strength of 0.1 - 0.5 and less. Approximate activity coefficients for typical groundwater constituents were provided by Hem (1989). At an ionic strength of 0.01 the activity coefficients for the monovalent species are near 0.91, for divalent species 0.67 and for trivalent species 0.45. This means that only 91, 67 and 45 % of total concentration is “active” in speciation.

Ionic strength is therefore an important chemical parameter as it affects inhibition of chemical reactions and prevents them from taking place. When the ionic shielding effect limits the effective concentration of a solute more mineral containing the solute can be dissolved and the overall mineralization of water increases. This mechanism plays a great role in arid zones where evaporites mobilized by groundwater increase dissolution of other minerals.

Concentrations of dissolved constituents increase from the east to the west following a similar decrease in precipitation. The geometric mean concentration of dissolved solids range from less than 100 mg/l at the base of the NE slopes of the Drakensberg Mountains to more than 3400 mg/l in the Western Karoo, representing a concentration factor in excess of 30 fold due to an increasing "rainfall deficit" (rainfall : evapotranspiration) towards the Western Karoo.

Most of the Karoo Basin has TDS in the range of 450-1000 mg/l, which is not excessive by any standards. High concentrations are limited to westernmost and southernmost edges of the Basin, especially to groundwater in the Dwyka Formation. This water is partly of a connate origin. As mentioned earlier, the relatively well-defined picture of TDS may be skewed by the fact that fresh water related to dolerite structures was sampled most often. The groundwater quality in the sedimentary sequence is regarded as poorer due to longer residence time.

pH is an important parameter to consider when studying the quality of groundwater. According to these measurements Karoo aquifers have in general a rather high pH, in the range of 8.0-8.5. Only a relatively small part of the Karoo Basin on the east has pH less than 7.5, where rainfall (and carbonic acid activity) is comparatively higher than in the other parts of the Karoo.

High pH values are rather typical for dry desert-like climates. Occurrences of pH greater than 7.5 are however not limited to dry areas only. In the northern and north-eastern part of the basin the high and "low" pH zones are next to each other. The pH variations in those terrains most probably reflect differences in groundwater residence times.

Low pH values broadly encountered in the Witbank and Newcastle areas are probably influenced by measurements obtained from the numerous coal-mines in the area, which contain pyrite.

This section describes the concentrations of major constituents found in Karoo aquifers. All constituents, except nitrate, show an east-west trending increase in concentration.

### 5.5.5.2. Major Cations

**Calcium** and bicarbonate are usually the dominant ions in recharge water, at the beginning of the groundwater cycle. For most parts of the Karoo calcium occurs in relatively low mean concentrations, commonly between 30-80 mg/l (**Figure 5.5.5.2.A**). Lower Ca ranges of between 10-30 mg/l occur in the eastern Karoo and around Lesotho. Calcium is balanced by alkalinity in the central and eastern Karoo, and by sulphate in the western Karoo. Elevated calcium concentrations occur in the extreme west, mainly in the Dwyka Formation, and in the high evaporation / low recharge area around Rietbron.

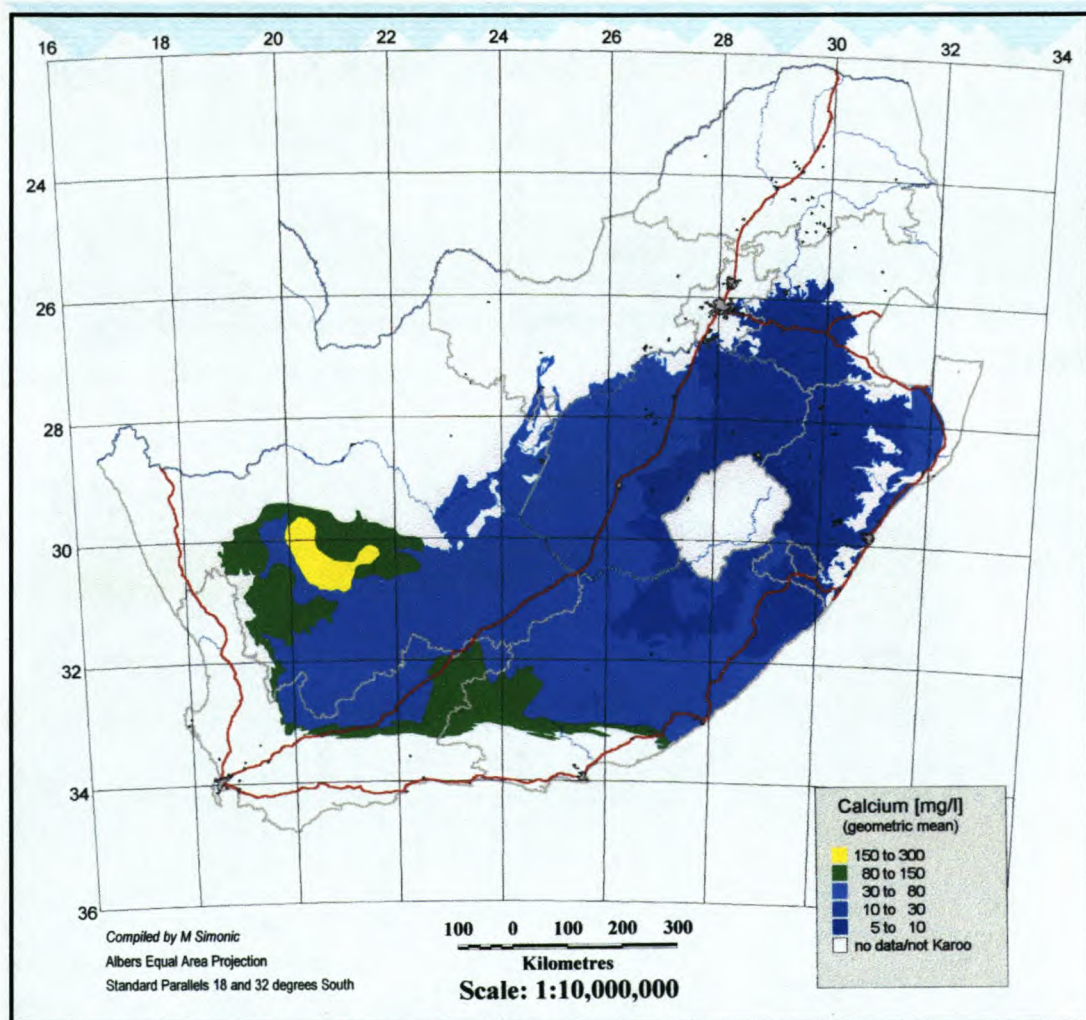


**Figure 5.5.5.2.A.** Calcium concentrations expressed as a geometric mean within each lithological unit.

**Magnesium** reveals a similar distribution pattern to calcium (**Figure 5.5.5.2.B**), but does not occur at the same concentration levels as calcium. Rather low ranges are encountered in the south-western portion of the Basin. Magnesium is seldom more abundant than calcium, suggesting that magnesium minerals are not as readily soluble as calcium. The Ca:Mg ratio for most parts of Karoo is between 1.1 and 4.0. Groundwater from the Dwyka Formation in the Barkly West area has Ca:Mg values slightly below 1.0.

Calcium and magnesium ions participate in a property that is known as *total hardness*. Based on this property groundwater in Karoo is regarded as hard in most parts. Very soft to soft groundwater is found in the eastern and northern part of the Karoo. The western edge of the Karoo Basin contains groundwater that is very hard to extremely hard.

The concentration of **sodium** is more variable than that of calcium (**Figure 5.5.5.2.C**). Most of the Karoo has sodium concentrations within acceptable drinking limits, i.e. below 100 mg/l. The coastal sections of Karoo rocks in Kwazulu-Natal and the Eastern Cape show elevated sodium concentrations, that on average exceeding 100 mg/l. This is most likely the impact of the sea-born salts in which sodium dominates as the main cation.

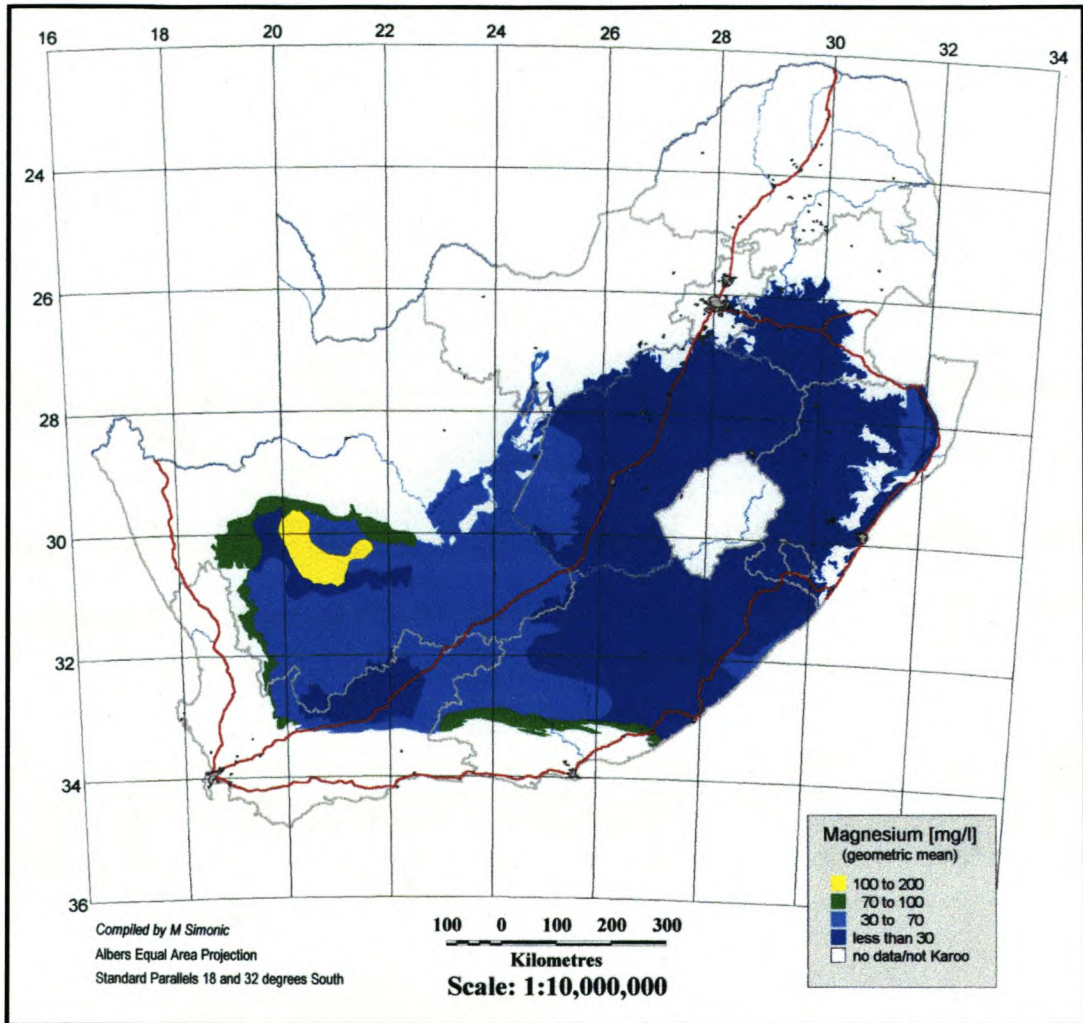


**Figure 5.5.2.B. Magnesium concentrations expressed as geometric mean over elementary lithological units.**

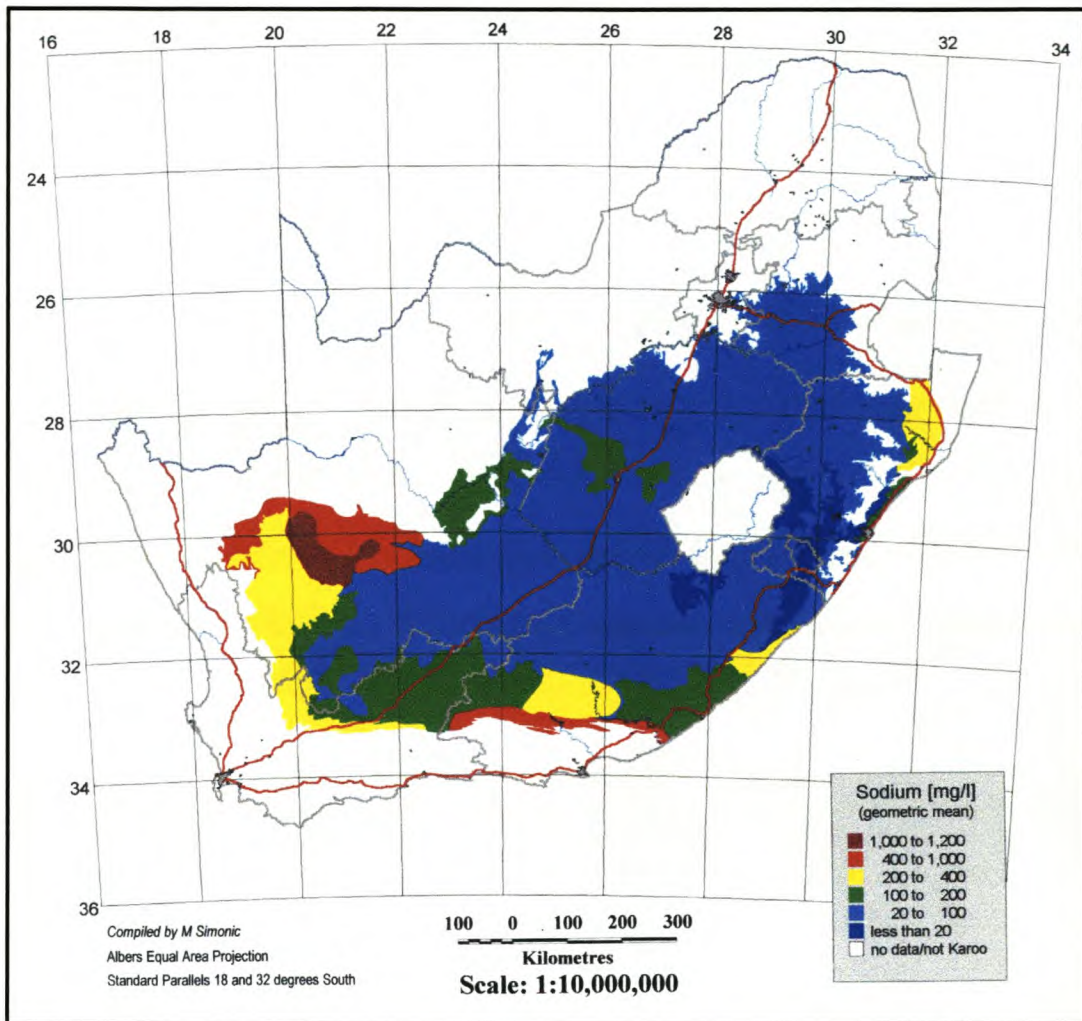


**Figure 5.5.5.2.C. Sodium concentrations expressed as geometric mean over elementary lithological units.**

Sodium almost exactly mirrors the distribution of **chloride**, suggesting the two ions are closely associated. It also suggests that the process of Ca-Na exchange is not significant on a regional basis. If the exchange model is not dominant, then most of the sodium chloride concentration is of meteoric origin, i.e. coming from rainfall and subsequently concentrating due to evaporation.

If the meteoric origin theory is true then the Na:Cl ratio should be approximately equal to 1. However when inspecting Na:Cl ratio map (**Figure 5.5.5.2.D**) the values close to 1 cover only a small area of the Basin, i.e. a narrow strip along the Indian Ocean, the western and south-western edges of the Karoo Basin.

In addition to rainfall there is therefore an additional source of sodium. This is especially the case in the eastern half of Karoo where sodium ions are correlated with alkalinity rather than by chloride.

**Potassium** concentrations seldom exceed 10-20 mg/l. Potassium ions are easily adsorbed by the aquifer material and therefore can seldom reach significant concentrations in groundwater.

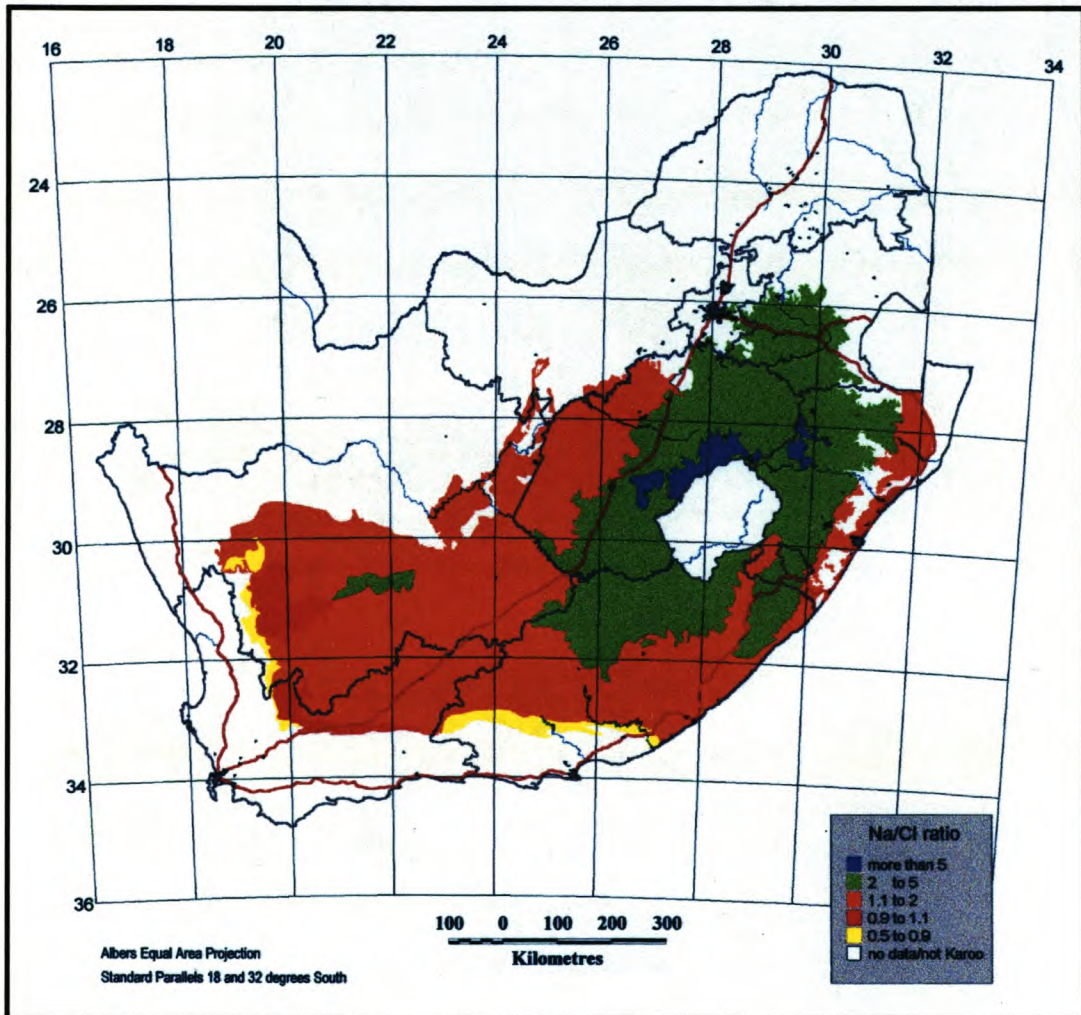


**Figure 5.5.5.2.D. Spatial Distribution of the Na:Cl ratio in the Karoo Basin.**

### 5.5.5.3. Major Anions

Bicarbonate and carbonate are represented by the **total alkalinity**. In the dynamic systems they are formed by introduction of carbon dioxide with rainfall and by the biological activities in the soil. Further dissolution of carbonates in the aquifer material introduces additional alkalinity into solution until the solubility limit is reached. Relatively low total alkalinity concentrations occur in groundwater of low ionic strength in the eastern portion of the Karoo Basin. The exception is the most eastern segment of Karoo rocks around Nongoma where groundwater quality is affected by relatively high mineralization.

The total alkalinity increases towards the center of the basin and averages between 200-300 mg/l. In the south-western section of the Basin the alkalinity decreases, probably due to solubility limits of  $\text{CaCO}_3$  and part of alkalinity may be lost to precipitation of carbonate minerals. Calcite fracture incrustations are common in the Western Karoo.

In order to understand the development of alkalinity, it is important to know the partial pressures of carbon dioxide in groundwater. The accurate computation of carbon dioxide requires accurate field measurements of pH and alkalinity. Although these field measurements are not available for establishing **accurate  $\text{CO}_2$  partial pressures**, the spatial distribution of  $\text{pCO}_2$  (expressed as  $\log \text{pCO}_2$ ) do illustrate the major differences in  $\text{CO}_2$  activity in various parts of the Karoo. Relatively high pressures are documented in the central part of the Basin where alkalinity is also high. High  $\text{pCO}_2$  values are also encountered in the Dwyka sediments in the Eastern Cape, where the partial pressures are some 10 fold higher than the atmospheric pressure.

On the other hand,  $\text{pCO}_2$  close to that of atmospheric pressure are found in the central part of the Western Karoo, on southern Highveld and east of Lesotho in Kwazulu-Natal. Low partial pressures develop within an environment where there is either insufficient  $\text{CO}_2$  as a result of low organic carbon content in soil, or where most of  $\text{CO}_2$  was depleted by reactions occurring in the aquifer.

Alkalinity is not the only process requiring the presence of  $\text{CO}_2$ . Dissolution of silicate minerals is also a process where  $\text{CO}_2$  is consumed. Availability of  $\text{CO}_2$  is therefore the factor limiting to some extent the weathering and dissolution processes.

**Chloride** and **sulphate** concentrations seem to be well correlated (**Figures 5.5.5.3.A and B**). Chloride however dominates over sulphate in most areas of the Karoo Basin, a fact already mentioned by Bond (1946). Chloride shows obvious enrichment in the coastal strips along the Indian Ocean and is also profuse along the western margins of the Basin. In the north-western section both ions show relatively high concentrations exceeding 1000 mg/l. The low-recharge area around Rietbron shows elevated concentrations of chloride, as well as sulphate. Long groundwater residence times, poor irrigation practices and saline influxes via rivers are noted as the probable causes for these high concentrations.

High **nitrate** concentrations do not pose any regional health-risk problems, but do occur locally in excessive concentrations. High concentrations occur in the Dwyka rocks of the northern portion of the western Karoo (**Figure 5.5.5.3.C**). This however does not mean that the nitrate problem can be completely disregarded. Numerous locally elevated nitrate concentrations have been reported from different parts of the Karoo, most of which are related to point source contamination of the groundwater from the surface.

**Fluoride** concentrations are usually elevated in acid igneous rocks. These rocks do not occur in the Karoo Basin. The fluoride concentrations often correlate with pH. However, inspection of pH values and mean fluoride concentration maps (**Figure 5.5.5.3.D**) do not show any apparent correlation either. Evaporation and long-residence time processes seem to be the most viable processes responsible for fluoride concentrations in the Karoo aquifers.

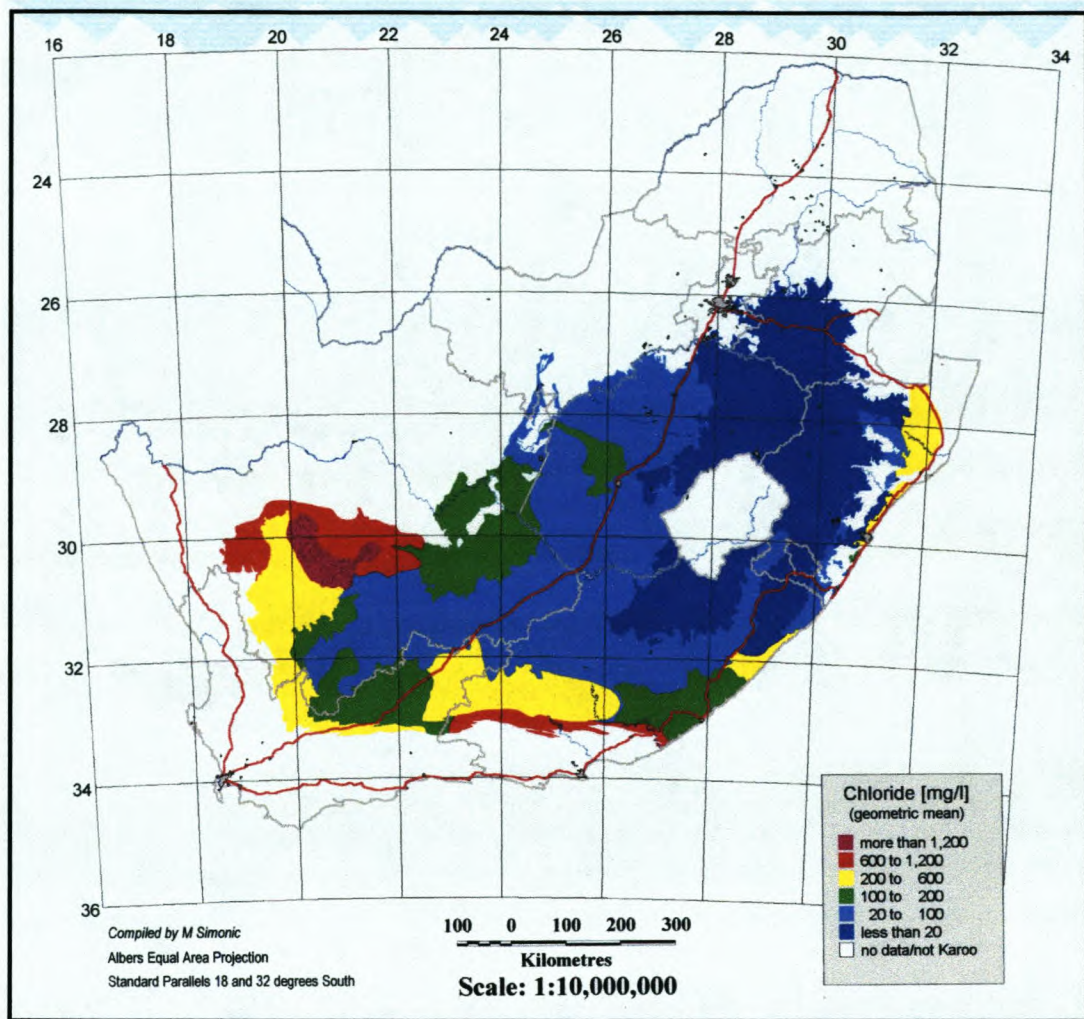


**Figure 5.5.5.3.A. Chloride concentrations expressed as geometric means over representative lithological units**

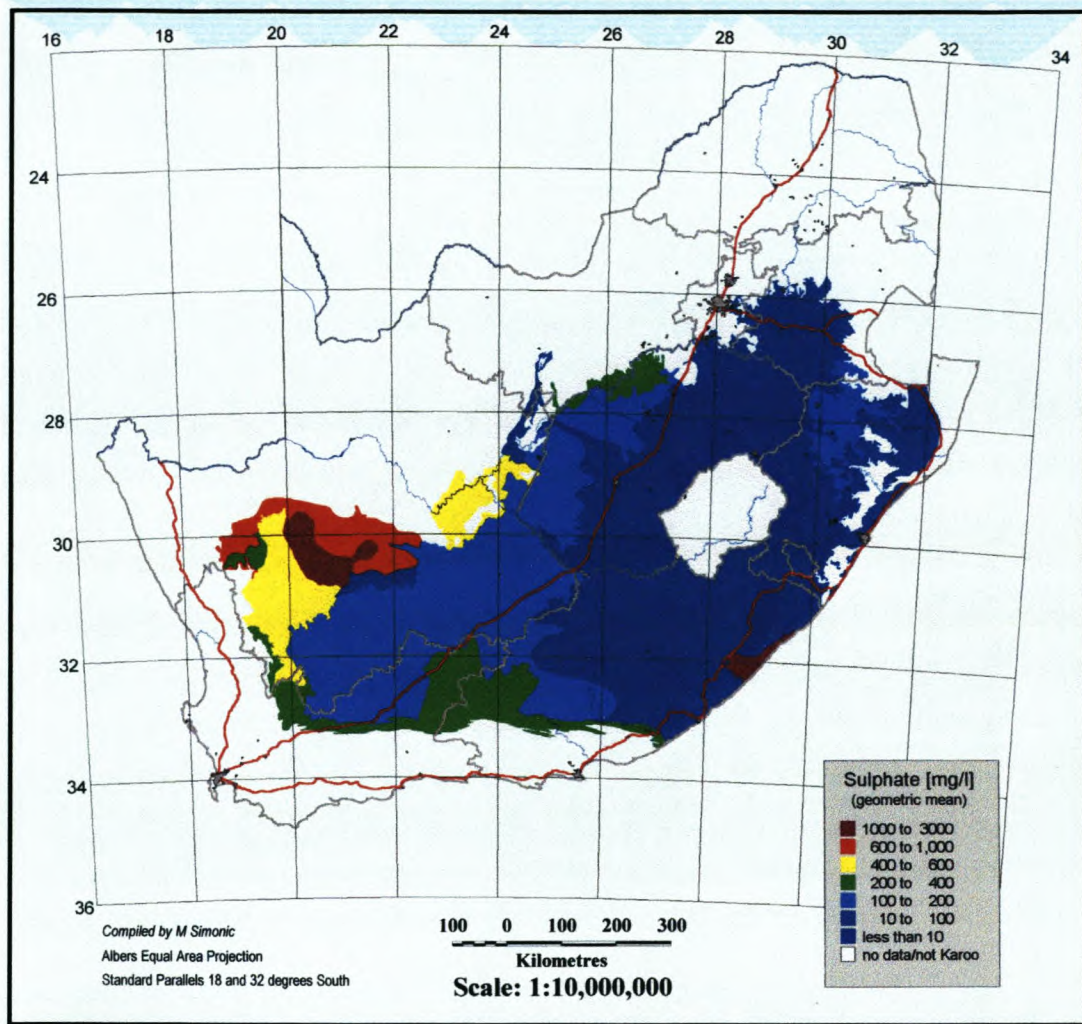


**Figure 5.5.5.3.B. Sulphate concentrations expressed as geometric means over representative lithological units.**

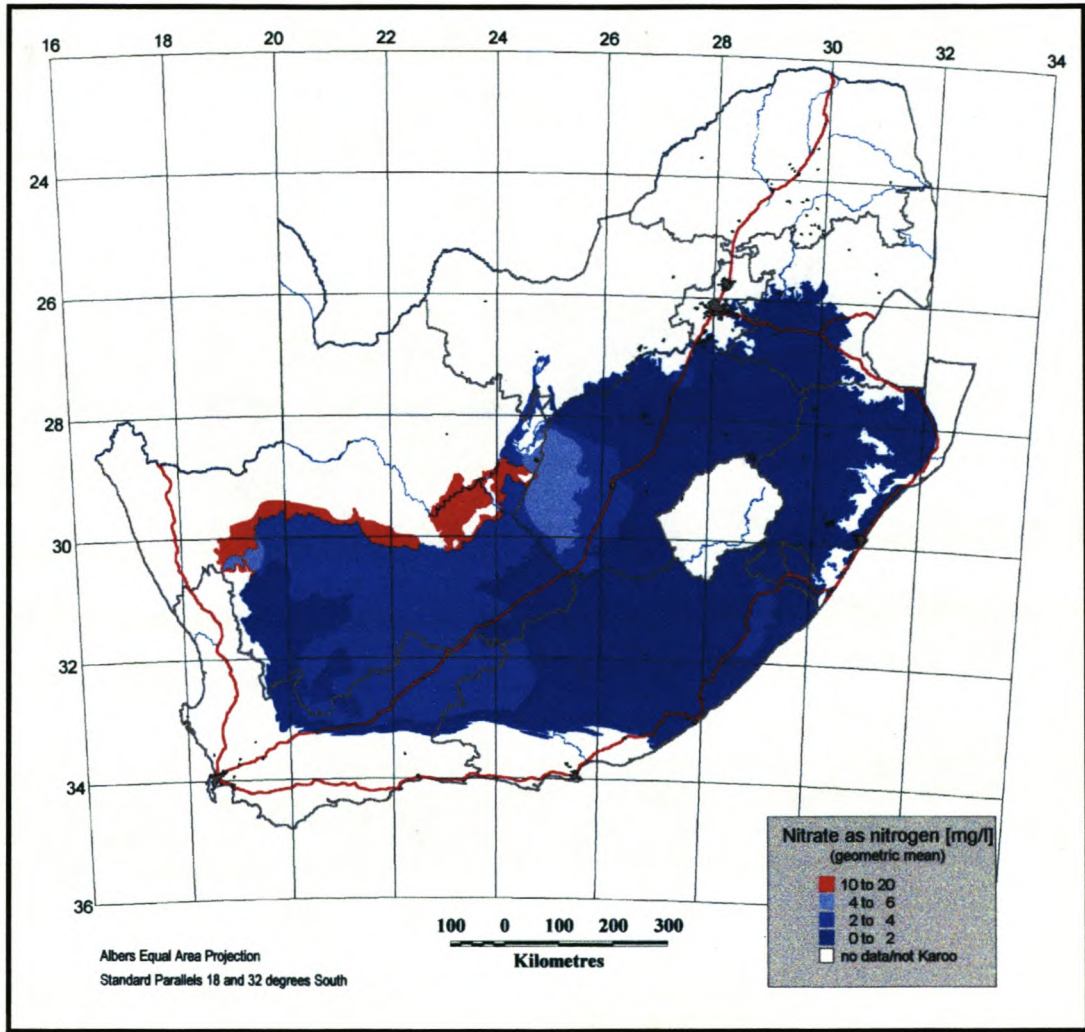


**Figure 5.5.5.3.C. Nitrate (as nitrogen) concentrations expressed as geometric means over representative lithological units.**

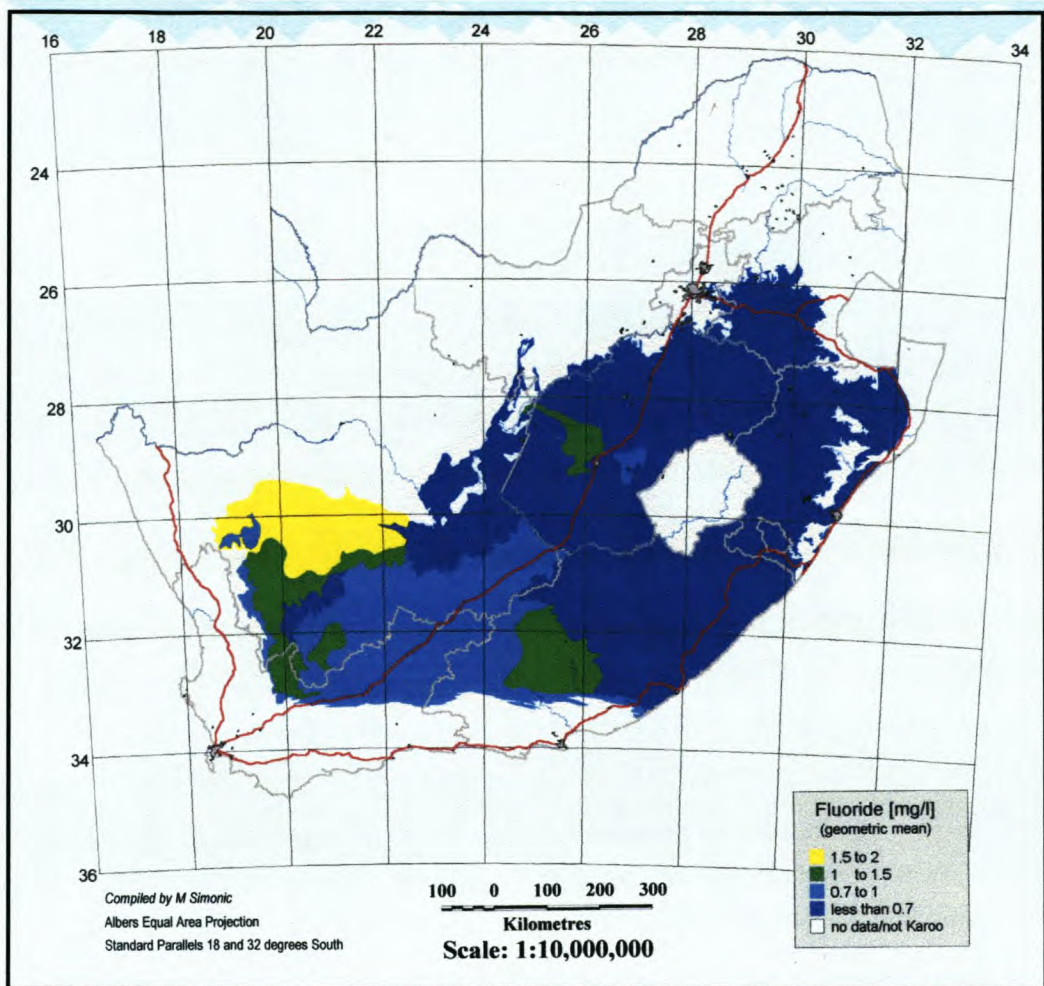


**Figure 5.5.5.3.D. Fluoride concentrations expressed as geometric means over representative lithological units.**

#### 5.5.5.4. Silica

The concentration ranges of silica (as  $\text{SiO}_2$ ) in groundwater are a measure of the silicate weathering processes. The bulk of matrix of Karoo aquifers is composed of silicate minerals. Silicates are much more resistant to weathering than for example the carbonates and the rate of dissolution is slower. The dissolution of silicates is irreversible and the products of dissolution usually form secondary minerals or quartz. The sources of silica in Karoo aquifers are mainly minerals like feldspar, albite and anorthite.

The highest mean concentrations of silica in groundwater occur in the northern half of the central Basin. The mean concentrations are 15-25 mg/l. Other regions have lower mean concentrations, controlled by solubility of the silicate minerals.

#### **5.5.6. Variability of the major constituents**

Presented maps do not give a complete picture on the groundwater quality as they provide *only mean concentrations assigned to representative lithological units*. No information is provided on how variable the concentrations for the particular units are. In order to provide the reader with an estimate on variability of assessed concentrations the following measure of variability was computed:

The *standard deviations* (SD) from selected log-transformed constituents (Ca, Mg, Na, T-Alk, SO<sub>4</sub>, Cl) were normalized using the Lilliefors transformation (the transformation factor is the mean). The normalized SD were summed up and mapped. It must be remembered that variability is directly proportional to the mean. Higher relative variability in the eastern part of the Karoo does not necessarily mean that the concentration ranges in the eastern part are higher.

#### **5.5.7. Groundwater quality with respect to drinking water guidelines**

Groundwater quality in the Karoo aquifers varies considerably. This is not surprising bearing in mind the areal extent of the Karoo Basin and variety of different hydrological regimes represented. After inspection of the spatial distribution of all the ions presented it is obvious that most groundwater quality problems occur in the western half of the Karoo Basin, especially along the edges, as well as portions of the eastern Karoo, i.e. in the vicinity of Nongoma. Local pollution sources may negatively effect groundwater in area which are generally mapped as favorable for drinking purposes, and thus all groundwater intended for drinking purposes should be assessed by a professional hydrogeologist or water quality scientist.

Constituents that most typically exceed drinking water quality guidelines are *sulphate, nitrate and fluoride*. In the western Karoo, especially within the Dwyka rocks, this list includes almost all the major constituents. However, this does not propose that there is no potential for groundwater development in these regions. The geometric means represent values somewhere in the middle of the frequency curve of the measured values, which implies that some samples will exceed guidelines and others will not.

In future it will be necessary to focus on the development of methods to assess further chemical parameters in addition to those presently being monitored. The industrial development and use of chemical agents in agriculture will require the measurement of other constituents that may be harmful in minute quantities.

## CHAPTER 6

### Conclusions and Recommendations

#### 6.1. Introduction

Statistical (descriptive, correlation matrices and factor analysis), graphical (Stiff, Piper and hydrogeochemical maps) and hydrogeochemical (isotopes and saturation state calculations) techniques were employed to assess groundwater characteristics of the geologically different fractured rock aquifers at different depths in the study area. The main factors (hydrogeochemical) and processes (exchange reactions, etc.) that determine groundwater chemistry variations (quality) in space and time were identified by means of chemical, isotope and  $^{14}\text{C}$ -dating analyses, in order to test for a "second, deeper seated aquifer system", with different characteristics.

Six sites were selected for exploration drilling by the Department of Water Affairs and Forestry at Loxton. Different structural parameters were used to select each site: type of fracture, major lineaments, orientation, stress-field, reactivation, structural domain and roughness, as well as density of fracturing.

The fracturing associated with and the morphology of the ring-structures may result in the development of discrete hydrological units (groundwater compartments), with excellent storage and recharge conditions.

All the objectives outlined in *Chapter 1* have been met and will be discussed in the following conclusions.

## 6.2. Groundwater chemistry and variations

Groundwater in the study area evolves from a Ca / Mg -HCO<sub>3</sub> type water, towards an Ca-SO<sub>4</sub> type water, indicating that several processes are occurring in the evolution sequence.

Groundwater in Loxton does not comply with the emulated flow path sequence, formulated by Chebotarev (*Freeze and Cherry, 1979*). There is no indication of TDS increase with evolution in the groundwater probably due to the large number of groundwater types occurring.

The chemical composition of groundwater is controlled by (*Adams, 1998*):

- Recharge of the aquifers by CO<sub>2</sub> charged precipitation, along preferred pathways. Carbonate minerals are mostly dissolved at topographic highs (Na-HCO<sub>3</sub>), with leaching of evaporitic salts in topographic lows (Na-SO<sub>4</sub>) to the unsaturated zone being the dominant process. Direct infiltration is also possible at lower lying areas. Fracture zones will favor recharge. The content of Na and Cl increases from topographic highs to lows, indicated also by the fresher water from high lying areas, where its not subjected to concentration (evapotranspiration) as in the low lying areas.
- Evolution of Ca / Mg -HCO<sub>3</sub> type water, towards a Ca-SO<sub>4</sub> type water is controlled by processes of dissolution, precipitation and primarily cation exchange processes. Dissolution and precipitation of mineral phases is the control mechanism for the reaction of ionic species in solution. Cation exchange may be responsible for the formation of Na-SO<sub>4</sub> water types. Ca-Cl type water can be the result of reverse cation exchange, by which attached Ca is exchanged for Na, possibly due to refreshing of older, more saline water with fresher Ca-type water. The Ca concentration equilibrium is disrupted by the precipitation of calcite, leading to the dissolution of minerals such as gypsum, containing ions that can replace the precipitated elements.

The main factors determining groundwater composition in the study area are geology, topography, the arid environment (evapotranspiration) and anthropogenic activities in the area. Vertical stratification plays a significant role and is not always overridden by lateral chemical changes, as a function of distance away from a mineralized zone.

### 6.3. Groundwater characteristics

Although groundwater type development may occur simultaneously within the fractured aquifer, no definite trend can be identified in terms of the groundwater type distribution for the study area versus different structures or distance from these structures. A regional groundwater evolution pattern in a NE-SW direction could be identified.

The main water type found in the area is a water type not dominated by any anions or cations in particular. The second is a water type in which Na-SO<sub>4</sub> is dominant, followed by a Na-HCO<sub>3</sub> dominated water and to a lesser extent a Ca-SO<sub>4</sub> type water. Depicting the different water types graphically indicates the dominance (91%) of the four water types mentioned above, in the Loxton area. The other nine percent of groundwater in the area is represented by NaCl and Ca / Mg-HCO<sub>3</sub> type water.

The main cause of groundwater salinity is the infiltration of evaporated water to the subsurface, suggested by the isotopic enrichment of  $\delta^{18}\text{O}$  and  $\delta^2\text{H}$ , indicating very slow recharge from ponded water during excessive rainfall events. This evaporated water infiltrates the subsurface through preferential pathways.

Hydraulic and hydrological factors greatly influence groundwater quality. Dolerite dykes and sills on one hand and fracture / fault sets on the other often control the mode of groundwater flow, availability of rainfall recharge and groundwater velocity and hence the residence time of water in the subsurface. Openness of groundwater systems is important in terms of availability of electron acceptors and carbon dioxide (*Woodford et al., in press*).

Difference in Cl and  $\delta^{18}\text{O}$  indicate different infiltration conditions and that the water may be unrelated, probably due to mixing of different water bodies.

There is a fair difference in isotopic values between surface measurements and measurements taken at depth, enforcing the possibility of a "second deeper seated aquifer". The water with the lower  $^{18}\text{O}$  values, for samples at depth suggest that the water has a source further inland, from rainfall on the range to the NE, the Hexrivierberge or Pramberge, which has greatly depleted  $^{18}\text{O}$  values relative to SMOW.

Barite could be the source for barium in the feldspar (e.g. celsian Ba[Al<sub>2</sub>Si<sub>2</sub>O<sub>8</sub>]) and biotite, feldspar, plagioclase, calcite, zeolite, apatite, perovskite, of the geological material. Biotite, K-feldspars, plagioclase, muscovite, illite, phlogopite, zeolites, apatite and orthoclase may be

source for potassium. Pyroxenes, biotite, magnetite, plagioclase, chlorite, calcite, ilmenite, pyrite, garnet, apatite and olivine may be the manganese source. Fluoride ions in the groundwater may be derived from the apatite and fluorite minerals (biotite, calcite, phlogopite, monticellite, zeolite) in the area. These indicate the influence of geology on the groundwater chemistry (*Adams, 1998*).

Calcite saturation controls the calcium concentration in the groundwater, as Ca ions are consumed by calcite saturation. The dissolution of gypsum, with a consequent increase in Ca concentration, causes calcite precipitation (*Appelo and Postma, 1994*). The removal or addition of Ca in solution, is also controlled by cation exchange processes.

The precipitation of calcite causes a decrease in  $\text{CO}_3$ , causing the dissolution of other carbonate minerals (i.e. strontianite). This and cation exchange processes are probably the cause of strontianite oversaturation (*Adams, 1998*).

Gypsum ( $\text{CaSO}_4$ ) is also a major source of  $\text{SO}_4$  in the groundwater of the area.  $\text{SO}_4$  is then reduced to  $\text{H}_2\text{S}$ , the "rotten egg" odour of groundwater in the area. Gypsum undersaturation may be a result of Ca loss, due to cation exchange and common ion effects, whereby barium is the preferred ion to attach to  $\text{SO}_4$ , forming barite. Barite ( $\text{BaSO}_4$ ) equilibrium controls barium concentrations and could also be less soluble than gypsum (*Adams, 1998*).

An oversaturation of fluoride exists in the groundwater, as fluoride dissolution may be caused by complexing effects, reducing free Ca and fluoride activities (*Nordstrom and Jenne, 1977*). Oversaturation of most of the mineral phases is probably due to an increase of ions, as a result of cation exchange and dissolution of minerals in the water rock interaction.

A strong correlation exists between Na and a moderate correlation between  $\text{SO}_4$ , with electrical conductivity (EC). These relationships are a clear indication of the main contributing elements to groundwater salinity. The moderate correlation between Pb, Li and strong correlation of Sr with EC, indicate the concentration increase of these elements, as the salinity of the water increases.

A mild carbonic acid ( $\text{H}_2\text{CO}_3$ ) forms, as the initial precipitation is charged with  $\text{CO}_2$  in the atmosphere. If availability of carbon dioxide is limited, hydrolysis of calcite (and silicates) occurs and the resulting hydroxyl ion may be involved in further reactions. In this way iron present in clay minerals may be leached out to form ferric hydroxide (*Woodford et al., in press*).

Iron is released naturally in the aquatic environment, by the weathering and leaching of sulphide ores (Pyrite,  $\text{FeS}_2$ ) in igneous, sedimentary and metamorphic rocks. Iron is only released under reducing conditions (DWAF, 1993).

Fluoride concentrations in surface and groundwater are high in the Karoo (DWAF, 1993). It is thought that fluoride is the ion mainly responsible for the dissolution of beryllium, scandium, niobium, tantalum and tin in natural water (DWAF, 1993).

Three possible sources of fluoride in Karoo aquifers are (Woodford *et al.*, *in press*):

1. Leaching and concentration of fluorine from rocks and soils during weathering and alteration processes.
2. Dissolution of secondary hydrothermal–pneumatolytic fluoride-rich minerals.
3. Circulation and regional-flow of a deeper-seated (thermal) groundwater.

During recent drilling in the Loxton area, where elevated fluoride values are known to occur, typical hydrothermal F-bearing fracture mineralization was commonly encountered - apophyllite in association with calcite (Woodford and Chevallier, 1998). This evidence points to a relationship between age, origin, temperature and fluoride content of groundwater in certain areas of the Karoo Basin.

The pH of water is largely controlled by the amount of carbonates, bicarbonates and dissolved carbon dioxide ( $\text{CO}_2$ ) in the water (El Ghandour *et al.*, 1985), it is also governed by the type of contamination bases, degree of ionisation, extent of hydrolysis and buffering action. High pH values are rather typical for dry desert-like climates. The pH variation in such terrains most probably reflects the differences in groundwater residence times. The high groundwater pH in Loxton is due to the residence time and cation exchange reactions.

Potassium ions are easily adsorbed by the aquifer material and therefore can seldom reach significant concentrations in groundwater, as indicated by the low potassium values in the groundwater of Loxton.

TDS in groundwater is controlled by the chemical composition of the host rock, as well as by the age (residence time) of the water, making these two parameters essential in hydrogeochemical data interpretation. The total dissolved solids concentration depends largely on the chemistry of

the host rock, rather than on the flow rate of the underground water. Calcrete may be responsible for high TDS values in this system of fresh and brackish water.

Nitrates are the main pollutants from animal, human waste and bacterial-activity in Loxton. A common source of nitrates in agricultural areas is the mineralization of natural soil's organic nitrogen and leaching thereof, when a virgin field is turned to tillage. The source of nitrate in the area may be due to nitrogen in the soils from animal wastes, containing more or less 5% nitrogen of its dry mass (urea), which is hydrolyzed and decomposed to ammonia (*Alexander, 1961*).

Point source nitrate contamination (*Sites 2 & 5*) is the result of anthropogenic activities as it's superimposed on the hydrogeochemical contour map, over the topographic and geochemical effects of the groundwater. Interestingly enough termite mounds were reported in Australia as being responsible for elevated nitrate concentrations on regional basis (*Barnes et al, 1992*).

Evaporation is the main process that may concentrate  $\text{NO}_x\text{-N}$ , which is easily leached out of surface soil mixing zone by water, due to its negative ionic charge and low adsorption potential (*Shirmohammadi et al, 1991*).

High B (illite) concentrations tend to be a sign of pollution, although in Loxton it's from the geology. Li (chlorite, pyroxene, apatite) is usually found as an impurity of sodium and potassium minerals (*Galvin 1996*).

Most of the groundwater samples taken at depth indicated a  $^{14}\text{C}$ -dating of century age ( $\pm 200$  years), although in a evolutionary sequence the water is not such a old (evolved) water type, supporting the statements made above about the migration of deeper seated water and thus a "second deeper seated aquifer system".

High evaporation rates in the Western Karoo induce a continuous concentration of solutes as the flushing-effect is at a minimum. The combination of a long groundwater residence time and evapotranspiration results in the reported high salt concentrations of groundwater in the Western Karoo (*Woodford et al., in press*).

The chemical character of the groundwater is predominantly controlled by the infiltration of evaporated surface and subsurface water, the topographical nature of the catchments, geological influences (i.e. the process of dissolution, precipitation and ion exchange) and the influence of man.

#### **6.4. Groundwater model**

A fracture rock mass can be considered a multi-porous medium, consisting of two main components, namely matrix rock blocks and fractures. Fractures are conductive conduits for flow, whilst the matrix blocks may be permeable or impermeable and most of the storage is contained within the permeable matrices (*Kirchner and Van Tonder, 1995*). Density of fractures may be a factor in storing significant amounts of water, which depends on the lithology and structural components of the geological setting. Fractures may close at depth, in response to the weight of the overburden and fracture dewatering. Wright stated in 1994 that openings typically develop in the upper part of the earth's crust, generally restricted to the upper 100 m.

Van Wyk (1963) and Vegter (1992) state that the porosity of Karoo sediments appears to be higher nearer the earth's surface, probably due to weathering and leaching of the rocks within the upper 30m. Similarly, the primary porosity of the sediments is expected to decrease with depth due to increasing lithostatic pressures and temperatures.

Aquifers in the Beaufort Group will thus not only be multi-layered, but also multi-porous with variable thicknesses. The contact plane between two different sedimentary layers causes a discontinuity in the hydraulic properties of the aquifer.

The Karoo dolerite includes a wide range of petrological facies and consists of an interconnected network of dykes and sills. It is nearly impossible to single out any particular intrusive or tectonic event, nevertheless it appears that a very large number of fractures were intruded simultaneously by magma and that the dolerite intrusive network acted as a shallow stockwork-like reservoir.

A low primary porosity and permeability is characteristic for the Karoo rock. Yields of boreholes are increased in brittle deformation zones, associated with dolerite intrusives, faults and fold axes (*Johnson, 1997; Woodford et al., 1996 and unpub.*). This fracturing of arenaceous units and argillaceous layers, leads to the higher secondary porosity and permeability achieved. Sedimentary rock units do not constitute reliable aquifers in the absence of fractures and joint systems. Jointing is common along intrusive contacts, being of particular value on the up-slope side of the hydraulic gradient in the Karoo sediments (*Robins, 1980*).

The amount of recharge is influenced by vegetative cover, topography, the type and nature of soils and the intensity and frequency of precipitation (*US Dept. of the Interior, 1981*). Groundwater levels tend to rise after rainy periods with heavy storms, due to the joints penetrated by the boreholes being in hydraulic continuity with the joints that are open to recharge (*Robins,*

1980). In Karoo aquifers the favored recharge mechanism is flow along preferred pathways (Van Tonder and Kirchner, 1990). Groundwater moves from levels of higher potential energy to areas with lower potential energy levels in general, which is essentially the result of elevation and pressure (Davis and De Wiest, 1966). Generally, shallow water levels occur in areas of outcrop and recharge, while deep water levels coincide with basement depressions which have thickened beds and lack of recharge (Levin, 1981).

On the local scale, the geometry, attitude, degree of weathering and fracturing of dykes influence the hydrological properties of individual structures. For example, thick dykes do not necessarily deform the country rocks more than do thin dykes, but the former may be more porous because of their granularity upon weathering. Emplacement of an en-échelon dyke is associated with complex stress fields and strong deformation of the host-rock, make it a good drilling target for high-yielding boreholes. The hydrology of a particular dyke is related to a complex interplay of these parameters and can thus vary dramatically along the strike of the structure.

Calcrete deposits (formed in arid and semi-arid areas or as a weathering product of dolerite) often form excellent, albeit localised, sources of groundwater due to (Woodford *et al.*, *in press*):

- An exceptionally higher rate of recharge from rainfall than the average of 2-5% for Karoo aquifers (Kirchner *et al.*, 1991), and
- Dissolution of the calcrete results in highly permeable zones within the deposits, as well as enhancing their storage capacity.

Isotopes can provide information on groundwater origin, recharge and mobility in the Karoo Basin. However, the full potential of such environmental tracer techniques may be achieved only when they can be integrated into well-conducted geohydrological investigations or groundwater development programs. The Loxton area provided a very complex study of different systems and processes.

Three distinct groundwater types, based on chemical and isotope data, was found by Talma (1981) in sandstone, siltstone and shales intruded by dolerite dykes and covered by colluvium in the Beaufort Group near Venterstad, also emulated in this study:

- I. Recent (<20 years) Ca, Mg, HCO<sub>3</sub>-water;
- II. Very pure (Old) Na HCO<sub>3</sub>-water and;
- III. Old NaCl-water, with little Ca<sup>2+</sup> and HCO<sub>3</sub><sup>-</sup>.

## **6.5. Hydrogeochemical conditions of groundwater**

Karoo formations display variable water quality properties. Lateral changes in climatic patterns seem to be the main factor controlling the diversity of the mineralization and water types occurring in Karoo rocks. This variability is caused by differences in rainfall, recharge, evaporation, topography, soil type and thickness, vegetation cover and human activities (Woodford *et al.*, *in press*).

Local topography has an influence on the local groundwater quality. Flat lying areas act as sinks (i.e. rivers and valleys) for groundwater, which is usually of a much poorer quality (> 149 mS/m) than groundwater in sloping areas (i.e. hills and foothills), which tend to be fresher (Adams, 1998).

Once groundwater reaches a natural boundary (hills), the EC seems to decrease, as groundwater drains towards the lower lying areas, where it becomes static or stagnant, with a concurrent increase in EC. The flatter lying areas have sufficient unconsolidated overburden, which is used for agricultural purposes, with the subsequent effects of irrigation causing the EC to rise (Adams, 1998).

The high salinity of groundwater is an indication of the influence of the geological materials on groundwater, as the major source of solutes. The infiltration of evaporated surface water and the leaching of soluble salts in the unsaturated zone, are the major processes controlling groundwater chemistry, verified in statistical, isotope and hydrochemical analyses. Intrusions and the fractures that accompany these structures act as useful conduits for groundwater flow.

Man's influence is superimposed on the topographical and geochemical effects on the subsurface water, indicating a source of contamination (NO<sub>3</sub>).

Due to the nature of groundwater flow, which varies significantly from area to area, local groundwater quality variations are significant and anomalies to the large-scale generalizations are prevalent. Micro-scale differences occur due to the nature of groundwater flow in Karoo rocks, namely the resulting variations within matrix and fracture components of the groundwater flux. The residence times are often different for these two main components and give rise to the differences in mineralization and solute proportion in passing groundwater (Woodford *et al.*, *in press*).

Topography does not absolutely determine chemical composition, which may be due to other factors like residence time (evapotranspiration) and geology.

Ions like calcium (Ca), sulphate (SO<sub>4</sub>) and chloride (Cl), all tend to increase in discharge regions. Potassium (K) shows an increase to the west of the topographic high, but is not controlled by the salinity of water, but sourced from the geological material in the area. Nitrate (NO<sub>3</sub>) shows the effect of land use practices, as isolated occurrences (Site 6 & 2) of high levels of nitrate are indicative of anthropogenic sources, for no nitrogen containing geological material exists within the study area.

The exchange capacity of clay minerals allows for the dissolution of more calcite (oversaturation) than would otherwise dissolve. The process also mobilizes significant amounts of sodium into solution and can lead to excessively alkaline solutions as observed in the low pH of groundwater in Loxton.

Statistical analysis showed that the main ions involved in cation exchange reactions at Loxton are:

Na-Ca; Sr-Ca and Sr-Na.

The major exchangeable ions Na-Ca, Sr-Ca and Sr-Na, all correlate positively. The elemental concentrations in the groundwater may be due to cation exchange processes.

The sodium concentration increase, accompanies the decrease in dissolved magnesium, calcium and potassium concentration, the latter being adsorbed on the interbedded and confining shales, in exchange for the desorbed sodium ions (*Tredoux and Kirchner, 1981*). The equilibrium of the calcium-magnesium-carbonic acid-calcite system is disturbed by the decrease of calcium and magnesium concentration in solution, resulting in the dissolution of additional calcite (*Tredoux and Kirchner, 1981*). The calcium ions are also exchanged for sodium in solution, with the overall effect of these reactions being an increase in sodium, alkalinity and pH, with a concurrent decrease of calcium and magnesium (*Tredoux and Kirchner, 1981*). This is also true for the study at Loxton.

Evapotranspiration masks the signature of various chemical processes like cation exchange reactions and should therefore not be sought after in a data set of a complex geological area, due to aquifer heterogeneity (*Woodford et al., in press*).

Contributing factors in progressive mineralization along a flow path are the type, distribution and adsorptive capacity of the geological matrix, the porosity and permeability of rocks and sediments and the course followed by water (*Kauffman, 1977*). Freeze and Cherry (1979) postulated that the order in which groundwater encounters strata of different mineralogical compositions exerts an important control on the water chemistry. It was also stated that as groundwater flows through strata of different mineralogical composition, it undergoes adjustments caused by imposition of new mineralogical controlled thermodynamic constraints. Water may attain local equilibrium in some strata, with respect to some mineral phases, but the continuous flow of the water causes disequilibrium as the water moves into strata comprising of different minerals (*Freeze and Cherry, 1979*).

Dolerite and carbonatite intrusions act as significant groundwater conduits, as these intrusions occur along fractures. Kimberlites and major joints associated with the Cape Orogeny, may only represent a break in the rock formations, as they are not filled with the same rock types and material, giving them poor geohydrological properties and rendering them poor groundwater targets.

Mega-joints and -faults showing signs of reactivation are more important from a geohydrological perspective as they are more deep-seated features and can act as conduits for groundwater flow. These structures (EW & NNW lineaments) are open under the modern tectonic stresses (WNW) and are potentially good drilling targets (*Woodford et al., in press*).

Statistical techniques together with graphical methods and hydrogeochemical techniques are suitable and simple tools for groundwater characterization.

## **6.6. Recommendations**

The Karoo Basin is characterised by fractured rock aquifers that are dissected by numerous dolerite intrusions. These conditions produce a complex hydrogeological system, which complicates the study and development of groundwater. Universal models of groundwater flow hardly apply to these conditions, and the geohydrologist needs additional tools with which to understand the movement and chemical evolution of groundwater. Environmental isotope techniques and their use in Karoo aquifers are intended to draw attention to this powerful and efficient tool to be used by geohydrologists. The potential of environmental isotopes has not

been properly exploited in the main Karoo Basin, and their use in groundwater investigations is encouraged.

As yet, no applications of nitrogen isotopes in the main Karoo Basin have been reported. However, the usefulness of this method is likely to increase. No nitrogen isotope study has been conducted in the study at Loxton.

To unravel the geological influence (influence of the uranium province) on groundwater chemistry is probable if exact geological profiles and sampling of boreholes at specific lithological units are conducted.

The establishing of a monitoring program could identify the effects of abstraction on groundwater quality, as well as determine seasonal influences. Point specific protected zones may protect the groundwater from the infiltration of pollutants.

The sun-powered submersible pump was operational with the 200m pipe, for sampling and with use of the flow-through sell. Sampling is however a time consuming process with this pump and can be frustrating if conditions (sunlight) is not optimal.

There are no distinct answers provided for the control by the geological structures on groundwater quality within the study. This project should be seen as a beginning for a basis of further study to provide the concrete answers needed to manage groundwater projects in the fractured rock aquifers of the Karoo.

## References

- Adams, S., (1998): ***The chemical groundwater characteristics of the Sutherland area, Northern Cape***. University of the Western Cape, Earth Science Department.
- Alexander, M., (1961): ***Introduction to soil microbiology***. Wiley, New York.
- Allsop, H.L., Bristow, J.W., Smith, C.B., Brown, R., Gleadow, A.J.W., Kramers, J.D. and Garvie, O.G., (1986): ***A summary of radiometric dating methods applicable to kimberlites and related rocks***. Fourth Intern. Kimberlite Conf., Perth, J. Ross ed., Vol.1, GSA special Publ. No 14, 343 - 357.
- Andrews, J. N., (1972): ***Mechanism of radon release in rock matrices and entry into ground water***. Trans. Inst. Min. Metal. Section B81, 198.
- Appelo, C.A.J. & Postma D., (1994): ***Geochemistry, groundwater and pollution***. A.A. Balkema Publishers, Rotterdam.
- Arad, A., Kafri, U., Halicz, L. & Brenner, I., (1986): ***Genetic Identification of the Saline Origins of Groundwater in Israel by Means of Minor Elements***. Chemical Geology, 54, 251-270.
- Ashley, R.P. & Lloyd, J.W., (1978): ***An example of the use of factor analysis and cluster analysis in groundwater chemistry interpretation***. Journal of Hydrology, 39, 355-364.
- Atomic Energy Corporation (AEC) (1990): ***Correlation between rainfall and groundwater quality throughout the Republic of South Africa. Addendum to: A report on the results of phase I of the ground water quality study of the Republic of South Africa***. Report No. AEC-89/73(B/R). Atomic Energy Corporation, Pelindaba.
- Barnes, C. J., Jacobson, G. & Smith, G. D., (1992): ***The origin of high-nitrate ground waters in the Australian arid zone***. Journal of hydrology; V. 137, Issue 4, Issue 1, 181-197.
- Beekman, H. E., Gieske, A. and Selaolo, E. T., (1996): ***GRES: Groundwater recharge studies in Botswana 1987-1996***. Botsw. Jnl of Earth Sci. 3, 1-17.

Bodmer H.P., (1994): ***The use of seismological data to predict overpressures***. Bull. Swiss. Assoc. Petroleum Geol, und-Eng., vol.61, 139, 69-81.

Boehmer, W.K. and Boonstra, J., (1986): ***Flow to wells in Intrusive Dykes***. Akademisch Proefschrift. Vrije Universiteit, Amsterdam.

Bond, G.W., (1946): ***A geochemical survey of the underground water supplies of the Union of South Africa***. Dept. of Mines, Geological survey Memoir, V41, 216.

Botha, J. F., Verwey, J. P., Van der Voort, I., Vivier, J. J. P., Colliston, W. P. and Loock, J. C., (1998): ***Karoo Aquifers. Their Geology, Geometry and Physical Behaviour***. WRC Report No 487/1/98. Water Research Commission, P.O. Box 824, Pretoria 0001.

Bredenkamp, D.B., (1995): ***An overview of quantitative estimation of groundwater recharge and aquifer storativity***. Ground water recharge and rural water supply. Geological society of South Africa, Midrand, South Africa.

Bredenkamp, D.B., Botha, L.J., Van Tonder, G.J. & Van Rensburg, H.J., (1995): ***Manual of the quantitative estimation of groundwater recharge and aquifer storativity***. Report No. TT 73/95. Water Research Commission, Pretoria.

Bredenkamp, D. B., Verhagen, B. Th. and Botha, L., (1998): ***Hydrogeological and isotopic assessment of the response of a fractured multi-layered aquifer to long term abstraction***. Final report on project K5/565 to the Water Research Commission.

Bricker, O.P. & Jones, B.F., (1995): ***Main factors affecting the composition of natural waters***. In B. Salbu and E. Steiness (Eds). Trace elements in natural waters. CRC Press, Boca Raton.

Brink A.B.A., (1985): ***Engineering geology of Southern Africa, Post-Gondwana deposits***. Vol. 4, Building Publication Pretoria, 332.

BRGM., (1978): ***Groundwater investigation at Beaufort West (Salt River)***. Bureau de Recherches Geologiques et Minieres, Technical Report for DWA&F, Contract No. W6018, Paris.

Burger, C.A.J., Hodgson F.D.I. and Vand der Linde P.J., (1981): ***Hidrouliese eienskappe van akwifere in die Suid-Vrystaat. Die ontwikkeling en evaluering van tegnieke vir die bepaling***

**van die ontginningspotensiaal van grondwaterbronne in die Suid-Vrystaat en in Noord-Kaapland, Volume 2.** Institut vir Grondwaterstudies.

Burke, K., (1996): ***The African Plate***. S.afr.J.Geol., 99 (4), 341 - 409.

Busenberg, E. and Plummer, L. N., (1992): ***Use of chlorofluorocarbons ( $CCl_3F$  and  $CCl_2F_2$ ) as hydrologic tracers and age-dating tools: the alluvial and terrace system of central Oklahoma***. Water Res. Res; V28, No.9. 2257-2283.

Chevallier L. and Woodford A.C., (1999): ***Morpho-tectonics and mechanism of emplacement of the dolerite rings and sills of the Western Karoo, South Africa.***, S.Afr.J.Geol., Vol. 102 (1), 43-54.

Chevallier L. and Woodford A.C., (in press.): ***Influence of dolerite ring-structures on the occurrence of groundwater in Karoo Fractured Aquifers: a morpho-tectonic approach***. Water Research Commission, Project Number K5/937, Pretoria.

Coetzee, D.S., (1983): ***The deformation style between Meirings Poort and Beaufort West***. In: A.P.G. Söhnge and I.W. Hälbig (eds), Geodynamics of the Cape Fold Belt. Geol. Soc. S. Afr. Spec. Publ., No 12, 101 - 113.

Cogho, V.E., Van Niekerk, L.J., Pretorius, H.P.J. and Hodgson, F.D.I., (1992): ***The development of techniques for the evaluation and effective management of surface and ground water contamination in the OVS goldfields***. Report No. K5/244. Water Research Commission, Pretoria.

Cole, D.I., Labuschagne L.S., Söhnge, Stettler E.H. and Scheinder G.I.C., (1991): ***Aeroradiometric survey for uranium and ground follow-up in the Main Karoo Basin***. Geol. Surv., Memoir 76, 172 + map.

Cole, D.I., (1992): ***Evolution and development of the Karoo Basin***. In: de Wit M.J. and Ransome I.G.D. (Eds.) Inversion tectonics of the Cape Fold Belt, Karoo and Cretaceous Basins of Southern Africa. Balkema, Rotterdam, 87 - 99.

Craig, H., (1961): ***Standards for reporting concentrations of deuterium and oxygen-18 in natural waters***. Science, 133, 1833-1834.

- Davis, S.N. and De Wiest, R.J.M., (1966): **Hydrology**. John Wiley and Sons, New York.
- Dawdy, D.R. & Feth, J.H., (1967): **Application of factor analysis in study of chemistry of groundwater quality, Mojave River Valley, California**. Water Resources Research, 3, 2, 505-510.
- De Beer, J.H. & Blume, J., (1985): **Geophysical and hydrogeological investigations of the groundwater resources of western Hereroland, SWA/Namibia**. Transaction of the Geological Society of South Africa, 88, 483-493.
- Deer, W.A., Howie, R.A. & Zussman, J., (1992): **An introduction to the Rock Forming Minerals**. Longman Scientific & Technical, England.
- De la Rue Winter, H. and Venter, J.J., (1970): **Lithostratigraphic correlation of recent deep boreholes in the Karoo - Cape sequence**. In: Proceedings of the 1970 Gondwana Symposium, 395 - 408.
- De Wet, J.J., (1975): **Carbonatites and related rocks at Salpeter Kop, Sutherland, Cape Province**. Annals University of Stellenbosch, Ser. A1, 1, 193-232.
- De Wit, M.C.J., (1996): **The distribution and stratigraphy of inland alluvial diamond deposits in South Africa**. Afr. Geos. Rev., 3, No2, 175 - 189.
- D'Hoore, J., (1954): **Proposed classification of the accumulation zones of free sesquioxides on a genetic basis**. African Soils, Vol.3, 66 - 81.
- Domenico, P.M. & Schwartz, F.W., (1990): **Physical and Chemical Hydrogeology**. John Wiley & Sons, New York.
- Drever, J.I., (1988): **The geochemistry of natural water**. Second Edition. Prentice Hall Inc., New Jersey.
- Duane, M.J. and Brown, R., (1992): **Geochemical open-system behaviour related to fluid-flow and metamorphism in the Karoo Basin**. In: de Wit M.J. and Ransome I.G.D. (Eds.) Inversion tectonics of the Cape Fold Belt, Karoo and Cretaceous Basins of Southern Africa. Balkema, Rotterdam, 127 - 140.

Duncan R.A., Hargraves R.B. and Brey G.P., (1978): ***Age, paleomagnetism and chemistry of melilite basalts in the Southern Cape, South Africa.*** Geol. Mag., 115, 317 - 327.

Duncan, R.A., Hooper, P.R., Ehacek, J., Marsh, J.S. and Duncan, R.A., (1997): ***The timing and duration of the Karoo igneous event, Southern Gondwana.*** J. Geophys.Res., 102, 18127 - 18138.

Du Toit, A.L., (1920): ***The Karoo Dolerites- a study in Hypabyssal Intrusion.*** Trans. Geol. Soc. S. Afr., V23, 1-42.

Du Toit, A.L., (1954): ***The geology of South Africa.*** Oliver and Boyd, Edinburgh.

DWA&F (1993): ***South Africa Water Quality Guidelines - Volume 1, Domestic use.*** Department Water Affairs and Forestry, Pretoria.

El Ghandour, M.F.M., Khalil, J.B. & Atta, S.A., (1985): ***Distribution of carbonates, bicarbonates and pH values in ground water of the Nile delta region, Egypt.*** Ground Water, 23, 1, 35-41.

Ellis, F. and Schloms, B.H.A., (1981): ***A note on the dorbanks (duripans) of South Africa.*** Palaeoecology of Africa and the surrounding islands, vol. 15, 149 - 158.

Enslin, J.F., (1950): ***Geophysical methods of tracing and determining contacts of dolerite dykes in Karoo sediments in connection with the siting of boreholes for water.*** Trans. geol. Soc. S Afr., V53, 193-204.

Fetter, C.W., (1988): ***Applied Hydrogeology.*** Second Edition. Merrill Publishing Co., Columbus.

Fontes, J-C., (1980): ***Enviromental isotopes in groundwater hydrology.*** In: Handbook of environmental isotope geochemistry 1 P Fritz & J-C Fontes (Eds.) Elsevier, 75-140.

Freeze, A. L. and Cherry, J. A., (1979): ***Groundwater.*** Prentice-Hall Inc., Englewood Cliffs, New Jersey.

Galvin, A.M., (1996): ***Occurences of metals in waters: An overview.*** Water SA, 22, 7-18.

Gordon, R.G., and Stein S., (1992): ***Global tectonics and space geodesy***. *Science*, 256, 333-342.

Gordon, R.G., (1995): ***Plate motions, crustal and lithospheric mobility, and palaeomagnetism: Prospective viewpoint***. *J. geophys. Res.*, V100, 24367-24392.

Gordon-Welsh, J.F., (1974): ***Hydrological phenomena in the southwestern Cape associated with the Ceres earthquake***. In "The Earthquake of 29 September 1969 in the Southwestern Cape Province, South Africa", *Geol. Surv. S. Afr. Seismol. Ser. 4*, 25-30.

Greeff, G.J., (1968): ***Fracture systems and the kimberlite intrusions of Griqualand West***. University of Stellenbosch, Department of Geology.

Greeff, G.J., (1991): ***The geohydrology of a typical catchment in the Cape Supergroup, Breë River Valley***. University of Stellenbosch, Department of Geology.

Greeff, G.J., (1994): ***Groundwater contribution to streamflow salinity in a Bokkeveld Shale Catchment, Breede River Valley, RSA***. *Ground Water*, 32, 33-70.

Hälbich, I.W. and Swart, J., (1983): ***Structural zoning and dynamic history of the cover rocks of the Cape Fold Belt***. In: A.P.G. Söhne and I.W. Hälbich (eds), *Geodynamics of the Cape Fold Belt*. *Geol. Soc. S. Afr. Spec. Publ.*, No 12, 75 - 100.

Hallbauer D.K., Chevallier L. and Woodford A.C., (1995): ***The application of capillary ion analysis to the geochemistry of ground water from Western Karoo Aquifers***. *Ground Water Recharge and Rural Water Supply*, 26 -28 sept 1995, Midrand. Extended Abstract.

Hancock, P.L. and Engelder, T., (1989): ***Neotectonic joints***. *Soc. Am. Bull.*, V101, 1197 - 1208.

Hartnady, C.J.H., (1990): ***Seismicity and plate boundary evolution in southeastern Africa***. *S Afr. J. Geol.*, V93, 473 - 484.

Hartnady, C.J.H. and Woodford, A.C., (1996): ***A feasibility investigation of the relationship between near-surface neotectonic crustal stress and groundwater occurrence in a Karoo fractured-rock aquifer***. Research proposal to the Water Research Commission.

Hartnady, C.J.H., (1998): ***A review of the earthquake history and seismotectonic interpretation of the kingdom of Lesotho***. In: Melis and Duplessis consulting Engineers (Eds.), Review of the current stage of knowledge of the seismotectonic setting of Lesotho and its significance in predicting seismic design parameters for the Katse and Mohale Dams and further phases of the LHWP. Lesotho Highlands Water Project contract No 1028., Workshop in Maseru, 25 may, 1998. 37.

Heaton, T.H.E., (1984): ***Sources of the nitrate in phreatic groundwater in the western Kalahari***. Journal of Hydrology, 67, 249-259.

Heaton, T.H.E., (1986): ***Isotopic studies of nitrogen pollution in the hydrosphere and atmosphere: a review***. Chem. Geol. (Isot. Geosc. Sect.) V59, 87-102.

Helweg, O.J., (1978): ***Regional groundwater management***. Ground Water, 16, 5, 318-321.

Hem, J.D., (1989): ***The study and interpretation of the chemical characteristics of natural water***. Third Edition. U.S. Geological Survey Water-Supply Paper 2254. U.S. Geological Survey.

Henderson, P., (1986): ***Inorganic Geochemistry***. Pergamon Press, Oxford.

Hitchon, B., Billings, G.K. & Klovan, J.E., (1971): ***Geochemistry and origin of formation waters in the western Canada sedimentary basin-III. Factors controlling chemical composition***. Geochimica et Cosmochimica Acta, 33, 567-598.

Holmes, P.J. and Reynhardt, J.H., (1989): ***Late Cenozoic alluvial gravels in the vicinity of Aliwal North***. Suid- Afrik. Tydsk. vir Wetenskap. Vol. 85, 65 - 68.

Hübner, H., (1986): ***Isotope effects of nitrogen in the soil and biosphere***. In: Handbook of Environmental Isotope Geochemistry 2 (P Fritz & J-C Fontes, Eds) Elsevier. 361-426.

Hughes, D.A. & Sami, K., (1991): ***The Bedford catchments. An introduction to their physical and hydrological characteristics***. Report No. 138/1/92. Water Research Commission, Pretoria.

Hunter D.R. and Reid D.L., (1987): ***Mafic dykes swarms of Southern Africa***. In: Halls H.C. & Fahrig W.F. (Eds.), Mafic Dyke Swarms. Spec. Pap. geol. Assoc. Canada, 34, 445-456.

IAEA (1983): **Guidebook on nuclear techniques in hydrology**. Tech. Rep. Series 206. IAEA, Vienna.

Johnston, R.J., (1989): **Multivariate statistical analysis in geography**. Longman Group Ltd., Harlow.

Johnson, M.R., Van Vuuren, C.J., Visser, J.N.J., Cole, D.I., Wickens, H. de V., Christie, A.D.M., Roberts, D.L., and Brandl, G., (1997): **The foreland Karoo Basin, South Africa**. In: R.C. Selley (Ed.), African Basins. Sedimentary Basins of the World, 3. Elsevier, Amsterdam.

Katz, B.G., (1989): **Influence of mineral weathering reactions on the chemical composition of soil water, springs and groundwater, Catoctin Mountains, Maryland**. Hydrological Processes, 3, 185-202.

Katz, B.G. & Choquette, A.F., (1991): **Aqueous geochemistry of the sand-and-gravel aquifer**. Northwest Florida. Ground Water, 29, 1, 47-55.

Kauffman, R.F., (1977): **Land and water use impacts on Ground Water quality in Las Vegas Valley**. Ground Water, 15, 1, 81-89.

Kent, L.E. and Enslin, J.F., (1965): **Ground-water prospecting methods used in the Republic of South Africa**. Ann. Geol. Surv. SA, V4, 151-156 + 4 folders.

Kent, L.E., (1972): **Springs, In Eeden, O.R., 1972, The geology of the Republic of South Africa**. An Explanation to the 1:1 000 000 map, 1970. Special publication 18, Geological Survey, Department of Mines, 71-74.

Kirchner, J. O. G., Van Tonder, G. J. and Lukas, E., (1991): **Exploitation Potential of Karoo Aquifers**. WRC Report No 170/1/91. Water Research Commission, P.O. Box 824, Pretoria 0001.

Kirchner, J. O. G., (1994): **Investigation into the contribution of ground water to the salt load of the Breede River, using natural isotopes and chemical tracers**. Report No.344/1/95. Water Research Commission, Pretoria.

Kirchner, J. O. G. & Van Tonder, G.J., (1995): **Proposed guidelines for the execution, evaluation and interpretation of pumping tests in fracture-rock formations**. Water SA, 21, 3, 187-200.

Kok, T.S., (1982): ***Municipal Water Supply from Jagersfontein Mine, Orange Free State.*** Department of Water Affairs & Forestry, Directorate Geohydrology Technical Report GH1482, Pretoria, South Africa.

Kruger, J.C. and Kok, T.S., (1976): ***Die voorkoms van grondwater in dolerietgange in dele van Noordoos-Vrystaat.*** Department of Water Affairs & Forestry, Directorate Geohydrology Technical Report GH1482, Pretoria, South Africa.

Kruseman, G.P. & De Ridder, N.A., (1990): ***Analysis and Evaluation of Pumping Test Data.*** International Institute for Land Reclamation and Improvement (ILRI), Wageningen, vol. 47.

KwaZulu-Natal Hydrogeological mapping project (1995): ***Units 8, 9, 10 and 11.*** Department of Water Affairs and Forestry, Pretoria, Empangeni. 11 reports (geographic units 1 to 11) + maps.

Langmuir, D., (1971): ***The geochemistry of some carbonate group waters in central Pennsylvania.*** *Geochimica et Cosmochimica Acta*, 29, 1, 1023-1045.

Leiscewitz, A.F., (1979): ***Nelspoort – Salt River groundwater investigation.*** Technical Report GH3124, Department of Water Affairs and Forestry, Pretoria.

Levin, M., (1981): ***The geology, hydrology and hydrochemistry of an area between the Kuruman and Orange Rivers, North Western Cape.*** *Transaction of the Geological Society of South Africa*, 84, 177-190.

Levinson, A.A., (1980): ***Introduction to exploration geochemistry. Second edition.*** Applied Publishing Ltd., Calgary.

Lynch, S.D., Reynders, A.G. & Schulze, R.E., (1994): ***Preparing input data for a national-scale groundwater vulnerability map of Southern Africa.*** *Water SA*, 20, 239-246.

Maclear, L.G.A. and Woodford A.C., (1995): ***Factors affecting spring-flow variations at Uitenhage Springs, Eastern Cape.*** In *Groundwater 95 - Groundwater Recharge and Rural Water Supply*, 26-28 September 1995, Volkswagen Conference Centre, Midrand, South Africa.

Malomo, S., Okufarasin, V.A., Olorunniwo, M.A. & Ormode, A.A., (1990): **Groundwater chemistry of weathered zone aquifers of an area underlain by basement complex rocks.** Journal of African Earth Sciences, 11, 3/4, 327-371.

Maske S., (1966): **The petrography of the Ingeli Mountain Range.** Annale Universiteit van Stellenbosch, Vol. 41, 108.

Mazor, E., Bielsky, M., Verhagen, B.Th., Sellschop, J.P.F., Hutton, L. and Jones, M.T., (1980): **Chemical composition of groundwaters in the vast Kalahari Flatland.** Journal of Hydrology, 48, 147-165.

Mazor, E. and Verhagen, B. Th., (1983): **Dissolved ions, stable and radioactive isotopes and noble gases in thermal waters of South Africa.** J. of Hydrology V63, 315-329.

Mazor, E., (1991): **Applied chemical and isotopic groundwater hydrology.** Open University Press. 274.

Meyer, R. en van Zijl, J.S.V., (1980): **Die ontwikkeling en evaluasie van tegnieke vir die bepaling van die ontginningspotensiaal van grondwaterbronne in die Doornberg-breuksone.** Finale verslag Deel 2(b): Venterstad-omgewing - Geofisiese studies. Water Research Commission Project K5/28.

Mook, W.G., (1994): **Principals of isotope hydrology: Introductory course on isotope hydrology.** Centre of Isotope Research, University of Groningen.

Newton, A.R., (1987): **The fracture pattern around the Sutherland diatreme, Cape Province, from remote sensing.** South African Journal of Geology, 90, 2, 99-106.

Newton, A.R., (1993): **Thrusting on the northern margin of the Cape Fold Belt, near Laingsburg.** S.Afr.J.Geol., 96 (1/2), 22 - 30.

Nixon P.H. and Kresten P., (1973): **Butha-Buthe swarm and associated kimberlite blows. In: P.H. Nixon Ed., Lesotho kimberlites.** Lesotho National Development Corporation. 197 - 206.

Nixon P.H., Boyd F.R. and Boctor N.Z., (1983): **East Griqualand kimberlites.** Trans. Geol. Soc. S. Afr., 86, 221 - 236.

Nordstrom, D.K. & Jenne, E.A., (1977): ***Fluorite solubility equilibria in selected geothermal water***. *Geochimica et Cosmochimica Acta*, 41, 175-188.

Olivier H.J., (1972): ***Geohydrological investigation of the flooding of shaft 2, Orange - Fish tunnel, North eastern Cape Province***. *Trans. Geol Soc. S. Afri.*, 75, 197- 219.

Ophori, D.U. & Toth, J., (1988): ***Patterns of ground-water chemistry, Ross Creek Basin, Alberta, Canada***. *Ground Water*, 27, 1, 20-55.

Parker, L.V., (1994): ***The effect of groundwater sampling devices on water quality: A literature review***. *Groundwater Monitoring Review*, Spring 1994, 130-141.

Parsons, R.P., (1986): ***The exploration and evaluation of groundwater ubits south and west of Graaff-Reinet, Cape Province, South Africa***. Unpubl. MSc. Thesis, Rhodes University, Grahamstown.

Parsons, R. and Tredoux, G., (1993): ***The development of a strategy to monitor groundwater quality on a national scale***. Report No. 482/1/93. Water Research Commission, Pretoria.

Partridge, T.C., (In press): ***Of diamonds, Dinosaurs and diastrophism: 150 million years of landscape evolution in Southern Africa***. The 25th Alex Du Toit memorial lecture 1997.

Partridge, T.C. and Maud, R.R., (1987): ***Geomorphic evolution of Southern Africa since the Mesozoic***. *South African Journ. Geol.*, 90, 179 - 208.

Paver, G.L., Simpson, D.J., Freeman, C.J., and Clark, M.A., (1943): ***The location of underground water by geological and geophysical methods***. Compiled from Technical Work of the Unit 42<sup>nd</sup> Geological Section, South African Engineering Corps, U.D.F., M.E.F. April 1943, published by G.H.Q and printed M.M.P. & P Coy., S.A.E.C.

Piper, A.M., (1944): ***A graphic procedure in the geochemical interpretation of water analysis***. *Transaction of the American Geophysical Union*, 25, 914-923.

Plummer, L.N., Prestemon, E.C. & Parkhurst, D.L., (1992): ***An interactive code (NETPATH) for modeling net geochemical reactions along a flow path***. Water Resources Investigation Report 91-4078. U.S. Geological Survey.

Reeder, S.W., Hitchon, B. & Levinson, A.A., (1972): ***Hydrogeochemistry of the surface water of the Mackenzie River drainage basin, Canada - I. Factors controlling inorganic composition.*** *Geochimica et Cosmochimica Acta*, 36, 825-865.

Rethati, L., (1983): ***Groundwater in Civil Engineering.*** Elsevier Scientific Publishing Co., Amsterdam.

Robins, N.S., (1980): ***A review of groundwater resources and well yields in Swaziland.*** *Transaction of the Geological Society of South Africa*, 83, 1-4.

Rose, A.W., Hawkes, H.E. and Webb, J.S., (1979): ***Geochemistry in mineral exploration.*** Second Edition. Academic Press, London.

Roux, P.W., (1981): ***Interaction between climate, vegetation and runoff in the Karoo.*** In H. Maaren (Ed.). Workshop on the effect of rural land use and catchment management on water resources. Department Water Affaires and Forestry, Pretoria.

Roux, P.W. and Opperman, D.P.J., (1986): ***Soil erosion.*** In Cowling, Roux and Pieterse (Eds.). *The Karoo biome: a preliminary synthesis. Part I - Physical environment.* South African National Scientific Programmes. Report No. 124. Foundation for Research and Development.

Rowell, D.M. and de Swart, A.M.J., (1976): ***Diagenesis in Cape and Karoo sediments, South Africa and its bearing on their hydrocarbon potential.*** *Trans. geol. Soc. S. Afr.*, 81-145.

Sami, K., (1992): ***Recharge mechanisms and geochemical processes in a semi-arid sedimentary basin, Eastern Cape, South Africa.*** *Journal of Hydrology*, 139, 27-48.

Schot, P.P. and Van der Waal, J., (1992): ***Human impact on regional groundwater composition through intervention in natural flow patterns and changes in land use.*** *Journal of Hydrology*, 134, 297-313.

Schot, P.P. and Wassen, M.J., (1993): ***Calcium concentrations in wetland groundwater in relation to water sources and soil conditions in the recharge area.*** *Journal of Hydrology*, 141, 197-217.

Seward, P., (1982): ***Possibilities for groundwater development in the Vanwyksvlei area.*** Technical Report GH3225, Department of Water Affairs and Forestry, Pretoria.

Shirmohammadi, A., Magette, W.L. & Shoemaker, L.L., (1991): ***Reduction of nitrate loadings to groundwater***. Groundwater Monitoring Review, Winter 1991, 112-117.

Sibson, R.H., (1990): ***Rupture nucleation on unfavorably oriented faults***. Bull. Seism. Soc. Am., 80/6, 1580-1604.

Simonis, J.J. and Kok, T.S., (1989): ***Notes on the hydrogeological characteristics of the more important waterbearing formations in South Africa with special reference to possible groundwater pollution***. Technical Report No. GH 3641. Department of Water Affairs and Forestry, Pretoria.

Smart, M.C., (1994): ***Mimosadale wellfield long term yield and future groundwater development at Graaff Reinet***. DWA&F Technical Report GH 3836, Pretoria.

Smith C.B., Allsopp, H.L., Kramers, J.D., Hutshinson, G. and Roddick, J.C., (1985): ***Emplacement ages of Jurassic - Cretaceous South African kimberlites by Rb - Sr method on phlogopite and whole-rock samples***. Trans. Geol. Soc. S. Afr., 88, 249 - 266.

Smith, R.H.M., (1990): ***A review of stratigraphy and sedimentary environments of the Karoo Basin of South Africa***. J. Afr. Earth Sc., 10, 117-137.

Smith, R.M.H., Eriksson, P.G., & Botha, W.J., (1993): ***A review of the stratigraphy and sedimentary environments of the Karoo-aged basins of Southern Africa***. J. Afr. Earth Sc., 16, 143-169.

Smith C.B., Clark T.C., Barton E.S. and Bristow J.W., (1994): ***Emplacement ages of kimberlite occurrences in the Prieska region, Southwest border of the Kaapvaal Craton, South Africa***. Chem. Geol., 113, 149-169.

Sowayan, A.M. & Allayla, R., (1989): ***Origin of the saline ground water in Wadi Ar-Rumah, Saudi Arabia***. Ground Water, 27, 4, 481-490.

Stear, W.M., (1980): ***Sedimentary environment of the Beaufort West Group uranium province in the vicinity of Beaufort West, South Africa***. PhD thesis, Univ. Port Elizabeth (unpubl.).

Steffen, Robertson and Kirsten (SRK) (1997): **Beaufort West Municipality: Brandwacht Aquifer and Wellfield Groundwater Flow Model**. (Kotze J C and Rosewarne P N), Steffen, Robertson & Kirsten report: 227331/3, Cape Town.

Storey, B.C. and Kyle, P.R., (1997): **An active mantle mechanism for Gondwana breakup**. South Africa. S.Afr.J.Geol., 100 (4), 283 - 290.

Swan, A.R.H. and Sandilands, M., (1995): **Introduction to geological data analysis**. Blackwell Science Ltd., Oxford.

Talma, A.S., (1981): **Chemical changes in groundwater and their reaction rates**. Transactions of the Geological Society of South Africa, 84, 99-105.

Tankard, A.J., Eriksson, K.A., Hunter, D.R., Jackson, M.P.A., Hobday, D.K., and Minter, W.E.L., (1982): **Crustal Evolution of Southern Africa**. Springer-Verlag, New York, 523.

Thomas R.J., Du Plessis A., Fitch F.J., Marshall C.G.A., Miller J.A, von Brunn V. and Watkeys M.K., (1992): **Geological studies in southern Natal and Transkei: implication for Cape Orogen**. In: De Wit M.J. and Ransome I.G.D. (Eds), Inversion tectonics of the Cape Fold Belt, Karoo and Cretaceous Basins of Southern Africa. Conference on inversion tectonics of the Cape Fold Belt Proceedings, South Africa. Balkema, Rotterdam. 229 - 236.

Tordiffe, E.A.W., (1978), unpubl. Ph.D. Thesis: **Aspects of the hydrochemistry of the Karoo Sequence in the Great Fish River Basin, Eastern Cape Province, with special reference to the groundwater quality**. Univ. O.F.S.

Tredoux, G., (1993): **A preliminary investigation of the nitrate content of groundwater and limitations of the nitrate input**. Report No. 368/1/93. Water Research Commission, Pretoria.

Tredoux, G. and Kirchner, J.O.G., (1981): **The evolution of the chemical composition of artesian water in the Auob sandstone (Namibia/SWA)**. Transaction of the Geological Society of South Africa, 84, 169-175.

US Department of the Interior (Water and Power Resources Services) (1981): **Ground Water Manual**. John Wiley and Sons, New York.

Usunoff, E.J. and Guzman-Guzman, A., (1989): ***Multivariate analysis in hydrochemistry: An example of the use of factor and correspondence analysis***. Ground Water, 27, 1, 27-34.

Vandoolaeghe, M.A.C., (1979): ***Middelburg geohydrological investigation***. Unpublished Technical Report GH3072, Directorate:Geohydrology, Department of Water Affairs, Cape Town.

Vandoolaeghe, M.A.C., (1980): ***Queenstown geohydrological investigation***. Unpublished Technical Report GH3135, Directorate:Geohydrology, Department of Water Affairs, Cape Town.

Van Tonder, G.J. and Kirchner, J.O.G., (1990): ***Estimation of natural groundwater recharge in the Karoo aquifers of South Africa***. Journal of Hydrology, 121, 395-419.

Van Wyk, W.L., (1963): ***Groundwater studies in northern natal, zuland and surrounding areas***. Memoir 52, Geological Survey of South Africa, 133.

Veevers, J.J., Cole, D.I. and Cowan, E.J., (1994): ***Southern Africa: Karoo Basin and Cape Fold Belt***. In: Veevers, J.J. & Powell, C. McA. (Eds.), Permian-Triassic Pangean Basins and Foldbelts Along the Panthalassan Margin of Gondwanaland. Mem. Geol. Soc. Am., 184, 223–279.

Vegter, J.R., (1992): ***An evaluation of ground water exploitation and its potential for urban use, De Aar***. Hydrogeological consulting report to the Directorate of Geohydrology, Department of Water Affairs and Forestry, Pretoria, South Africa.

Venter, J.M., Mocke, C. and De Jager, J.M., (1986): ***Climate***. In Cowling, Roux and Pieterse (Eds.). The Karoo biome: a preliminary synthesis. Part I - Physical Environment. South African National Scientific Programmes Report No. 124. Foundation of Research and Development.

Verhagen, B. Th., (1984): ***Environmental isotope study of a groundwater supply project in the Kalahari of Gordinia***. Isotope Hydrology 1983. IAEA Vienna. 415-432.

Verhagen, B. Th., (1985). ***Isotope hydrology of ground waters of the Kalahari, Gordinia***. Transactions of the Geological Society of South Africa, 88, 517-522.

Verhagen, B. Th., Geyh, M. A., Froehlich, K. and Wirth, K., (1991): ***Isotope hydrological methods for the quantitative evaluation of ground water resources in arid and semi-arid areas***. Research reports: Fed. Ministry for Econ. Coop., FRG. ISBN 3-8039-0352-1.

Verhagen, B. Th., Butler, M. J., Levin, M. and Walton, D.G., (1996): ***Investigation of ground water pollution associated with waste disposal: development of an environmental isotope approach***. Final report to the Water Research Commission on Project K5/311.

Verwoerd, W.J., Viljoen, E.A. and Chevallier, L., (1995): ***Rare metal mineralization at the Salpeterkop carbonatite complex, Western Cape Province, South Africa***. Journal of African Earth Sciences, 21, 1, 171-186.

Visser, J.N.J., (1997): ***Deglaciation sequences in the Permo-Carboniferous Karoo and Kalahari basins of southern Africa: a tool in the analysis of cyclic glaciomarine basin fills***. Sedimentology, Vol.44, 507-521.

Visser, J.N.J. and Botha, B.J.V., (1980): ***Meander channel, point-bar, crevasse splay and aeolian deposits from the Elliot Formation in Barkly Pass, northeastern Cape***. Trans. Geol. Soc. S. Afr., 83, 55-62.

Visser, H.N; von Backström, J.W; Keyser, U; van der Westhuizen, J.M; Marais, J.A.H; Coetzee, C.B; Schumann, F.W; van Wyk, W.L; de Villiers, S.B; Coertze, F.J; Wilke, P.P; de Jager, D.H; Rilett, M.H. and Toerien, B., (1963): ***Gips in die Republiek van Suid Afrika***. Geological Survey Handbook No 4, 134 + maps.

Vogel, J.C., (1970): ***Carbon-14 dating of ground water***. In: Isotope Hydrology 1970. 225-240. IAEA, Vienna.

Vogel, J. C. and van Urk, H., (1975): ***Isotopic composition of groundwater in semi-arid regions of southern Africa***. J. of Hydrol. V25, 23-36.

Vogel, J.C., and Heaton, T.H.E., (1980(a)): ***The isotopic, chemical and dissolved gas concentrations in groundwater near Venterstad, Cape Province***. CSIR, Technical report 391, Natural Isotopes Division, Pretoria.

Vogel, J.C., Talma, A.S. and Heaton, T.H.E., (1980(b)): ***Natural isotope studies of the groundwater in the Beaufort West area***. CSIR, Pretoria. Final report Kon/Gf/74/1; K 5/28.

Weaver, J.M.C., (1992): ***Groundwater sampling - A comprehensive guide for sampling methods***. Water Research Commission, Pretoria.

Weaver, J.M.C., (1992): ***Groundwater sampling - an abbreviated field guide form for sampling methods***. Water Research Commission, Pretoria, vol. Project No. 339.

Weaver, T.R. and Bahr, J.M., (1991): ***Geochemical evolution in the Cambrian-Ordovician sandstone aquifer, Eastern Wisconsin: II. Correlation between flow paths and groundwater chemistry***. Ground Water, 29, 4, 510-515.

Weaver, J.M.C., Conrad, J.E. and Eskes, S.J.T., (1993): ***Valley calcretes: another Karoo ground water exploration target***. Proc. Convention: Africa needs ground water. Ground Water Division, GSSA, Univ. of the Witwatersrand, Johannesburg, Vol. I, Paper 8.

Weaver, J.M.C., Talma, A.S. and Cavé, L.C., (1996): ***Geochemistry and isotopes for resource evaluation in the fractured rock aquifers of the Table Mountain Group***. Report No. ENV/S-C96058. Council for Scientific and Industrial Research, Stellenbosch.

Wending, J., Fillion, E. and Trouillard, J.M., (1994): ***Geometrie de la fracturation et écoulements. Perméabilité et porosité directionnelles en milieu sédimentaire fracturé. Sites de Tabuk et Tayma (Arabie Saoudite)***. Report BRGM A 01865 (Orléans), 54.

White, R.S., (1997): ***Mantle plume origin for the Karoo and Ventersdorp flood basalts, South Africa***. S.Afr.J.Geol., 100 (4), 271 - 282.

Woodford, A.C., (1989): ***Preliminary evaluation of aquifer tests conducted in the South-Eastern / Burgerville areas, southeast of De Aar***. Department of Water Affairs & Forestry, Technical Report GH3645, Pretoria.

Woodford A.C. & Chevallier L., (1996): ***Regional characterisation and mapping of Karoo fractured aquifer systems - An integrated approach using a geographical information system and digital image processing***. Department of Water Affairs.

Woodford A.C. and Chevallier L., (1998): ***Regional characterisation and mapping of Karoo fractured aquifer systems - An integrated approach using a geographical information system and digital image processing***. Water Research Commission Project report K5/653 in preparation.

Woodford, A.C. and Chevallier L., (in press): ***Hydrogeology of the dolerite breccia-plugs of the Western Karoo***. SA Water. Unpublished report.

Woodford, A.C., Botha, J.F., Chevallier, L., Hartnady, C., Johnson, M., Meyer, R., Simoncic, M., van Tonder, G. and Verhagen, B. Th., (in press): ***Hydrogeology of the Main Karoo Basin: Current Knowledge and Research Needs***. WRC Report, Project 860.

Wright, A., (1994): ***Groundwater: The Cinderella of the South African water industry***. SAICE Journal, First Quarter, 1-5.

Zawada, P.K., Meuller, A., Greeff, G. & Test, Z., (1998): ***Trace elements as possible palaeosalinity indicators for the Ecca and Beaufort Group mudrocks in the southwestern Orange Free State***. S.-Afr. Tydskr. Geol., **91(1)**, 18-26.

Zoback, M.L. and Zoback, M.D., (1980): ***State of stress in the conterminous United States***. J. Geophys. Res., **V85**, 6113 - 6156.

Zoback, M.L., (1992): ***First- and second-order patterns of stress in the lithosphere: The World Stress Map Project***. J. geophys. Res., **V97**, 11702-11728.

## **APPENDIX A**

### **DATA TABLES**

LOXTON	BOREHOLE NR.	LATITUDE	LOGITUDE	TOPOGRAPHY	GEOLOGY	FRACTURE	H <sub>2</sub> O - LEVEL (m)	SAMPLE DEPTH (m)	H <sub>2</sub> O-TYPE
SITE 1	G39981	3146461	2234894	Slope	KIMBERLITE	KIMBERLITE	10.53	18	Cl and Na dominant
	G39982	3146378	2234911	Slope	KIMBERLITE	DRY/KIMBERLITE	12.33	50	Na - SO <sub>4</sub>
	G39984	3146475	2234914	Slope	KIMBERLITE	MUDSTONE/QUARTZ	10.18	60	Na-HCO <sub>3</sub>
	G39984	3146475	2234914	Slope	KIMBERLITE	MUDSTONE/QUARTZ	10.18	90	No Dominant +/-
	G39985	3146473	2234914	Slope	DOLERITE	DOLERITE/QUARTZ	10.07	60	Mg-HCO <sub>3</sub> and or Ca
	G39986	3146476	2234905	Slope	SANDSTONE	DRY/SANDSTONE	11.51	50	No Dominant +/-

LOXTON	BOREHOLE NR.	LATITUDE	LOGITUDE	TOPOGRAPHY	GEOLOGY	FRACTURE	H <sub>2</sub> O - LEVEL (m)	SAMPLE DEPTH (m)	H <sub>2</sub> O-TYPE
SITE 2	G39987	3166430	2211573	Flat	DOLERITE	DOLERITE/CALCITE/MUDSTONE	11.02	97	Cl and Na dominant
	G39988	3166170	2212011	Flat	DOLERITE	SAND-&MUDSTONE	8.91	121	Ca - SO <sub>4</sub>
	G39989	3166216	2212011	Flat	DOLERITE	SAND-&MUDSTONE/CALCITE	8.98	124	Na - SO <sub>4</sub>
	G39990	3166192	2212011	Flat	SANDSTONE	SAND-&MUDSTONE	8.98	148	Na - SO <sub>4</sub>
	G39991	3166228	2212011	Flat	DOLERITE	DOLERITE/MUDSTONE	8.98	180	Ca - SO <sub>4</sub>
	G39992	3166232	2212011	Flat	SANDSTONE	SAND-&MUDSTONE/CALCITE	9.11	93	Ca - SO <sub>4</sub>
	G39993	3166243	2212011	Flat	DOLERITE	DOLERITE/CALCITE/APOPHYLLITE	8.95	172	Ca - SO <sub>4</sub>
	G39994	3166258	2212011	Flat	MUDSTONE	MUDSTONE/CALCITE	9.04	194	Ca - SO <sub>4</sub>
	G39995	3166441	2211567	Flat	MUDSTONE	SAND,SILT-&MUDSTONE	9.84	50	Ca - SO <sub>4</sub>
	G40002	3166419	2211580	Flat	DOLERITE	MUDSTONE/PYRITE	10.79	187	Na - SO <sub>4</sub>
	G40004	3166203	2211456	Flat	DOLERITE	MUDSTONE	10.6	12	No Dominant +/-

LOXTON	BOREHOLE NR.	LATITUDE	LOGITUDE	TOPOGRAPHY	GEOLOGY	FRACTURE	H <sub>2</sub> O - LEVEL (m)	SAMPLE DEPTH (m)	H <sub>2</sub> O-TYPE
SITE 3	G39998	3165117	2235486	Riverbed	DOLERITE	DOLERITE/CALCITE	5.45	24	No Dominant +/-
	G39998	3165117	2235486	Riverbed	DOLERITE	DOLERITE/CALCITE/PYRITE	5.45	90	Na - SO <sub>4</sub>
	G39999	3165135	2235486	Riverbed	MUDSTONE	SAND-&MUDSTONE/CALCITE/PYRITE	5.35	61	No Dominant +/-
	G40000	3165094	2235486	Riverbed	MUDSTONE	MUDSTONE/CALCITE/SANDSTONE	5.68	57	Na - SO <sub>4</sub>
	G40001C	3165129	2235486	Riverbed	DOLERITE	DOLERITE/CALCITE/SANDSTONE	4.54	20	Na - SO <sub>4</sub>
	G40003	3165071	2235486	Riverbed	MUDSTONE	SAND-&MUDSTONE	4.79	46	Na - SO <sub>4</sub>
	G40005	3165292	2235319	Flat	DOLERITE	DOLERITE/CALCITE	9.47	50	No Dominant +/-
	G40006	3165292	2235306	Flat	MUDSTONE	SAND-&MUDSTONE	7.25	82	No Dominant +/-
	G40007	3165292	2235324	Flat	MUDSTONE	SAND-&MUDSTONE	9.06	54	No Dominant +/-
	G40008	3165292	2235344	Flat	MUDSTONE	MUDSTONE/CALCITE/PYRITE	8.8	184	No Dominant +/-
	G40009	3165117	2235250	Flat	MUDSTONE	SANDSTONE	8.8	23	No Dominant +/-
	G40009	3165117	2235250	Flat	MUDSTONE	SANDSTONE	8.8	60	No Dominant +/-

LOXTON	BOREHOLE NR.	LATITUDE	LOGITUDE	TOPOGRAPHY	GEOLOGY	FRACTURE	H <sub>2</sub> O - LEVEL (m)	SAMPLE DEPTH (m)	H <sub>2</sub> O-TYPE
SITE 4	G39996	3155769	2226681	Flat	KIMBERLITE	KIMBERLITE/CALCITE	20.55	59	Na - SO <sub>4</sub>
	G39997	3155763	2226703	Flat	KIMBERLITE	SAND-&MUDSTONE	19.36	59	No Dominant +/-
	G39997	3155763	2226703	Flat	MUDSTONE	SAND-&MUDSTONE	19.36	93	No Dominant +/-

LOXTON	BOREHOLE NR.	LATITUDE	LOGITUDE	TOPOGRAPHY	GEOLOGY	FRACTURE	H <sub>2</sub> O - LEVEL (m)	SAMPLE DEPTH (m)	H <sub>2</sub> O-TYPE
SITE 5	G40010	3142111	2253419	Flat	MUDSTONE	SANDSTONE	11.43	95	Na-HCO <sub>3</sub>
	G40011	3142111	2253427	Flat	MUDSTONE	SANDSTONE/CALCITE	11.51	68	No Dominant +/-
	G40011	3142111	2253427	Flat	MUDSTONE	MUDSTONE/CALCITE	11.51	90	Na - SO <sub>4</sub>
	G40012	3142110	2253438	Flat	DOLERITE	DOLERITE/CALCITE	12.88	67	Na - SO <sub>4</sub>

LOXTON	BOREHOLE NR.	LATITUDE	LOGITUDE	TOPOGRAPHY	GEOLOGY	FRACTURE	H <sub>2</sub> O - LEVEL (m)	SAMPLE DEPTH (m)	H <sub>2</sub> O-TYPE
SITE 6	G40013	3143078	2271316	Slope	DOLERITE	DOLERITE/CALCITE	16.16	21	Na-HCO <sub>3</sub>
	G40014	3143076	2271315	Slope	DOLERITE	DOLERITE	16.3	32	Na-HCO <sub>3</sub>
	G40015	3142956	2271260	Slope	MUDSTONE	SANDSTONE	12.37	23	Na-HCO <sub>3</sub>
	G40016	3142960	2271255	Slope	DOLERITE	DOLERITE/CALCITE	11.7	27	Na - SO <sub>4</sub>
	G40017	3142974	2271245	Slope	MUDSTONE	MUDSTONE/CALCITE/PYRITE	11.39	19	Na-HCO <sub>3</sub>
	G40018	3143081	2271319	Slope	DOLERITE	SAND-&MUDSTONE	16.27	90	Cl and Na dominant
	G40019	3143066	2271347	Slope	DOLERITE	DOLERITE/CALCITE	16.95	25	Na-HCO <sub>3</sub>
	G40020	3143064	2271347	Terrace	DOLERITE	SANDSTONE/CALCITE/PYRITE	17.24	47	Na-HCO <sub>3</sub>
	G40020	3143064	2271347	Terrace	DOLERITE	DOLERITE/CALCITE	17.24	90	Na - SO <sub>4</sub>

LOXTON	BOREHOLE NR.	H <sub>2</sub> O-TYPE	BOREHOLE LOCATION	DISCUSSION
SITE 1	G39981	Cl and Na dominant	On Kimberlite (up-slope)	Na from pyroxene, melillite, perovskite and zeolites - Indicates an end point water in a evolution sequence
	G39982	Na - SO <sub>4</sub>	70 m - On Kimberlite (up-slope)	Na from pyroxene, melillite, perovskite and zeolites - Water due to mixing influences
	G39984	Na-HCO <sub>3</sub>	63 m - On Dolerite	Na from pyroxene, biotite and plagioclase - Ion exchanged water (Same water as at 90m)
	G39984	No Dominant +/-	63 m - On Dolerite	Water associated with dissolution or mixing (Same water as at 60m)
	G39985	Mg-HCO <sub>3</sub> and or Ca	63-1.6 m - On Dolerite	Ca from pyroxene, plagioclase and biotite & Mg from pyroxene, magnetite, biotite and olivine - Water associated with mafic igneous rocks
	G39986	No Dominant +/-	70 m - Kimberlite left side (up-slope)	Water resulting from dissolution or mixing

LOXTON	BOREHOLE NR.	H <sub>2</sub> O-TYPE	BOREHOLE LOCATION	DISCUSSION
SITE 2	G39987	Cl and Na dominant	On Displacement	Na from pyroxene, biotite and plagioclase - End pointwater in a evolution sequence
	G39988	Ca - SO <sub>4</sub>	On Dolerite (up-slope)	Ca from feldspars, plagioclase, calcite, pyroxene and biotite - Recharged water in lavas
	G39989	Na - SO <sub>4</sub>	On Dolerite (up-slope)	Na from feldspars, plagioclase, pyroxene and biotite - Water due to mixing influences
	G39990	Na - SO <sub>4</sub>	Dolerite top side (up-slope)	Na from feldspars, plagioclase and biotite - Water due to mixing influences
	G39991	Ca - SO <sub>4</sub>	Dolerite bottom side (up-slope)	Ca from calcite, pyroxene and biotite - Recharged water in lavas
	G39992	Ca - SO <sub>4</sub>	Dolerite bottom side (up-slope)	Ca from feldspars, plagioclase and calcite - Recharged water in lavas
	G39993	Ca - SO <sub>4</sub>	Dolerite bottom side (up-slope)	Ca from calcite, pyroxene, biotite and apophyllite - Recharged water in lavas
	G39994	Ca - SO <sub>4</sub>	Dolerite bottom side (up-slope)	Ca from feldspars, plagioclase and calcite - Recharged water in lavas
	G39995	Ca - SO <sub>4</sub>	Displacement left side	Ca from feldspars, plagioclase and calcite - Recharged water in lavas
	G40002	Na - SO <sub>4</sub>	Side of Displacement and Dolerite	Na from pyroxene, plagioclase and biotite - Water due to mixing influences
	G40004	No Dominant +/-	Side of Displacement and Dolerite	Water resulting from dissolution or mixing

LOXTON	BOREHOLE NR.	H <sub>2</sub> O-TYPE	BOREHOLE LOCATION	DISCUSSION
SITE 3	G39998	No Dominant +/-	On Dolerite Dyke	Water resulting from dissolution or mixing
	G39998	Na - SO <sub>4</sub>	On Dolerite Dyke	Na from pyroxene, plagioclase and biotite - Water due to mixing influences
	G39999	No Dominant +/-	193 m - Lower side of Dolerite (up-slope)	Water resulting from dissolution or mixing
	G40000	Na - SO <sub>4</sub>	193 m - Upper side of Dolerite	Na from biotite, feldspars and plagioclase - Water due to mixing
	G40001C	Na - SO <sub>4</sub>	On Dolerite Dyke	Na from biotite, feldspars, plagioclase and pyroxene - Water due to mixing
	G40003	Na - SO <sub>4</sub>	194 m - Top side of Dolerite	Na from biotite, feldspars and plagioclase - Water due to mixing
	G40005	No Dominant +/-	136 m - On Displacement (up-slope)	Water resulting from dissolution or mixing
	G40006	No Dominant +/-	136 m - Left side of Displacement (up-slope)	Water resulting from dissolution or mixing
	G40007	No Dominant +/-	136 m - Right side of Displacement (up-slope)	Water resulting from dissolution or mixing
	G40008	No Dominant +/-	136 m - Right side of Displacement	Water resulting from dissolution or mixing
	G40009	No Dominant +/-	Side of Displacement and Dyke	Water resulting from dissolution or mixing
	G40009	No Dominant +/-	Side of Displacement and Dyke	Water resulting from dissolution or mixing

LOXTON	BOREHOLE NR.	H <sub>2</sub> O-TYPE	BOREHOLE LOCATION	DISCUSSION
SITE 4	G39996	Na - SO <sub>4</sub>	On Kimberlite	Na from pyroxene, melillite, perovskite and zeolites - Water due to mixing influences
	G39997	No Dominant +/-	25 m - Right of Kimberlite in Mega Joint	Water resulting from dissolution or mixing (Same water as at 93m)
	G39997	No Dominant +/-	26 m - Right of Kimberlite in Mega Joint	Water resulting from dissolution or mixing (Same water as at 59m)

LOXTON	BOREHOLE NR.	H <sub>2</sub> O-TYPE	BOREHOLE LOCATION	DISCUSSION
SITE 5	G40010	Na-HCO <sub>3</sub>	Left side of Dolerite Dyke (up-slope)	Na from biotite, plagioclase and feldspars - Ion exchanged water
	G40011	No Dominant +/-	On Dolerite Dyke	Water resulting from dissolution or mixing
	G40011	Na - SO <sub>4</sub>	On Dolerite Dyke	Na from biotite, pyroxene and plagioclase - Water due to mixing
	G40012	Na - SO <sub>4</sub>	Right side of Dolerite Dyke	Na from biotite, pyroxene and plagioclase - Water due to mixing

LOXTON	BOREHOLE NR.	H <sub>2</sub> O-TYPE	BOREHOLE LOCATION	DISCUSSION
SITE 6	G40013	Na-HCO <sub>3</sub>	On 6 m - wide Dolerite Dyke	Na from pyroxene, biotite and plagioclase - Ion exchanged water
	G40014	Na-HCO <sub>3</sub>	Upper side of 6 m - wide Dolerite Dyke	Na from pyroxene, biotite and plagioclase - Ion exchanged water
	G40015	Na-HCO <sub>3</sub>	On 16 m - wide Dolerite Sill	Na from feldspars, biotite and plagioclase - Ion exchanged water
	G40016	Na - SO <sub>4</sub>	On 16 m - wide Dolerite Sill	Na from pyroxene, biotite and plagioclase - Water due to mixing influences
	G40017	Na-HCO <sub>3</sub>	Side of 16 m - wide Dolerite Sill	Na from biotite, feldspars and plagioclase in sandstone - Ion exchanged water
	G40018	Cl and Na dominant	On 6 m - wide Dolerite Dyke (up-slope)	Na from biotite, feldspars, plagioclase and pyroxene - End point water in a evolution sequence
	G40019	Na-HCO <sub>3</sub>	Side of both Dolerite Structures	Na from pyroxene, biotite and plagioclase - Ion exchanged water
	G40020	Na-HCO <sub>3</sub>	Side of both Dolerite Structures	Na from biotite, plagioclase, feldspars and pyroxene - Ion exchanged water
G40020	Na - SO <sub>4</sub>	Side of both Dolerite Structures	Na from pyroxene, biotite and plagioclase - Water due to mixing influences	

LOXTON	BOREHOLE NR.	H <sub>2</sub> O-TYPE	TOPOGRAPHY	SAMPLE DEPTH (m)	ISOTOPE AND <sup>14</sup> C - DISCUSSION
SITE 1	G39981	Cl and Na dominant	Slope	18	Indicates an end point water in a evolution sequence - Other Recharge Mechanism - <b>Century</b>
	G39982	Na - SO <sub>4</sub>	Slope	50	Water due to mixing influences
	G39984	Na-HCO <sub>3</sub>	Slope	60	Ion exchanged water - Other Recharge Mechanism - <b>Decade</b>
	G39984	No Dominant +/-	Slope	90	Water associated with dissolution or mixing - Other Recharge Mechanism
	G39985	Mg-HCO <sub>3</sub> and or Ca	Slope	60	Water associated with mafic igneous rocks - Other Recharge Mechanism
	G39986	No Dominant +/-	Slope	50	Water resulting from dissolution or mixing

LOXTON	BOREHOLE NR.	H <sub>2</sub> O-TYPE	TOPOGRAPHY	SAMPLE DEPTH (m)	ISOTOPE AND <sup>14</sup> C - DISCUSSION
SITE 2	G39987	Cl and Na dominant	Flat	97	End point water in a evolution sequence - Intense Evaporation
	G39988	Ca - SO <sub>4</sub>	Flat	121	Recharged water in lavas
	G39989	Na - SO <sub>4</sub>	Flat	124	Water due to mixing influences - Intense Evaporation
	G39990	Na - SO <sub>4</sub>	Flat	148	Water due to mixing influences - Intense Evaporation
	G39991	Ca - SO <sub>4</sub>	Flat	180	Recharged water in lavas
	G39992	Ca - SO <sub>4</sub>	Flat	93	Recharged water in lavas - Intense Evaporation - <b>Century</b>
	G39993	Ca - SO <sub>4</sub>	Flat	172	Recharged water in lavas
	G39994	Ca - SO <sub>4</sub>	Flat	194	Recharged water in lavas
	G39995	Ca - SO <sub>4</sub>	Flat	50	Recharged water in lavas
	G40002	Na - SO <sub>4</sub>	Flat	187	Water due to mixing influences
	G40004	No Dominant +/-	Flat	12	Water resulting from dissolution or mixing - Other Recharge Mechanism

LOXTON	BOREHOLE NR.	H <sub>2</sub> O-TYPE	TOPOGRAPHY	SAMPLE DEPTH (m)	ISOTOPE AND <sup>14</sup> C - DISCUSSION
SITE 3	G39998	No Dominant +/-	Riverbed	24	Water resulting from dissolution or mixing - Other Recharge Mechanism - <b>Decade</b>
	G39998	Na - SO <sub>4</sub>	Riverbed	90	Water due to mixing influences - Other Recharge Mechanism - <b>Decade</b>
	G39999	No Dominant +/-	Riverbed	61	Water resulting from dissolution or mixing - Other Recharge Mechanism
	G40000	Na - SO <sub>4</sub>	Riverbed	57	Water due to mixing - Other Recharge Mechanism
	G40001C	Na - SO <sub>4</sub>	Riverbed	20	Water due to mixing
	G40003	Na - SO <sub>4</sub>	Riverbed	46	Water due to mixing
	G40005	No Dominant +/-	Flat	50	Water resulting from dissolution or mixing - Intense Evaporation
	G40006	No Dominant +/-	Flat	82	Water resulting from dissolution or mixing - Intense Evaporation
	G40007	No Dominant +/-	Flat	54	Water resulting from dissolution or mixing - Intense Evaporation
	G40008	No Dominant +/-	Flat	184	Water resulting from dissolution or mixing
	G40009	No Dominant +/-	Flat	23	Water resulting from dissolution or mixing - Direct Recharge - <b>Decade</b>
	G40009	No Dominant +/-	Flat	60	Water resulting from dissolution or mixing - Intense Evaporation - <b>Decade</b>

LOXTON	BOREHOLE NR.	H <sub>2</sub> O-TYPE	TOPOGRAPHY	SAMPLE DEPTH (m)	ISOTOPE AND <sup>14</sup> C - DISCUSSION
SITE 4	G39996	Na - SO <sub>4</sub>	Flat	59	Water due to mixing - Intense Evaporation
	G39997	No Dominant +/-	Flat	59	Water resulting from dissolution or mixing - Intense Evaporation - <b>Decade</b>
	G39997	No Dominant +/-	Flat	93	Water resulting from dissolution or mixing - Intense Evaporation - <b>Decade</b>

LOXTON	BOREHOLE NR.	H <sub>2</sub> O-TYPE	TOPOGRAPHY	SAMPLE DEPTH (m)	ISOTOPE AND <sup>14</sup> C - DISCUSSION
SITE 5	G40010	Na-HCO <sub>3</sub>	Flat	95	Ion exchanged water - Intense Evaporation
	G40011	No Dominant +/-	Flat	68	Water resulting from dissolution or mixing - Intense Evaporation - <b>Century</b>
	G40011	Na - SO <sub>4</sub>	Flat	90	Water due to mixing - Intense Evaporation - <b>Century</b>
	G40012	Na - SO <sub>4</sub>	Flat	67	Water due to mixing - Intense Evaporation

LOXTON	BOREHOLE NR.	H <sub>2</sub> O-TYPE	TOPOGRAPHY	SAMPLE DEPTH (m)	ISOTOPE AND <sup>14</sup> C - DISCUSSION
SITE 6	G40013	Na-HCO <sub>3</sub>	Slope	21	Ion exchanged water - Intense Evaporation
	G40014	Na-HCO <sub>3</sub>	Slope	32	Ion exchanged water
	G40015	Na-HCO <sub>3</sub>	Slope	23	Ion exchanged water - Intense Evaporation
	G40016	Na - SO <sub>4</sub>	Slope	27	Water due to mixing influences - Intense Evaporation - <b>Century</b>
	G40017	Na-HCO <sub>3</sub>	Slope	19	Ion exchanged water - Intense Evaporation
	G40018	Cl and Na dominant	Slope	90	End point water in a evolution sequence - Intense Evaporation - <b>Century</b>
	G40019	Na-HCO <sub>3</sub>	Slope	25	Ion exchanged water - Intense Evaporation
	G40020	Na-HCO <sub>3</sub>	Terrace	47	Ion exchanged water - Intense Evaporation - <b>Century</b>
	G40020	Na - SO <sub>4</sub>	Terrace	90	Water due to mixing influences - Intense Evaporation - <b>Century</b>

## **APPENDIX B**

### **CHEMICAL ANALYSES**

## HBASE GROUNDWATER CHEMICAL ANALYSIS FOR LOXTON

Borehole Nr.	Date	Time	Depth m	Al mg/L	NH4-N mg/L	Sb mg/L	As mg/L	Ba mg/L	HCO3 mg/L	B mg/L	Cd mg/L
G39981	20000107	10h00	18	0.01	0.033	0.009		0.01	45	0.02	
G39982	20000109	10h00	50	0.01	0.605	0.024	0.002	0.05	43	0.536	
G39984	20000108	10h00	60		0.023	0.001	0.048	0.002	290	0.845	
G39984	20000108	11h00	90	0.01	0.012	0.029	0.047	0.001	256	0.135	
G39985	20000109	10h00	60	0.01		0.048		0.001	279	0.106	
G39986	20000109	10h00	50			0.047		0.016	186	0.109	
G39987	20000110	10h00	97	0.08	0.095	0.042		0.006	46	0.627	0.001
G39988	20000110	10h00	121	0.1		0.038		0.001	139	1.396	0.001
G39989	20000110	10h00	124	0.01		0.055	0.074	0.001	69	1.283	
G39990	20000110	10h00	148	0.16	0.325	0.049	0.042	0.002	42	1.081	
G39991	20000110	10h00	180		0.057	0.035	0.029	0.004	143	1.612	
G39992	20000111	10h00	93		0.027	0.033	0.061	0.015	232	1.455	
G39993	20000110	10h00	172	0.07	0.023	0.047	0.107	0.003	167	0.842	
G39994	20000110	10h00	194	0.19	0.057	0.082		0.005	89	1.258	
G39995	20000110	10h00	50		0.123	0.009		0.005	40	1.64	
G39996	20000110	10h00	59	0.27	0.016	0.003	0.055	0.022	349	1.368	0.002
G39997	20000111	10h00	59		0.017			0.023	395	0.544	
G39997	20000111	11h00	93		0.016			0.029	390	0.337	0.001
G39998	20000113	10h00	24	0.17	0.020	0.003		0.009	461	0.316	0.001
G39998	20000113	11h00	90	0.01	0.029		0.026	0.007	417	0.464	
G39999	20000112	10h00	61		0.012			0.009	232	0.521	
G40000	20000112	11h00	57	0.29	0.083			0.009	487	0.405	
G40001C	20000112	10h00	20		0.364		0.091	0.008	510	0.478	
G40002	20000110	10h00	187	0.11	0.027	0.011	0.022	0.015	162	0.442	
G40003	20000112	10h00	46	0.07	0.019	0.004	0.081	0.011	162	0.921	
G40004	20000111	10h00	12	0.12	0.016	0.031	0.072	0.023	432	0.964	
G40005	20000113	10h00	50	0.12	0.013	0.002	0.005	0.007	320	0.212	
G40006	20000112	10h00	82	0.01	0.008	0.008	0.046	0.013	335	0.217	
G40007	20000112	10h00	54	0.1			0.035	0.013	394	0.126	
G40008	20000112	10h00	184					0.021	441	0.325	0.001
G40009	20000113	10h00	23	0.11	0.009		0.05	0.012	302	0.381	
G40009	20000113	11h00	60	0.22	0.020	0.024	0.064	0.012	228	0.662	
G40010	20000114	10h00	95	0.05			0.041	0.007	303	0.884	
G40011	20000118	10h00	68	0.02			0.062	0.001	139	0.522	
G40011	20000118	11h00	90	0.08			0.052		116	0.674	
G40012	20000114	10h00	67	0.14			0.027		162	0.736	
G40013	20000114	10h00	21				0.067	0.003	279	0.751	
G40014	20000114	10h00	32	0.15			0.076	0.007	256	0.497	
G40015	20000114	10h00	23	0.09	0.023		0.001	0.01	281	0.464	
G40016	20000117	10h00	27		0.064	0.008	0.055	0.002	279	0.406	
G40017	20000114	11h00	19	0.2	0.056			0.013	274	0.459	
G40018	20000117	10h00	90	0.05				0.003	186	0.517	
G40019	20000114	10h00	25	0.13	0.017	0.015	0.07	0.012	279	1.17	
G40020	20000115	10h00	47	0.08			0.013	0.005	285	0.649	
G40020	20000115	11h00	90	0.12			0.015	0.005	210	0.517	
R 1	20000117	11h00	1	0.08			0.062	0.005	28	0.807	

**HBASE GROUNDWATER CHEMICAL ANALYSIS FOR LOXTON**

Borehole Nr.	Ca mg/L	CaHard mg/L	CO3 mg/L	Cl mg/L	Cr mg/L	Co mg/L	Cu mg/L	EC mS/m	F mg/L	Ion-bal %	Fe mg/L	Langel. mg/L
G39981	13	32	2	169		0.015		43	0.2	-3.11	0.02	0.07
G39982	8	20	2	80	0.006		0.011	38.1		2.77	0.02	-0.18
G39984	60	150		55	0.005		0.008	62.8	0.4	4.74	0.03	-0.02
G39984	59	147		54	0.008		0.009	62.9	0.5	-4.45	0.03	-0.08
G39985	60	150		54	0.004		0.009	63.7	1	-4.78	0.02	-0.03
G39986	60	150		71	0.008		0.011	62	0.6	1.82	0.09	-0.19
G39987	64	160		160	0.004		0.011	298	1.9	-0.77	0.02	-2
G39988	586	1463		117	0.015		0.011	161.8	1.2	-3.57	0.03	-0.11
G39989	205	512		135	0.011		0.007	146.1	1.5	-1.8	0.03	-0.17
G39990	191	477	2	110	0.006		0.01	316	1.8	-1.49	0.03	0.93
G39991	506	1263		216	0.005		0.01	286	1.9	4.74	0.03	-0.1
G39992	505	1261		98	0.008		0.01	139.9	1.3	-2.98	0.02	0.38
G39993	443	1106		115	0.009		0.008	150.3	2	2.01	0.02	0.33
G39994	350	874		89	0.012	0.005	0.009	199.3	1.4	-0.43	0.03	-0.46
G39995	679	1695	3	125	0.01		0.007	305	1.1	-3.46	0.03	1.56
G39996	32	80	3	223	0.01		0.012	105.3	0.1	-4.05	0.06	0.39
G39997	106	265		178	0.004		0.011	127.1	0.8	4.6	0.02	-0.01
G39997	112	280		171	0.007		0.009	127.4	0.8	-4.12	0.02	0.01
G39998	110	275	1	250	0.006		0.009	162.2	0.6	-1.09	0.02	0.24
G39998	106	265	1	251	0.006		0.013	166.9	0.7	-0.27	0.03	0.17
G39999	119	297		241	0.01		0.009	161.6	0.8	4.85	0.02	-0.02
G40000	68	170	1	255	0.006		0.015	166.7	0.7	-0.84	0.02	0.04
G40001C	72	180	1	242	0.015		0.011	159.7	0.5	-2.46	0.02	0.08
G40002	91	227		267	0.006		0.01	146.8	1.4	1.06	0.03	-0.48
G40003	96	240		196	0.07		0.009	134.8	0.9	-0.74	0.04	-0.43
G40004	132	330	1	134	0.006		0.01	115	0.8	-3.85	0.02	0.4
G40005	107	267		77	0.013		0.01	92.8	0.5	-1.61	0.02	-0.06
G40006	106	265		89	0.002			84.9	0.5	-3.16	0.03	0.05
G40007	102	255		196	0.009	0.004	0.009	137.1	0.7	3.39	0.02	0.18
G40008	102	255	1	215	0.005		0.003	158.1	0.5	-3.18	0.03	0.19
G40009	134	335		196	0.007		0.007	134.1	0.9	-0.65	0.02	-0.04
G40009	155	387		187	0.006		0.012	141.6	0.9	-1.79	0.03	0.08
G40010	41	102		54	0.005		0.013	49.1	1.5	3.78	0.02	-0.37
G40011	41	102		71	0.003		0.003	43.1	1.8	-0.38	0.03	-0.66
G40011	24	60		62	0.008		0.011	35.5	2.2	1.05	0.05	-0.76
G40012	22	55		98	0.007		0.011	60.7	1.3	-4.96	0.04	-1.07
G40013	36	90		98	0.008		0.011	65.7	1.1	-0.8	0.04	-0.54
G40014	30	75		100	0.005		0.008	62.7	0.7	0.69	0.02	-0.55
G40015	51	127		116	0.002		0.003	80.6	0.7	3.36	0.02	-0.3
G40016	51	127		143	0.006		0.013	84.2	0.6	-1.97	0.02	-0.21
G40017	46	115		147	0.008		0.005	63.1	0.3	-2.84	0.08	-0.46
G40018	32	80		125	0.002		0.014	64.2	1.7	-1.05	0.02	-0.55
G40019	41	102		100	0.004		0.014	65.4	0.7	-1.2	0.03	-0.49
G40020	41	102		116	0.004		0.01	65.1	1.3	-4.84	0.05	-0.28
G40020	30	75		117	0.01		0.011	63.5	1.8	-4.39	0.05	-0.63
R 1	2	5		87	0.002		0.013	2.3		-2.96	0.03	

## HBASE GROUNDWATER CHEMICAL ANALYSIS FOR LOXTON

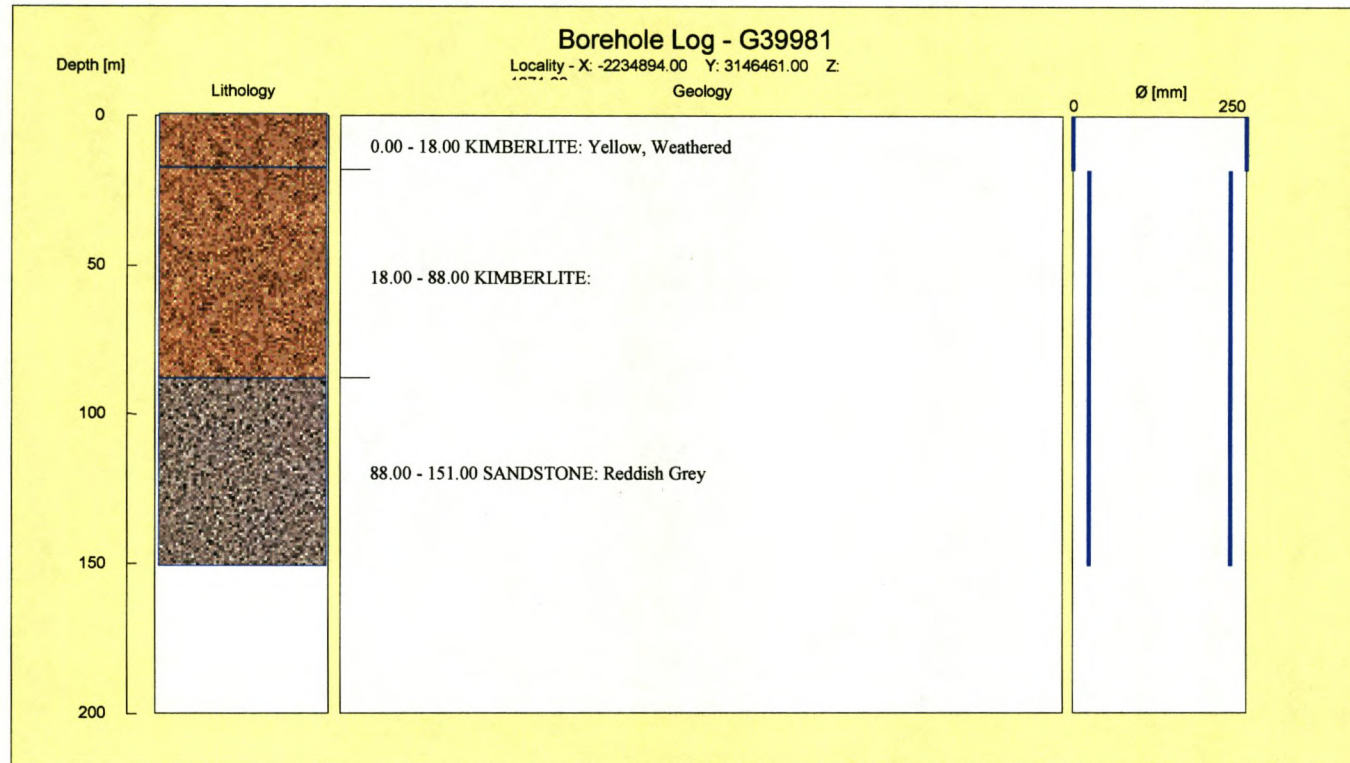
Borehole Nr.	Pb mg/L	Li mg/L	Mg mg/L	MgHard mg/L	Mn mg/L	Mo mg/L	Ni mg/L	NO3-N mg/L	pH mg/L	P.AIk mg/L	PO4 mg/L	K mg/L
G39981		0.005	1	4	0.011			0.003	8.8	9	0.132	16.4
G39982		0.116	7	29	0.018	0.048	0.219	0.016	8.8	9		8.2
G39984	0.011	0.047	10	41		0.046		0.024	7.3		0.061	33.7
G39984		0.059	32	132		0.054	0.004	0.226	7.3			1.2
G39985		0.06	31	128		0.148	0.005	0.025	7.3		0.043	5.3
G39986	0.039	0.37	31	128		0.046	0.017		7.3		0.043	5.9
G39987	0.066	0.996	2	8		0.035	0.007	0.003	6.1		0.068	8
G39988	0.056	0.496	3	12	0.002	0.07	0.012	0.007	6.8		0.074	8.6
G39989	0.031	0.466	3	12	0.002	0.065			7.4		0.095	22.9
G39990	0.084	0.943	1	4		0.07	0.011	0.002	8.7		0.126	22.9
G39991	0.015	0.746	1	4	0.008	0.06			6.8		0.157	1.4
G39992	0.037	0.35	14	58	0.028	0.044	0.023		7.1		0.025	17.6
G39993	0.021	0.297	14	58	0.033	0.033	0.008		7.2			4.1
G39994	0.01	0.755	5	21	0.016	0.072			6.8			10.3
G39995	0.013	0.586	3	12		0.06	0.013		8.9		0.166	8.8
G39996		0.695	14	58		0.044	0.026	0.043	8	58	0.150	17.2
G39997	0.023	0.154	59	243	0.152	0.066	0.012	0.186	7		0.061	13.8
G39997		0.161	58	239	0.14	0.029	0.003	0.188	7		0.175	5.2
G39998	0.008	0.163	62	255	0.131	0.054	0.001	0.025	7.2		0.052	5.2
G39998	0.034	0.251	62	255	0.181	0.01	0.011		7.2			5.2
G39999	0.046	0.189	75	309		0.074		0.193	7.2			14.7
G40000	0.034	0.197	77	317		0.049	0.018	0.080	7.2			14.7
G40001C		0.199	77	317		0.043	0.01	0.092	7.2		0.003	5.8
G40002	0.029	1.021	52	214	0.043	0.047			7		0.064	4.5
G40003	0.034	0.467	17	70		0.042	0.016	0.003	7			2.4
G40004	0.018	0.145	55	226	0.093	0.038	0.01	0.628	7.3			8.2
G40005	0.023	0.214	36	148		0.07	0.003	0.005	7		0.012	3.8
G40006		0.168	42	173		0.041	0.009	0.113	7.1		0.123	7.5
G40007	0.031	0.211	56	231		0.117	0.014	0.017	7.2		0.080	14.3
G40008		0.207	66	272		0.023	0.008	0.318	7.2		0.104	14.3
G40009		0.356	31	128	0.011	0.058		0.013	7			3.2
G40009		0.454	32	132		0.044	0.007	0.005	7.2		0.154	1.9
G40010	0.002	0.07	10	41		0.037		0.793	7.1		0.034	1.2
G40011		0.372	10	41		0.036	0.009	0.004	7.1		0.089	0.6
G40011		0.445	5	21		0.042	0.004		7.3		0.040	0.9
G40012		0.545	1	4		0.038	0.021		6.9			21.1
G40013	0.028	0.268	8	33		0.026	0.014		7			21.1
G40014		0.236	16	66		0.026	0.001		7.1		0.028	0.9
G40015	0.016	0.24	19	78		0.039	0.008	0.015	7.1			1.5
G40016		0.311	12	49	0.002	0.046	0.014		7.2			1.2
G40017		0.314	8	33		0.023	0.011	0.005	7		0.003	1.7
G40018		0.273	9	37		0.032	0.006		7.2			0.6
G40019	0.036	0.311	20	82		0.024	0.008		7		0.064	1.2
G40020	0.005	0.159	20	82		0.015			7.2		0.034	1.9
G40020	0.019	0.251	12	49		0.01	0.002		7.1			1.4
R 1		0.27	1	4	0.02	0.03	0.004	0.190	6.2			1.7

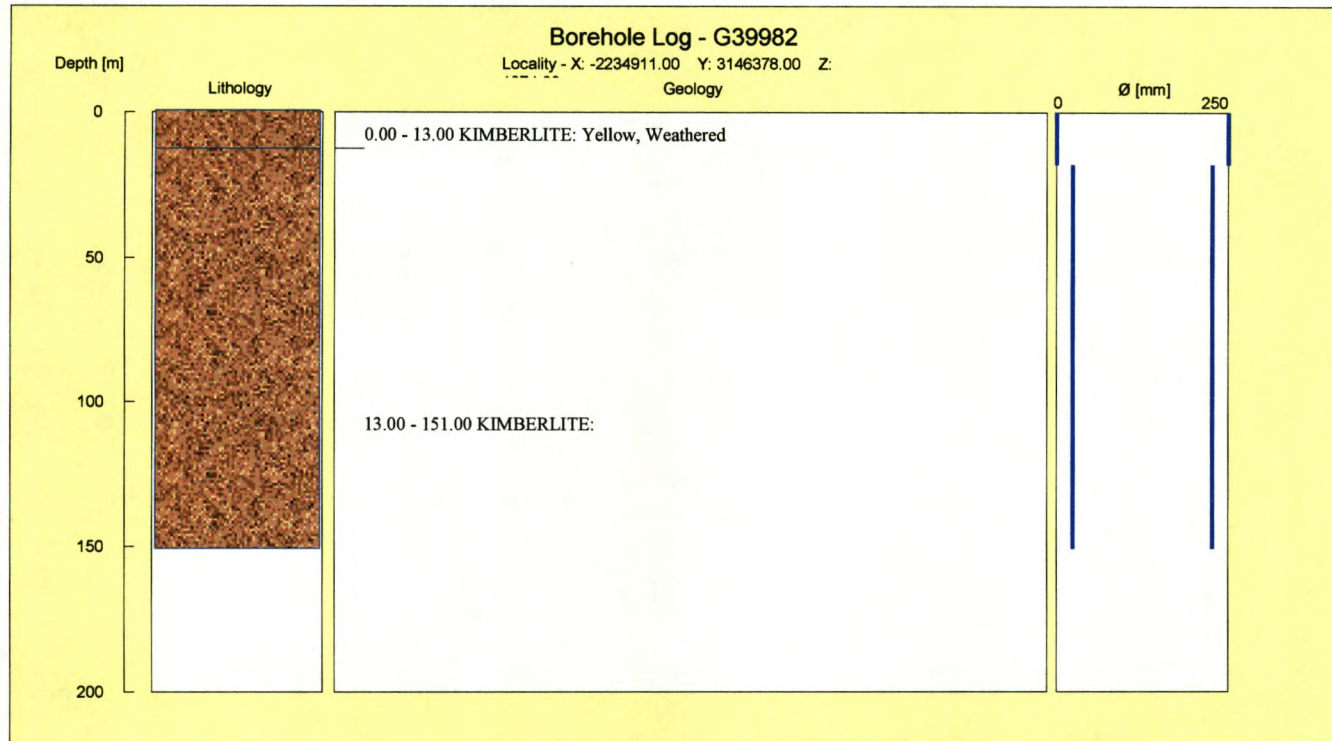
**HBASE GROUNDWATER CHEMICAL ANALYSIS FOR LOXTON**

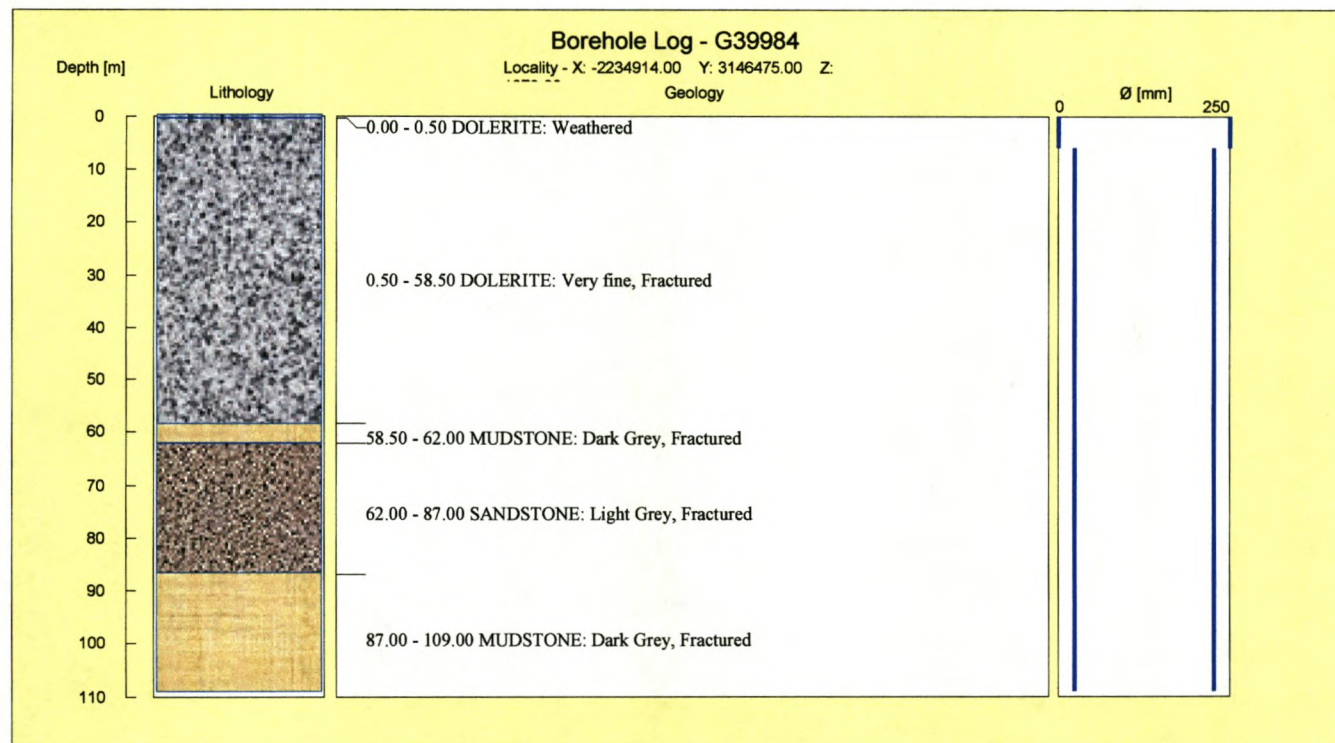
Borehole Nr.	Se mg/L	Si mg/L	Na mg/L	Sr mg/L	S mg/L	SO4 mg/L	T.Alk mg/L	TDS(EC)	U mg/L	V mg/L	Zn mg/L
G39981	0.006	0.1	94	0.021	0.05		40	301		0.001	0.941
G39982	0.215	2.6	86	1.032	26.46	79	38	267	0.077	0.014	
G39984	0.086	0.1	93	0.869	25.75	77	238	440	0.038	0.024	
G39984	0.047	6.9	54	0.965	47.13	141	210	440		0.018	
G39985		6	48	0.904	38.5	115	229	446		0.021	
G39986	0.053	5.9	49	0.764	39.49	118	153	434		0.025	
G39987		3.6	123	7.629	58.98	177	38	2086		0.017	
G39988	0.115	2	357	2.146	688.79	2063	114	1133		0.027	0.001
G39989		3.1	347	2.656	354.4	1061	57	1023		0.013	
G39990		2.4	347	10.718	354.44	1062	38	2212	0.001	0.017	
G39991		1.9	252	8.005	393.12	1177	117	2002		0.013	1.085
G39992	0.06	2.1	300	3.921	571.6	1712	191	979		0.012	
G39993		3.9	182	3.341	384.41	1151	137	1052		0.014	
G39994	0.082	3.1	341	7.186	468.77	1404	73	1395		0.014	
G39995		1.9	345	6.33	778.48	2332	38	2135		0.015	
G39996	0.068	2	345	8.664	122.41	367	291	737		0.013	
G39997	0.034	4.5	159	3.873	69.36	208	324	890	0.022	0.017	0.006
G39997		3.1	112	4.006	86.67	260	320	892	0.029	0.009	0.004
G39998	0.103	3.1	199	2.941	82.96	248	379	1135		0.022	
G39998	0.109	2.8	255	3.463	124.65	373	343	1168		0.016	
G39999		2.9	207	2.236	141.6	424	191	1131		0.023	
G40000	0.048	2.9	265	1.197	108.85	326	400	1167	0.039	0.025	
G40001C		3.3	265	1.461	119.67	358	419	1118		0.027	
G40002	0.012	2.9	205	2.06	116.02	347	133	1028		0.017	
G40003	0.035	2.9	188	3.81	102.69	308	133	944	0.095	0.022	0.004
G40004	0.008	3.7	150	1.475	133.49	400	355	805		0.012	0.033
G40005		4.1	77	1.957	75.04	225	263	650		0.015	
G40006	0.02	2.7	75	1.196	79.59	238	275	594		0.02	
G40007		2.6	137	1.832	47.21	141	324	960		0.012	
G40008		2.9	190	1.87	113.07	339	362	1107		0.008	
G40009		3	190	3.313	116.78	350	248	939		0.021	
G40009	0.016	3.4	198	4.132	171.35	513	187	991	0.034	0.012	
G40010		3.4	150	0.6	33.68	101	249	344		0.029	
G40011	0.009	3.3	62	0.391	19.88	60	114	302	0.044	0.029	
G40011	0.069	2.8	80	0.242	20.08	60	95	249		0.017	
G40012		2.2	91	0.041	12.53	38	133	425	0.051	0.028	
G40013	0.053	2.4	100	1.034	1.08	3	229	460		0.017	
G40014		2.9	100	0.672	0.5	2	210	439	0.049	0.025	
G40015	0.071	18.3	102	1.171	1.71	5	231	564		0.016	
G40016	0.056	3.1	122	1.303	9.31	28	229	589		0.025	
G40017	0.033	3.3	122	1.329	2.41	7	225	442		0.018	
G40018	0.009	2.5	97	1.199	0.58	2	153	449		0.021	
G40019	0.039	2.8	97	0.75	11.31	34	229	458		0.019	
G40020	0.023	4.2	89	0.653	6.16	18	234	456		0.023	
G40020		3.4	91	0.658	3.9	12	172	445		0.014	
R 1	0.012	3.2	68	0.615	7.42	22	23	16		0.013	

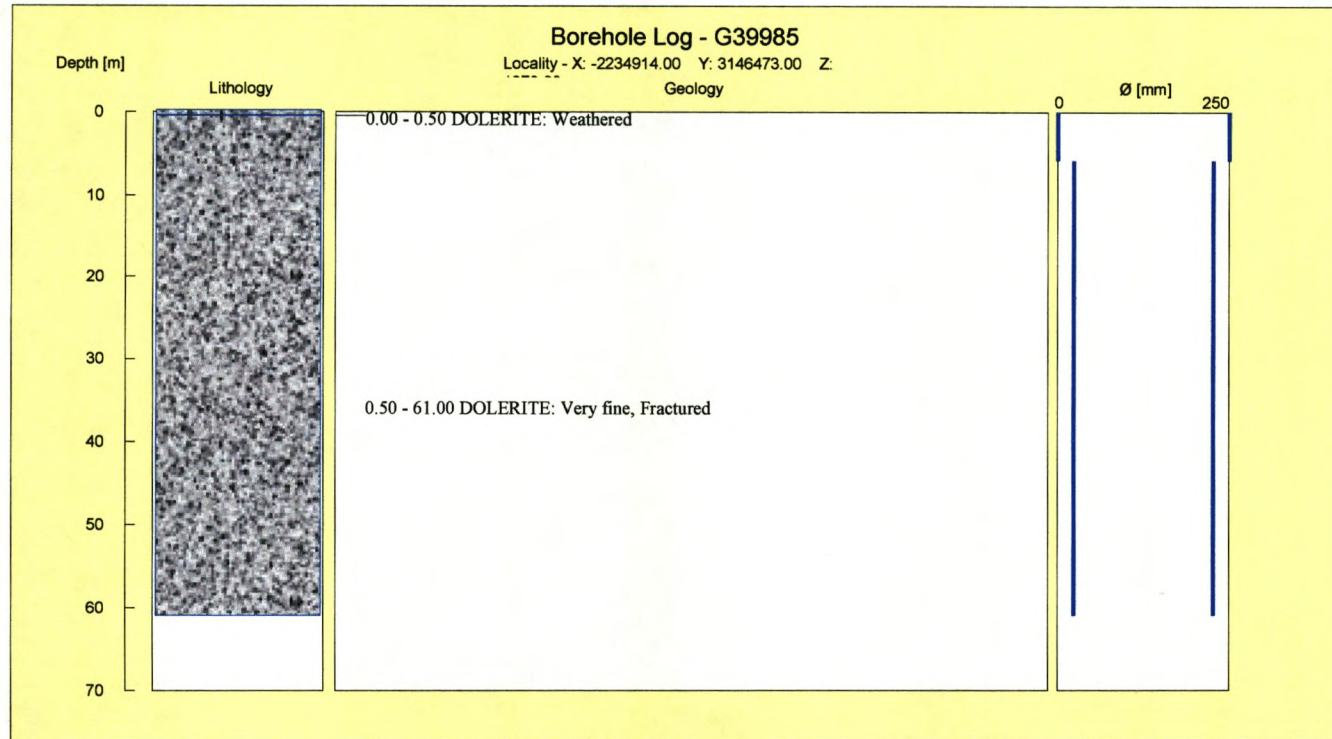
## **APPENDIX C**

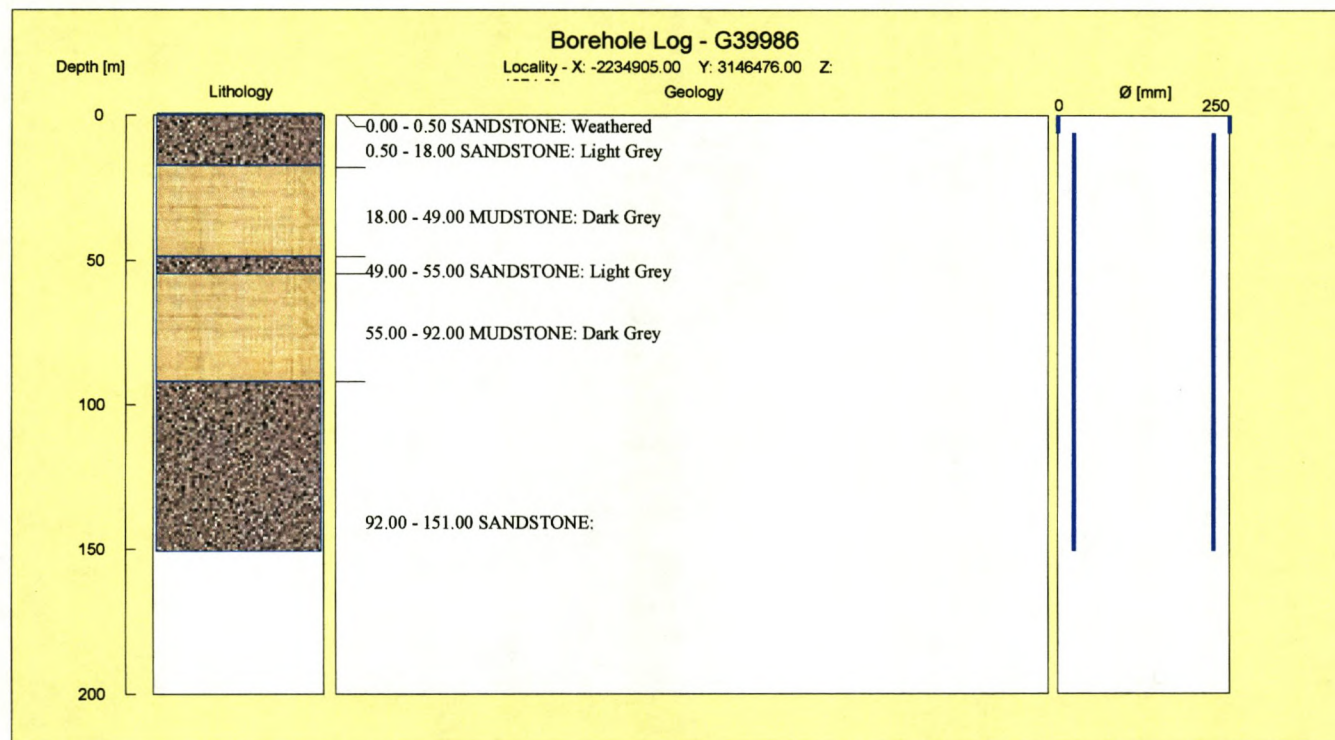
### **GEOLOGICAL INFORMATION**

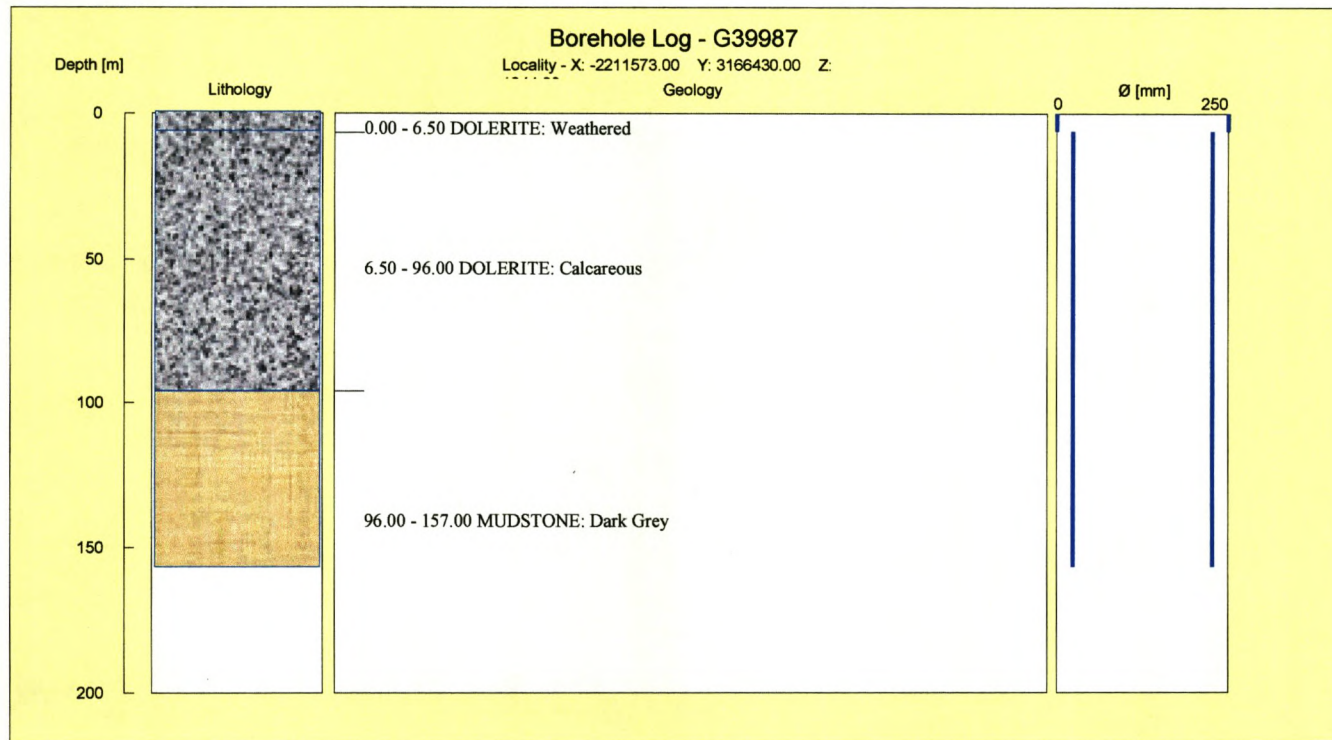


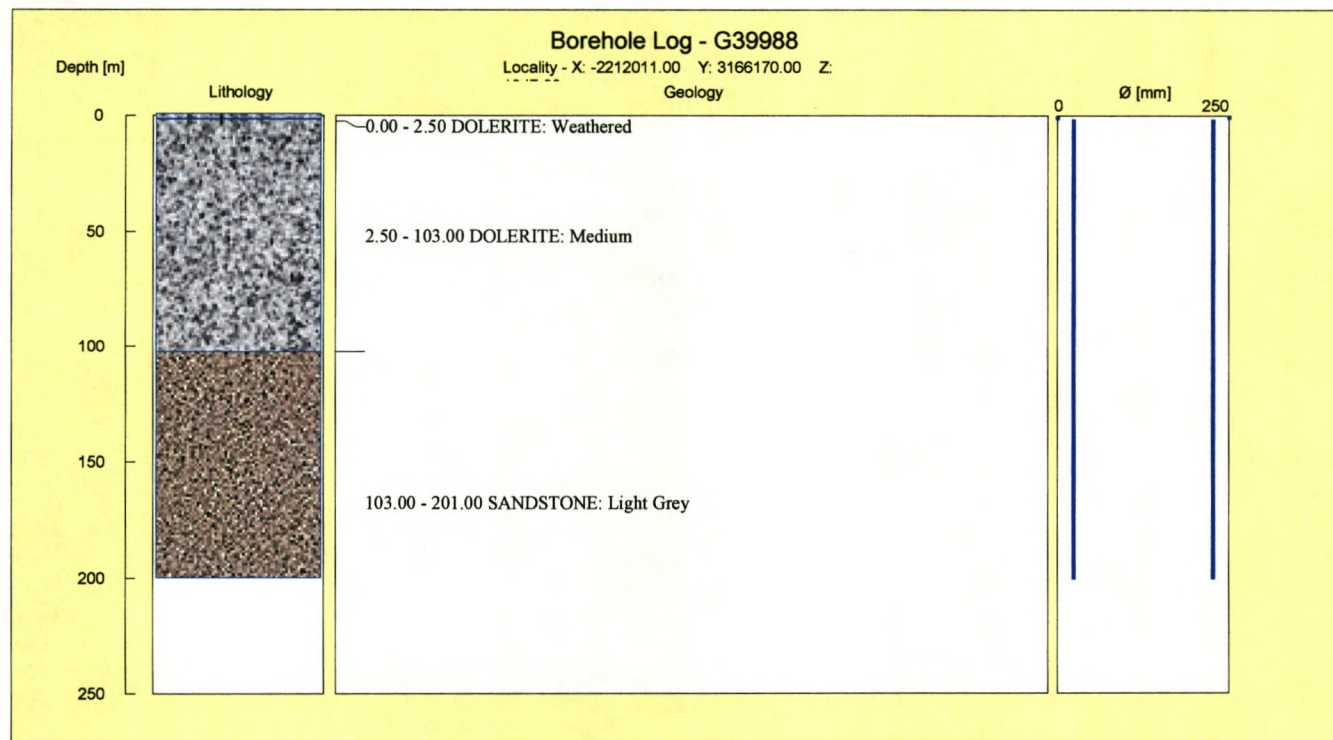




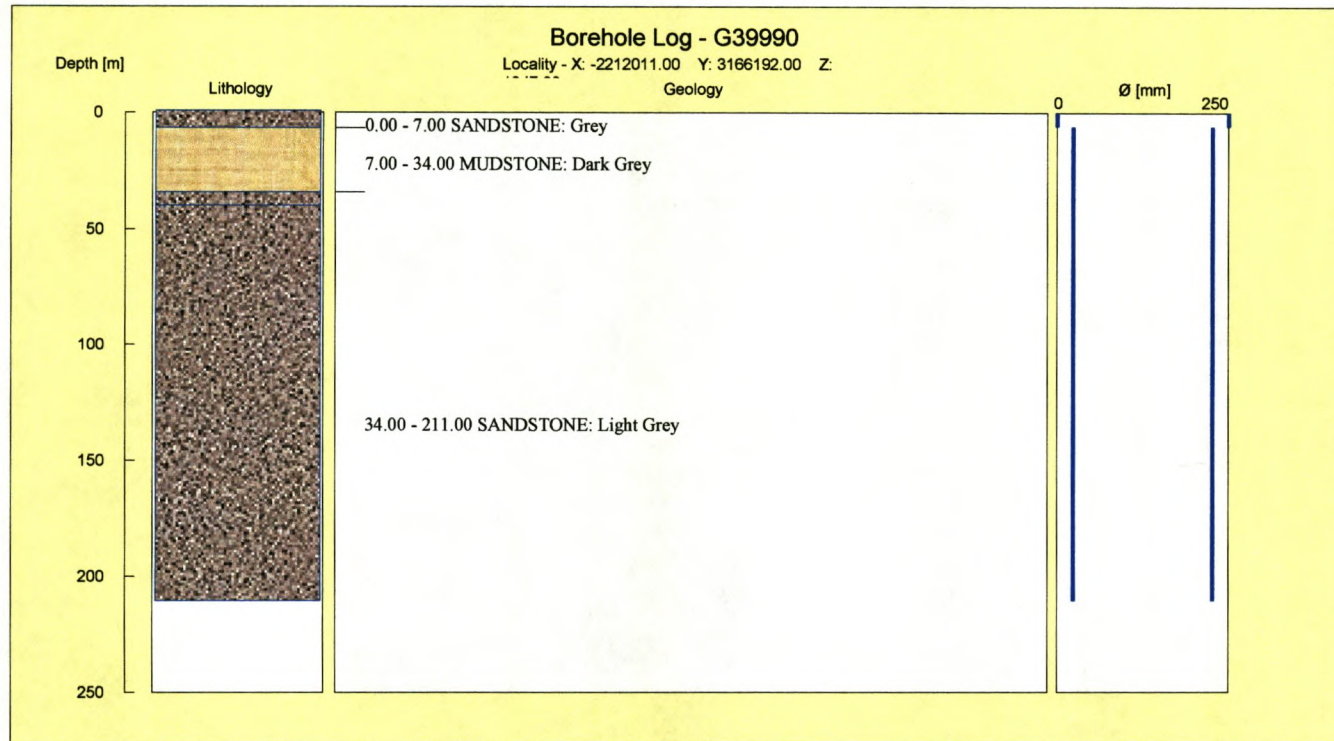


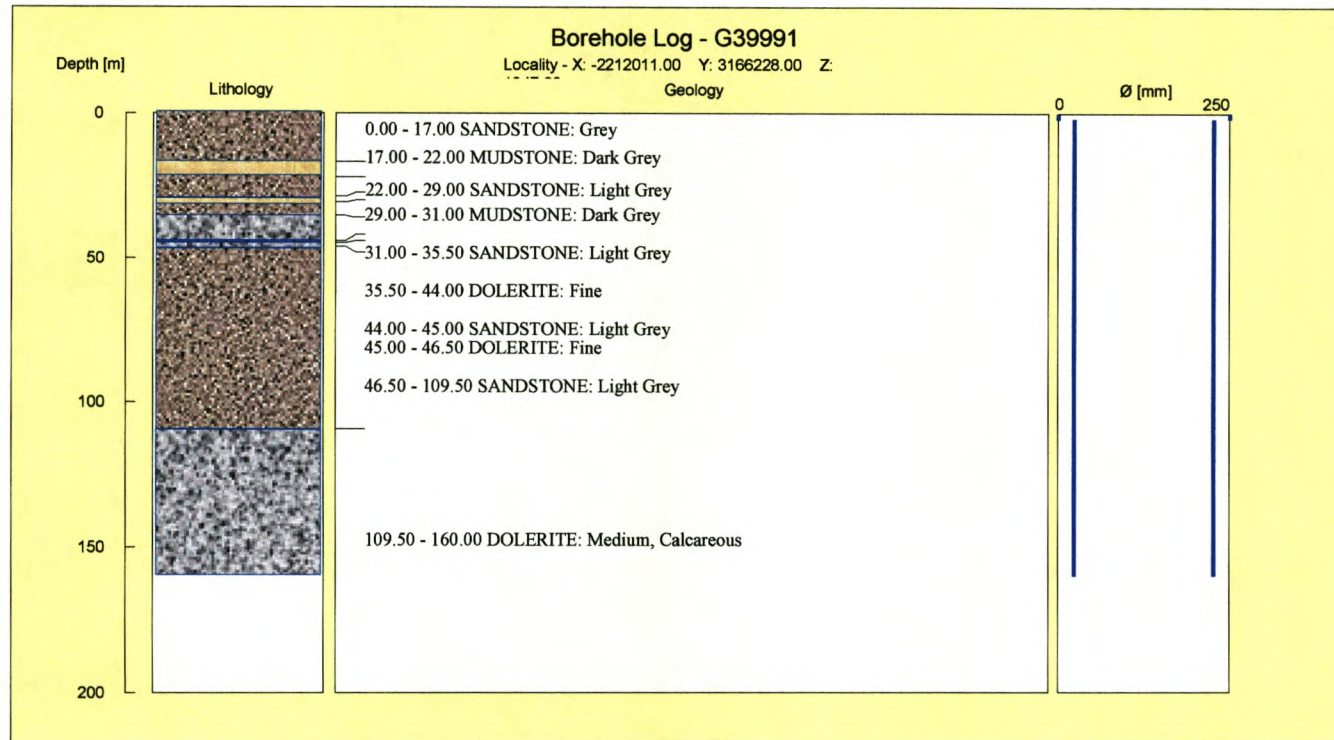


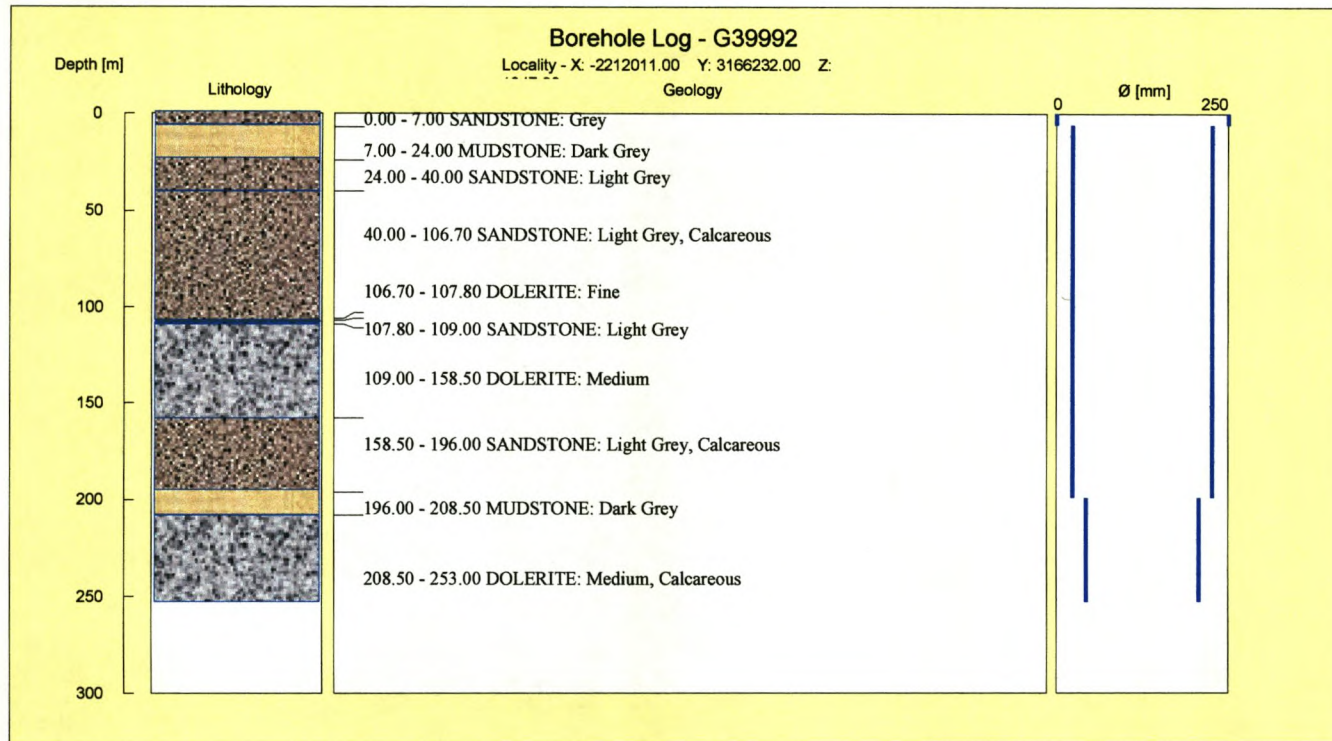




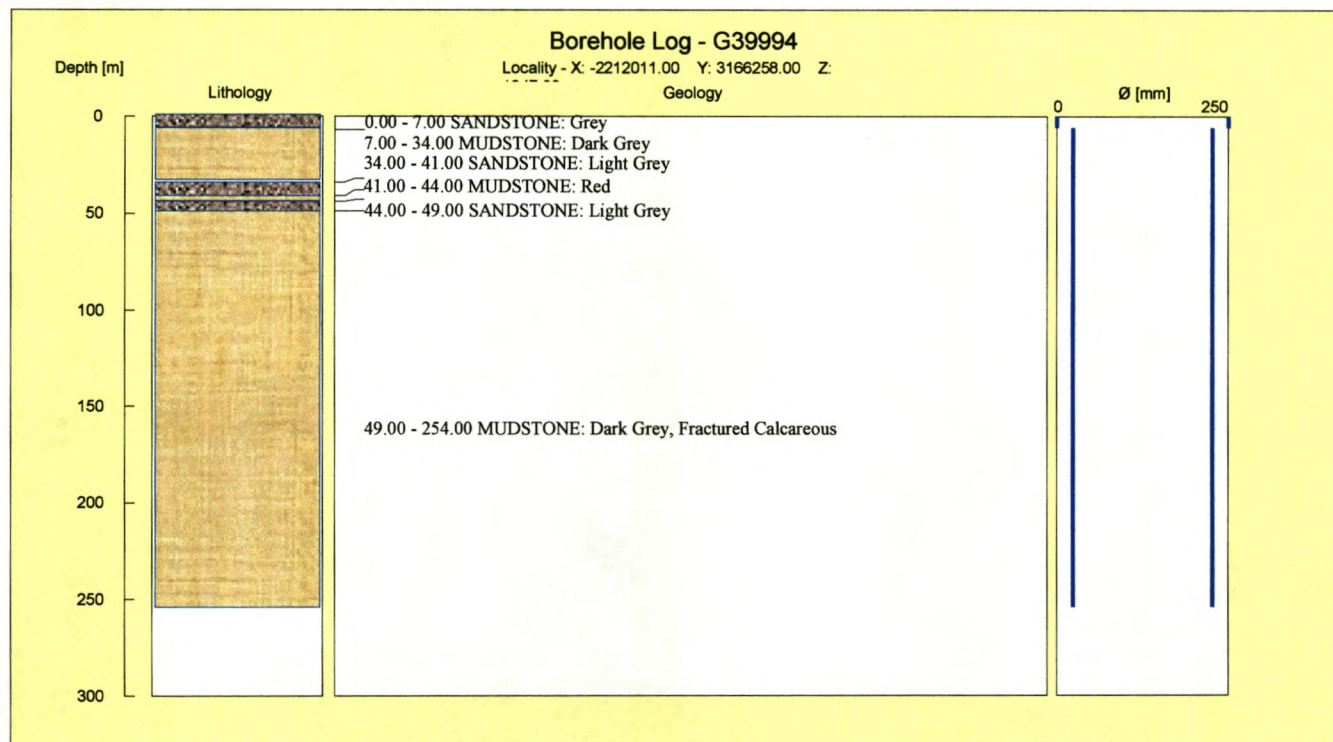




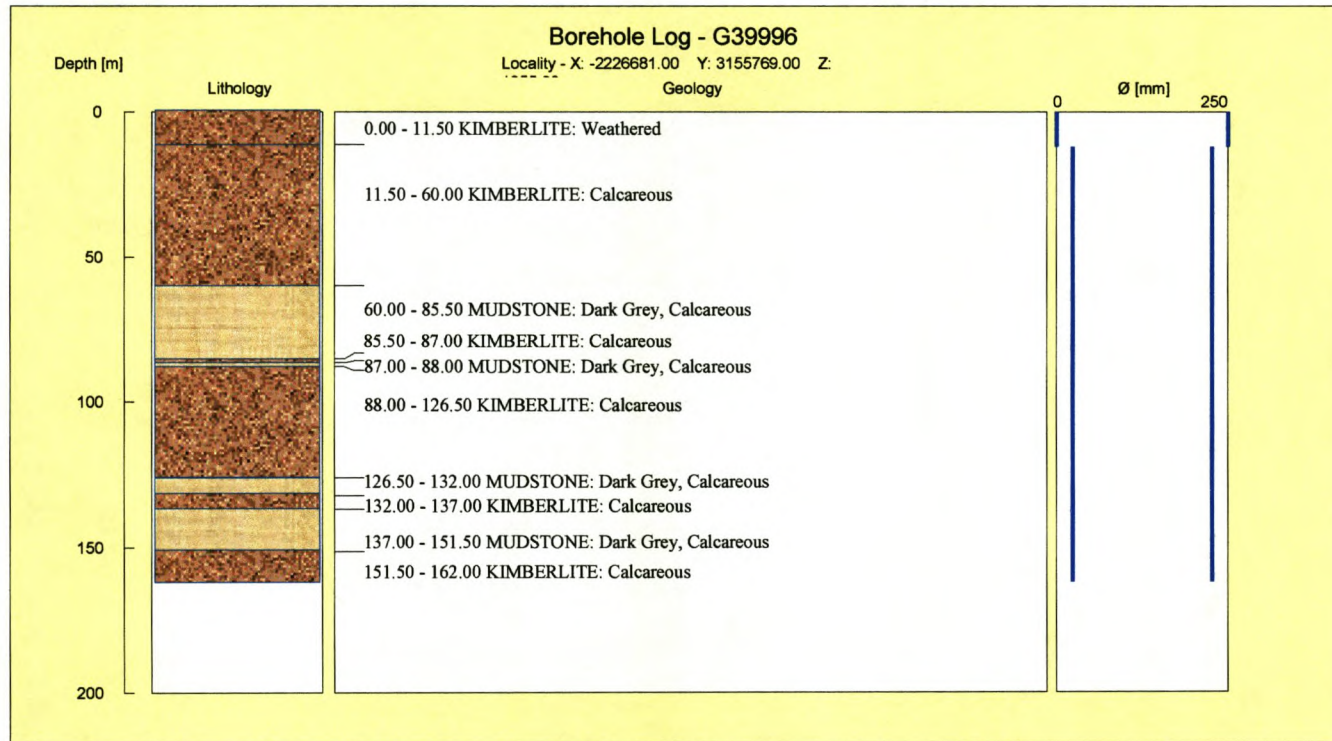


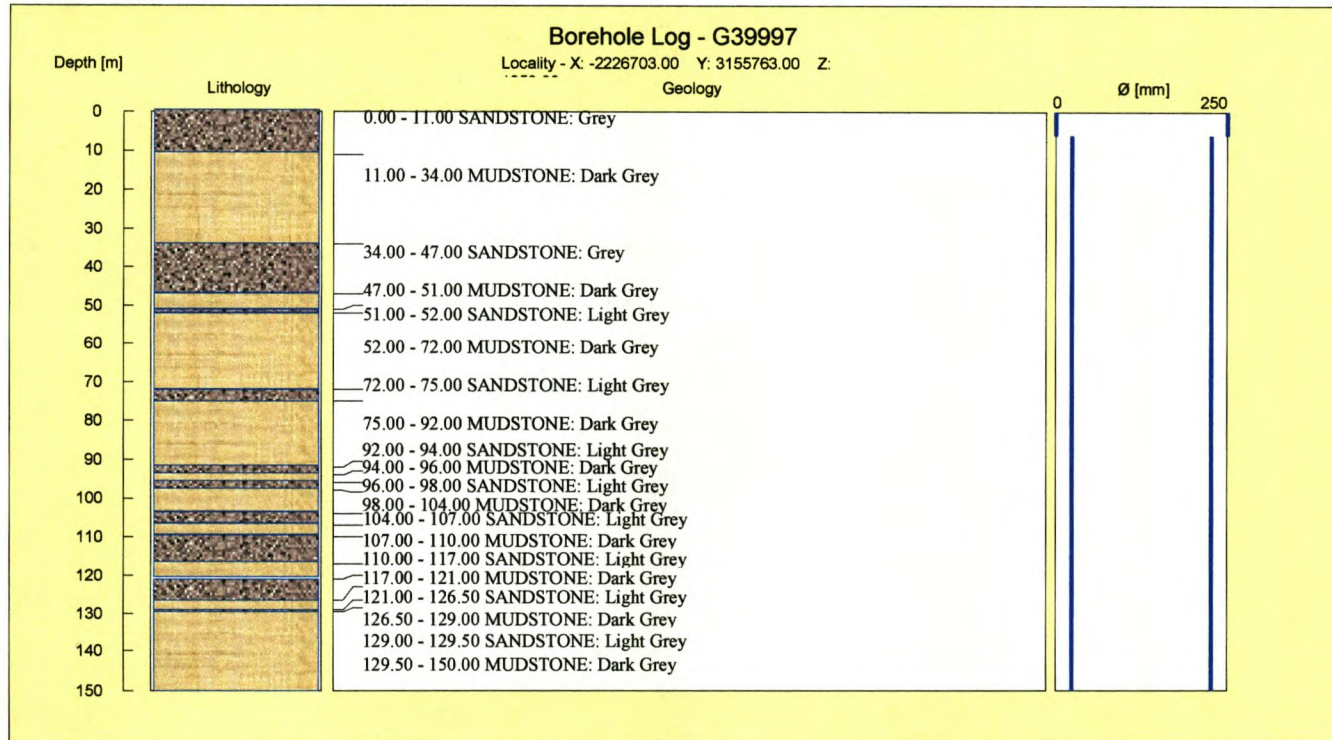


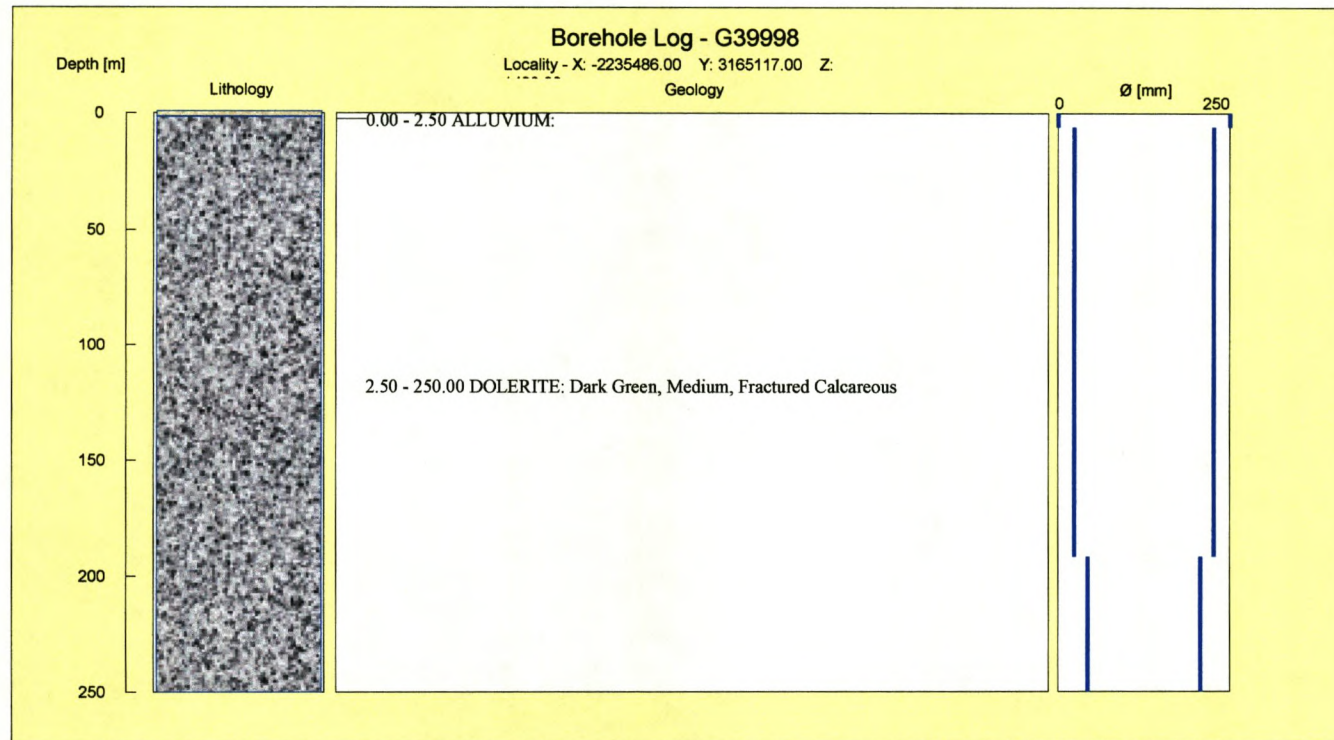


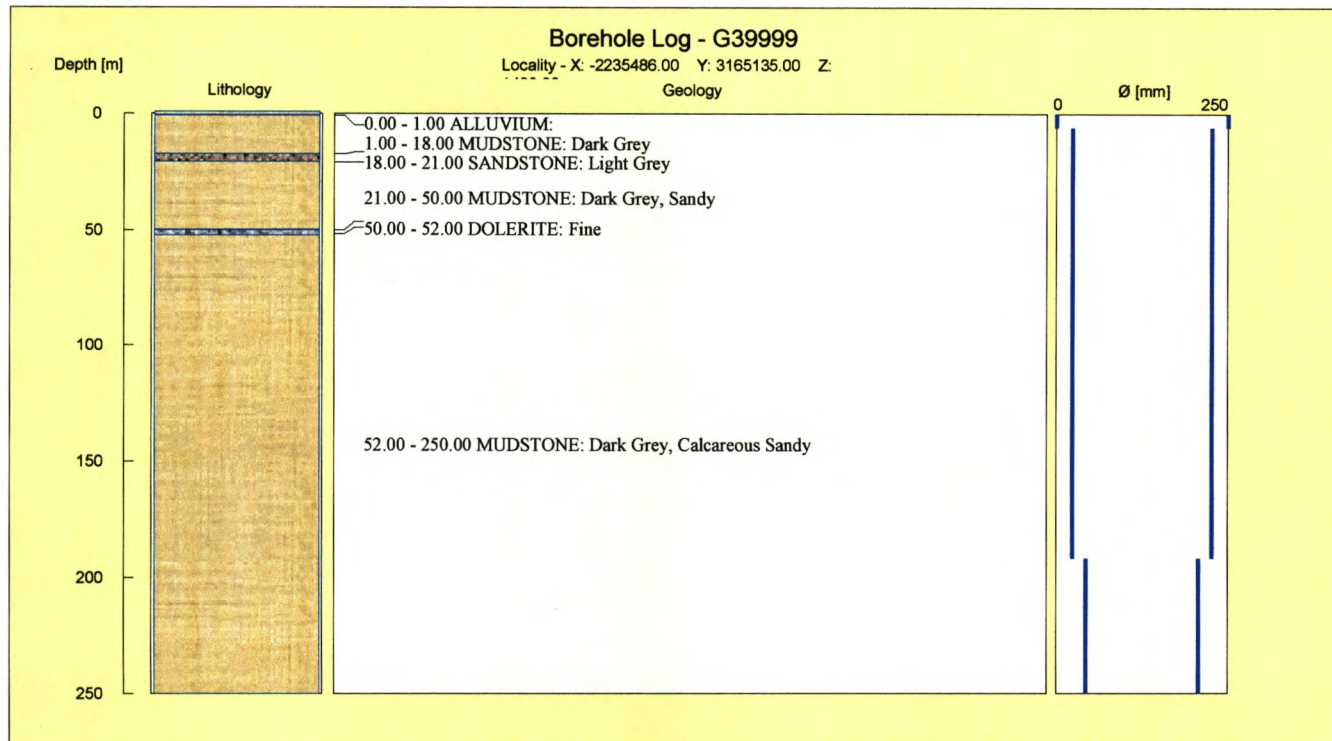


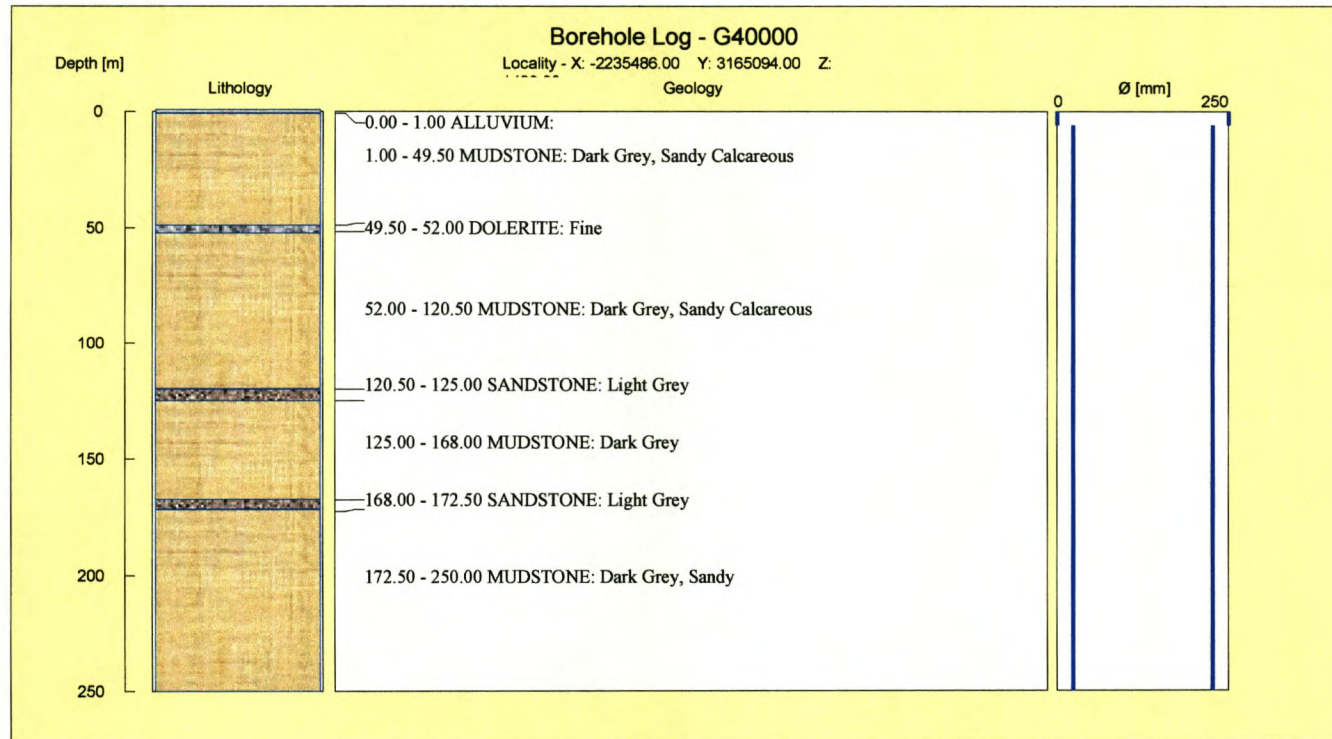


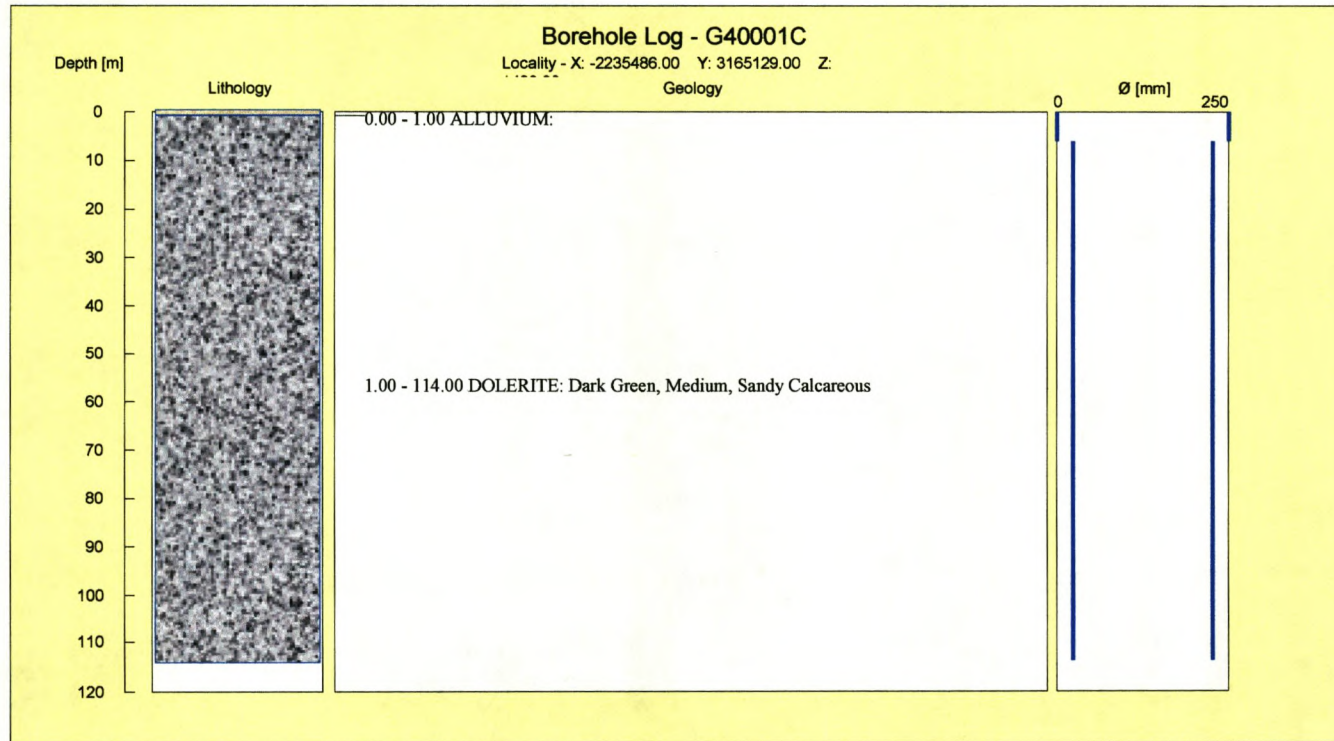


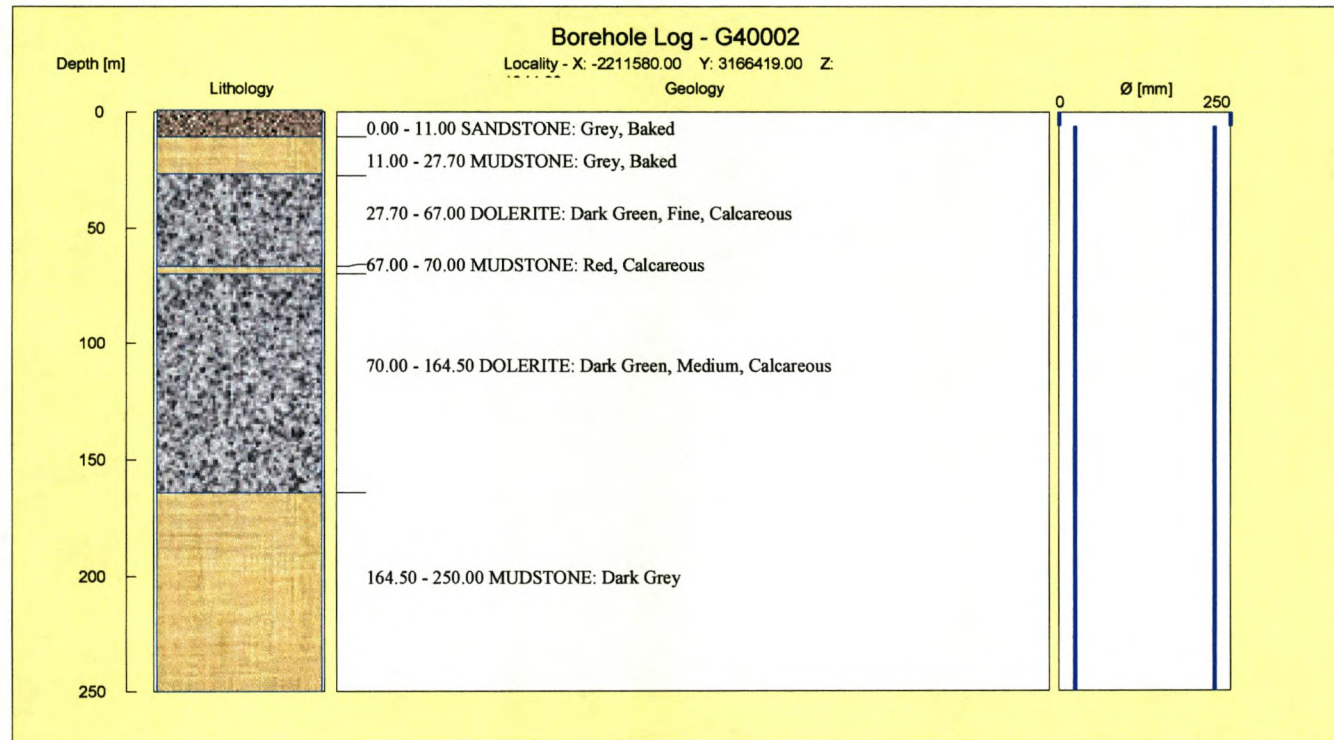


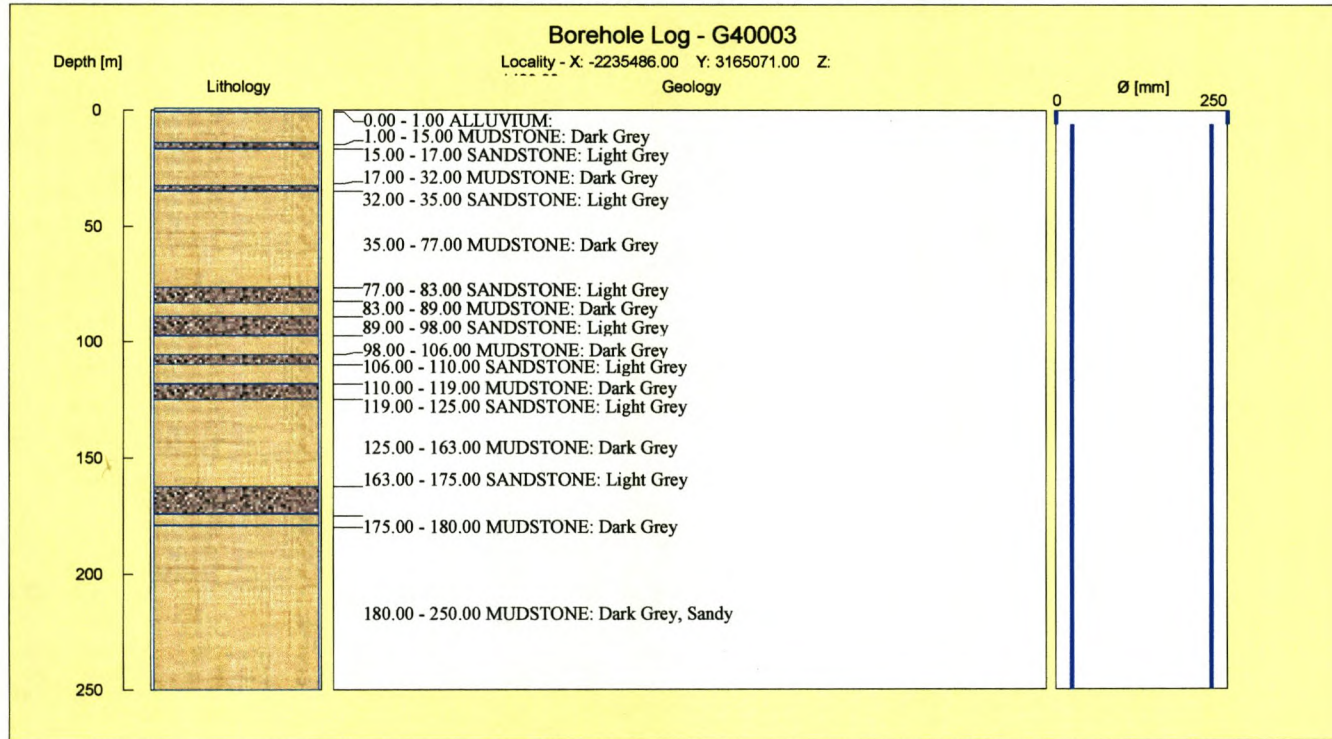


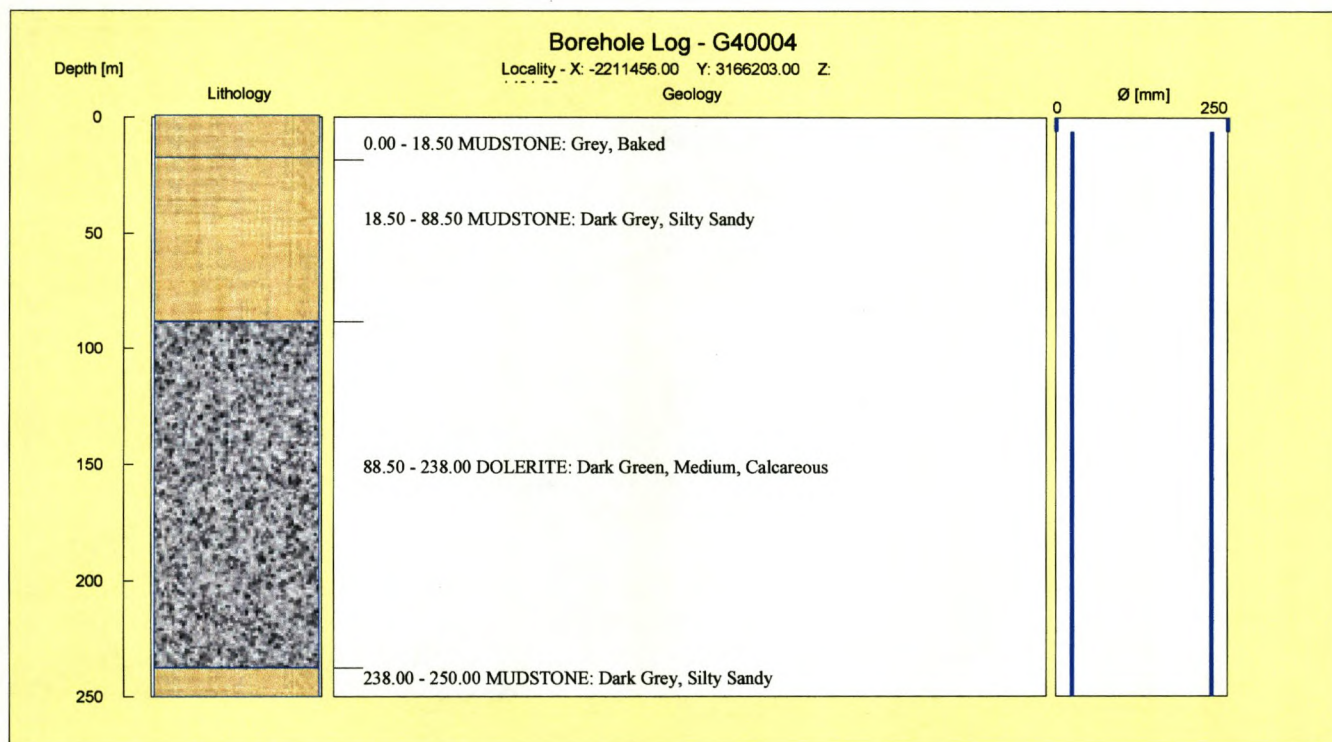


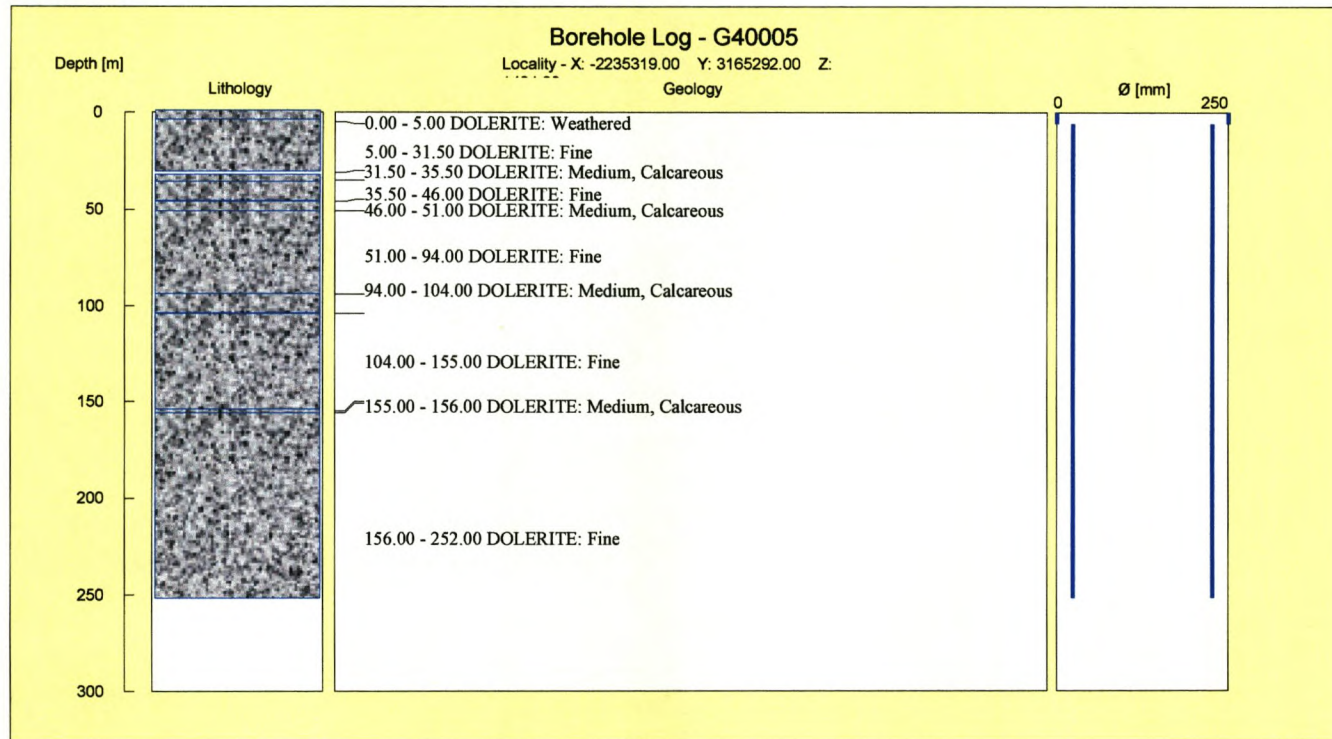


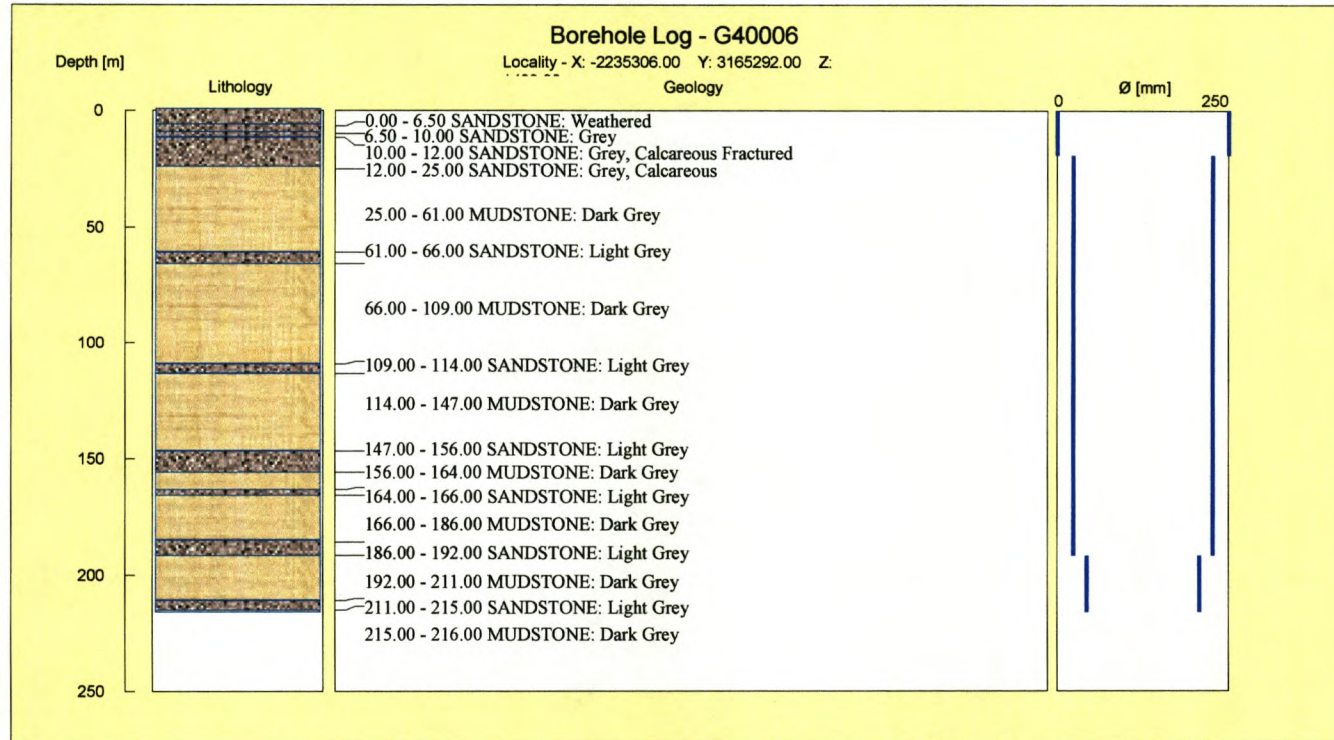


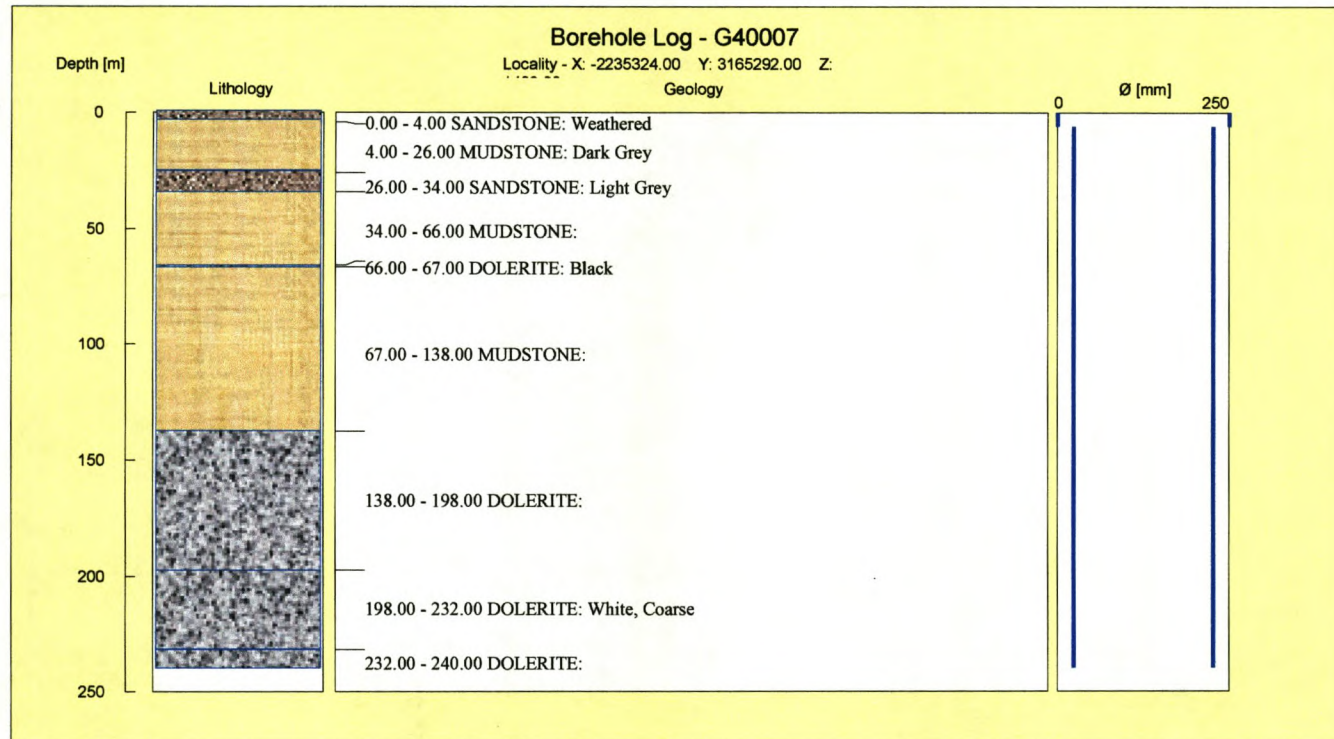


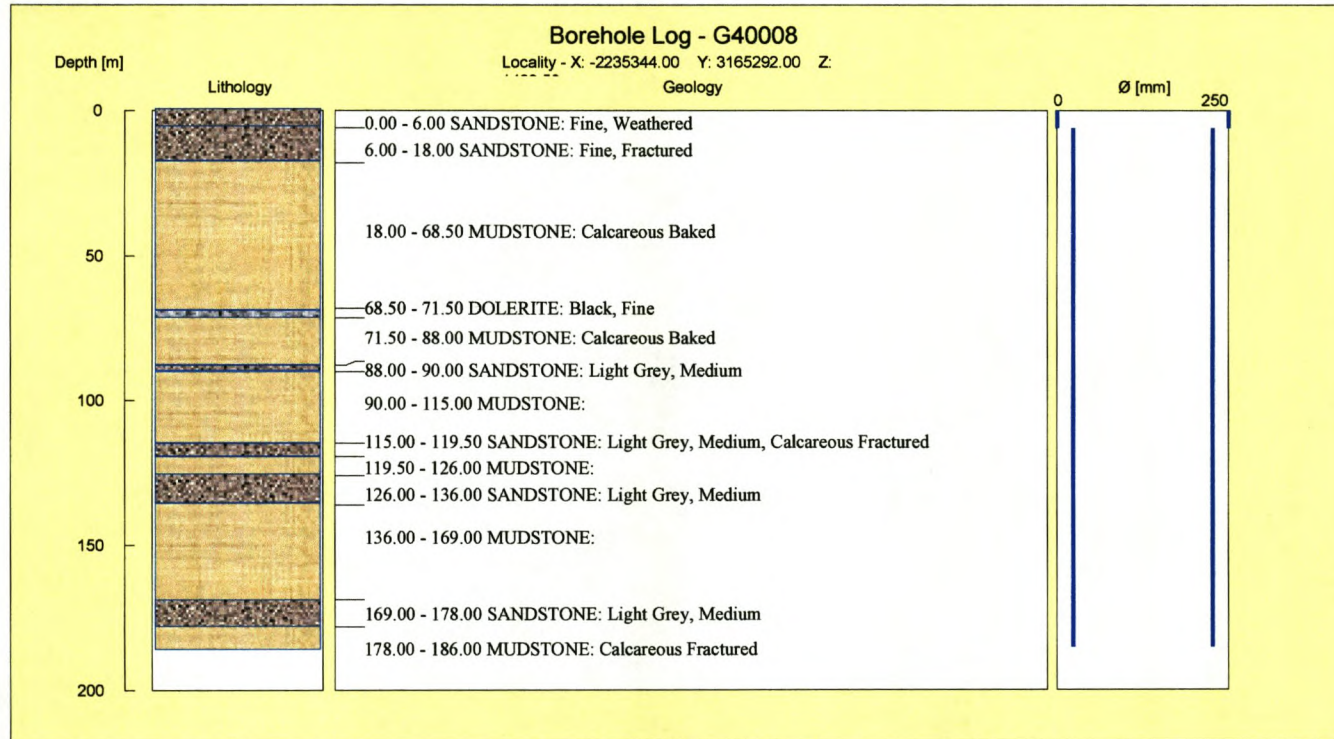


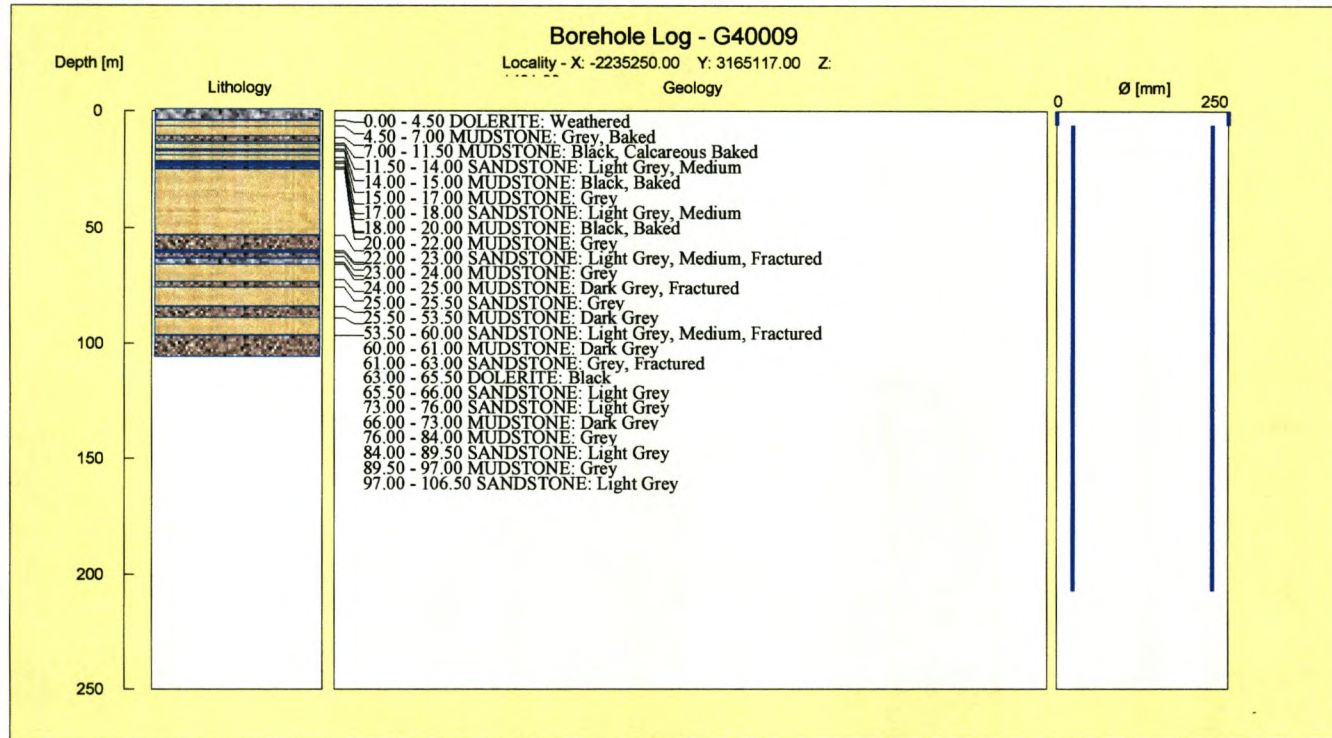


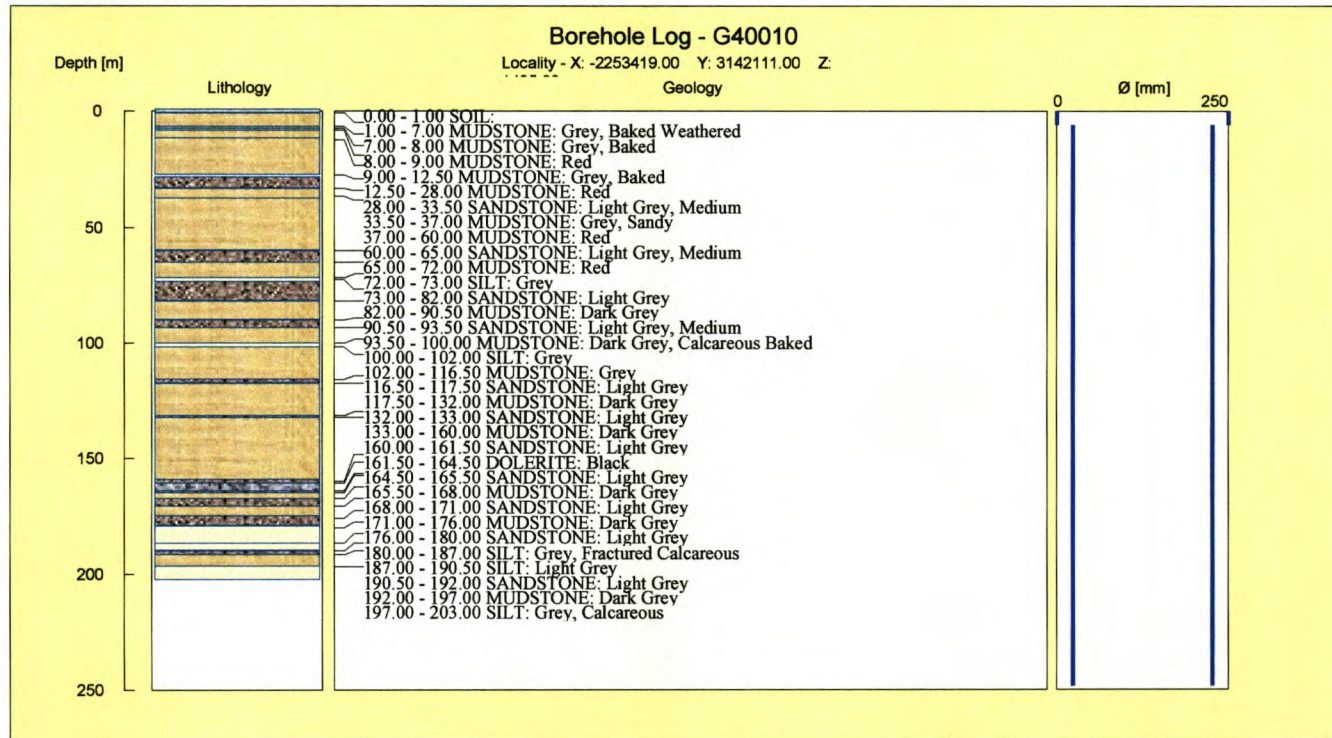


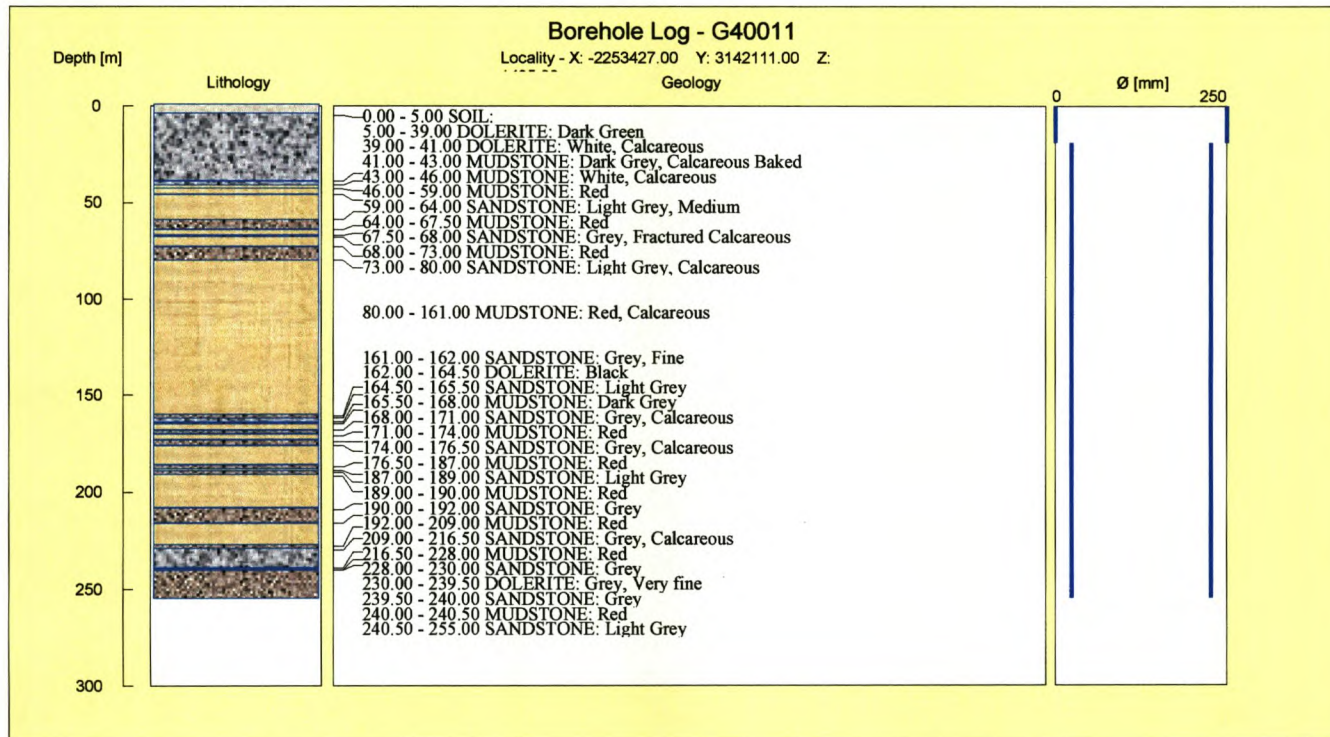


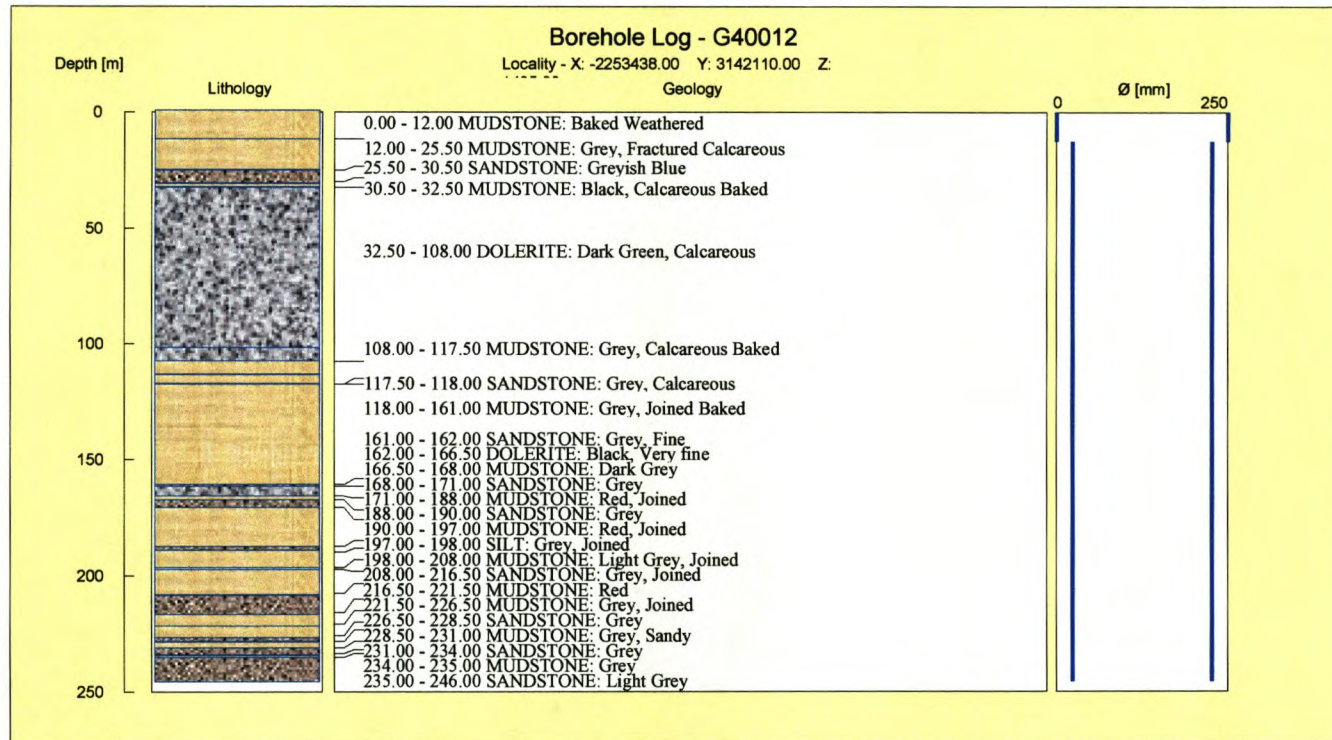


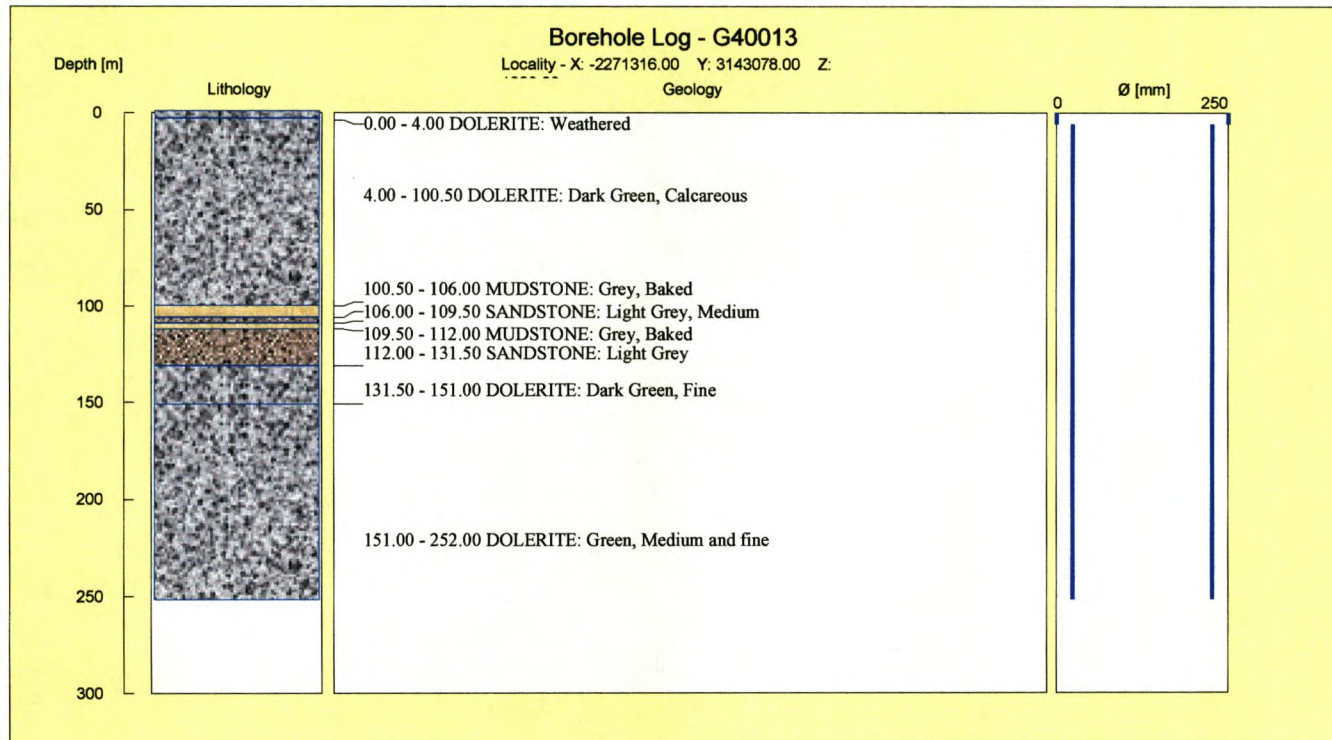


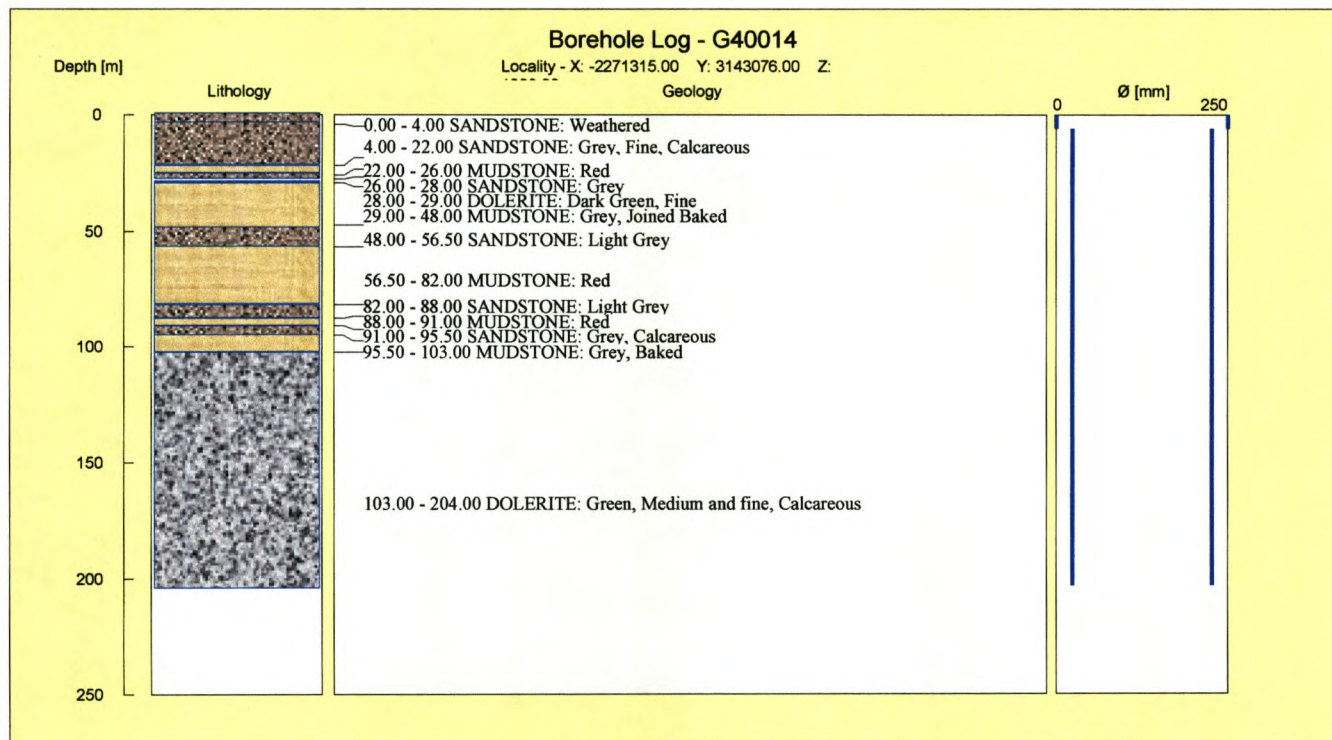


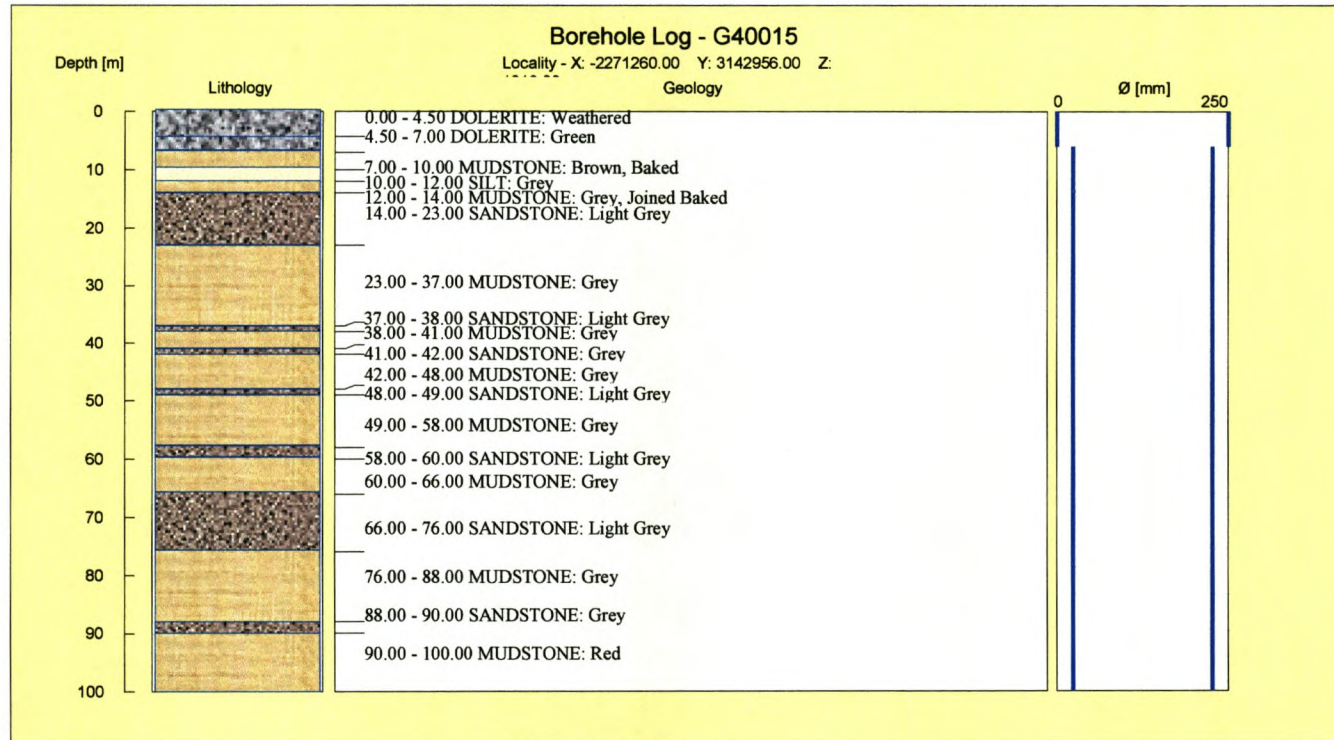


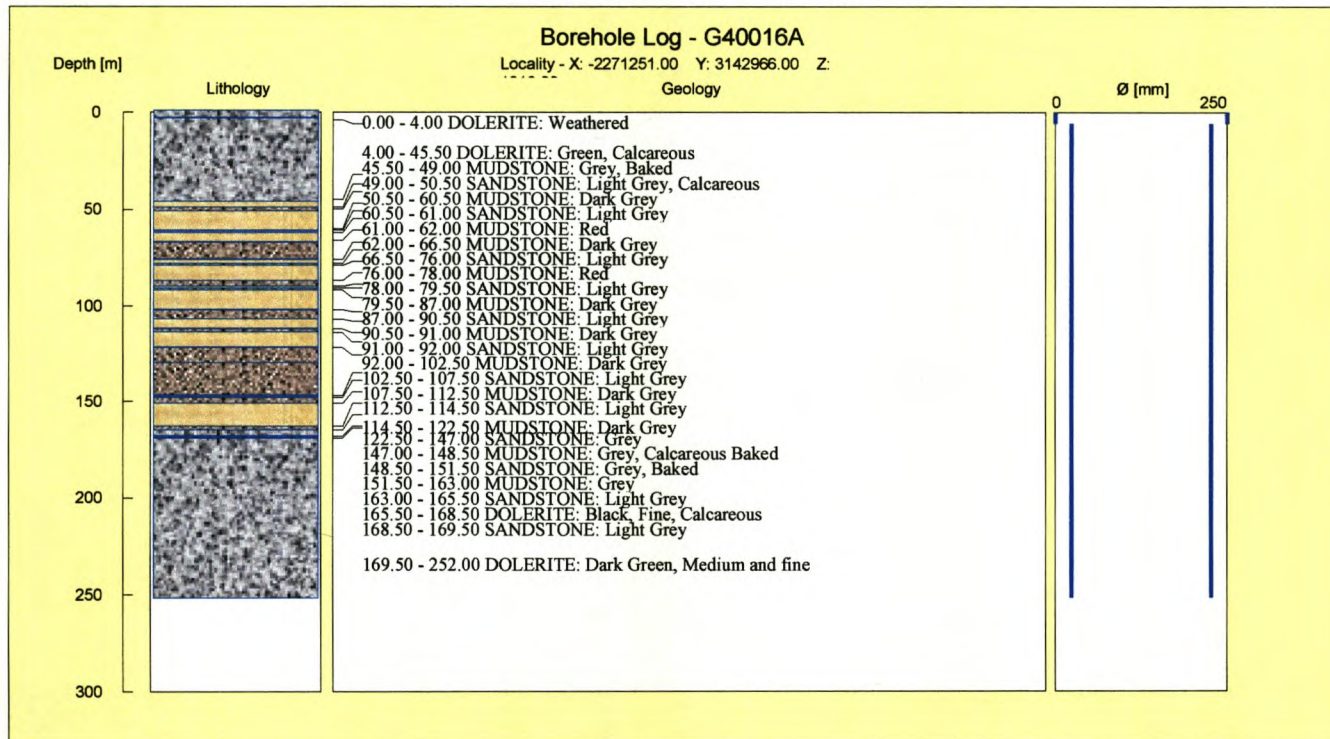


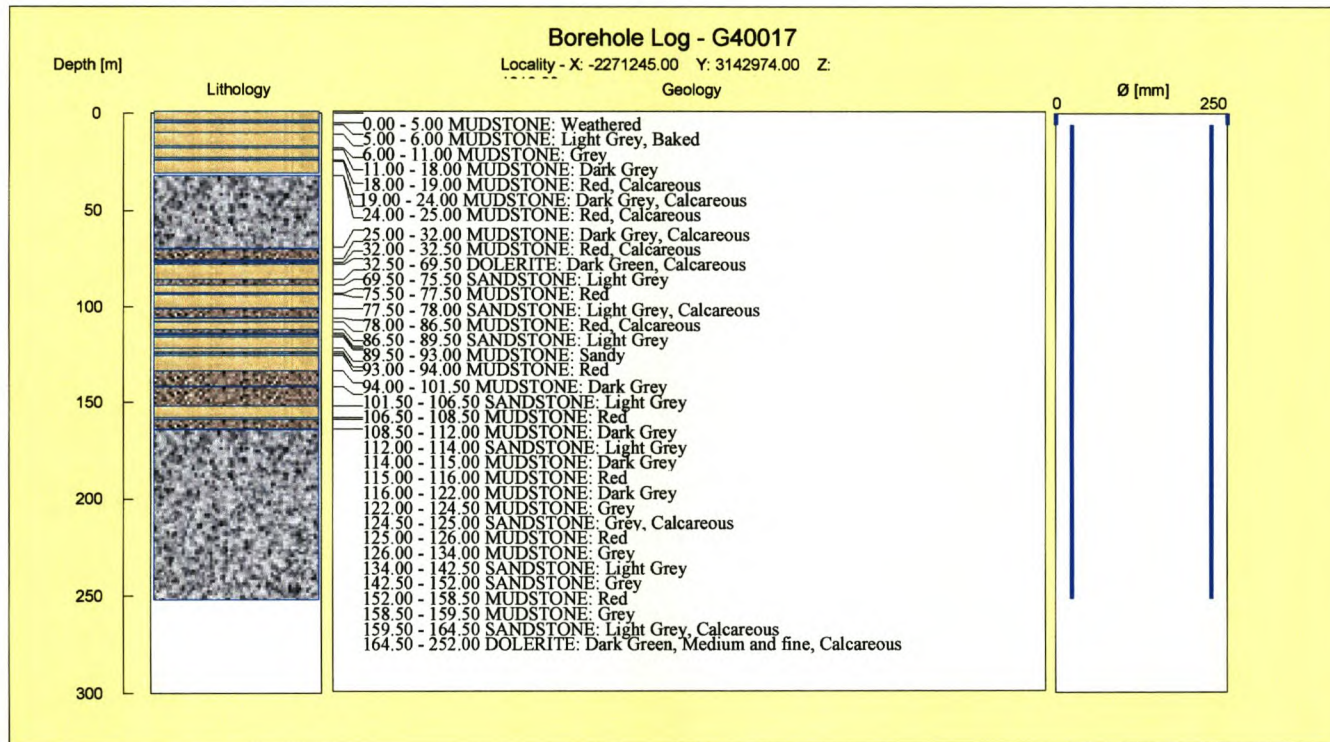


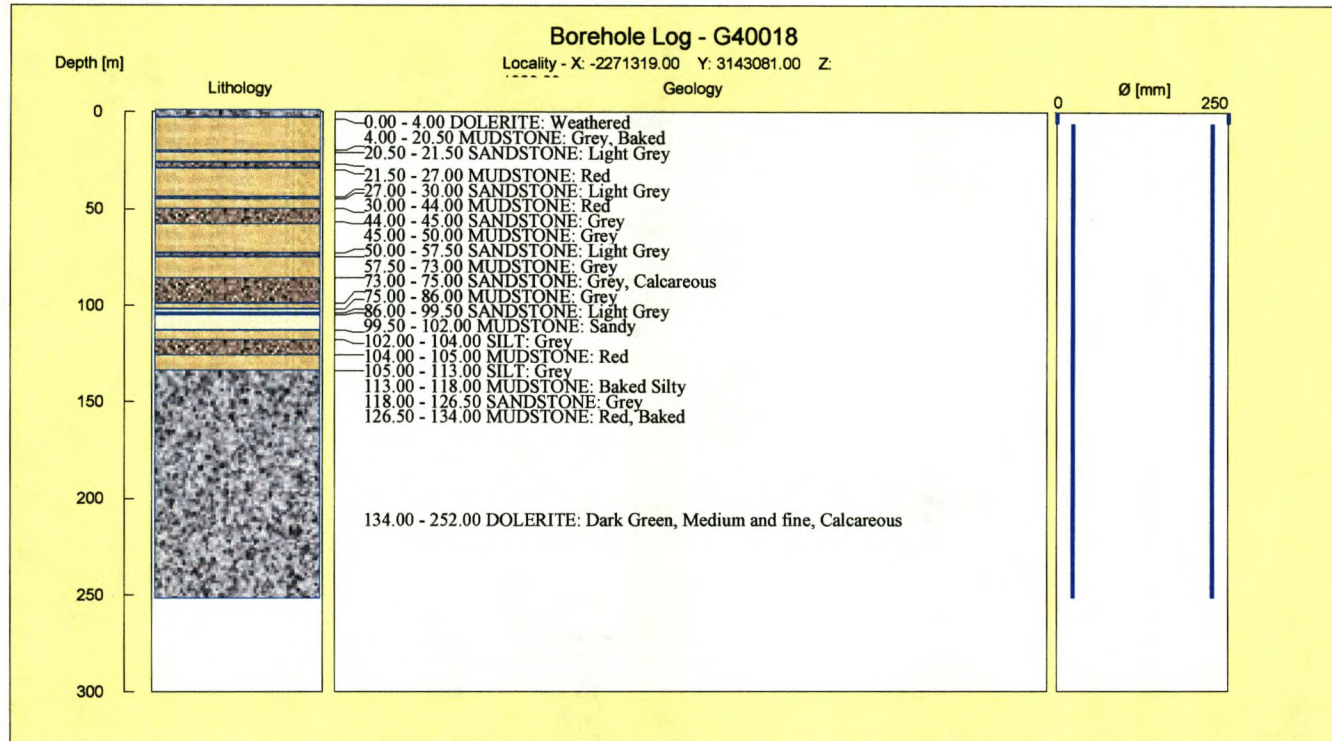


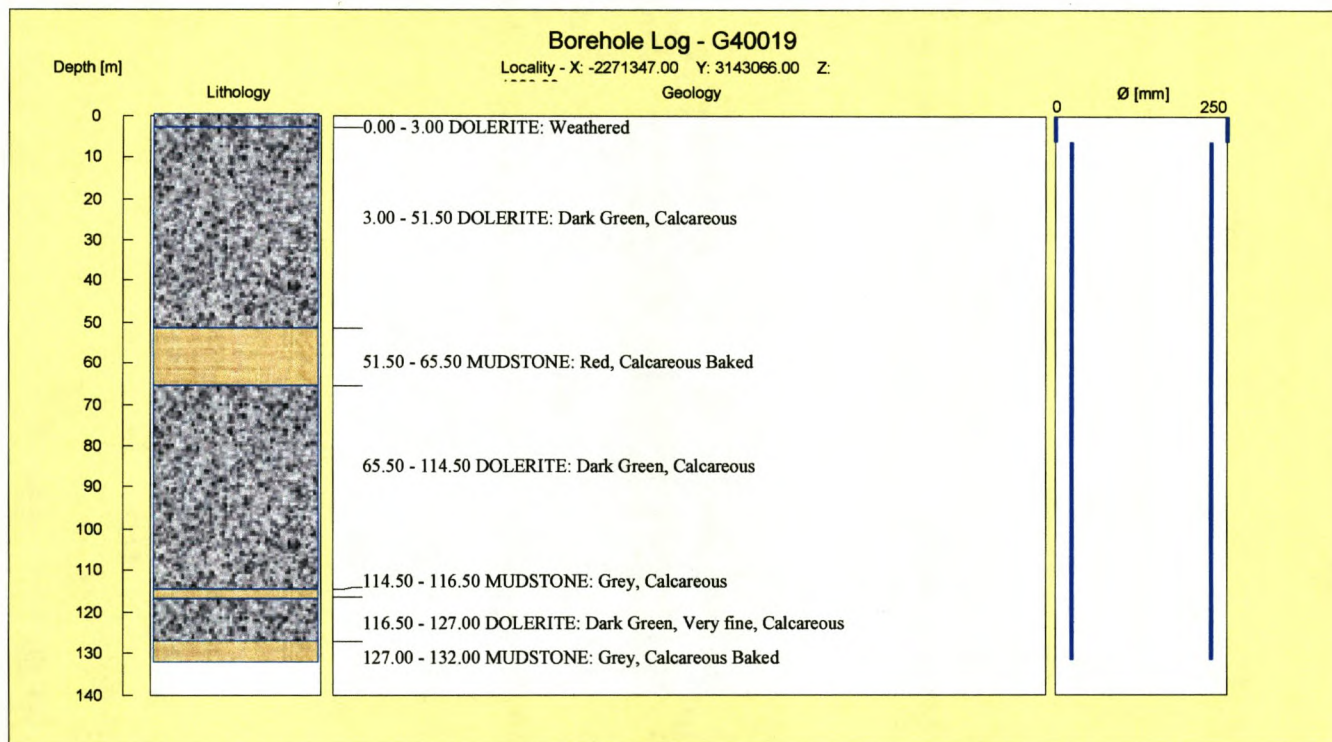


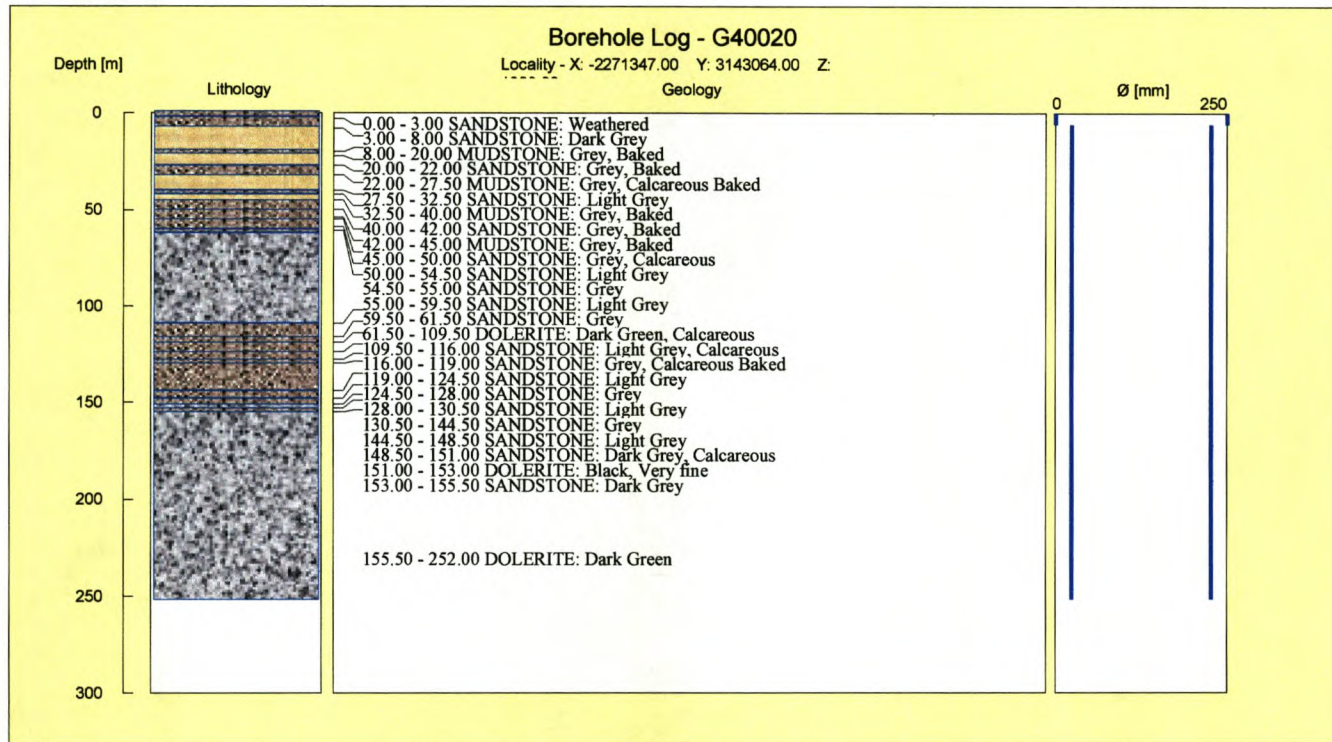












## **APPENDIX D**

### **LOG - ACTIVITIES**

## GROUNDWATER CHEMISTRY - LOG ACTIVITIES

	Ca <sup>+2</sup>	Mg <sup>+2</sup>	Na <sup>+</sup>	K <sup>+</sup>	Fe <sup>+2</sup>	Mn <sup>+2</sup>	Al <sup>+3</sup>	Ba <sup>+2</sup>	Sr <sup>+2</sup>	Cl <sup>-</sup>	HCO <sub>3</sub> <sup>-</sup>	SO <sub>4</sub> <sup>-2</sup>	NO <sub>3</sub> <sup>-</sup>	H <sub>3</sub> BO <sub>3</sub>	HPO <sub>4</sub> <sup>-1</sup>	F <sup>-</sup>	Li <sup>+</sup>	NH <sub>4</sub> <sup>+</sup>	CO <sub>3</sub>	
G 39981	-3.489	-4.386	-2.388	-3.377	-6.446	-6.698	-6.431	-7.138	-6.620	-2.322	-3.132			-5.733	-5.857	-4.978	-6.142	-5.368	-3.080	
G 39982	-3.700	-3.541	-2.427	-3.678	-6.446	-6.485	-6.431	-6.439	-4.929	-2.646	-3.152	-3.085	-5.845	-4.305			-4.777	-4.361	-3.099	
G 39984 (60)	-2.825	-3.386	-2.393	-3.064	-6.270			-7.837	-5.003	-2.809	-2.323	-3.096	-5.845	-4.107	-6.190	-4.676	-5.169	-5.845	-2.284	
G 39984 (90)	-2.832	-2.880	-2.629	-4.513	-6.270		-6.431	-8.138	-4.958	-2.817	-2.377	-2.833	-4.784	-4.903		-4.580	-5.070	-6.146	-2.337	
G 39985	-2.825	-2.894	-2.680	-3.868	-6.446		-6.431	-8.138	-4.986	-2.817	-2.340	-2.922	-5.669	-5.008	-5.345	-4.279	-5.063		-2.300	
G 39986	-2.825	-2.894	-2.671	-3.821	-5.793			-6.933	-5.059	-2.698	-2.516	-2.910		-4.996	-6.345	-4.500	-4.273	-4.500	-2.474	
G 39987	-2.797	-4.085	-2.271	-3.689	-6.446			-5.528	-7.359	-4.060	-2.345	-3.122		-4.236	-6.148	-4.000	-3.843	-5.146	-3.070	
G 39988	-1.834	-3.907	-1.807	-3.656	-6.269	-7.437	-5.430	-8.136	-4.610	-2.480	-2.641	-1.667	-6.145	-3.888	-6.109	-4.198	-4.144		-2.597	
G 39989	-2.290	-3.908	-1.820	-3.232	-6.269	-7.438	-6.430	-8.137	-4.518	-2.419	-2.946	-1.956		-3.925	-5.999	-4.102	-4.172		-2.897	
G 39990	-2.321	-4.385	-1.820	-3.232	-6.269			-5.226	-7.836	-3.912	-2.508	-3.161		-3.999	-5.877	-4.023	-3.866	-4.627	-3.109	
G 39991	-1.898	-4.385	-1.959	-4.445	-6.269	-6.836			-7.535	-4.038	-2.214	-2.629		-3.826	-5.782	-3.999	-3.968	-5.367	-2.585	
G 39992	-1.898	-3.238	-1.883	-3.345	-6.445	-6.292			-6.961	-4.348	-2.557	-2.419		-3.870	-6.587	-4.164	-4.296	-5.668	-2.378	
G 39993	-1.956	-3.239	-2.101	-3.979	-6.445	-6.221	-5.585	-7.660	-4.418	-2.488	-2.562	-1.921		-4.108		-3.977	-4.368	-5.844	-2.519	
G 39994	-2.058	-3.686	-1.828	-3.578	-6.269	-6.535	-5.151	-7.438	-4.085	-2.599	-2.835	-1.834		-3.933		-4.132	-3.962	-5.367	-2.788	
G 39995	-1.770	-3.907	-1.822	-3.646	-6.268				-7.437	-4.140	-2.451	-3.182		-3.817	-5.757	-4.236	-4.072	-5.066	-3.129	
G 39996	-3.097	-3.239	-1.823	-3.356	-5.968			-4.999	-6.795	-4.004	-2.201	-2.242	-5.544	-3.897	-5.800	-5.278	-3.999	-5.845	-2.205	
G 39997 (59)	-2.577	-2.615	-2.160	-3.452	-6.446	-5.558			-6.776	-4.354	-2.299	-2.188		-4.867	-4.298	-6.190	-4.375	-4.653	-5.845	-2.152
G 39997 (93)	-2.553	-2.622	-2.312	-3.876	-6.446	-5.593			-6.675	-4.339	-2.316	-2.194		-4.867	-4.506	-5.735	-4.375	-4.634	-5.845	-2.157
G 39998 (24)	-2.561	-2.593	-2.062	-3.876	-6.445	-5.622	-5.200	-7.183	-4.474	-2.151	-2.121	-2.588	-5.669	-4.534	-6.260	-4.500	-4.629	-5.8447	-2.086	
G 39998 (90)	-2.577	-2.593	-1.954	-3.876	-6.269	-5.482	-6.430	-7.292	-4.403	-2.149	-2.165	-2.410		-4.367		-4.433	-4.441	-5.669	-2.129	
G 39999	-2.527	-2.510	-2.045	-3.424	-6.445				-7.183	-4.593	-2.167	-2.419		-4.316		-4.375	-4.564	-6.146	-2.379	
G 40000	-2.770	-2.499	-1.938	-3.424	-6.445		-4.968	-7.183	-4.864	-2.143	-2.097	-2.469	-5.243	-4.426		-4.433	-4.546	-5.243	-2.062	
G 40001	-2.745	-2.499	-1.938	-3.828	-6.445			-7.234	-4.777	-2.165	-2.077	-2.428	-5.191	-4.354	-7.490	-4.579	-4.542	-4.589	-2.042	
G 40002	-2.643	-2.669	-2.049	-3.939	-6.269	-6.106	-5.389	-6.961	-4.628	-2.123	-2.575	-2.442		-4.388	-6.168	-4.132	-3.832	-5.669	-2.532	
G 40003	-2.620	-3.155	-2.087	-4.212	-6.145		-5.586	-7.096	-4.361	-2.257	-2.576	-2.494		-4.069		-4.324	-4.172	-5.845	-2.532	
G 40004	-2.482	-2.645	-2.185	-3.678	-6.445	-5.771	-5.351	-6.776	-4.773	-2.422	-2.149	-2.380	-4.346	-4.049		-4.375	-4.679	-5.845	-2.113	
G 40005	-2.573	-2.829	-2.475	-4.012	-6.446		-5.352	-7.292	-4.651	-2.663	-2.280	-2.630	-6.146	-4.707	-6.889	-4.579	-4.511	-6.146	-2.242	
G 40006	-2.577	-2.762	-2.486	-3.717	-6.270		-6.431	-7.024	-4.865	-2.600	-2.260	-2.606	-5.105	-4.697	-6.889	-6.076	-4.433	-4.517	-2.153	
G 40007	-2.594	-2.637	-2.224	-3.436	-6.446		-5.431	-7.023	-4.679	-2.257	-2.190	-2.833	-5.845	-4.933	-6.076	-4.433	-4.517		-2.105	
G 40008	-2.594	-2.566	-2.082	-3.436	-6.269			-6.815	-4.670	-2.217	-2.140	-2.452	-4.641	-4.521	-5.959	-4.579	-4.525		-2.105	
G 40009 (23)	-2.475	-2.894	-2.082	-4.087	-6.445	-6.698	-5.389	-7.058	-4.422	-2.257	-2.305	-2.438	-6.146	-4.452		-4.324	-4.289	-6.146	-2.266	
G 40009 (60)	-2.412	-2.880	-2.064	-4.313	-6.269		-5.088	-7.058	-4.326	-2.277	-2.427	-2.272	-6.146	-4.212	-5.792	-4.324	-4.184	-5.845	-2.386	
G 40010	-2.990	-3.386	-2.185	-4.513	-6.446		-5.732	-7.292	-5.164	-2.817	-2.304	-2.978	-4.248	-4.087	-6.449	-4.102	-4.996		-2.265	
G 40011 (68)	-2.990	-3.386	-2.569	-4.814	-6.270		-6.130	-8.138	-5.350	-2.698	-2.642	-3.204		-4.316	-6.028	-4.023	-4.271		-2.598	
G 40011 (90)	-3.223	-3.687	-2.458	-4.638	-6.048		-5.528		-5.559	-2.757	-2.721	-3.204		-4.205	-6.377	-3.936	-4.193		-2.675	
G 40012	-3.260	-4.386	-2.402	-3.268	-6.145		-5.285		-6.330	-2.558	-2.576	-3.403		-4.167		-4.165	-4.105		-2.533	
G 40013	-3.046	-3.483	-2.361	-3.268	-6.145			-7.660	-4.928	-2.558	-2.340	-4.505		-4.158		-4.237	-4.413		-2.300	
G 40014	-3.126	-3.182	-2.361	-4.638	-6.446		-5.255	-7.293	-5.115	-2.549	-2.377	-4.681		-4.337	-6.537	-4.433	-4.468		-2.337	
G 40015	-2.895	-3.107	-2.353	-4.416	-6.446		-5.477	-7.138	-4.874	-2.485	-2.337	-4.283	-5.845	-4.367		-4.433	-4.461	-5.845	-2.297	
G 40016	-2.895	-3.306	-2.275	-4.513	-6.446	-7.439			-7.837	-4.827	-2.394	-2.340		-4.425		-4.500	-4.348	-5.368	-2.300	
G 40017	-2.940	-3.483	-2.275	-4.362	-5.844		-5.130	-7.024	-4.819	-2.382	-2.347	-4.137	-6.146	-4.372	-7.491	-4.801	-4.344	-5.368	-2.308	
G 40018	-3.098	-3.431	-2.375	-4.814	-6.446		-5.732	-7.661	-4.864	-2.453	-2.516	-4.681		-4.320		-4.048	-4.405		-2.474	
G 40019	-2.990	-3.085	-2.375	-4.513	-6.270		-5.317	-7.058	-5.067	-2.549	-2.340	-3.451		-3.965	-6.169	-4.433	-4.348	-5.845	-2.300	
G 40020 (47)	-2.990	-3.085	-2.412	-4.313	-6.048		-5.528	-7.439	-5.127	-2.485	-2.330	-3.727		-4.221	-6.449	-4.165	-4.640		-2.291	
G 40020 (90)	-3.126	-3.306	-2.402	-4.446	-6.048		-5.352	-7.439	-5.124	-2.481	-2.463	-3.903		-4.320		-4.023	-4.441		-2.422	
R 1	-4.302	-4.386	-2.529	-4.362	-6.270	-6.439	-5.528	-7.439	-5.154	-2.610	-3.338	-3.640	-4.868	-4.127			-4.410		-3.282	

## GROUNDWATER SATURATION INDICES

	Calcite	Aragonit	Dolomite	Siderite	Rhodochr	Strontit	Witherit	Gypsum	Anhydrit	Celestit	Barite	Hydroxap	Fluorite	Gibbs(c)	Al(OH)3a	Hematite	Goethite	Fe(OH)3a	Vivianit	Pyrolusi	
G 39981	-8.555	-8.419	-17.351	-10.959	-11.17	-9.3	-8.564					-4.422	-10.478	7.479	10.067	-4.862	-0.599	4.891	-36	39.578	
G 39982	-8.457	-8.31	-16.989	-10.863	-11.115	-9.269	-8.572	-4.581	-4.346	-6.623	-10.041										42.078
G 39984 (60)	-8.477	-8.333	-17.078	-10.887		-9.27	-8.563	-4.581	-4.359	-6.631	-9.978	-3.376	-10.605		8.355	11.084	-3.677	-1.155	4.891		
G 39984 (90)	-8.461	-8.315	-17.01	-10.869		-9.269	-8.57	-4.581	-4.348	-6.625	-10.025		-10.64	8.303	11.024	-3.747	-1.122	4.891	-36		
G 39985	-8.464	-8.318	-17.022	-10.872		-9.269	-8.568	-4.581	-4.35	-6.626	-10.017	-3.161	-10.634	8.274	10.991	-3.786	-1.104	4.891	-36		
G 39986	-8.482	-8.339	-17.099	-10.892		-9.271	-8.561	-4.581	-4.363	-6.633	-9.964	-3.457	-10.595			-4.038	-0.986	4.891	-36		
G 39987	-8.47	-8.325	-17.048	-10.879		-9.269	-8.565	-4.581	-4.354	-6.628	-9.999	-3.26	-10.621	8.212	10.918	-3.871	-1.064	4.891	-36		
G 39988	-8.468	-8.322	-17.039	-10.876	-11.122	-9.269	-8.566	-4.581	-4.352	-6.627	-10.006	-3.224	-10.626	8.234	10.944	-3.84	-1.079	4.891	-36	41.735	
G 39989	-8.473	-8.329	-17.062	-10.883	-11.126	-9.27	-8.564	-4.581	-4.356	-6.629	-9.989	-3.314	-10.614	8.178	10.878	-3.917	-1.043	4.891	-36	41.573	
G 39990	-8.474	-8.329	-17.064	-10.883		-9.27	-8.564	-4.581	-4.356	-6.629	-9.988	-3.323	-10.612	8.172	10.872	-3.924	-1.039	4.891	-36		
G 39991	-8.476	-8.332	-17.076	-10.886	-11.128	-9.27	-8.563	-4.581	-4.358	-6.631	-9.98	-3.368	-10.607			-3.962	-1.021	4.891	-36	41.476	
G 39992	-8.458	-8.312	-16.996	-10.865	-11.116	-9.269	-8.571	-4.581	-4.347	-6.624	-10.036	-3.061	-10.647			-3.701	-1.144	4.891	-36	42.029	
G 39993	-8.467	-8.321	-17.034	-10.875	-11.121	-9.269	-8.567	-4.581	-4.352	-6.627	-10.009		-10.628	8.246	10.958	-3.825	-1.086	4.891	-36	41.767	
G 39994	-8.473	-8.329	-17.062	-10.883	-11.126	-9.27	-8.564	-4.581	-4.356	-6.629	-9.989		-10.614	8.178	10.878	-3.917	-1.043	4.891	-36	41.573	
G 39995	-8.465	-8.319	-17.024	-10.873		-9.269	-8.568	-4.581	-4.35	-6.626	-10.015	-3.17	-10.633			-3.794	-1.101	4.891	-36		
G 39996	-8.463	-8.317	-17.017	-10.871		-9.269	-8.569	-4.581	-4.349	-6.625	-10.02	-3.143	-10.636	8.286	11.004	-3.77	-1.112	4.891	-36		
G 39997 (59)	-8.519	-8.38	-17.238	-10.929	-11.152	-9.282	-8.558	-4.585	-4.394	-6.653	-9.876	-3.986	-10.529			-4.49	-0.774	4.891	-36	40.362	
G 39997 (93)	-8.465	-8.319	-17.027	-10.873	-11.12	-9.269	-8.568	-4.581	-4.351	-6.626	-10.014	-3.179	-10.632			-3.801	-1.097	4.891	-36	41.816	
G 39998 (24)	-8.452	-8.304	-16.965	-10.857	-11.111	-9.269	-8.576	-4.581	-4.343	-6.622	-10.058	-2.941	-10.664	8.412	11.152	-3.599	-1.192	4.891	-36	42.244	
G 39998 (90)	-8.448	-8.3	-16.948	-10.853	-11.108	-9.27	-8.579	-4.582	-4.341	-6.622	-10.07		-10.673	8.453	11.199	-3.544	-1.218	4.891	-36	42.36	
G 39999	-8.453	-8.306	-16.972	-10.859		-9.269	-8.575	-4.581	-4.344	-6.623	-10.053		-10.66			-3.622	-1.181	4.891	-36		
G 40000	-8.453	-8.306	-16.972	-10.859		-9.269	-8.575	-4.581	-4.344	-6.623	-10.053		-10.66	8.395	11.131	-3.622	-1.181	4.891	-36		
G 40001	-8.451	-8.303	-16.96	-10.856		-9.269	-8.577	-4.581	-4.343	-6.622	-10.062	-2.923	-10.666			-3.583	-1.199	4.891	-36		
G 40002	-8.474	-8.33	-17.067	-10.884	-11.126	-9.27	-8.564	-4.581	-4.357	-6.63	-9.986	-3.332	-10.611	8.166	10.865	-3.932	-1.036	4.891	-36	41.541	
G 40003	-8.45	-8.302	-16.955	-10.855		-9.269	-8.578	-4.581	-4.342	-6.622	-10.065		-10.669	8.436	11.179	-3.567	-1.207	4.891	-36		
G 40004	-8.52	-8.381	-17.24	-10.929	-11.153	-9.283	-8.558	-4.585	-4.395	-6.653	-9.875		-10.528	7.748	10.379	-4.498	-0.77	4.891	-36	40.346	
G 40005	-8.457	-8.31	-16.991	-10.864		-9.269	-8.572	-4.581	-4.346	-6.624	-10.039	-3.042	-10.65	8.349	11.078	-3.685	-1.152	4.891	-36		
G 40006	-8.457	-8.31	-16.989	-10.863		-9.269	-8.572	-4.581	-4.346	-6.623	-10.041	-3.033		8.355	11.084	-3.677	-1.155	4.891	-36		
G 40007	-8.456	-8.309	-16.984	-10.862		-9.269	-8.573	-4.581	-4.345	-6.623	-10.044	-3.015	-10.654	8.366	11.098	-3.662	-1.163	4.891	-36		
G 40008	-8.462	-8.316	-17.015	-10.87		-9.269	-8.569	-4.581	-4.349	-6.625	-10.022	-3.133	-10.638			-3.763	-1.115	4.891	-36		
G 40009 (23)	-8.536	-8.399	-17.293	-10.943	-11.161	-9.29	-8.56	-4.588	-4.411	-6.663	-9.843		-10.504	7.62	10.231	-4.671	-0.689	4.891	-36	39.982	
G 40009 (60)	-8.469	-8.324	-17.046	-10.878		-9.269	-8.566	-4.581	-4.353	-6.628	-10.001	-3.251	-10.622	8.217	10.925	-3.863	-1.068	4.891	-36		
G 40010	-8.451	-8.304	-16.962	-10.856		-9.269	-8.576	-4.581	-4.343	-6.622	-10.06	-2.932	-10.665	8.418	11.158	-3.591	-1.196	4.891	-36		
G 40011 (68)	-8.456	-8.309	-16.984	-10.862		-9.269	-8.573	-4.581	-4.345	-6.623	-10.044	-3.015	-10.654	8.366	11.098	-3.662	-1.163	4.891	-36		
G 40011 (90)	-8.451	-8.304	-16.962	-10.856		-9.269	-8.576	-4.581	-4.343	-6.622	-10.06	-2.932	-10.665	8.418	11.158	-3.591	-1.196	4.891	-36		
G 40012	-8.451	-8.303	-16.96	-10.856		-9.269	-8.576	-4.581	-4.343	-6.622	-10.06		-10.666	8.424	11.165	-3.583	-1.199	4.891	-36		
G 40013	-8.456	-8.309	-16.984	-10.862		-9.269	-8.573	-4.581	-4.345	-6.623	-10.044		-10.654			-3.662	-1.163	4.891	-36		
G 40014	-8.458	-8.312	-16.996	-10.865		-9.269	-8.571	-4.581	-4.347	-6.624	-10.036	-3.061	-10.647	8.337	11.064	-3.701	-1.144	4.891	-36		
G 40015	-8.462	-8.316	-17.013	-10.87		-9.269	-8.569	-4.581	-4.349	-6.625	-10.024		-10.639	8.297	11.017	-3.755	-1.119	4.891	-36		
G 40016	-8.488	-8.346	-17.125	-10.899	-11.135	-9.272	-8.559	-4.581	-4.367	-6.636	-9.947		-10.583			-4.121	-0.947	4.891	-36	41.141	
G 40017	-8.458	-8.312	-16.996	-10.865		-9.269	-8.571	-4.581	-4.347	-6.624	-10.036	-3.061	-10.647	8.337	11.064	-3.701	-1.144	4.891	-36		
G 40018	-8.455	-8.308	-16.982	-10.862		-9.269	-8.573	-4.581	-4.345	-6.623	-10.046		-10.655	8.372	11.104	-3.654	-1.166	4.891	-36		
G 40019	-8.461	-8.315	-17.008	-10.868		-9.269	-8.57	-4.581	-4.348	-6.625	-10.027	-3.106	-10.641	8.309	11.031	-3.739	-1.126	4.891	-36		
G 40020 (47)	-8.469	-8.324	-17.043	-10.878		-9.269	-8.566	-4.581	-4.353	-6.627	-10.002	-3.242	-10.623	8.223	10.931	-3.855	-1.072	4.891	-36		
G 40020 (90)	-8.48	-8.336	-17.09	-10.89		-9.271	-8.562	-4.581	-4.361	-6.632	-9.97		-10.6	8.11	10.8	-4.008	-1	4.891	-36		
R 1	-8.48	-8.336	-17.09	-10.89	-11.13	-9.271	-8.562	-4.581	-4.361	-6.632	-9.97			8.11	10.8	-4.008	-1	4.891	-36	41.38	

GROUNDWATER SATURATION INDICES

Hausmani	Manganit	Pyrochro	PCO2	H2-gas	NH3-gas	Melanter	Alunite	K-Jarosi
58.244	25.34	15.2	-1.59	-3.199	1.544			
62.11	25.34	15.2	-1.42	-3.131	1.858	-2.263	-0.861	-8.874
			-1.46	-3.148	1.78	-2.215		-9.171
			-1.43	-3.135	1.839	-2.251	-0.975	-8.946
			-1.43	-3.137		-2.245	-1.038	-8.985
			-1.47	-3.152		-2.204		-9.241
			-1.45	-3.142	1.806	-2.231	-1.176	-9.071
61.578	25.34	15.2	-1.44	-3.14		-2.236	-1.126	-9.04
61.328	25.34	15.2	-1.45	-3.145		-2.224	-1.251	-9.117
			-1.46	-3.145	1.792	-2.223	-1.264	-9.125
61.179	25.34	15.2	-1.46	-3.147	1.782	-2.217		-9.164
62.033	25.34	15.2	-1.42	-3.132	1.851	-2.259		-8.898
61.629	25.34	15.2	-1.44	-3.14	1.819	-2.239	-1.101	-9.024
61.328	25.34	15.2	-1.45	-3.145	1.794	-2.224	-1.251	-9.117
			-1.43	-3.138	1.827	-2.244		-8.993
			-1.43	-3.136	1.833	-2.247	-1.013	-8.969
59.456	25.34	15.2	-1.54	-3.178	1.642	-2.134		-9.699
61.704	25.34	15.2	-1.44	-3.138	1.825	-2.242		-9
62.365	25.34	15.2	-1.4	-3.127	1.878	-2.276	-0.733	-8.795
62.545	25.34	15.2	-1.39	-3.124	1.893	-2.285	-0.644	-8.739
			-1.41	-3.128	1.872	-2.272		-8.819
			-1.41	-3.128	1.872	-2.272	-0.772	-8.819
			-1.4	-3.126	1.883	-2.278		-8.779
61.278	25.34	15.2	-1.46	-3.146	1.79	-2.221	-1.276	-9.133
			-1.4	-3.125	1.887	-2.281	-0.682	-8.763
59.432	25.34	15.2	-1.54	-3.178	1.64	-2.133	-2.198	-9.707
			-1.42	-3.132	1.856	-2.261	-0.874	-8.882
			-1.42	-3.131	1.858	-2.263	-0.861	-8.874
			-1.41	-3.13		-2.265	-0.836	-8.859
			-1.43	-3.136		-2.249		-8.961
58.868	25.34	15.2	-1.57	-3.188	1.595	-2.107	-2.479	-9.882
			-1.45	-3.142	1.808	-2.232	-1.164	-9.063
			-1.4	-3.126		-2.277	-0.721	-8.787
			-1.41	-3.13		-2.265	-0.836	-8.859
			-1.4	-3.126		-2.277	-0.721	-8.787
			-1.4	-3.126		-2.278	-0.708	-8.779
			-1.41	-3.13		-2.265		-8.859
			-1.42	-3.132		-2.259	-0.899	-8.898
			-1.43	-3.136	1.837	-2.25	-0.988	-8.953
60.661	25.34	15.2	-1.49	-3.156	1.74	-2.191		-9.325
			-1.42	-3.132	1.851	-2.259	-0.899	-8.898
			-1.41	-3.13		-2.267	-0.823	-8.851
			-1.43	-3.135	1.841	-2.253	-0.962	-8.938
			-1.44	-3.141		-2.234	-1.151	-9.055
			-1.47	-3.15		-2.209	-1.4	-9.21
61.03	25.34	15.2	-1.47	-3.15		-2.209	-1.4	-9.21